Responses to DNA damage within *Arabidopsis* stem cell niches

A thesis submitted to the University of East Anglia for the degree of

Doctor of Philosophy

Nick Fulcher

John Innes Centre

Norwich, UK

July 2010

ABSTRACT

Plants are sessile by nature so are unable to escape environmental hazards that can potentially induce DNA damage. Any negative impacts of DNA damage exerted on stem cell populations could affect growth or be passed onto future generations. In animals, programmed death of stem cells with damaged DNA is important to prevent cancer and protect the germline. It has been assumed that programmed cell death (PCD) does not play an important role in plants, partly due to the absence of the key genes implicated in DNA damage-induced cell death. The aim of this project was to identify mechanisms plants use to safeguard their stem cell populations against genomic damage.

The initial hypothesis was derived from early work in *Zea mays* where the quiescent centre (QC), a group of slowly dividing cells at the centre of the root stem cell niche, was proposed to act as a genetically stable template for neighbouring stem cells. It was thought that the QC could activate cell divisions after DNA damage to form a new population of root initials. While testing this hypothesis in *Arabidopsis*, instead of activation of the QC, I saw that root initials were preferentially killed in response to mild treatment with agents that cause DNA double strand breaks.

Cell death was found to depend on transduction of DNA damage signals by key signalling kinases ATM (ATAXIA-TELANGIECTASIA MUTATED) and ATR (ATM and RAD3-RELATED), showing that it was a genetically programmed response and not a consequence of DNA damage itself. In addition, mutants defective in DNA repair by non-homologous end joining (NHEJ) were shown to exhibit spontaneous death of stem cells in the absence of DNA damaging agents.

Dying stem cells did not show the morphological hallmarks of apoptosis but instead showed autophagic-like intracellular vesicles within dying root initials. Analysis of mutants defective in autophagy however showed no impact on cell death within stem cells of the root, suggesting additional cell death mechanisms may complement autophagy.

Experiments were also adapted to the shoot meristem; stem cells within the shoot apex were also shown to be selectively killed after DNA damage treatments. Cell death was dependent on ATM as in the root, but not on ATR, suggesting different roles for these signalling kinases in the root and shoot.

Finally, experiments investigating recovery of the root after DNA damage showed root growth resumed after treatment. Cell death was found to be largely reduced up to 3 days after treatment; surrounding cells were found to expand into space left by dying root initials. Results from this thesis provide evidence for the role of PCD in protecting stem cell populations from DNA damage in plants.

ACKNOWLEDGEMENTS

This work was funded by the Biotechnology and Biological Sciences Research Council (Grant BB/B511927/1).

I'd like to thank my supervisor Robert Sablowski for his excellent guidance and support throughout the PhD. I'd also like to thank the members of the Sablowski lab, past and present, whose discussion and advice have been a great help. A big thanks goes to Gerardo Acosta-Garcia for his help at the start of the project and for teaching me many lab protocols. Thank you to my advisor Mary Byrne for taking part in the supervisory meetings and also for the comments on the thesis.

Thank you to the people who supplied seeds and materials that are mentioned throughout the thesis. Special thanks go to Frank Luhana at the Norfolk and Norwich Hospital for his help and patience with the x-ray experiments. Also, I'd like to thank Sue Bunnewell for the root tip sectioning and electron microscopy.

I'd like to thank my close friends and family who have supported me throughout my time at university and the PhD. Finally, special thanks go to Lauren, whose love and support has helped me a huge amount over the past few years.

Thank You!

TABLE OF CONTENTS

ABBREVIATIONS

ACR4	ARABIDOPSIS CRINKLY4
AG	AGAMOUS
AP1	APETALA1
ARF	Auxin response factor
AS	ASYMMETRIC LEAVES
ATG	AUTOPHAGY-RELATED
ATM	Ataxia-Telangiectasia Mutated
ATR	Ataxia-Telangiectasia Mutated and Rad3-related
ATRIP	ATR interacting protein
BARD1	BRCA1-associated ring domain protein 1
BBM	BABY BOOM
BDL	BODENLOS
BP	BREVIPEDICELLUS
BRCA1	Breast cancer associated gene 1
CARD	Caspase-recruitment domain
CDK	Cyclin dependent kinases
CHK	Checkpoint kinase
CK	Cytokinin
CLV3	CLAVATA3
Col	Columbia
CPD	cyclobutane pyrimidine dimers
CZ	Central zone
DAB	3’-diaminobenzidine
DNA	Deoxyribonucleic acid
DNA-PK	DNA dependent protein kinase
dNTP	Deoxynucleotide triphosphate
DSB	Double strand DNA break
DTT	Dithiothreitol
EDTA	Ethylenediaminetetraacetic Acid
EIN2	ETHYLENE INSENSITIVE 2
ESCs	Embryonic stem cells
ET	Ethylene
FADD	Fas-associated death domain
FD	Fluorescein diacetate
GA	Gibberellins
GFP	Green fluorescent protein
GM	Germination media

GUS	β-glucuronidase
HR	Homologous recombination
IPT7	ISOPENTENYL TRANSFERASE 7
IR	Ionizing radiation
JKD	JACKDAW
KAPP	Kinase-associated protein phosphatase
KNAT	KNOTTED-like in *Arabidopsis thaliana*
KNOX	Class 1 KNOTTED-like HOMEOBOX
LB	Lysogeny broth
L*er*	Landsberg *erecta*
LFY	LEAFY
LIGIV	DNA ligase IV
MGP	MAGPIE
M-MLV	Moloney murine leukemia virus
MP	MONOPTEROS
MRE11	Meiotic recombination 11
MRN	MRE11/RAD50/NBS1 complex
NBS1	NIJMEGEN BREAKAGE SYNDROME 1
NPA	N-1-Naphthylphthalamic Acid
MMS	Methyl methanesulfonate
NHEJ	Non homologous end joining
OC	Organising centre
OXI1	OXIDATIVE SIGNAL-INDUCIBLE 1
PARP	Poly(ADP-ribose) Polymerase
PCD	Programmed cell death
PCR	Polymerase chain reaction
PE	Phosphatidylethanolamine
PI	Propidium iodide
PIN	PIN-FORMED
PLT	PLETHORA
PPT	Phosphinothricin
pRB	RETINOBLASTOMA
PZ	Peripheral zone
QC	Quiescent centre
RAM	Root apical meristem
RCD1	RADICAL INDUCED CELL DEATH 1
RNA	Ribonucleic acid
RNAi	RNA interference

ROP	Rho-like GTPases
ROS	Reactive oxygen species
RPA	Replication binding protein A
RT	Reverse transcription
RZ	Rib zone
SA	Salicylic acid
SAM	Shoot apical meristem
SCR	SCARECROW
SHR	SHORTROOT
SID	SALICYLIC ACID INDUCTION–DEFICIENT
SOB	Super optimal broth
ssDNA	Single stranded DNA
STM	SHOOTMERISTEMLESS
TALE	Three-amino acid loop extension
T-DNA	Transfer DNA
TEM	Transmission electron microscopy
TERT	Telomerase
TEV	Tobacco etch virus
Ub	Ubiquitin
UV	Ultraviolet
WOX5	WUSCHEL-RELATED HOMEOBOX PROTEIN 5
WS	Wassilewskija
WT	Wild type
WUS	WUSCHEL
X-Gluc	5-bromo-4-chloro-3-indolyl-β-D-glucuronide
X-Gal	5-bromo-4-chloro-3-indolyl-β-D-galactopyranoside
XRCC4	X-ray repair cross complementing protein 4

Chapter 1 - General introduction

1.1. Introduction to *Arabidopsis* stem cell populations

1.1.1. Meristem definitions and functions

Stem cell niches are specialized microenvironments containing small pools of pluripotent cells that contribute to the formation of new tissues and organs (Tucker and Laux 2007). These cells remain within the confines of the niche until they are displaced by cell division, releasing them from short-range signals that prevent differentiation (Sablowski 2004). Stem cell populations act within almost all multicellular organisms to maintain growth and development, however, the contribution of these populations to formation of the adult body differs greatly between animals and plants. In animals, the body plan is established within the embryo through rapid proliferation of embryonic stem cells (ESCs) (Heyer *et al.* 2000). Post-embryonic growth then proceeds to increase the size of the organism. Plant development contrasts largely to this by maintaining growth of organs post-embryonically; development of all tissues and organs occurs after seed germination through the actions of root and shoot meristems.

In plants, two separate stem cell populations are established early on in embryo development. The shoot apical meristem (SAM) is involved in the formation of all aerial structures and floral organs; the root apical meristem (RAM) mediates growth of the root system which enables the plant to absorb nutrients from its surroundings. Stem cell populations contained within shoot and root meristems are controlled by short-range signalling mechanisms that influence population size and pluripotency. This section therefore aims to summarise interactions between signals involved in stem cell maintenance.

1.1.2. Organisation of the shoot apical meristem and generation of floral organs

The structure of the SAM is highly organised into distinct layers and zones which allow for the generation of new organs and also the preservation of undifferentiated stem cells for future organogenesis (Fletcher 2002). This organisation is controlled by a number of gene interactions that have been well characterised (Doerner 2001, Fletcher 2002, Sablowski 2004, Sablowski 2007). These reviews highlight two separate levels of SAM organisation summarised in figure 1.1., tunica-corpus organisation and central/peripheral zones (CZ/PZ). The SAM is organised into 3 clonally distinct layers consisting of the L1, L2 (tunica) and L3 (corpus), the L1 cells give rise to epidermal cells, whereas the L2 and L3 cells produce internal portions of the plant (Abe *et al.* 1999). Cell divisions within the first two surface layers are anticlinal (dividing in only 1 plane) whereas the L3 layer corpus cells exhibit periclinal division (divide in multiple planes).

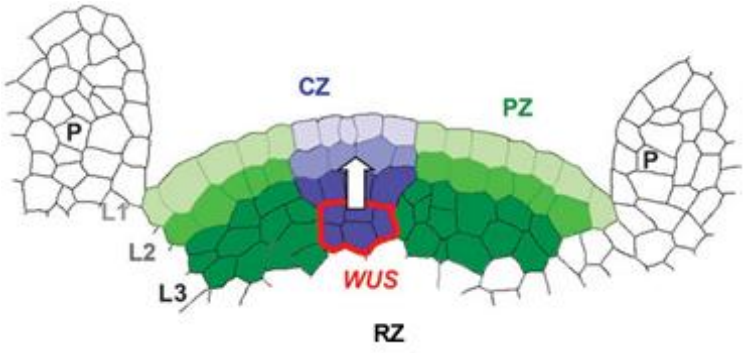

Figure 1.1. Organisation of the shoot apical meristem (SAM)
A graphical representation showing levels of shoot apical meristem organisation in *Arabidopsis*. Clonally distinct layers L1, L2 and L3 are shown in green to light green; the organising centre is outlined in red, these cells express stem cell identity gene *WUSCHEL*. The arrow indicates *WUS* signalling to the overlying central zone (CZ) where it induces *CLV3* expression, the CLV3 peptide then signals to the CLV1 & 2 receptors to form a dimer which represses *WUS*. The meristem displaces cells from the stem cell niche to the surrounding peripheral zone (PZ) and rib zone (RZ) where they differentiate to form new organ primordia and stem tissue. (Image Source – Sablowski 2007).

The stem cell population in the SAM is located in layers L1 to L3 at the meristem centre, their progeny are progressively displaced towards the

periphery of the meristem where they are recruited into organ primordia (Doerner 2001). Clonal analysis has shown that stem cell specificity is not permanent and cells differentiate once displaced from the central zone (CZ) (Baurle and Laux 2003). Directly below the CZ is the organizing centre (OC) which signals to the overlaying stem cells contained within the CZ controlling their number and pluripotency (Mayer *et al.* 1998). The basal end of the meristem consists of the rib zone (RZ) which eventually gives rise to tissues within the stem (Kuhlemeier and Reinhardt 2001). Once the population within the CZ becomes large enough, cells are displaced to the peripheral and rib zones (PZ & RZ) where they form new organs.

A current model proposes that the size of the stem cell population in the SAM is controlled by a negative feedback regulation between two pathways that promote or restrict stem cell numbers (Brand *et al.* 2002). The *WUSCHEL* (*WUS*) gene encodes a nuclear-localized homeodomain protein that has been shown to specify stem cell identity along with *SHOOTMERISTEMLESS* (*STM*) (Brand*, et al.* 2002, Laux *et al.* 1996, Mayer*, et al.* 1998). *WUS* was first characterised in a paper by Laux *et al.* (1996) where homozygous *wus-1* mutants were found to terminate shoot and floral meristems prematurely. WUS was eventually found to play a role in organising stem cell fate in the shoot meristem (Mayer*, et al.* 1998). *WUS* expression is confined to a small group of meristem cells called the organising centre (OC) by a negative feedback loop involving signalling by three CLAVATA proteins (CLV1, 2 and 3) (Brand*, et al.* 2002). In this loop, WUS migrates to the CZ and promotes transcription of the polypeptide signalling ligand *CLAVATA3* (*CLV3*). CLV3 is able to migrate to the OC where it binds with the CLV1/CLV2 receptor complex. *CLV1* encodes an LLR-receptor kinase whereas *CLV2* encodes for a similar receptor lacking an intracellular domain (Baurle and Laux 2003). Once activated, the intracellular CLV1 kinase domain induces a signalling cascade involving a kinase-associated protein phosphatase (KAPP) and ROP, a member of a family of Rho-like GTPases (Fletcher 2002). This signalling

pathway inhibits expression of *WUS*; WUS therefore acts to inhibit its own activity by promoting the CLV signalling pathway. Once WUS levels are downregulated by CLV signalling, *CLV3* is not induced leading to its own downregulation. When CLV3 levels are reduced, WUS levels are able rise again in the absence of high *CLV3* expression providing an inhibitory feedback loop.

WUS expression is also detected within the early floral meristem but is downregulated upon onset of carpel formation (Lenhard *et al.* 2001). Flowers arise on the flanks of indeterminate shoot meristems and are produced by determinate floral meristems (Fletcher 2002). Floral meristems are determined by LEAFY (LFY) and APETALA1 (AP1), these transcription factors activate overlapping expression of homeotic genes involved in floral organ development (Parcy *et al.* 2002). The floral meristem is terminated through inhibition of *WUS* by AGAMOUS (AG), a MADS domain transcription factor involved in carpel formation. *AG* mutants retain their stem cell population controlled by *WUS* resulting in indeterminate flower formation (Lenhard*, et al.* 2001).

STM is a member of the KNOX (Knotted-like Homeobox) gene family with a large super-class of homeodomain (HD) proteins that contain a three-amino acid loop extension (TALE) motif in the homeodomain (Long *et al.* 1996, Scofield and Murray 2006). *KNOTTED1* (*ZmKN1*) from maize was the first characterised homeobox gene to have involvement in the maintenance of the SAM (Scofield and Murray 2006). The *Arabidopsis* genome contains four class I KNOX genes: *STM*, *KNAT1*/*BREVIPEDICELLUS* (*BP*), *KNOTTED*-like from *Arabidopsis thaliana 2* (*KNAT2*) and *KNAT6* (Hay *et al.* 2004). *STM* has been shown to restrict the initiation of organs to the flanks of the meristem through the repression of *ASYMMETRIC LEAVES1* (*AS1*) and *AS2* which in turn also repress the expression of KNOX genes *KNAT1*, *KNAT2* and *KNAT6* (Baurle and Laux 2003, Byrne *et al.* 2000, Byrne *et al.* 2002). *KNAT1* and *KNAT2* are also expressed within the meristem and are involved in maintaining cells in an undifferentiated state. *AS1* encodes a myb protein which negatively regulates homeobox genes *KNAT1* and

KNAT2 but is itself regulated by *STM*. Combined ectopic expression of *WUS* and *STM* has been shown to establish meristem cells and induce cell division indicating their role in specifying stem cell fate (Gallois *et al.* 2002).

In addition to the interactions of stem cell regulatory genes, plant hormones have also shown to be essential in regulating homeostasis of the shoot meristem (Tucker and Laux 2007). Early experiments showed high cytokinin (CK) levels to be essential for the formation of shoot structures from callus tissue (Skoog and Miller 1957). More recently, Jasinski *et al.* (2005) showed dexamethasone inducible STM was able to induce ectopic expression of *ISOPENTENYL TRANSFERASE 7* (*AtIPT7*), a key CK biosynthesis gene. In addition, Yanai *et al.* (2005) used the LhG4/pOp transcriptional system to express *AtIPT7* under the control of the *STM* promoter. This was found to repress meristem termination observed in the *stm-1* mutant. A common model is proposed by these papers which suggest a role for KNOX genes in regulation of CK biosynthesis in the SAM. The interaction between KNOX genes and CK biosynthesis is also proposed to play a role in excluding gibberellins (GA) from the SAM. This depletion of GA in the SAM would act to limit GA to leaf primordia, where it functions to mediate growth of new organs. KNOX genes were originally found to suppress the expression of GA biosynthetic genes in the shoot meristem of tobacco (Sakamoto *et al.* 2001). STM was also found to interact with *AtGA2ox2* and *AtGA2ox4* suggesting a direct role in activating genes with a role in GA-degradation in *Arabidopsis* (Jasinski*, et al.* 2005). Together, these results suggest an antagonistic relationship between cytokinins and gibberellins; STM could help to maintain growth homeostasis in the shoot apex by activating CK and repressing GA (Sablowski 2007). Plants therefore exhibit overlapping regulatory mechanisms that control boundaries of stem cell populations.

1.1.3. Structure of the root apical meristem

Mechanisms for regulating the stem cell niche within the root tip are relatively distinct in comparison to the shoot meristem. The stem cell niche of the root meristem consists of the quiescent centre (QC) and the surrounding stem cells known as the root initials (indicated in figure 1.2.). QC identity is defined by slow mitotic cycles displayed by cells within the centre of the niche. Early experiments in *Zea mays* roots first identified these slowly dividing cells through experiments tracking incorporation of thymidine-^{3}H (Clowes 1961); the QC was eventually estimated to divide after 174 hrs in a later paper (Clowes 1965). Subsequent experiments have determined the role of the QC in controlling the fate of surrounding cells. Van den Berg *et al.* (1997) used laser ablation to remove the QC, resulting in differentiation of neighbouring cells. These studies concluded that short-range signals were being released from the QC to prevent differentiation of surrounding cells. Cells within direct contact with the QC are dubbed the root initials; division of meristem initials yields one daughter cell which remains as an initial and one daughter which breaks contact with the QC to begin differentiation (Sablowski 2004). Establishing QC identity and position is therefore deemed important for the activity of the stem cell niche in the root.

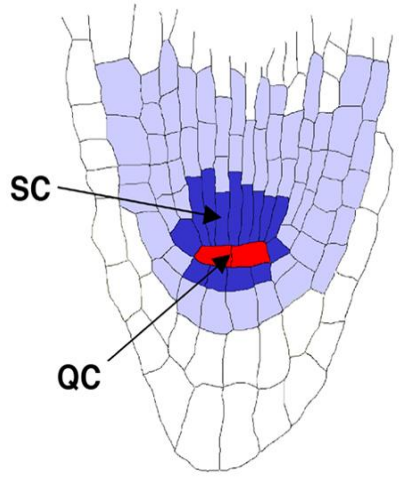

Figure 1.2. Structure of the root meristem
The stem cell niche of the root meristem is centred on the quiescent centre (QC). This group of slowing dividing cells is known to function as an organiser of stem cell fate. The QC releases signals to surrounding stem cells (SC) known as the root initials to prevent their differentiation. Cell division of the root initials yields two daughter cells, one remaining within the niche and one being displaced. Root initials that are displaced from signals of the QC go on to become differentiated and form tissue structures of the root. (Image source: Sablowski 2004).

Positional information for maintenance of the QC is proved from transport of the phytohormone auxin to the root tip. The exact sites of auxin biosynthesis

are unknown, synthesised auxin is transported to tissues where it activates cell signalling responses to influence growth and development (Benjamins and Scheres 2008). This transport is mediated by PIN-FORMED (PIN) membrane bound auxin transport proteins. PIN proteins function within the cell to mediate polar transport of auxin; direction of auxin transport is therefore indicated by the position of PIN proteins (Feraru and Friml 2008). Auxin flow is directed in the root through stele cells where an auxin maximum is established in the root tip (Teale *et al.* 2005). This auxin gradient was first identified by Frimil *et al.* (2003) utilising a *DR5rev::GFP* marker to observe auxin response. Auxin levels were found to be shifted to the basal portion of the embryo upon formation of the root meristem. PIN proteins were found to be essential in establishing this gradient, exposure to N-1-Naphthylphthalamic Acid (NPA) which blocks functionality of PIN proteins created a perturbed auxin gradient. Also, *PIN1* expression was found to localise within cells directing polar auxin transport towards the basal end of the embryo. Computer simulations modelling auxin flow through the root showed localisation of PIN proteins was sufficient to establish the auxin maximum at the root tip (Grieneisen *et al.* 2007). It eventually became evident that this high level of auxin was essential to establish the root meristem through interactions with specific auxin response genes.

Auxin response regulators *MONOPTEROS* (*MP*) and *BODENLOS* (*BDL*) are active at auxin peak levels where they function to induce *PLETHORA* (*PLT*) genes. *MP* was first characterised by Berleth & Jürgens (1993) in a mutant screen yielding seedlings lacking the basal pattern elements, root and hypocotyl. MP was found to be essential for formation of the root meristem, elements of the shoot meristem however were observed to be unaffected. To assess post-embryonic functions of MP, Przemeck *et al.* (1996) produced adult *mp* plants through generation of adventitious roots. Inflorescence meristems of *mp* plants were shown to resemble those of *pin1* mutants defective in the generation of flowers and leaves. This paper therefore was able to link MP to auxin transport,

the distinct phenotypic differences between *mp* and *pin1* however suggested distinct roles of each protein. Eventual sequence analysis of the *MP* gene revealed conserved regions with *AUXIN RESPONSE FACTOR 1* (*ARF1*) suggesting a role in auxin signalling (Hardtke and Berleth 1998). Another gene, *BDL*, was also found to be involved in formation of the root, a mutant derived from a mutagenised L*er* population showed similar embryonic phenotypes as described in the *mp* mutant. BDL was subsequently identified as a negative regulator of MP highlighting an important interaction between these proteins in establishing the root meristem (Hamann *et al.* 2002).

The relationship between BDL and MP in activating PLT is regulated via a negative feedback loop as described by Benjamins & Scheres (2008). Research into auxin dependent genes has led to the identification of AUX/IAA and ARF (AUXIN RESPONSE FACTOR) protein families, interactions between these genes is known to form a feedback loop to regulate auxin dependent gene expression. The interaction between MONOPTEROS (MP/ARF5) and BODENLOS (BDL/IAA12) is well characterised in the formation of the *Arabidopsis* root meristem. A representation of the model which describes how auxin dependent genes are regulated is shown in figure 1.3. High auxin levels activate SCF^{TIR1} ubiquitin protein ligase (TIR1 is involved in auxin perception) which is involved in targeting AUX/IAA (BDL in this case) genes for ubiquitin dependent degradation. Once ARFs (MP in the case of the root) are released from the inhibitory interaction between them and AUX/IAA proteins, they are able to induce expression of auxin related genes including AUX/IAA. Induction of AUX/IAA means more inhibition creating a negative feedback loop.

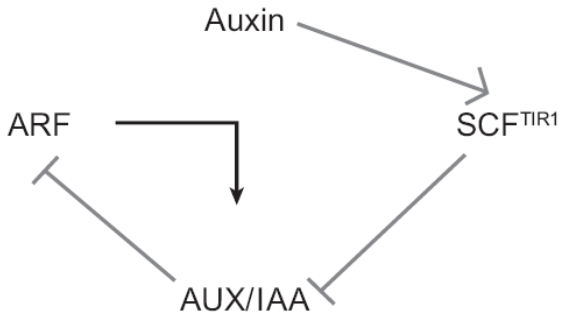

Figure 1.3. Model for auxin dependent feedback mechanism in the root meristem
High auxin levels activate SCF^{TIR1} ubiquitin protein ligase which targets AUX/IAA proteins for degradation by the proteosome. Upon release from inhibitory interaction with AUX/IAA proteins, ARFs are able to initiate transcription of auxin dependent genes. ARFs are also able to regulate their own transcription through upregulating AUX/IAA expression. These interactions are thought to act in the root meristem to mediate positioning of the QC at sites of auxin maxima. (Image source: Benjamins & Scheres 2008)

One known gene family induced downstream of MP activity is *PLETHORA (PLT)* (Tucker and Laux 2007). *PLT* genes were first characterised by Aida *et al.* (2004), *plt1-4 plt2-2* double mutants were found to exhibit extremely reduced root growth compared with wild type WS seedlings. The *PLT* family was eventually found to contain 4 homologs essential for root growth. Triple mutants of *plt1*, *plt2* and *plt3* result in a rootless phenotype and additional loss of the 4th *PLETHORA* gene, *BABY BOOM* (*BBM*), results in a complete lack of hypocotyl and root (Galinha *et al.* 2007). This quadruple mutant resembles mutants of MP; PLT genes are therefore proposed to function in establishing the QC in the root tip.

In addition to positioning by *PLETHORA* genes, the GRAS family transcription factors *SCARECROW (SCR)* and *SHORTROOT (SHR)* are also needed to specify QC identity (Aida*, et al.* 2004). *SCR* and *SHR* were identified through screening of mutagenised seeds which displayed retarded root growth (Benfey *et al.* 1993, Scheres *et al.* 1995). These genes were eventually found to be essential in patterning of the root meristem. The putative transcription factor SHR is expressed within the stele, SHR protein was found to translocate to the adjacent QC and activate expression of *SCR* (Nakajima *et al.* 2001). SCR was subsequently found to be essential for establishing the QC, *scr-1* mutants failed to specify QC identity and lack expression of QC25 and QC46 GUS markers (Sabatini *et al.* 2003). Transcriptional regulation by SCR induces expression of genes relevant to maintenance of QC identity. Known target genes of SHR/SCR

activity include *MAGPIE* (*MGP*) and *JACKDAW* (*JKD*) which can regulate activity of *SCR* and *SHR* (Welch *et al.* 2007).

Stem cell regulatory networks initially appeared to be very different in comparison of root and shoot meristems. The search for related mechanisms has until recently not shown any similarity to that of the CLV3-WUS feedback loop in the shoot. More recent discovery of related genes in the root as suggested similar roles for feedback loops in stem cell maintenance within shoot and root meristems.

1.1.4. Similarities and differences between root and shoot stem cell niches

Similarities between maintenance of stem cell populations in shoot and root meristems has long been under speculation. Characterisation of the *WOX5* (*WUSCHEL-RELATED HOMEOBOX PROTEIN 5*) gene by Sarkar *et al.* (2007) provided the first solid evidence for related pathways between shoot and root meristems. Stem cells within the shoot require WUS activity to specify them as undifferentiated; a WUS-dependent signal travels to the stem cell population from the underlying organising centre. This activates expression of *CLV3* which has an inhibitory impact on WUS expression forming the negative feedback loop which maintains the stem cell population. Experiments with the WUSCHEL-related WOX5 protein show promising results highlighting a similar feedback mechanism.

Expression of *WOX5* is very specific to the QC; lack of expression in the *wox5-1* mutant causes columella initials to differentiate which is evident from the appearance of unusually large columella cells (Sarkar*, et al.* 2007). This therefore suggests WOX5 is a key signalling protein involved in maintaining surrounding root initials in an undifferentiated state. Interestingly, expression of the *WOX*5 gene within the shoot meristem can replace the function of *WUSCHEL*

in *wus-1* mutants, rescuing them from meristem termination (Sarkar*, et al.* 2007). Various studies have also highlighted CLV3-like activity in regulating *WOX5* expression in the QC, mirroring the feedback mechanisms in the shoot. CLE40 has been suggested as having similar function to CLV3 in the shoot by regulating expression of *WOX5* within the QC (Stahl *et al.* 2009). *CLE40* is thought to be expressed within differentiated columella cells; migration to the QC is thought to repress *WOX5* expression through the ARABIDOPSIS CRINKLY4 (ACR4) receptor (De Smet *et al.* 2008, Stahl*, et al.* 2009). These papers therefore provide evidence for the role of similar feedback mechanisms that control stem cell number in shoot and root meristems.

The role of hormones in establishing stem cell boundaries also shows similarities and differences between shoot and root meristems. Auxin has shown to be involved in establishing leaf and flower formation and regulation for phylotaxy in the SAM (Reinhardt *et al.* 2003). Exogenously added auxin was found to induce leaf and flower formation in PIN1 mutants defective for auxin transport. As described earlier in this chapter, auxin is key in establishing positional information for the QC in the root meristem. Clear differences for requirement of auxin distribution therefore seem to occur in shoot and root tissues. The role of cytokinins also appears to be different between shoot and root meristems. Dello Ioio *et al.* (2007) showed application of exogenous CK caused significant reduction in the size of the root meristem. Mutants disrupted in CK signalling and biosynthesis also showed increased meristem size. This contrasts to the shoot meristem where CK is essential in maintaining homeostasis of stem cell populations in the SAM (Jasinski*, et al.* 2005). Hormones are essential in maintenance of both shoot and root meristems; they however can play very different roles.

Both root and shoot meristems have seen shown to utilise an organising centre to control signalling to surrounding cells in order to maintain them as undifferentiated. This is a common feature but cell division rates within these

two populations differ greatly. The QC, the proposed organising centre of the root, divides very infrequently. Surrounding root initials divide at a faster rate, but still undergo divisions much slower than other surrounding meristem cells (Dolan *et al.* 1993). This contrasts to the OC of the shoot which divides more frequently than the overlaying stem cell population (Reddy *et al.* 2004). Large differences are therefore observed comparing shoot and root meristems including different roles for hormones and varying cell division rates.

1.1.5. Effects of the environment on meristems

Stem cell populations function throughout the lifetime of a plant to maintain post-embryonic growth of tissues and organs. This however also means they are exposed to various environmental conditions that could exert negative impacts on their growth. Plants lack a reserve germline and generate gametes late in development; any negative effects of environmental conditions could also affect future generations. It is well known that exposure to many environmental factors such as UV, high salinity and drought can result in DNA damage, causing genomic instability (Kotchoni and Gachomo 2006). It is therefore important to understand how plant stem cell populations have evolved to deal with genotoxic environmental conditions.

1.2. DNA damage: formation and recognition of double stranded DNA breaks

1.2.1. Mechanisms of DNA damage in response to biotic and abiotic stress

The nature of plants, being sessile and depending on photosynthesis for energy, means they have no means of escaping harmful genotoxic environmental conditions. Abiotic factors including heavy metal toxicity, high salinity, low temperature, drought and UV irradiation have shown to contribute to a rise in DNA damage in plants (Kotchoni and Gachomo 2006). In addition, invasion of pathogens, fungi and insects are known to elicit DNA damage induced cell death through the hypersensitive response (Gechev *et al.* 2006). Each of these environmental factors initiates DNA damage through a common mechanism known as the "oxidative burst" which results in rapid generation of reactive oxygen species (ROS) (Apel and Hirt 2004). ROS have DNA cleaving properties which can create genomic instability through generation of double stranded DNA breaks (DSBs); their production is however linked to signalling mechanisms in plants that control cellular responses to environmental stress.

ROS production occurs endogenously through normal cellular metabolic processes. This is a result of aerobic metabolism mechanisms in plants using photosynthesis and photorespiration for energy (Kotchoni and Gachomo 2006). ROS intermediates such as $O_2^{\bullet-}$, H_2O_2 and hydroxyl radicals can often leak out of the electron transport chain during photosynthesis (Apel and Hirt 2004). The chloroplast is therefore deemed to be the key organelle involved in ROS production. Once thought of as unwanted by-products of metabolism, ROS are now known to act as key signalling intermediates involved in activating downstream stress responses (Wong and Shimamoto 2009). Miller *et al.* (2009) identified *RESPIRATORY BURST OXIDASE HOMOLOG D* (*RBOHD*) in *Arabidopsis*

to be involved in elevating ROS levels after exposure to heat and cold stress, high light intensity and high salinity levels. NADPH oxidases are well characterised in their ability to generate ROS by channelling electrons from NADPH inside the cell to join with molecular oxygen forming $O_2^{\bullet-}$ (DeLeo and Quinn 1996). This increase in ROS levels was suggested by Miller *et al.* (2009) to enable a rapid, long distance signalling mechanism to quickly initiate plant responses to these harmful environmental conditions. ROS production is therefore not solely linked to mistakes in the electron transport chain, but is also controlled by membrane bound proteins to mediate stress perception.

Under normal conditions, antioxidant enzymes such as superoxide dismutase (SOD) counteract the harmful effects of ROS production (Mittler 2002). However, exposure to extreme environmental conditions results in excessive ROS production, elevating ROS levels over the threshold by which antioxidant enzymes can support. This production is also enhanced by drought, salt and temperature stress (also combined with high-light levels) which affects CO_2 fixation in photosynthesis (Mittler *et al.* 2004). The balance of ROS levels, if not maintained by antioxidant mechanisms, is then able to act on cellular components causing molecular damage.

ROS accumulation is known to induce DNA damage through addition to double bonds of DNA bases and hydrogen abstraction (Cooke *et al.* 2003). ROS molecules are highly reactive and contain unpaired electron valence shells (Banerjee *et al.* 2003). This high level of reactivity means ROS can oxidise many molecules, the major target being DNA which contains many electron-rich bases (Roldan-Arjona and Ariza 2009). Oxidative attack involving hydrogen abstraction on sugar molecules causes fragmentation leading to subsequent DNA breaks; addition of the hydroxyl radical to pyrimidines can also form stable DNA lesions that affect DNA structure (Roldan-Arjona and Ariza 2009). Collapse of sugar molecules therefore result in the formation of DSBs, which if left unrepaired can have a catastrophic effect on cell integrity and survival.

ROS accumulation is described as a natural response to environmental stress, a number of chemical and irradiation treatments can however induce ROS mediated DNA damage. Drugs such as the bleomycin family are known to create DSBs through similar mechanisms used in ROS attacks. DNA cleavage by bleomycin is known to involve interaction with Fe(II)· and O_2 which causes hydrogen abstraction at pyrimidine nucleotides of preferred sites containing 5'-GC and 5'-GT sequences (Claussen and Long 1999). Similarly, exposure to ionizing radiation (IR) also causes DNA damage through direct and indirect mechanisms involving ROS. IR is known to directly damage DNA by displacing electrons from DNA molecules; IR can also displace electrons from H_2O creating clusters of ROS (Roldan-Arjona and Ariza 2009). ROS attack and mechanisms of ROS-like treatments can therefore cause damage DNA by forming stable lesions or mediating the break of DNA strands. Exposure to UV can also upregulate ROS production, UV is however able to alter the chemical structure of DNA creating lesions known as photoproducts. The most common of these photoproducts are cyclobutane pyrimidine dimers (CPDs) and (6-4) pyrimidine-pyrimidone photoproducts, which form as a result of covalent linkage between adjacent pyrimidine bases (Batista *et al.* 2009). Presence of such lesions can result in the stalling of replication forks which can subsequently collapse forming a DSB. These treatments described can therefore be used to study effects of DNA damage in plants by directly generating DSBs through ROS related mechanisms.

1.2.2. DNA damage perception and activation of downstream signalling events

Various chemical agents and environmental conditions act on DNA to induce DSBs; organisms have however evolved complex molecular pathways in order to deal with such lesions. These signalling events are well studied in animals due to links with cancer predisposition in certain genetic diseases. Through these

studies, signalling proteins have been identified with a role in the perception of DNA damage which initiates several responses which act in cell cycle arrest, DNA repair and in the event of extensive DNA damage, cell death. A well-established model has been described in animals that functions in DSB recognition and activation of downstream processes.

The primary sensor of this model involves a complex of three proteins known as the MRN complex (MRX in budding yeast) (Czornak *et al.* 2008). This complex exhibits multiple functions in DSB signalling gained from the unique function of each of its components. Three integral parts of this complex consist of MRE11, RAD50 and NBS1 in humans. MRE11 is proposed to act as an exonuclease which functions in DSB repair by resecting exposed DSB ends making them compatible for religation (Paull and Gellert 1998). RAD50 is known to associate directly with MRE11 and functions to tether DSB ends (de Jager *et al.* 2001). The long coiled coil domains of RAD50 act as a flexible bridge, anchoring exposed DSB ends (Czornak*, et al.* 2008). The third protein, NBS1 (nijmegen breakage syndrome 1), has shown ability to recruit key signalling transducer ataxia-telangiectasia mutated (ATM) to the site of a double strand break (Falck *et al.* 2005). The combined role of the MRN complex is to bind broken DNA ends, keep ends in close contact, process them to allow for rejoining and signal to activate DNA repair and cell cycle arrest.

Ataxia telangiectasia (AT) is an autosomal recessive disease in humans, patients homozygous for mutations in ataxia-telangiectasia mutated (*ATM*) display sensitivity to ionizing radiation and predisposition to cancer (Savitsky *et al.* 1995). This gene has since shown to encode for a crucial transducer of signalling responses to DNA damage (Zhou *et al.* 2006). ATM was initially shown to sequester within unstressed cells as a dimer; in the event of DNA damage, ATM was shown to autophosphorylate on ser1981 causing dissociation and allowing subsequent activation of downstream targets (Bakkenist and Kastan 2003). Lee & Paull (2005) first provided evidence for MRN complex in the

recruitment of ATM to DSBs; MRN was suggested to bind exposed DNA, recruit ATM and cause ATM dimer dissociation leading to its subsequent activation. ATM has however shown to amplify DNA damage signalling in addition to acting on targets that conduct DNA repair, this is mediated through phosphorylation of H2A histone variant H2AX (Burma *et al.* 2001). By phosphorylating H2AX at sites proximal to the DSB, adaptor protein MDC1 is recruited and binds forming γH2AX foci (Stucki and Jackson 2006). This interaction creates a "landing platform" enabling more ATM molecules to bind and therefore further amplifies the DNA damage response. This damage recognition system has however recently found to be more complex than initially thought.

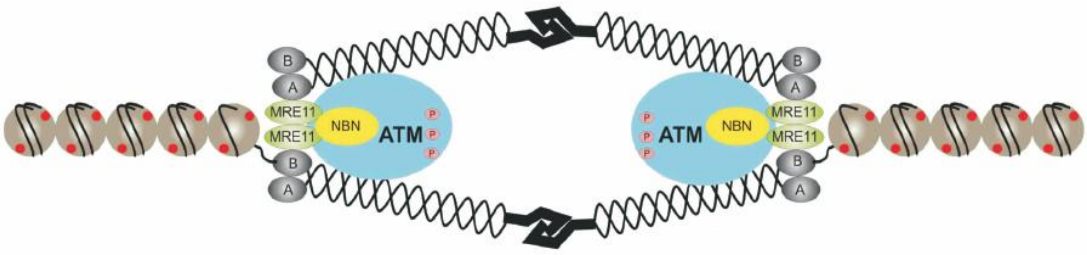

Figure 1.4. Localisation of the MRN complex to sites of DSBs
Generation of a double stranded DNA break (DSB) is known to be perceived by the MRN complex, the primary sensor of DNA damage. The MRN complex is proposed to activate downstream responses which include DNA repair, cell cycle arrest and cell death (in extreme circumstances). Components of the MRN complex act to bridge the gap between broken ends, resect them to enable religation and signal to downstream transducers. (Image source: Czornak 2008)

In addition to formation of γH2AX foci, ubiquitination has more recently been discovered to also play a role in activation of downstream DNA repair. Ubiquitination is primarily used in targeting of proteins for degradation, attachment of single or polyubiquitin chains acts to label proteins for proteolysis by the proteosome (Hochstrasser 1996). This process has however been shown not to function solely in protein degradation but also in regulatory signals in many molecular pathways (Panier and Durocher 2009). A model has been proposed to act after MDC1 binding in ubiquitination of H2A-type histones. Activated MDC1 is recognised by RNF8, an E3 ubiquitin ligase (Marteijn *et al.* 2009). RNF8 in conjunction with UBC13 attaches Ubiquitin to chromatin surrounding the site of a DSB. RNF168 further acts to amplify ubiquitination on

H2A amplifying the signal (Doil *et al.* 2009). A heterodimer consisting of breast cancer associated gene 1 (BRCA1) and BRCA1-associated ring domain protein 1 (BARD1) is then recruited to the DSB through interaction with adaptor proteins which recognise and bind these Ub modifications (Panier and Durocher 2009). This heterodimer showed E3 ligase ability implicating a role in amplifying ubiquitin signalling at break sites. BRCA1 also has many downstream targets including interactions with DNA repair mechanisms and cell cycle arrest (Deng 2006, Deng and Wang 2003).

ATR (ATM & Rad3-related) is another key DNA damage signalling kinase closely related to *ATM* (Zhou and Elledge 2000). Activation of these related proteins has however shown to be very different. As mentioned, ATM is activated in response to DSBs through the MRN complex; this contrasts to ATR, which has been shown to respond directly to replication stress (Ward *et al.* 2004). It has been observed that replication binding protein A (RPA) is involved in DNA replication and binds to ssDNA at the replication fork (Dutta and Stillman 1992). In the event of fork stalling, ATR interacting protein (ATRIP) mediates recruitment of ATR through RPA binding (Niida and Nakanishi 2006). Activation of *ATR* leads to overlapping functions in cell cycle arrest by activating CHK1 (Bucher and Britten 2008). Mammalian studies have therefore revealed ATM and ATR proteins as key signalling transducers of DNA damage.

Recognition of DSBs by the MRN complex is a well established model in animals, the presence of a related complex in plants is however not certain. Homologous genes are present for each component of the MRN complex in the *Arabidopsis* genome. Both *AtMRE11* and *AtRAD50* homozygous mutants display increased sensitivity to DNA damage along with defects in fertility (Bundock and Hooykaas 2002, Gallego *et al.* 2001). The NBS1 homolog has also shown to interact with MRE11 in yeast two-hybrid experiments, *nbs1-1* however showed no difference in response to UV or X-ray irradiation compared to wild type or any defects in fertility (Waterworth *et al.* 2007). The role of these genes in plant-

mediated perception of DSBs is therefore not confirmed, although likely due to sequence homology with mammalian counterparts.

BRCA1 and BARD1 proteins that are recruited to DSBs through interactions with Ub are also present within the *Arabidopsis* genome. Lafarge and Montané (2003) first identified the *AtBRCA1* gene and showed its expression was strongly induced after treatment with γ-rays. The *AtBARD1* gene was also identified in a later paper by Reidt *et al.* (2006) which showed AtBRCA1 binding and sensitivity to mitomycin C. AtBARD1 has more recently shown to exhibit additional roles in the maintenance and organization of the shoot apical meristem (Han *et al.* 2008). Mutant allele's *bard1-1* and *bard1-2* used by Reidt *et al.* (2006) were shown to display residual AtBARD1 activity compared to the fully null *bard1-3* allele. The newly characterised *bard1-3* mutant was found to contain an enlarged *WUSCHEL* expression domain suggesting a role in the repression of WUS activity. AtBARD1 was subsequently shown to form a protein-DNA complex on the WUS promoter and interact with the SYD chromatin remodelling complex. This is thought to repress *WUS* transcription through inhibition of chromatin remodelling essential for *WUS* expression. Ubiquitin dependent DSB signalling remains unstudied in plants; presence of these orthologous genes however suggests a role for *AtBRCA1* and *AtBARD1* in DNA damage signalling.

In addition to MRN components, homologous *ATM* and *ATR* genes have also been identified. *ATM* mutants have shown to be sensitive to DNA damage and to display partial sterility (Garcia *et al.* 2003, Garcia *et al.* 2000). The *AtATR* mutant showed sensitivity to replication blocking agents hydroxyurea and UV irradiation (Culligan *et al.* 2004). *Arabidopsis ATRIP* has also shown sensitivity to replication blocking drugs (Sweeney *et al.* 2009). As described earlier in this chapter, ATM activation leads to phosphorylation of histone variant H2AX which acts to amplify the signalling response. This process has also shown to occur in *Arabidopsis*, a paper by Friesner *et al.* (2005) showed γ-H2AX phosphorylation

after exposure to IR using a plant specific antibody. This phosphorylation was found to be defective in the *atm* mutant but not *atr*. It also appears the roles for ATM and ATR are conserved between animals and plants, little is known about which downstream targets they activate in plants.

Events controlling activation of DNA damage responses therefore are dependent on initiation of key signalling transducers ATM and ATR. Upon activation, ATM and ATR trigger downstream amplification of signalling through H2AX phosphorylation and ubiquitination dependent on RNF8 and BRCA1/BARD1. In addition, many other proteins act downstream of ATM and ATR to mediate DNA repair and cell cycle arrest including BRCA1 and p53 (Deng 2006). This review will focus on each of these aspects beginning with DNA repair.

1.3. Mammalian DNA repair pathways

1.3.1. How does the cell repair a double strand DNA break?

Two pathways have been described in animal studies that act to rejoin double stranded DNA breaks; non homologous end joining (NHEJ) and homologous recombination (HR) (Pardo *et al.* 2009). These pathways are separated by the requirement for a homologous template which is used to accurately repair broken DNA ends. The NHEJ pathway is able to re-ligate broken DNA simply by processing exposed ends of a DSB and rejoining (Jackson 2002). This resection is mediated by the MRE11 component of the MRN complex (Paull and Gellert 1998). This contrasts to HR which uses a homologous template to repair DNA breaks based on sequence homology (Longhese *et al.* 2006). DNA replication proteins then act to amplify this region resulting in an accurate repair of the break. As this mechanism requires the homologous sequence such as a sister

chromatid, it is only active during late S-G2 phases of the cell cycle (Bernstein and Rothstein 2009). NHEJ by comparison is able to act at all times due to its ability to function without a homologous template, NHEJ is known to compete for DSBs even when a homologous sequence is present (Shrivastav *et al.* 2008). NHEJ is therefore the dominant cell cycle pathways by default, it is however relatively inaccurate by comparison. Processing of DSB ends to permit religation can introduce small deletions that could inflict a mutation which could potentially impact gene function (Hakem 2008). It has been shown that cell cycle stage is a major factor in the decision of which pathway is activated. CDK activity has shown to block HR by phosphorylating BRCA2, which activates HR proteins downstream of DNA damage (Esashi *et al.* 2005). Both pathways are therefore activated under optimum conditions by which they repair DNA, both share a common initiator through the MRN complex.

The initial step of NHEJ activation occurs through binding of the KU heterodimer to DSB ends processed by the MRN complex. KU70 and KU80 join and are loaded onto DNA ends to prevent further processing and acts to protect ends (Ramsden and Gellert 1998). DNA-dependent kinase catalytic subunit (DNA-PKcs) is recruited by KU heterodimer to the site of a DSB through a highly conserved C-terminal motif (Falck*, et al.* 2005). The DNA-PK holoenzyme is then involved in downstream recruitment of XRCC4/LIGIV which acts to re-ligate broken DNA ends previously anchored by MRN (Chen *et al.* 2000).

HR processes differ due to the requirement for greater nuclease dependent processing of DSB ends to create sufficient overhangs for recognition of homologous sequences. A review by Bernstein and Rothstein (2009) highlights each step of HR in detail. The MRN complex performs initial resection of the DSB in conjunction with DNA endonuclease SAE2; further progressive processing can also be performed using EXO1 or DNA2 nucleases. After this 5’ resection, exposed single strand ends are bound by RPA in order to protect them from processing by unrelated nucleases. RPA binding enables recruitment of the

RAD52 epistasis group of proteins (RAD52, RAD55, RAD57, RAD59, RAD54, RDH54), which interact with RAD51 to form a nucleofilament complex. This complex is able to recognise homologous sequences and forms Holliday junctions by invading sister chromatids. DNA polymerases then act to replicate over the broken region, upon completion, resolvase proteins such as GEN1 promote Holliday junction resolution resulting in two identical strands of DNA (Ip *et al.* 2008).

1.3.2. Similarities between DNA repair pathways in plants and animals

Plants are known to contain homologous genes for components of NHEJ and HR pathways. However, as with previously mentioned DNA damage sensory proteins, their function is implied from sequence homology with mammalian genes. For example, *Arabidopsis* contains NHEJ components *KU70* (Bundock *et al.* 2002), *KU80* (West *et al.* 2002), *XRCC4* (West *et al.* 2000) and *LIGIV* (van Attikum *et al.* 2003); *DNA-PK* is yet to be identified. Mutants of these *Arabidopsis* NHEJ genes have shown sensitivity to DNA damage in each of the cited papers which implies a direct role in DNA repair. Additional functions have also been described for *KU70* and *KU80* in plants. KU proteins have also shown to play an essential role for telomere maintenance, the *ku70* mutant exhibits increased telomere length along with DNA damage sensitivity (Bundock*, et al.* 2002). KU proteins have also been described to suppress formation of T-circles which occur after resolution of T-loops, the structure that forms at telomeres to act in chromosome end protection (Zellinger *et al.* 2007). It is therefore possible that functions of *Arabidopsis* NHEJ candidates are relatively similar compared to their mammalian relatives shown by sensitivity to DNA damage, but it is also possible extra players may contribute to DNA repair in plants.

Arabidopsis has also shown to contain mutants for genes implicated in homologous recombination (HR). The *AtRAD51* homolog was first identified by Li

et al. (2004) and was shown to be essential for meiosis; this paper however did not determine a role in DNA repair. Analysis of three *Arabidopsis RAD51* paralogs *AtRAD51B*, *AtRAD51C* or *AtXRCC2* by Bleuyard *et al.* (2005) showed no sensitivity to γ-rays but to mitomycin C. A later paper by Markmann-Mulisch (2007) showed the survival of the *rad51-1* mutant used by Li *et al.* (2004) mutant was not drastically affected by bleomycin treatment but was after mitomycin C. The *RAD54* homolog has also been identified in *Arabidopsis*; plants overexpressing *AtRAD54* displayed increased resistance to γ-irradiation (Klutstein *et al.* 2008). The role for homologous HR genes is therefore not clear in *Arabidopsis*; these genes may have evolved plant-specific functions removed from mammalian homologs.

1.4. Cell cycle control

1.4.1. Mammalian cell cycle

Cell division in animals consists of two main phases which act to replicate the genome correctly and segregate replicated chromosomes into two individual cells (Vermeulen *et al.* 2003). Synthesis (S) phase ensures DNA is replicated successfully; Metaphase (M) then acts to separate sister chromatids at the mitotic spindle, pulling them to polar ends of the cell which eventually forms two separate cells through cytokinesis. These two main phases are separated by cell cycle checkpoints which act to monitor progression of each phase, only allowing continuation after successful completion (Bucher and Britten 2008). The G1 checkpoint functions between the M-S phase transition and ensures correct conditions for DNA synthesis. The G2 checkpoint monitors accuracy of DNA replication in late S phase before entering into mitosis. Cells can also enter a state of quiescence by entering G0 just after M phase, in G0 phase the cell is not

cycling (Vermeulen*, et al.* 2003). This whole process is driven by a series of protein-protein interactions between cyclin dependent kinases (CDKs) and cyclins which govern progression into each phase.

Cyclin dependent kinases (CDKs) are key activators in cell cycle progression. Numerous components are involved in controlling their activity; their phosphorylation leads to activation of downstream cell cycle processes (De Veylder *et al.* 2007). The dynamics of cell cycle progression in animals and the role of CDKs are reviewed in detail by Vermeulen *et al.* (2003). Different CDKs are known to function in permitting entry into each stage of the cell cycle, three CDKs in G1 (CDK4, CDK6 and CDK2), CDK2 in S phase and CDK1 in M phase. Levels of CDKs remain at a steady state during the cell cycle; their activity is induced through binding of cyclins whose levels rise and fall during cell cycle progression. Stimulation from growth factors induces transcription of D-type cyclins which bind to CDK6 and CDK4 are essential for G1 entry, Cyclin E is then required to bind CDK2 for S phase entry. Cyclin A binds CDK2 to promote continuation through S phase. Entry into M phase at the late G2 checkpoint involved CDK1/cyclin A interaction, M phase progression is then mediated by CDK1/Cyclin B.

1.4.2. Plant cell cycle

In a similar mechanism to animals and in fact all eukaryotes, cell divisions in plants are controlled by CDK/cyclins interactions. The G1 and G2 checkpoints were first established in plants through experiments with sucrose starvation (Hof 1966). Using ^{3}H-thymidine incorporation, cell division was studied in sucrose limiting conditions, and was found to arrest in either G1 or G2 suggesting presence of checkpoints. This highlighted what appears to be a similar mechanism for cell cycle progression with plants exhibiting G1-S-G2-M phases of the cell cycle.

CDKs are also present in plants; seven classes (A-G) have been identified. Out of these seven, classes A, B, D, and F have been implicated in controlling the plant cell cycle, the remaining classes have shown possible roles outside of cell cycle control (Francis 2007). Identification of CDKs in plants has been mainly through homology with the PSTAIRE motif found in mammalian CDKs which mediates the interaction between CDKs and cyclins (Porceddu *et al.* 2001). *Arabidopsis* CDKA;1 has been found to carry this motif and is indeed important for regulation of the plant cell cycle (De Schutter *et al.* 2007). Generation of a dominant negative *Arabidopsis* CDKA;1 and subsequent overexpression within *BY-2* cells showed clear inhibition of cell cycle progression (Joubes *et al.* 2004). The dominant negative protein was thought to inhibit cell cycle by competitively binding cyclins but not initiating cell cycle progression. Plant specific B-type CDKs also contain motifs very similar to PSTAIRE described in A-type CDKs (Inze and De Veylder 2006). B-type CDKs are divided into type 1 and type 2 categories containing PPTALRE and PPTTLRE motifs respectively (Inze 2005). Dominant negative expression of *Arabidopsis* B-type CDK CDC2b in *BY-2* cells demonstrated a role in G2-M phase progression (Porceddu*, et al.* 2001). Little is known about the function of remaining CDK classes found in *Arabidopsis*. CDKD and CDKF have shown CDK-activating kinase (CAK) activity, CDKD requiring binding to cyclin H to regulate this function (Umeda *et al.* 2005). The role of CDKs in controlling progression through the cell cycle therefore appears to be relatively similar between plants and animals.

A similar role for cyclins in plants is also well established, clear differences however exist between plants and animals. *Arabidopsis* is known to contain approximately 32 cyclin genes; significantly more than described in other organisms (Inze 2005). This is divided up into 10 A-type, 11 B-type, 10 D-type, and 1 H-type cyclins (Inze and De Veylder 2006). D-type cyclins are thought to regulate the G1-S phase transition, A-type in S-M regulation and B-type in G2-M phase transition (Francis 2007). Evidence for the role of D-type

cyclins in plants show CYCD4;1 is found to activate CDKB2;1 at G2-M *in vitro* (Kono *et al.* 2003). It is however uncertain why so many classes of cyclins exist in plants. This maybe due to the flexibility of plants to respond to developmental and environmental cues, meaning these extra cyclins could act in more complex CDK interactions to control the cell cycle (Inze and De Veylder 2006).

1.4.3. DNA damage induced cell cycle control in animals and plants

Studies into cell cycle regulators in animals and plants show very similar mechanisms for pushing the cell through synthesis and mitosis stages. In the event of DNA damage, the cell cycle needs to stall allowing sufficient time for repair processes to be completed (Bucher and Britten 2008). Mechanisms of blocking CDK activity exist downstream of DNA damage signalling transducers to prevent interaction of CDKs and cyclins, these mechanisms are known as checkpoints.

A checkpoint can be classically defined as "a biochemical pathway that ensures dependence of one process upon another process that is otherwise biochemically unrelated" (Elledge 1996). Early work by Weinert & Hartwell (1988) first revealed the genetic basis of DNA damage checkpoints through work in *Saccharomyces cerevisiae*. The radiation sensitive mutant *rad9* was found to be defective in the activation of a G2 cell cycle arrest in response to x-ray irradiation. This placed *RAD9* in a pathway which acts downstream of DNA damage to control progression into S phase. Checkpoints are however not limited to DNA damage responses and can act to ensure integrity of other cellular processes. One example is the spindle checkpoint which monitors correct interactions between chromosomes and microtubules during formation of the mitotic spindle. Unsuccessful attachment of microtubules to kinetochores results in activation of the spindle checkpoint and delays the onset of anaphase (Musacchio and Hardwick 2002).

The G2-M phase cell cycle checkpoint is very well studied in animals. Upon DNA damage, MRN complex recruits ATM, which acts on downstream targets to allow arrest. ATR is also known to be recruited to sites of a DSB through interaction with RPA which binds to exposed ssDNA at break sites (Garcia-Muse and Boulton 2005). Direct targets of ATM and ATR are the checkpoint kinases 1 & 2 (CHK1 & 2), which are key in controlling cell cycle arrest (Bucher and Britten 2008). These kinases primarily act to phosphorylate CDC25, a dual specificity phosphatase that release CDKs from inhibitory phosphorylation (Karlsson-Rosenthal and Millar 2006). CDK phosphorylation is an important regulatory feature of CDK-cyclin binding; this phosphorylation can prevent binding of CDKs and cyclins preventing cell cycle progression. Inhibition of CDC25 arrests the cell cycle by preventing removal of inhibitory phosphates. In addition, WEE1 kinase can inhibit cell cycle progression by phosphorylating CDKs. CDC25 and WEE1 can therefore act as a switch regulating cell cycle progression downstream of DNA damage. *Arabidopsis* is known to lack CHK1 and CHK2 kinases (Cools and De Veylder 2009); also a functional CDC25 is yet to be identified (Dissmeyer *et al.* 2009). A *WEE1* homolog has been characterised and mediates *in vitro* phosphorylation of CDKA1;1 in *Arabidopsis* (De Schutter*, et al.* 2007). Further studies have suggested that phosphorylation of the CDKA;1 p-loop to be unimportant in DNA damage induced cell cycle arrest making WEE1 function irrelevant (Dissmeyer*, et al.* 2009). This does not however exclude the possibility that WEE1 functions to phosphorylate other CDKs other than CDKA;1 to arrest the cell cycle including the plant specific B-type CDKs.

Transition from G2-M phase and G1-S phase is possible through activation of checkpoint kinases (Bucher and Britten 2008); the retinoblastoma protein (pRB) is also able to regulate G1-S phase progression through binding of E2F proteins. The E2F family of transcription factors comprises of around 7 members (E2F1-E2F7) that requires association with DP proteins (DP1 and DP2) to function in activating downstream targets (Bracken *et al.* 2004). E2F family

members are repressed through binding of the retinoblastoma protein (pRB), in order to prevent cell proliferation. Under normal conditions, CDK4/cyclin D levels rise in G1, activated CDK4 phosphorylates pRB which releases E2F proteins from their inhibitory hold. E2F transcription factors are then free to permit entry into the next phase of the cell cycle through promoting transcription of target genes. Under stress conditions, the p53 protein acts downstream of ATM to block CDK4/cyclin D through activation of p21, a known CDK inhibitor (Child and Mann 2006). As no CDK4/cyclin D binding occurs, pRB is not phosphorylated and E2F proteins remain repressed and cell cycle arrests.

Arabidopsis also appears to contain a similar mechanism for mediating G1-S phase arrest. Three homologous E2F proteins have been identified (E2Fa, E2Fb and E2Fc) and two DPa proteins (DPa, DPb) (Francis 2007). The pRB protein has also been described in *Arabidopsis* to play a role in stem cell regulation, influencing stem cell division and differentiation (Wildwater *et al.* 2005). Retinoblastoma was found to bind E2F in tobacco, expression of cyclin D was found to overcome this repression activity (Uemukai *et al.* 2005). This interaction indicates a similar mechanism related to the mammalian pathway as cyclins are known to release pRB from its inhibitory hold on E2F proteins in animals. There is however a well documented lack of a p53 homologous gene within the *Arabidopsis* genome, which acts to induce expression of CDK inhibitor p21. The KRP family of proteins in *Arabidopsis* have been suggested to act as CDK inhibitors similar to p21 (De Veylder *et al.* 2001). Similarities between E2F-pRB induced cell cycle arrest do therefore seem to exist between animals and plants.

1.5. Programmed cell death (PCD) mechanisms in animals and plants

1.5.1. Apoptosis

Apoptosis is the prevalent mechanism of programmed cell death (PCD) in animals; its activation results in effective cell degradation (Bao and Shi 2007). Initiation of machinery involved in the apoptotic response can ensure cells are efficiently dismantled from within, which limits disruption to surrounding cells (Taylor *et al.* 2008). Broken down cellular organelles are absorbed into neighbouring cells through phagocytosis allowing recycling of these components. Certain cellular characteristics are exhibited by dying cells undergoing apoptosis; this includes condensation and fragmentation of the nucleus and formation of apoptotic bodies which are engulfed by adjacent cells (Elmore 2007). Activation of apoptosis involves a highly organised signalling pathway which requires intra and extracellular signals to initiate cell death.

Extrinsic activation of apoptosis is dependent on membrane bound receptors to trigger downstream signalling after binding their respective ligands. Many receptor and ligand partners have been observed to initiate apoptosis, the best characterised however are FasL/FasR and TNF-*α*/TNFR1 models (Elmore 2007). This signalling process is described by Wajant (2002); a trimeric complex of TNF/FAS receptors is able to form in the plasma membrane in the absence of a ligand. Interaction with the TNF/Fas ligand forms the death-inducing complex (DISC), which acts to recruit fas-associated death domain protein (FADD) to its intracellular death domain (Chinnaiyan *et al.* 1995). Chinnaiyan *et al.* (1995) showed this interaction was essential for initiation of apoptosis and overexpression of FADD was found to initiate apoptosis in a Fas ligand independent manner. FADD then functions to activate downstream activation of apoptosis specific molecules known as caspases (Cysteine-rich aspartate proteases) which act to break down cellular components.

The intrinsic pathway in comparison is activated by a diverse range of cellular stresses including DNA damage (Taylor*, et al.* 2008). Growth factor suppression, misfolded proteins and DNA damage signalling pathways are known to interact with members of the B-cell lymphoma-2 (BCL-2) family of proteins essential for regulation of apoptosis (Danial 2007). This family is characterised by the presence of BCL-2 homology (BH) domains involved in protein-protein interactions. The BCL-2 family is composed of 3 main groups including anti-apoptotic, pro-apoptotic and BH3-only proteins. Anti-apoptotic such as BCL-2 and BCL-XL bind to pro-apoptotic BCL-2 family members through BH domains, inhibiting their function (Gustafsson and Gottlieb 2007). BH3-only proteins are pro-apoptotic and comprise of 8 members, 3 of these (NOXA, PUMA & BID) are upregulated by p53 in the DNA damage response (Taylor*, et al.* 2008). BH-3-only proteins are then able to activate pro-apoptotic BAX and BAK which act in apoptosis (Gustafsson and Gottlieb 2007). This inhibitory protein-protein binding of BCL-2 family members affects the abundance of functional protein. In the event of cell death activation, higher levels of pro-apoptosis BCL-2 homologues will tip the balance and trigger cell death (Danial 2007). This family is known to regulate release of cytochrome-c from the mitochondria which is forms a complex known as the apoptosome essential in apoptosis activation (Taylor*, et al.* 2008). This regulation is mediated by either forming or blocking channels within the mitochondrial membrane.

The apoptosome is a multimeric complex formed from cytochrome-c, APAF-1 and ATP (Bao and Shi 2007). Cytochrome C and Procaspase-9 are released from the mitochondria due to actions of BCL-2 proteins. Cytosolic protein APAF-1 senses release of cytochrome C which oligomerises to form the wheel-shaped apoptosome, a process dependent on presence of dATP/ATP (Riedl and Salvesen 2007). Formation of the apoptosome is reviewed by Riedl & Salvesen (2007) and summarised in figure 1.5., In the absence of cytochrome C, APAF-1 is kept in an inactive monomeric state through its WD40 domains

which cause the protein to fold back on itself. Release of cytochrome C from the mitochondria is detected by APAF-1, cytochrome C binds to WD40 domains which opens into its uninhibited form. This molecule is then able to oligomerise to form the circular apoptosome. Activation of caspases is then mediated by the caspase-recruitment domain (CARD) at the centre of the apoptosome.

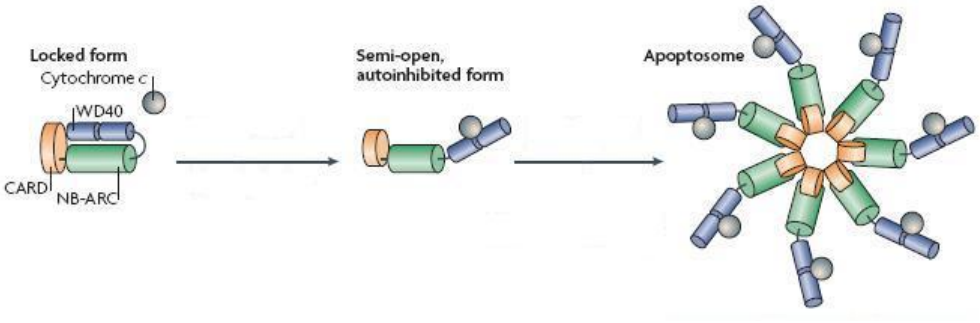

Figure 1.5. Formation of the mammalian apoptosome
The apoptosome is a crucial component of the intrinsic apoptosis pathway. Excessive cellular stress activates pro-apoptotic BCL-2 proteins which mediate release of cytochrome C from the mitochondria. Cytosolic APAF-1, which is kept in an inactive "locked" form, recognises cytochrome C which enables in to open into its uninhibited form. APAF-1 is then able to oligomerise to form the wheel shaped apoptosome, this is dependent on dATP/ATP. The apoptosome is then able to activate caspase activity through CARD domains present within Apaf-1. (Image adapted from review by Riedl & Salvesen 2007).

Cysteine-rich aspartate proteases, or caspases as they are commonly known, are specific to apoptotic cell death. Proteolytic activity of caspases is known to target structural components of the cell in order to break down the cell efficiently. These include the cytoskeleton, nuclear envelope and cell-cell adhesion sites (Taylor*, et al.* 2008). Caspases are retained within the cell as inactive precursors known as a zymogen, proteolytic processing of the zymogen forms the active protease (Kumar 2007). This processing is mediated by other caspases, activation of apoptosis leads to a cascade of proteolytic activity of zymogens. This cascade however has to start with a specific type of known as the initiator caspases, in mammals these include caspase-2, 8, 9 and 10 (Creagh *et al.* 2003). These caspases are initiated through either extracellular signals (Fas/TNF) or the intracellular apoptosome as mentioned above. Activation of these initiator caspases leads to proteolytic processing of effector caspases

(caspase 3, 6, and 7) which then function in breaking down of organelles (Creagh*, et al.* 2003).

1.5.2. Autophagy

Autophagy is another common pathway of cell death in animals; this form of PCD involves sequestering large segments of cytoplasm into membrane bound vesicles which are degraded within the lysosome (Klionsky 2007). These autophagic vesicles are referred to as the autophagosome, which fuses with the lysosome to form the autolysosome where cellular components are digested (Kroemer and Levine 2008). Two pathways of autophagy exist; Micro and macro autophagy. These pathways differ simply due to the extent of degradation; macro-autophagy involves sequestering larger portions of the cytoplasm (van Doorn and Woltering 2005). The actions of these pathways are however not specific to programmed cell death. During nutrient limiting conditions autophagy acts in cell survival by reducing the cells need for resources (Bassham 2007).

Formation of the autophagosome is essential for the initiation of autophagy; this process is controlled by the autophagy-related (*ATG*) genes. This family of around 30 members is able to form membrane bound vesicles through connecting with themselves and membrane lipids. This is known to occur through a similar process by which ubiquitin is attached to proteins targeted for proteolysis; ubiquitin (Ub) is activated by an E1 enzyme which transfers it to an E2 conjugating enzyme. An E3 ubiquitin ligase then recognises the target protein and mediates transfer of Ub from the E2 enzyme (Hochstrasser 1996). Conjugation of ATG proteins occurs in a similar way; function of ATG proteins is therefore compared to activities of E1, E2 and E3 enzymes. In this system, two ubiquitination-like pathways are known to exist in conjugating ATG proteins as reviewed by Geng and Klionsky (2008); ATG12-ATG5 and ATG8-PE (phosphatidylethanolamine, a membrane lipid). The first one

designates ATG12 as an ubiquitin-like (Ubl) protein, ATG7 acts as an E1 like enzyme attaching ATG12 to E2-like enzyme ATG10. There is no E3 like enzyme in this pathway; ATG5 and ATG16 bind ATG12 to form a multimeric complex. The second pathway, ATG8-PE, involves binding to the PE membrane lipid. In this process, Ubl protein ATG8 is transferred to ATG3 (E2-like) via ATG7 (E1-like). ATG8 is then attached to PE through E3-like activity of ATG12-ATG5. Conjugates of these two pathways act together in *de novo* synthesis of double membrane bound vesicles, ATG proteins then dissociate from the autophagosome upon completion.

1.5.3. Necrosis

Necrosis was originally described as an accidental form of cell death arising through exposure to extreme stresses (Reape *et al.* 2008). Morphological traits of necrosis are very different to apoptosis and autophagy, the primary observation is that cells swell and burst in an uncontrolled manner (Proskuryakov *et al.* 2003). It has however been shown that similar molecular pathways act to induce necrotic cell death without activating caspases. Fas, which acts as an extracellular trigger of apoptosis, has been shown to activate necrosis independently of caspases (Holler *et al.* 2000). Additionally, poly(ADP-ribose) polymerase (*PARP*) genes have been shown to activate necrotic death after DNA damage. PARPs function in the recognition of DSBs and can activate downstream processes through attaching chains of ADP-ribose to DNA damage effectors (Heeres and Hergenrother 2007). These chains of ADP-Ribose are produced from NAD+, 3 to 5 molecules of ATP are however required for synthesis of each molecule of NAD+ (De Block *et al.* 2005). Excessive DNA damage can therefore induce necrosis by depleting ATP causing metabolic stress.

1.5.4. Cell death pathways in plants

Little is known about molecular pathways that regulate cell death mechanisms in plants. These pathways are harder to define in plants due to physiological differences between animal and plant cells. One obvious difference is the presence of a cell wall; this prevents the defining feature of mammalian apoptosis, phagocytosis by neighbouring cells. As mentioned earlier, plants also lack key executioners of apoptosis including p53 and caspases (Bonneau *et al.* 2008, Cools and De Veylder 2009). Despite these differences, plants share common genes which mediate similar mechanisms of cell death.

Studies have reported the apparent lack of orthologous caspase sequences within the *Arabidopsis* genome; the metacaspase family of proteases present in plants have however been suggested to be functionally related to animal caspases (He *et al.* 2008). This began with the cloning of two metacaspases in *Arabidopsis*, AtMC4 and AtMC9 which were shown to be arginine/lysine proteases (Vercammen *et al.* 2004). They were however not shown to cleave known caspase substrates as identified by mammalian studies. Identification of another metacaspase gene, *AtMC8*, was shown to be up regulated after oxidative stress and mutants displayed reduced sensitivity to DNA damage (He*, et al.* 2008). This metacaspase was however also shown to not cleave known caspase substrates. The role of these proteases is therefore not clear in regulating an apoptosis-like mechanism in *Arabidopsis*. Their expression does however seem to correlate with cell death (He*, et al.* 2008).

Evidence for autophagy is *Arabidopsis* is more convincing, homologous ATG genes have been shown to play an essential role in plant autophagic processes. Evidence for autophagosome formation has been shown after treatment with the E-64 protease inhibitor, electron micrographs show clear formation of autophagic vesicles (Inoue *et al.* 2006). Homologous genes have been identified for many ATG genes including *ATG5* and *ATG7*, mutants for these

genes displayed increased sensitivity to nutrient limiting conditions and lack of vesicle formation after concanamycin A treatment (Thompson *et al.* 2005). Autophagy has also been linked to plant cell death, *ATG* mutants were shown to be defective in the hypersensitive response which initiated cell death surrounding sites of pathogen infection (Hofius *et al.* 2009). A clearer role for autophagy in plants is therefore better established than apoptosis-like mechanisms. It is possible that plants utilise autophagy as a primary mechanisms for cell death instead of apoptosis.

PARP genes have also been isolated within the *Arabidopsis* genome. Doucet-Chabeaud *et al.* (2001) characterised *PARP-1* and *PARP-2* in *Arabidopsis* and showed their expression was upregulated after exposure to ionizing radiation. A link between PARP activity and necrosis in plants is still yet to be established. Analysis of homologous cell death genes and similar cell morphology has therefore hinted at similarities between plants and animals, but little is understood about these pathways, specifically after DNA damage as cell death is not a characterised response to DNA damage in plants.

1.6. Objectives

Plant meristems are essential for growth of aerial structures and the root system in *Arabidopsis*. These stem cell populations act throughout the lifetime of the plant to mediate postembryonic growth and establish the germline. Studying how meristems respond to potentially harmful environmental conditions is important to understand how plants cope during development and growth.

The aim of this PhD project was to investigate responses to DNA damage specifically within Arabidopsis root and shoot meristems. To test this, plants were treated with various drugs that mimic DNA damage induced by ROS including bleomycin and Zeocin. Using mostly confocal imaging techniques and

mutants affected in responses to DNA damage, I then aimed to directly monitor responses within root and shoot meristems.

Chapter 2 – Effects of DNA damage on the *Arabidopsis* root meristem

2.1. Introduction

Plants grow and form new organs throughout their life cycle, all organs are created postembryonically from pluripotent stem cells present within the shoot and root meristems (Tucker and Laux 2007). In the *Arabidopsis* root meristem, these cells are known as the root initials, which surround the mitotically inactive quiescent centre (QC) (Hardtke 2006). The QC comprises a group of 3-4 cells undergoing long mitotic cycles (Dolan*, et al.* 1993, Fujie *et al.* 1993) that release signals to adjacent cells preventing their differentiation (van den Berg*, et al.* 1997). The presence of an organiser in the shoot also specifies stem cell identity (Sablowski 2007); similarities between stem cell maintenance in shoot and root meristems are discussed in Chapter 1. In addition to this function as an 'organiser' of cellular pattern, it has been suggested that the QC could act as a stem cell reservoir which divides to replace damaged initials (Ivanov 2007, van den Berg*, et al.* 1997)

The presence and function of the QC was addressed in early experiments with *Zea mays*. The QC and initials were identified as slowly dividing cells through experiments showing incorporation of tritium-labelled thymidine into mitotic cells (Clowes 1961). Cells of the *Zea* QC rarely incorporated labelled thymidine, root initials were shown to incorporate it at a much lower rate than surrounding meristem cells. Other studies showed that irradiation with x-rays resulted in initiation of QC division and loss of QC identity (Clowes 1959). These experiments were later adapted to *Arabidopsis* where the presence of a quiescent centre and surrounding initials was identified through ^{3}H-thymidine incorporation (Dolan*, et al.* 1993). This was confirmed more accurately by tracking incorporation of BrdU (Fujie*, et al.* 1993). Immunostaining with an anti-

BrdU antibody produced higher resolution images showing organelle DNA synthesis within the QC. These studies showed that central cells always synthesised organelle DNA but rarely nuclear DNA (Fujie*, et al.* 1993).

The nature of plants, being sessile and depending on photosynthesis for energy, means they have no means of escaping harmful genotoxic environmental conditions including UV irradiation, heavy metals, salinity and drought (Bray and West 2005). Genomic instability within stem cell populations of the shoot meristem could negatively impact the fitness of plants in future generations. Also, DNA damage in the root is known to have a detrimental effect on root growth affecting competition for nutrients in the soil (Culligan*, et al.* 2004, Culligan *et al.* 2006). It is therefore possible plants have evolved mechanisms to protect stem cell populations from genetic instability.

It remains unexplored whether DNA damage activates divisions of the QC in *Arabidopsis* and whether this is a mechanism for protecting the population of initials. The experiments described in this chapter were initially designed to address this question, *Arabidopsis* seedlings were treated with radiomimetic drugs and changes to the root meristem were monitored by confocal microscopy. Surprisingly, root initials were selectively killed in response to DNA damage suggesting programmed cell death as a mechanism to eliminate damaged stem cells.

2.2. Results

2.2.1. Root meristem shows disorganisation and loss of QC identity after treatment with the radiomimetic drug bleomycin

To assess DNA damage responses within the root meristem, the radiomimetic drug bleomycin was used to treat *Arabidopsis* roots. Bleomycin causes multiple types of molecular damage by attacking RNA and cell membranes (Burger 1998) but is predominately used to induce double-stranded DNA breaks (DSBs) (Culligan*, et al.* 2006). Bleomycin dependent DSBs are generated through oxidation of the deoxyribose moiety of DNA in the presence of oxygen and a redox-active metal ion e.g. Fe and Co (Liang *et al.* 2002). Because of these DNA damaging properties and wide use in *Arabidopsis*, bleomycin was the first treatment used to monitor meristem responses.

In order to follow cell morphology and QC identity within the meristem, a method of labelling cell outlines was required. The membrane marker 35S:GFP-LTI6B (Cutler *et al.* 2000) has been used previously in experiments to label cell outlines for live imaging (Campilho *et al.* 2006) and lineage analysis (Kurup *et al.* 2005). Seedlings containing the *35S:GFP-LTI6B* membrane marker were transferred to 1 µg/ml bleomycin containing media for 48 hrs, 5 seedlings were imaged by confocal microscopy and the other 5 transferred back to media without bleomycin for 48 hrs (Fig 2.1). The root meristem is usually a well defined structure with clear definition of QC cells and initials, but after 48 hrs of treatment the meristem structure appeared disorganised and contained unusually large cells (Fig 2.1b). Seedlings left to recover for 48 hrs on media without bleomycin showed apparent recovery of meristem structure (Fig 2.1d) although the QC was not clearly identified in either control or treated roots.

Based on experiments by Clowes (1959, 1961), the QC cells were predicted to survive DNA damaging treatments in order to repopulate damaged

initials. To monitor the behaviour of QC cells after bleomycin treatment, seedlings expressing the QC25 GUS marker were treated with 1 µg/ml bleomycin for 12, 24 and 48 hrs (Fig 2.2). 12 and 24hr treatments however show significant reduction in GUS activity within the QC and complete loss of expression after 48 hrs (Fig 2c, 2d). This suggested that one of the consequences of 48 hr exposure of the root meristem to bleomycin was loss of QC identity, which might or might not be followed by cell division.

Figure 2.1. Bleomycin induced disorganisation of root meristem structure

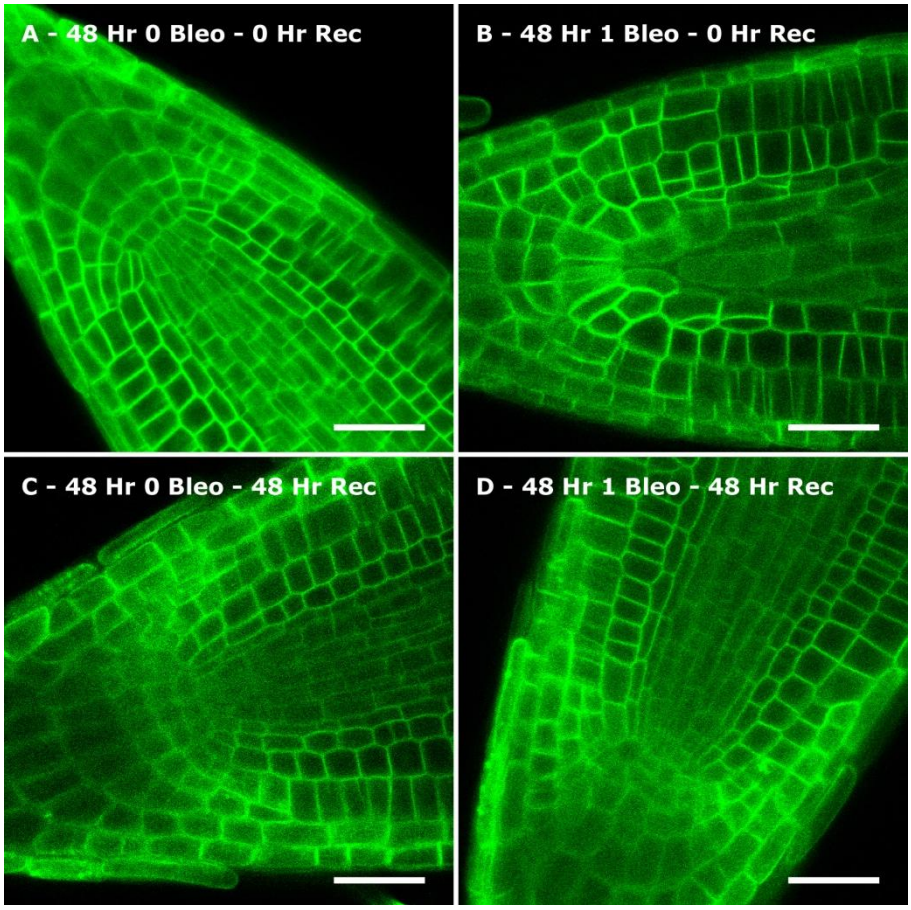

Transgenic 35S:GFP-LTI6B roots show meristem disorganisation after 48 hrs on 1 µg/ml bleomycin containing media. Roots were imaged immediately after treatment (**A** & **B**) and 48 hrs after recovery on media without bleomycin (**C** & **D**). Treated roots showed large disorganised cells after 48 hrs exposure (**B**), however the root appears to recover 48 hrs after treatment (**D**). (Scale Bars: 25 µm).

Figure 2.2. QC localised GUS expression was lost after bleomycin treatment

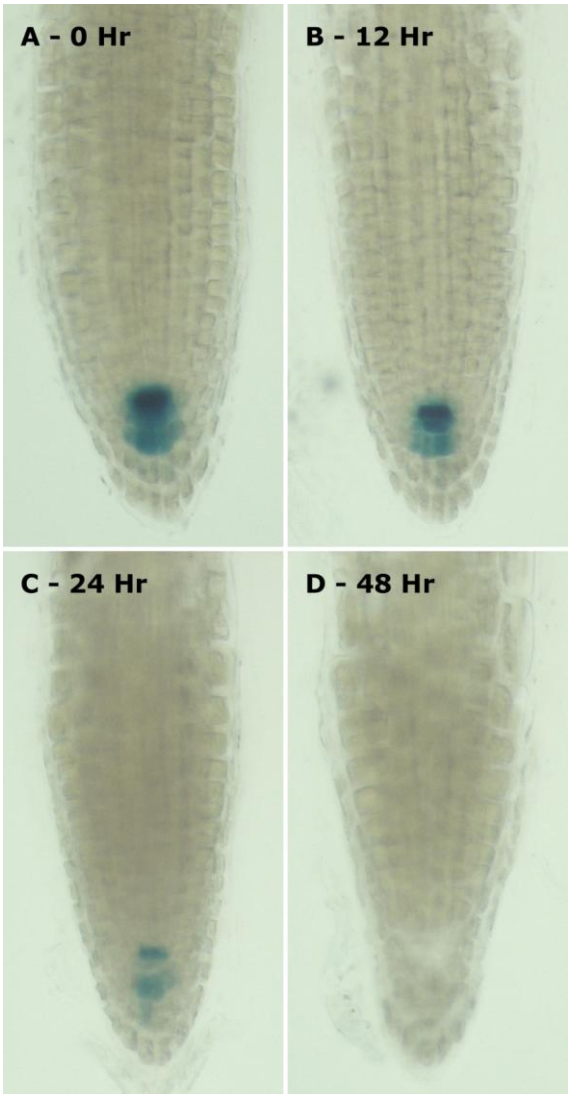

Seedlings expressing the QC marker QC25 showed loss of GUS expression after 48 hr bleomycin treatment. Untreated control seedlings showed QC localised GUS expression (**A**), Seedlings were treated for 12 Hrs (**B**), 24 Hrs (**C**) and 48 Hrs (**D**) on 1 µg/ml bleomycin supplemented media. Significant loss of GUS expression occurred after 24 Hrs (**C** & **D**).

2.2.2. Root initials were selectively killed in response to DNA damage induced by radiomimetic drugs

Auxin flow through the root meristem is known to specify positional information to establish QC identity (Hardtke 2006). As loss of GUS expression was experienced in QC marker lines after bleomycin treatment, investigating auxin flow after DNA damage might explain the disappearance of QC identity. To address how auxin transport is maintained in treated roots, DR5:GFP was used to show auxin levels in the disorganised meristem. DR5:GFP has been used previously to monitor the accumulation of auxin in the root tip (Blilou *et al.* 2005). After treatment for 24 hrs with 1 µg/ml bleomycin, roots were stained with propidium iodide to label cell outlines. Untreated root tips showed a peak of auxin in the QC and root cap cells (Fig 2.3a), roots treated for 24 hrs however showed unexpected cell death specifically within stele and columella root initials (Fig 2.3b). Propidium iodide is a widely used cell membrane stain in plant cells but also as a marker for loss of membrane integrity and cell death (Truernit and Haseloff 2008). Presence of the QC appears to be maintained in these 24 hr treated roots with QC cells still expressing GFP and not saturated with propidium iodide.

To further investigate auxin flow in treated roots we analysed PIN1:GFP expression. PIN proteins are essential in the polar transport of auxin and are used to show direction of auxin flow through the stele cells (Feraru and Friml 2008). High levels of GFP were detected within the stele cells of untreated roots (Fig 2.3c) where GFP expression was largely decreased after bleomycin treatment (Fig 2.3d).

To investigate whether death of root initials was a cell type-specific response to DNA damage that occurred throughout the meristem, the response to DNA damage was monitored using the CYCB1;1:GFP marker (Donnelly *et al.* 1999). In this line, cells stalling before entry into mitosis would be marked with

GFP indicating a likely G2 cell cycle arrest (Culligan*, et al.* 2004). In addition, microarray data on γ-irradiation-induced genes in *Arabidopsis* has shown *CYCB1;1* to be transcriptionally upregulated in response to DNA damage (Culligan*, et al.* 2006). This transcriptional upregulation was dependent on ATM, a key signalling intermediate in the DNA damage response pathway (see chapter 1 for broad review of DNA damage signalling). It is therefore possible CYCB1;1 is unique in plants and may have a dual role in DNA damage response and cell cycle control (Culligan*, et al.* 2006). CYCB1;1:GFP expression was weakly detected in untreated roots (Fig 2.3e) whereas treated roots showed high levels of GFP in cells surrounding the dead initials (Fig 2.3f). This suggests surrounding cells are responding to bleomycin treatment by arresting their cell cycle but not activating cell death.

Figure 2.3. Markers for auxin distribution and cell cycle arrest show cell death of root initials after bleomycin treatment

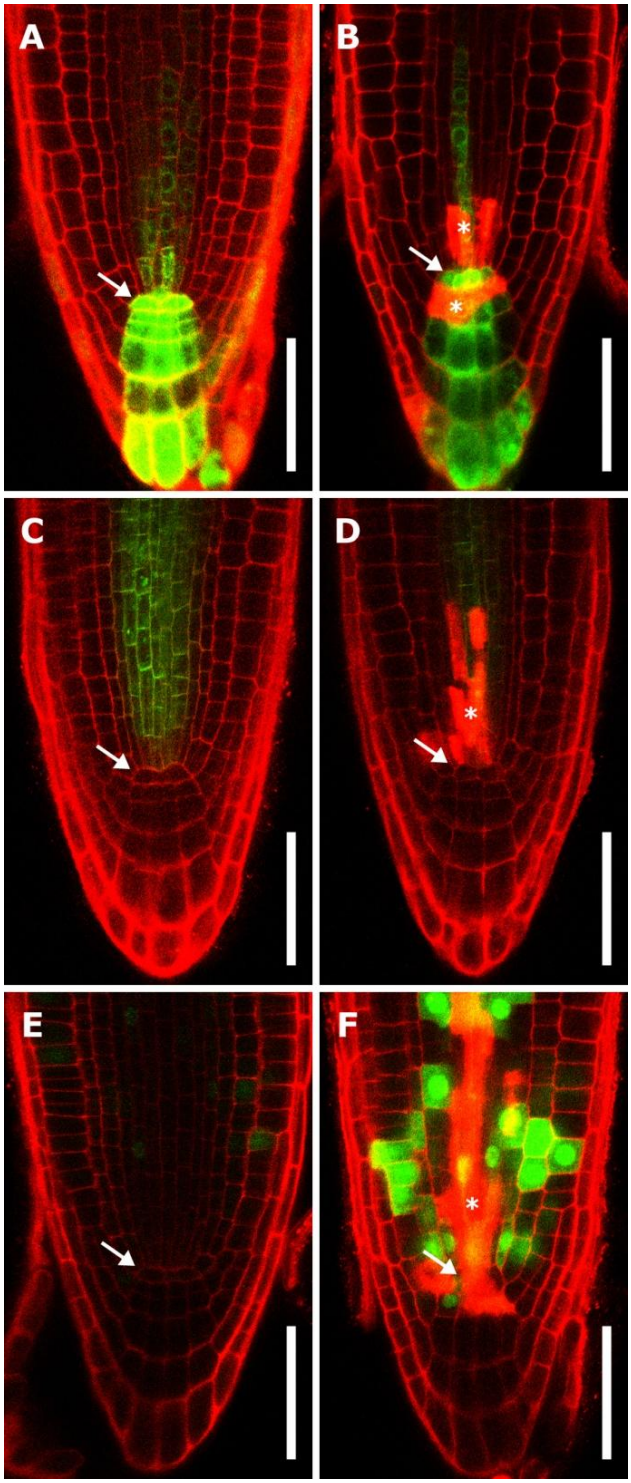

DR5:GFP, PIN1:GFP and CYCB1;1 seedlings treated with 1 µg/ml bleomycin for 24 hrs showed preferential death of root initials. Cell death was marked by propidium iodide which marks outline of living cells but enters dead cells. DR5:GFP untreated control (**A**) and treated (**B**). PIN1:GFP untreated (**C**) and treated (**D**). CYCB1;1:GFP untreated (**E**) and treated (**F**). Arrows and asterisks indicate the QC and dead cells, respectively. (Scale bars: 50 µm).

Because of the limited stability of bleomycin, zeocin was used in subsequent experiments to investigate the specific death of root initials. Zeocin is a member of the bleomycin family and has been previously used to monitor transcriptional activation of WEE1 after induction of DNA damage (De Schutter*, et al.* 2007). Zeocin stocks (Invitrogen) are stable for a longer period of time, are cheaper and are supplied as a prepared solution. I initially treated roots with varying concentrations of zeocin to see if a similar response was obtained as with bleomycin (Fig 2.4). Concentrations of 10 µg/ml resulted in the death of 1-2 root initials (Fig 2.4b) where 20 µg/ml resulted in death of the majority of stele and columella initials. Columella initials were observed to die less frequently than the stele initials. A concentration of 20 µg/ml was deemed ideal for further experiments as it was the lowest concentration able to induce death of the majority of initials whilst allowing QC survival. A higher concentration of 40 µg/ml also showed survival of QC but 60 µg/ml resulted in QC death in the majority of roots. To establish how early the initiation of cell death occurs, roots were treated for 8 and 16 hrs with 20 µg/ml zeocin (Fig 2.6). No cell death of initials was observed after 8 hrs whereas death of a few initials was already detected 16 hrs after treatment.

To further investigate survival of the QC after zeocin treatment, the WOX5:GFP QC specific marker (Sarkar*, et al.* 2007) was treated for 24 hrs with 20 µg/ml zeocin (Fig 2.5). Untreated roots showed very clear GFP expression within QC cells (Fig 2.5a). Treated roots exhibited death of initials and maintenance of GFP expression (Fig 2.5b). Zeocin treatments of CYCB1;1:GFP (Fig 2.5c & d) and DR5:GFP (Fig 2.5e & f) previously treated with bleomycin yielded similar results.

In order to confirm cells saturated by propidium iodide are correctly labelled as dead cells, an alternative cell death marker was required. Sytox orange has been used in other studies as a marker for cell death in *Arabidopsis* roots (Truernit and Haseloff 2008). Sytox was used in conjunction with

fluorescein diacetate to label living cells along with the LTI6B membrane marker (Fig 2.7). Sytox staining confirmed death of root initials, although Sytox appeared to be less sensitive than propidium iodide.

Figure 2.4. Zeocin induced cell death of root initials

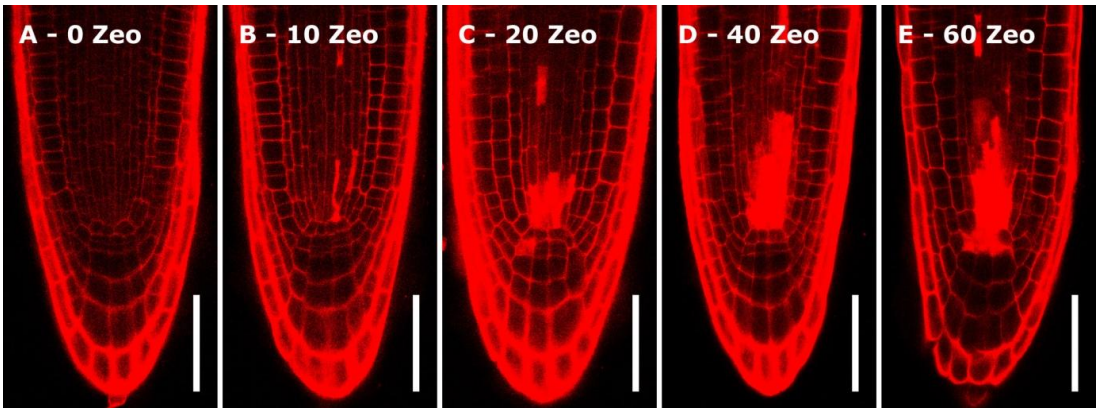

Varying concentrations of bleomycin family member zeocin also induced preferential death of root initials. Roots were treated at a number of concentrations (μg/ml) for 24 hrs on zeocin supplemented plates. (Scale bars: 50 μm).

Figure 2.5. Expression of QC marker WOX5:GFP is maintained after zeocin treatment

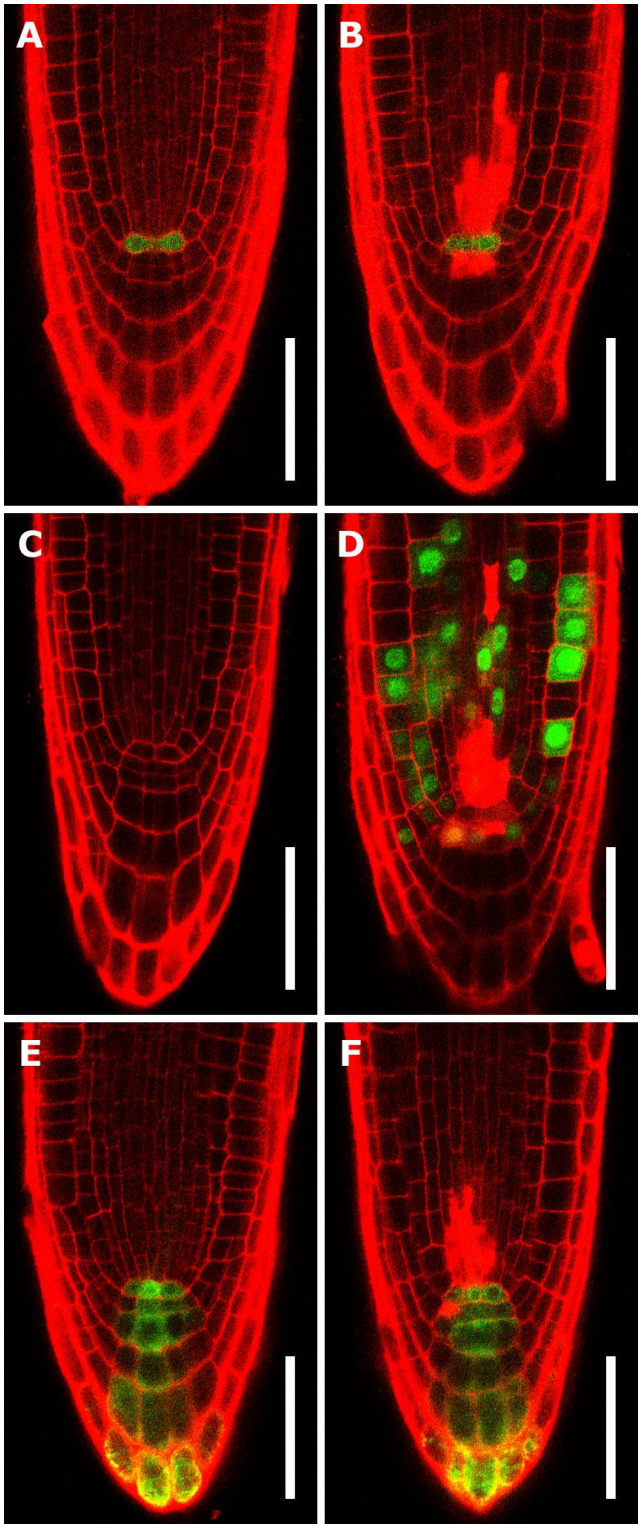

Surviving cells are identified as the QC through *WOX5:GFP* expression after 24 hr zeocin treatment at 20 µg/ml. WOX5:GFP untreated control (**A**) and treated (**B**). Zeocin treatments of CYCB1;1:GFP (**D**) untreated control (**C**) and DR5:GFP treated (**F**) and control (**E**) show similar results as witnessed with bleomycin. (Scale bars: 50 µm).

Figure 2.6. Cell death initiated at approximately 16 hrs after moving to zeocin

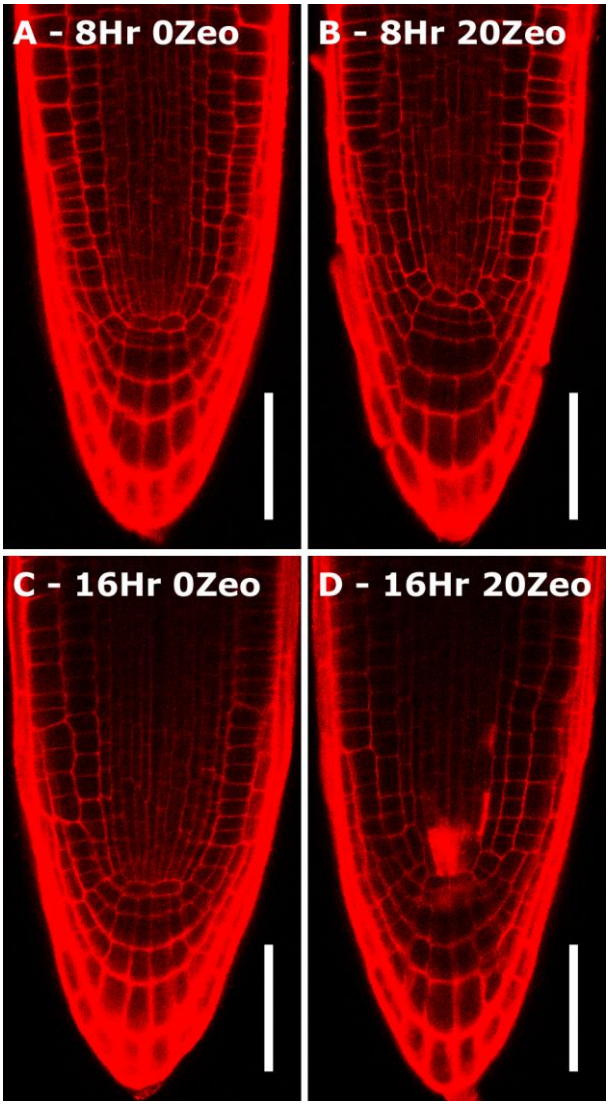

Roots begin to show death of initials 16 hrs after transfering to 20 µg/ml zeocin supplemented media. 8 hr treatments (**A**) control and (**B**) treated show no cell death, 16 hr treatments (**C**) control and (**D**) treated shows death of ~3 initials. (Scale bars: 50 µm).

Figure 2.7. Sytox staining labels dead initials after bleomycin and zeocin treatment

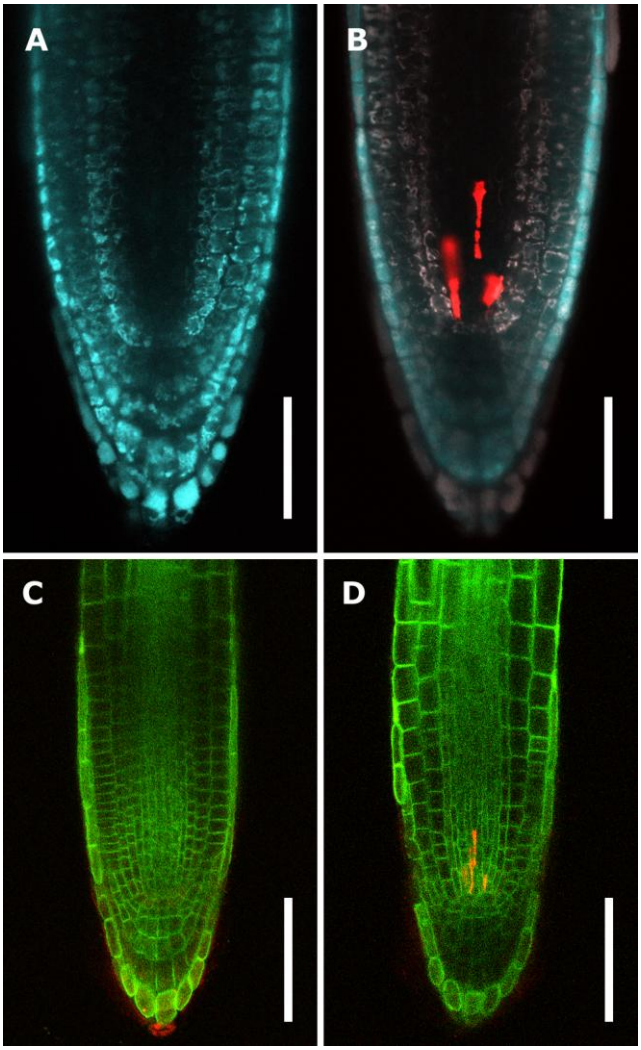

Death of root initials was also labelled with cell death stain Sytox orange. Wild type roots were co-stained with fluorescein diacetate to label living cells along with Sytox after 24 hrs bleomycin treatment at 1 µg/ml, (**A**) untreated and (**B**) treated. LTI6B membrane marker also showed Sytox stained initials after zeocin treatment, (**C**) untreated and (**D**) treated. (Scale bars: 50 µm).

2.2.3. Cell death responses varied with different genotoxic treatments

DNA damage can be generated by a wide array of drugs and treatments that damage DNA in different ways. Various treatments were used to induce thymine dimers (UV), DSBs (x-ray) and replication stress (hydroxyurea and aphidicolin). UV light is historically the most studied DNA damaging agent and is known to introduce lesions known as photoproducts. The most common photoproducts are pyrimidine dimers which result in a covalent linkage between two adjacent pyrimidine bases (Batista*, et al.* 2009). Covalently jointed bases can promote errors in DNA replication through incorrect transcription by translesion polymerases (TLPs) (Curtis and Hays 2007). X-rays induce DNA damage directly through ionization of DNA or indirectly through production of free radicals (Roldan-Arjona and Ariza 2009). Mechanisms of DNA damage through oxidation by reactive oxygen species (ROS) are discussed more extensively in chapter 1. Hydroxyurea (HU) and aphidicolin are known to affect DNA replication although via separate mechanisms, HU depletes dNTP pools whilst aphidicolin inhibits replicative polymerases (De Schutter*, et al.* 2007). Inhibition of DNA synthesis can lead to arrest in fork progression and subsequent collapse forming a DSB (Fram and Kufe 1982).

X-ray irradiation had a very similar effect on initials as bleomycin and zeocin (Fig 2.8b). Because x-rays are expected to cause uniform DNA damage across tissues and cells, selective death of the root initials indicates this is a cell specific response; root stem cells are unique in their ability to activate cell death compared to surrounding cells. Treatment with high UV-C levels however failed to cause initial specific death. UV irradiation was also uniform but showed high levels of death on the root surface (Fig 2.8d).

The ability of replication blocking drugs to cause DNA damage indirectly through fork collapse was thought to potentially initiate cell death. The effects of these drugs however showed differential responses in the root meristem. Cell

death was seen after treatment with hydroxyurea (HU) (Fig 2.9b), but not specifically in initials. Daughters of initials were shown to undergo cell death whereas the initials appeared unaffected. Experiments with aphidicolin used the CYCB1;1:GFP marker (Fig 2.9d), aphidicolin treatment did not induce cell death but did show a similar response in levels of CYCB1;1:GFP expression compared to zeocin and bleomycin treatments.

Toxic metals that occur naturally in soil could induce DNA damage within the root meristem through generation of reactive oxygen species (ROS) (Cho and Seo 2005). In order to relate the cell death responses to a naturally occurring stress, plants were treated with cadmium sulfate ($CdSO_4$) and aluminium chloride ($AlCl_3$). 24 hour treatments with both aluminium chloride (Fig 2.10b) and cadmium sulphate (Fig 2.10d) failed also to show death of root initials. Instead, death of the whole root was initiated at around 200 μM $CdSO_4$ and 300 μM $AlCl_3$. Varying concentrations from 0 to 400 μM were used for both $CdSO_4$ and $AlCl_3$, lower concentrations also showed no difference compared with untreated roots.

Figure 2.8. Irradiation with x-rays, but not UV preferentially killed root initials

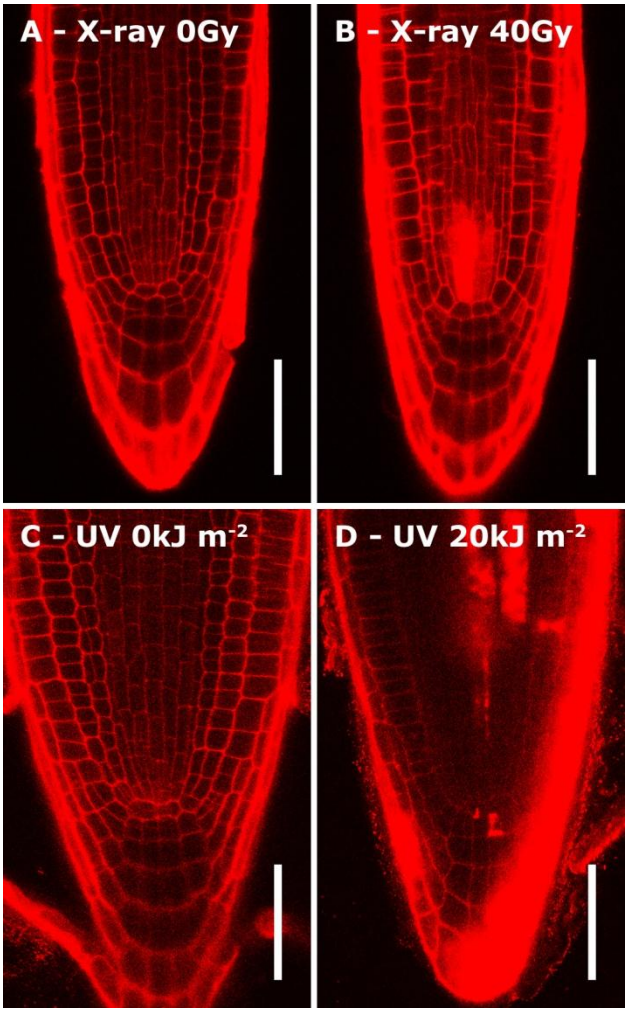

X-ray irradiation at 40 Gray induced cell death of root initials. Roots were irradiated on germination media and imaged after 24 hrs. (**A**) X-ray unirradiated control and (**B**) X-ray 40 Gray irradiation. UV-C irradiation caused cell death on root surface but not root initials. (**C**) UV control and (**D**) UV 20 kJ m^{-2} irradiation. (Scale bars: 50 μm).

Figure 2.9. Replication blocking agents showed varying cell death responses

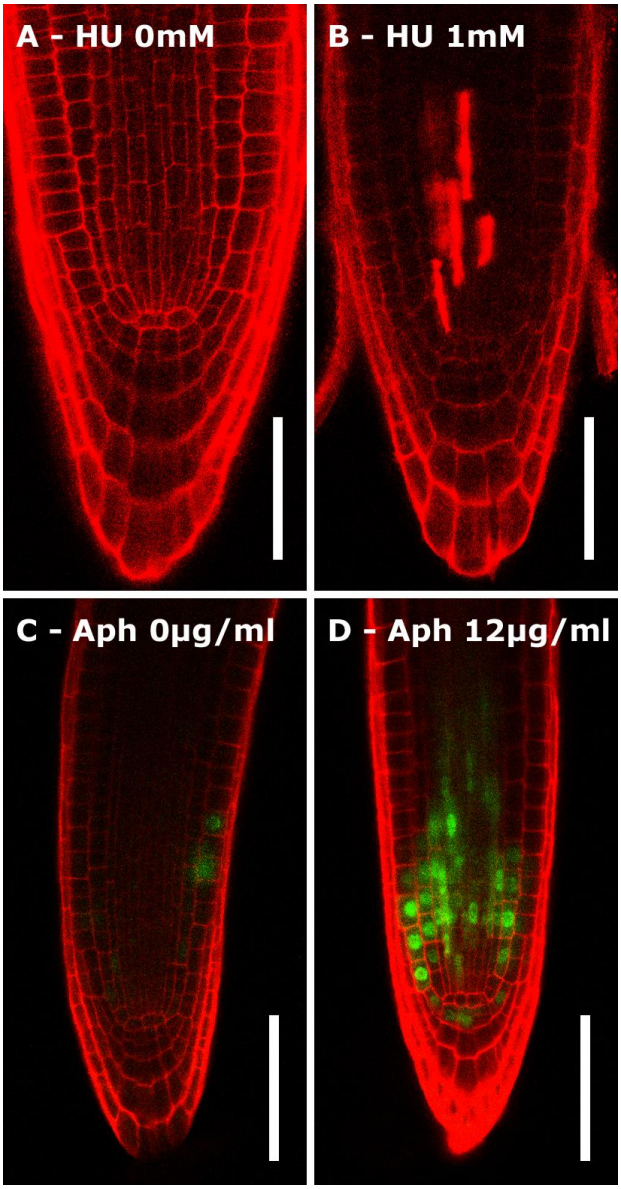

Treatment with HU caused death of daughter cells but not the initials themselves whereas aphidicolin showed cell cycle arrest but not cell death. HU treated Columbia seedlings (**A**) untreated and (**B**) 1 mM treated. Aphidicolin treated CYCB1;1:GFP (**C**) untreated and (**D**) 12 µg/ml treated. (Scale bars: 50 µm).

Figure 2.10. Treatment with heavy metals failed to selectively kill root initials

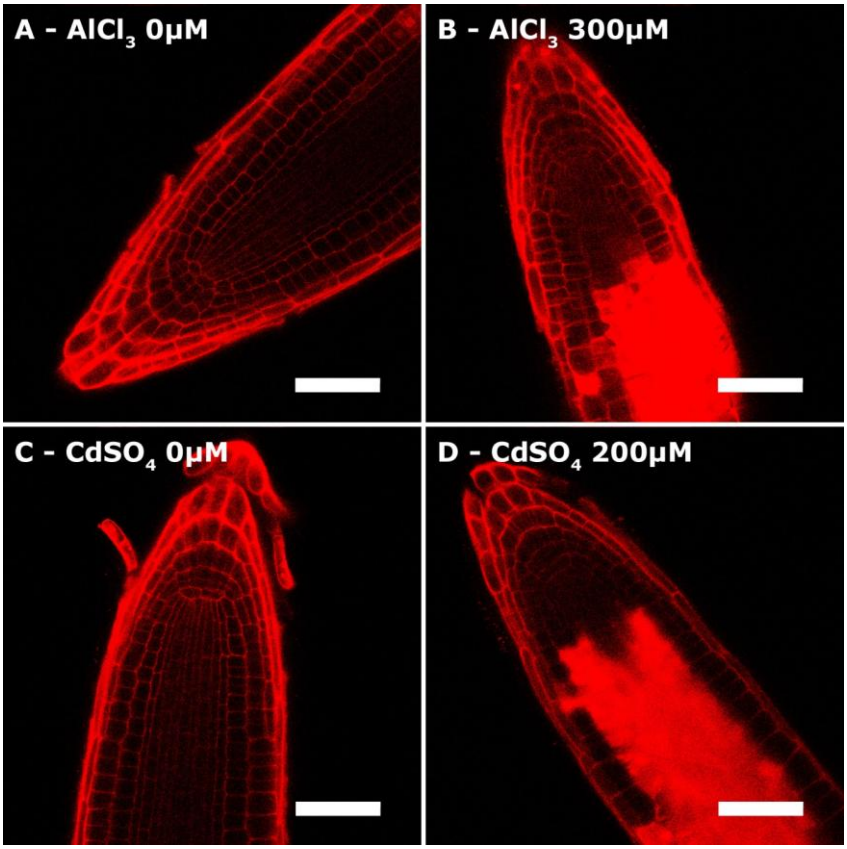

Treatments with Aluminium Chloride ($AlCl_3$) and Cadmium Sulfate ($CdSO_4$) for 24 hrs failed to show death of initials. Instead the whole root was killed after 24 hrs on (**B**) 300 µM $AlCl_3$ and (**D**) 200 µM $CdSO_4$. (Scale bars: 50 µm).

2.3. Discussion

My results showed that relatively low levels of DNA damage induced by radiomimetic drugs trigger selective death of root initials in *Arabidopsis*. It is well established that animal stem cells initiate programmed cell death (PCD) as a response to DNA damage (Rich *et al.* 2000, Schumacher *et al.* 2001). Selective death therefore appears to have also evolved as a mechanism to protect stem cell populations in plants. Such a response has not been shown previously; programmed cell death in response to DNA damage was presumed not to occur in plants. This is primarily due to the lack of key mediators involved in mammalian apoptosis such as p53, CHK1, CHK2 and caspases (Bonneau*, et al.* 2008, Cools and De Veylder 2009). Also, a key feature of apoptosis, engulfment of apoptotic bodies by surrounding cells, is not possible in plant cells due to thick cell walls preventing phagocytosis (van Doorn and Woltering 2005). Programmed cell death has however been shown to occur in xylem differentiation (Fukuda 1996) and the hypersensitive response (Hofius*, et al.* 2009). Possible pathways involved in activating death of root initials are discussed further in chapter 4.

Initial experiments showed disruption of meristem structure and subsequent recovery after bleomycin treatment. This disorganisation hinted at a possible recovery mechanism by which activation of QC division would repopulate damaged initials. As the QC cells exhibit long mitotic cycles, they could potentially repair DNA damage more accurately through homologous recombination, a relatively error free method of DNA repair (Bernstein and Rothstein 2009). A higher tolerance to genotoxic stress would provide a genetically stable template for repopulating the stem cell niche. Previous work with ethylene over-expressing plants showed QC divisions in *Arabidopsis* clearly identified by confocal microscopy (Ortega-Martinez *et al.* 2007). Using this approach, my initial aim was to verify whether the QC would activate division

after DNA damaging treatments. Following QC divisions proved difficult with the 35S:GFP-LTI6B line and QC cells were hard to identify, especially after exposure to DNA damage which caused meristem disorganisation. To circumvent the difficulties of identifying the QC based on cell morphology, I then used GUS expressing QC markers. Experiments with the QC25 marker showed unexpected reduction of expression after 48 hrs of bleomycin treatment. This suggests loss of QC identity after DNA damage; this could be a prelude for re-activation of cell division in the cells that made up the QC before DNA damage. On the other hand, expression of WOX5:GFP was maintained in 24 hr zeocin treated roots, suggesting that loss of QC identity occurred more slowly and required more damage than the cell death response seen in root initials.

The disappearance of QC25 expression after 48 hrs of bleomycin treatment could be explained by the longer exposure time used compared to the 24 hr exposure for WOX5:GFP treatments with zeocin. Higher zeocin treatments caused QC death in figure 2.4, 48 hr treatments will induce larger amounts of DNA damage than 24 hrs exposures. 24 hr bleomycin treatments however still showed greatly reduced GUS expression in figure 2.2. QC25 markers were originally derived from gene trap methods used to identify markers for QC identity; the promoter driving GUS expression is unknown. WOX5 on the other hand is known to act in the organising role of the QC by specifying surrounding initials as undifferentiated. The unknown nature of what is driving the expression of GUS in QC25 seedlings may produce differences in expression after DNA damage compared to that of the WOX5:GFP marker.

Auxin plays a key role in maintaining QC identity (Benjamins and Scheres 2008), loss of QC identity may be due to changes in auxin distribution. Auxin flow is mediated by the PIN family of auxin transport proteins (Feraru and Friml 2008). Cell death of the root initials could disrupt auxin flow through preventing expression of PIN proteins in the stele. *PIN1:GFP* expressing roots showed good levels of GFP within the stele prior to bleomycin treatment, this expression was

largely reduced in all stele cells and not just the initials after treatment. Experiments using the auxin response reporter DR5:GFP showed little evidence of changing auxin levels in the root tip after cell death induced by bleomycin and zeocin. From these results, it appears auxin distribution is maintained in the QC after DNA damage and is not strongly disrupted by cell death in neighbouring cells.

Early papers showed increased uptake of labelled thymidine in QC cells after x-ray treatment in *Zea* roots (Clowes 1961), activation of division could prevent expression of QC specific markers. Progression to zeocin treatments eventually showed that the QC survived lower doses of zeocin but died at around 40-60 µg/ml. This suggested there is a threshold of DNA damage to which the QC is able to withstand and potentially repopulate initials; too much damage causes death of the QC and termination of the root meristem. The length of the DNA damaging treatment probably also affects QC survival, considering the lack of QC in 35S:GFP-LTI6B after 48 hr exposure (Fig 2.1.) compared with 24 hrs with DR5:GFP (Fig 2.3b.). Survival of the mitotically inactive QC was also suggested to be connected with cell division rates rather than cell identity. However, this would not explain the specific death of the initials which are known to divide at a much slower rate than surrounding meristem cells (Dolan*, et al.* 1993).

These results show QC survival after low levels of DNA damage and cell death of surrounding stem cells. However, QC activation was not shown after bleomycin or zeocin treatments using methods described by Ortega-Martinez (2007). Further experiments were required to investigate QC divisions; methods used include cell lineage labelling and live imaging which are discussed in chapter 6.

While trying to analyse the behaviour of the QC after DNA damage, propidium iodide staining unexpectedly revealed selective death of root initials. This result raised the question whether selective death of stem cells plays a role

in the responses to DNA damage in the root meristem. A range of DNA damaging treatments were then used to further study the effects of DSBs, thymidine dimers, replication stress and toxic metals on initial specific cell death.

X-rays induced DSBs are used in the treatment of cancer in order to provoke cancerous cells into apoptosis (Muschel *et al.* 1998). Bleomycin and zeocin mimic damage caused by irradiation through generation of DSBs. The selective response of root initials to bleomycin and zeocin suggested a cell type-specific response, but the possibility remained that these drugs could accumulate or be metabolised differently in the initials, although the CYCB1;1:GFP experiments showed this was unlikely as surrounding meristem cells were shown to activate cell cycle arrest and not cell death. X-ray irradiation damages DNA uniformly across all tissues, so it was used to eliminate the possibility of drug collection at the root tip. Irradiation at around 40 Gray produced death of initials, a dose much lower than previous irradiation experiments (Culligan*, et al.* 2004, Garcia*, et al.* 2003).

In contrast to x-rays, irradiation with UV, known to create thymidine dimers and not DSBs, failed to induce death of initials and instead showed extensive cell death on the root surface. Previous experiments with UV-B in *Arabidopsis* show initiation of apoptotic-like cell death after UV treatment of protoplasts (Danon and Gallois 1998), UV treatments of roots showed death of epidermal cells, this suggests that maybe UV was absorbed by surrounding cells leaving initials unaffected by the irradiation. Earlier experiments by Curtis and Hays (2007) have addressed responses to UV irradiation in the root. Tolerance to UV-B irradiation is conferred by DNA translesion polymerases (TLPs) which synthesise DNA past UV induced lesions, although giving some risk of mutation. Root growth was analysed in TLP mutants AtPOLH-1 and AtREV3-2/2, double mutants were found to exhibit lower growth rates after UV irradiation. More importantly, propidium iodide staining revealed cell death in the meristem of these mutants after irradiation whereas wild type plants showed no cell death.

TLPs were suggested to enable plant roots to tolerate modest levels of UV induced replication stress. Actions of TLPs however potentially create harmful mutations; preventing cell death would not remove genetically unstable cells from the population. Reasons why cell death is prevented by TLPs requires further work to understand this mechanism of tolerating UV irradiation.

Replication stress is known to indirectly damage DNA by blocking progression of replication forks at S phase. Inhibition of replication forks can lead to their collapse and generation of DSBs (Fram and Kufe 1982). Hydroxyurea (HU) and aphidicolin are well known in their ability to prevent DNA replication although through different mechanisms. HU is responsible for inhibiting ribonuclease reductase (RNR) which catalyses a final reduction step in the production of dNTPs (Roa *et al.* 2009). Treatment with HU would result in depletion of the dNTP pool causing an arrest before the synthesis stage of the cell cycle. This contrasts to aphidicolin which prevents DNA replication by inhibiting polymerases ε and σ (Culligan*, et al.* 2004, Ikegami *et al.* 1978).

Previous experiments have shown that HU and aphidicolin have different effects on cell cycle progression (Culligan*, et al.* 2004). This paper characterised the ATR homolog in *Arabidopsis*, a key DNA damage signalling kinase identified from mammalian studies. The primary role of ATR in mammals in to activate cell cycle checkpoints specifically in response to replication stress (Ward and Chen 2001). *Arabidopsis ATR* mutants were shown to be particularly sensitive to HU and aphidicolin but not x-ray induced DNA damage highlighting a similar function in plants. Cell cycle progression in response to HU and aphidicolin was examined using the CYCB1;1:GUS marker which was introduced into both wild type and *atr* backgrounds. Wild type plants showed treatment with aphidicolin but not HU induced a G2 cell cycle arrest marked by induction of CYCB1;1:GUS. The ATR mutant failed to show a G2 arrest indicating *atr* as being essential in G2-M cell cycle progression. The paper describes a model by which HU is thought to induce a cell cycle arrest in G1 whereas aphidicolin induces a G2

arrest. Cells stalled at G1 due to continuous treatment with HU would not be permitted to enter S phase hence no CYCB1;1:GUS G2 labelled arrest after HU treatment. Aphidicolin treatment would allow entry into S phase due to sufficient dNTPs for DNA replication. Cells would however be unable to replicate any DNA due to inhibition of relevant DNA polymerases which would lead to a G2 arrest.

My results showed that, as seen for cell cycle arrest, cell death responses also differed after treatment with HU and aphidicolin. Aphidicolin treatments failed to show any cell death responses within the meristem, expression of the CYCB1;1:GFP was up regulated in a similar way as earlier experiments with bleomycin and zeocin, consistent with the results of Culligan *et al.* (2004) where aphidicolin activated CYCB1;1:GFP expression. In contrast, treatment with HU activated a cell death response after 24 hrs exposure, although this seemed to be more specific to daughters of initials rather than the initials themselves. The latter result could be explained if at least some of the HU-treated cells proceeded through the cell cycle with incompletely replicated DNA, leading to DSBs and consequently activation of cell death.

The death of stem cell daughters after HU treatment might also be a result of selective chromosome segregation (Armakolas and Klar 2006). A model for segregation of DNA strands was highlighted in an early review on the protection of stem cell populations (Cairns 1975). Most spontaneous mutations arise through errors in replication, semi-conservative replication means these mutations in would initially exist in a heterozygous state. Unless DNA repair corrects this problem, cell division will generate one mutant cell and one normal cell (Cairns 1975). This hypothesis was investigated in adult muscle satellite cells with BrdU pulse labelling (Shinin *et al.* 2006). BrdU labelled template strands were shown to be retained in satellite cells providing the first example of DNA cosegregation *in vivo*. Non random chromosome segregation from stem cells could therefore segregate damaged DNA to daughter cells in order to protect integrity of the stem cell niche.

Comparison of results obtained with agents that induce DSBs or replication stress raise the question whether cell cycle stage could plays a role in activating cell death responses in the initials. Treatments with replication blocking drugs had a lesser effect in causing initial specific cell death than treatments that induce DSBs directly. It was uncertain why DNA damage induced by replication stress did not also cause preferential death of initials. Mammalian cells have been shown to respond to HU and aphidicolin by predominately activating homologous recombination (HR) (Lundin *et al.* 2002, Rothkamm *et al.* 2003). Non-homologous end joining (NHEJ) is critical to repair IR-induced damage in all cell cycle stages whereas HR is shown to act exclusively in late S/G2 (Rothkamm*, et al.* 2003). In addition, mutants for HR are more sensitive to HU than wild type and NHEJ mutants, although NHEJ mutants displayed higher sensitivity than WT (Lundin*, et al.* 2002). It is therefore possible that replication stress causes cell cycle arrest in S phase resulting in DNA repair by HR. DSBs induced by IR, bleomycin and zeocin are predominately repaired by NHEJ, too many breaks would be catastrophic for the cell hence selective cell death. A difference in cell cycle stage could therefore explain the difference between replication blocking drugs and DSB inducing drugs in activating cell death.

In addition to agents that specifically cause DSBs or replication stress, I investigated the response to heavy metals ions in root initials, which are widespread natural toxicants (Kozhevnikova *et al.* 2007). Treatment with heavy metals aimed to put meristem recovery into context with a naturally occurring stress. Treatment with Cadmium has shown to enhance production of reactive oxygen species (ROS) in *Arabidopsis*, a concentration of 300 μM resulted in ~50% increase in ROS levels (Cho and Seo 2005). Aluminium and Cadmium experiments also found AtATR mutants to be less sensitive to toxic metals as well as maintaining QC identity marked by the QC46 GUS marker (Rounds and Larsen 2008). *Zea* roots were shown to activate QC divisions after treatment

with heavy metals (Kozhevnikova*, et al.* 2007). In my own experiments, 24 Hr treatments with varying concentrations of cadmium sulfate ($CdSO_4$) and aluminium chloride ($AlCl_3$) failed to trigger cell death in root initials. Cell death of the whole root was initiated at around 300 μM $AlCl_3$ and 200 μM $CdSO_4$. These experiments therefore failed to determine whether presence of heavy metals induces stem cell specific cell death. Further experiments are needed to place death of root initials into a naturally occurring context. It is possible that the multiple effects of acute exposure to toxic metals could have masked any specific responses in root initials; treatments at lower concentrations for longer time periods may be needed. ROS mediated molecular damage within cells is not solely confined to the generation of DSBs. ROS are also known to rapidly oxidise lipids in cellular membranes, proteins and other cellular components (Kotchoni and Gachomo 2006). Plants are subject to greater ROS production through the actions of photosynthesis and have therefore evolved elaborate protective mechanisms to control ROS levels (Gechev*, et al.* 2006). Knowledge of this regulation has progressed into a signalling network capable of controlling growth, cell cycle, programmed cell death, hormone signalling, biotic and abiotic stress responses and development (Mittler 2002). It is possible ROS mediated cell death does not necessarily activate cell death mechanisms as a direct result of DSBs, other signalling pathways could contribute to this. Also, other forms of cellular damage could also activate a cell death response.

In conclusion, treatments with DNA damaging treatments that directly cause DSBs resulted in a cell death response preferentially within the root initials. The quiescent centre was shown to survive these treatments suggesting these cells are more resistant to DNA damage, possibly through homologous recombination mediated DNA repair. The next question was whether this response was genetically controlled through pathways involved in perceiving and repairing DSBs in *Arabidopsis*.

Chapter 3 – Analysis of DNA damage perception and repair mutants

3.1. Introduction

DNA damage perception and repair pathways play an important role in maintaining genomic stability within animal cells in response to genotoxic stress. In comparison, little is known about these processes specifically in plants. Homologous genes for many of the DNA damage perception and repair proteins found in mammals have been identified in the *Arabidopsis* genome. Signalling pathways involved in downstream activation of DNA repair are therefore thought to be fairly conserved between plants and animals. The current model for mammalian DNA damage signalling is reviewed in chapter 1. In this model, the MRN complex acts to detect presence of double stranded DNA breaks (DSBs) within the genome (Czornak*, et al.* 2008). This complex initiates a signalling cascade which acts to arrest cell cycle progression and activate repair processes. Homologs of the MRN complex and many of its downstream signalling components have been shown to be sensitive to DNA damage in plants. Many of the interactions between these proteins is however not certain, it is possible plants may have evolved slight differences in DNA damage signalling.

Results from chapter 2 showed the stem cell population in the root to undergo cell death in response to DNA damaging treatments. The question however remained whether this response was dependent on DNA damage signalling. Mouse embryonic stem cell populations have previously shown to undergo apoptosis in response to low levels of DNA damage (Heyer*, et al.* 2000). Programmed cell death in these cells was dependent on ATM and p53 which function downstream of the MRN complex. The *p53* gene, dubbed "the guardian of the genome" (Lane 1992) is well known in its ability to initiate cell death in response to DNA damage (Garner and Raj 2008). *Arabidopsis* however

lacks a known *p53* homolog (Hefner *et al.* 2003). It still remained possible that ATM activates similar cell death mechanisms in plants in the absence of p53.

To investigate the role of DNA damage signalling mutants in activation of cell death in root initials, I selected a number of mutants covering a broad range of responses. This includes perception of DSBs, activation of repair pathways and cell cycle arrest. These mutants were treated with zeocin looking for any reduction or enhancement in cell death within the root meristem. Mutants unable to perceive DNA damage would be potentially unable to activate the downstream cell death response. I also aimed to test mutants with known genomic instability looking for the effect on root stem cells.

3.2. Results

3.2.1. Different accessions showed similar DNA damage induced cell death

To begin studying effects of DNA damage on signalling mutants, first it was essential to study cell death within different accessions of *Arabidopsis*. Mutants tested were sometimes of different ecotypes, it would first be essential to study the effect on wild type Columbia, Landsberg *erecta* (L*er*) and Wassilewskija (WS). These responses could be expected to be similar; however, the effects on plants derived from different geographical positions may differ in response to DNA damage.

Seedlings of Columbia, Landsberg and WS were treated with zeocin (20 µg/ml) for 24 hrs, stained with propidium iodide and imaged. Cell death was observed in the root initials of each accession (Fig 3.1.). Landsberg seedlings did however seem to be slightly more sensitive to zeocin treatment, activating more cell death within the root meristem (Fig 3.1d). The QC was still clearly visible within these treated seedlings, QC death was observed to occur at higher zeocin concentrations in chapter 2. No differences were observed between seedlings of Columbia and WS backgrounds. The figure produced (Fig 3.1.) represents control levels of cell death in wild type root initials. Please refer to this figure for comparison with cell death in wild type and mutant lines. All mutants used are in the Columbia background unless stated otherwise.

Figure 3.1. Different accessions of *Arabidopsis* showed similar responses to zeocin treatment

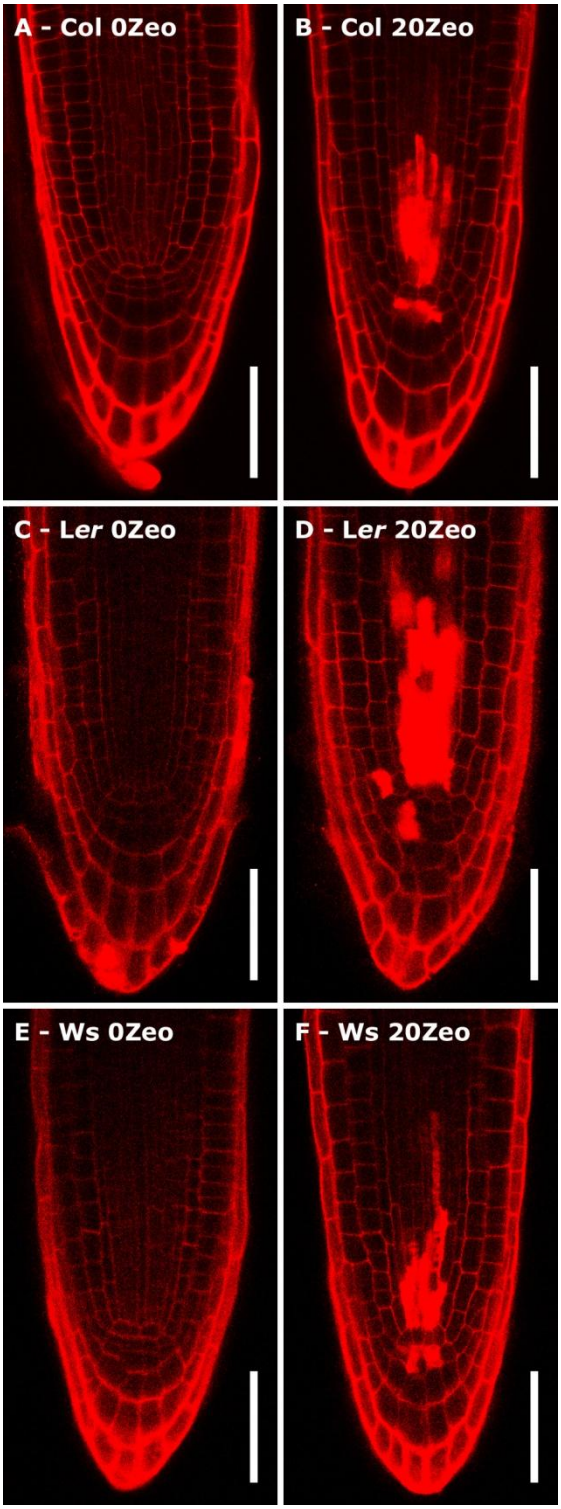

Columbia, Landsberg erecta and Wassilewskija seedlings were exposed to zeocin for 24 hrs (20 µg/ml). Cell death was found to occur in all three ecotypes, Seedlings of L*er* were however found to be slightly more sensitive to zeocin treatment. Please refer to this figure for comparison of wild type and mutant cell death levels. (Scale Bars: 50 µm).

3.2.2. Mutants affecting DNA damage perception by the MRN complex showed different cell death responses

The MRN complex is described in mammalian models for DNA damage signalling as the primary sensor of DNA breaks (Zhou*, et al.* 2006). This complex comprises of 3 proteins involved in separate functions to mediate activation of the DNA damage response (Pardo*, et al.* 2009). RAD50 is important to act as a bridge, anchoring broken DNA ends. MRE11 acts to resect broken DNA ends to provide compatibility for re-ligation. The signalling kinase NBS1 is then thought to signal downstream to key transducers ATM and ATR to mediate the damage response. For a full review of this process see chapter 1.

Arabidopsis contains homologous genes for each of the proteins involved in the MRN complex. Gallego *et al.* (2001) identified a *RAD50* homologous sequence, these mutants showed increased sensitivity to MMS and sterility. Bundock & Hooykass (2002) showed the *MRE11* mutant was also sensitive to DNA damaging agents and also exhibited telomere elongation. Waterworth *et al.* (2007) characterised the *AtNBS1* genes which also showed hypersensitivity to DNA damaging conditions and association with MRE11. Through identification of these homologous genes and interactions between them, it is possible the MRN complex also acts in *Arabidopsis* to initiate DNA damage response signalling and repair.

Mutants for *mre11-4* (unpublished, obtained from Chris West) and *nbs1* (Waterworth*, et al.* 2007) were treated with zeocin for 24 hrs, stained with propidium iodide and imaged. Results show two different zeocin concentrations for *mre11* and *nbs1* mutants (Fig 3.2.). Different zeocin stocks were found to induce different levels of cell death due to variable concentrations, although each was listed as 100 mg/ml as supplied from Invitrogen. Each new stock of zeocin was therefore calibrated in order to compare results to previous treatments. Wild type seedlings were exposed to varying concentrations of the

new zeocin stock; images of root tips were compared to those obtained with 20 µg/ml to assess the level of cell death in the initials and survival of the QC. All zeocin concentrations shown are therefore thought to be equal in ability to induce cell death in the wild type.

Homozygous *mre11* mutants are sterile; seedlings with non functional MRE11 are clearly identified by abnormal root morphology as seen by Bundock & Hooykass (2002). Roots of the unpublished *mre11-4* also exhibited the abnormal root structure and were easily identified from a heterozygous population. Results for *mre11-4* showed presence of cell death within the root initials even in the absence of zeocin (Fig 3.2a). Zeocin treatment seemed to have little effect on cell death which appeared to be similar as with untreated seedlings (Fig 3.2b). The *nbs1* mutant however showed no difference in cell death compared with wild type. Thus predicted components of the *Arabidopsis* MRN complex therefore showed different responses to zeocin treatment.

Figure 3.2. Components of the MRN complex showed different responses to zeocin

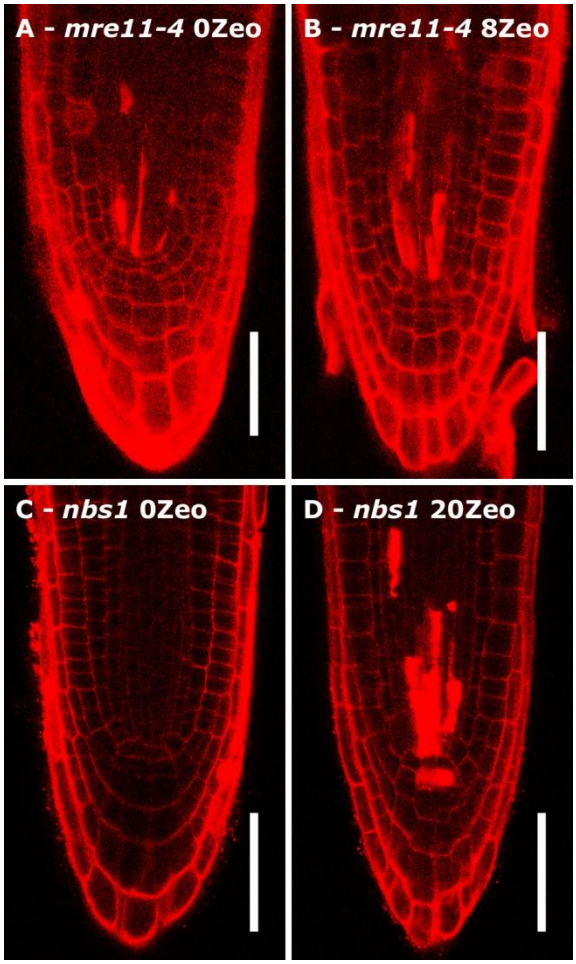

MRE11 (end resection) and NBS1 (downstream signalling) mutants were both treated with zeocin (20 µg/ml, 24 hrs) looking for effects of defective DNA damage perception on cell death. *mre11-4* showed death of initials in the absence of zeocin, cell death was not drastically increased after zeocin treatment (**A** & **B**). *nbs1* mutant seedlings (**C** & **D**) showed cell death levels similar to wild type (see fig 3.1. for wild type cell death levels). (Scale Bars: 50 µm).

3.2.3. ATM and ATR were found to be essential in the activation of DNA damage induced cell death

ATM and ATR are key signalling transducers which act downstream of the MRN complex in animals. *Arabidopsis* contains functional homologs of both *ATM* (Garcia*, et al.* 2003) and *ATR* (Culligan*, et al.* 2004) which are sensitive to DSBs and replication stress respectively. ATM and ATR activation is implicated in a wide range of downstream signalling in response to DNA damage including amplification of the damage response, cell cycle control and repair by HR or NHEJ depending on cell cycle stage (see chapter 1 for review).

To initially test whether these signalling kinases are essential in activating death of root initials, I exposed two *ATM* mutant alleles *atm-1* (WS background) and *atm-2* (Columbia) and the *ATR* allele *atr-2* to 20 µg/ml zeocin for 24 hrs. Cell death was found to be largely absent within these mutant lines (Fig 3.3.). A small amount of cell death remained in some seedlings (usually one cell); this was put down to the possible residual activity of ATM. In addition to zeocin treatments, *atm-1* and *atr-2* mutant alleles were exposed to 40 and 80 Gray of x-ray irradiation (Fig 3.4.). Results were similar to zeocin treatments at 40 Gray with cell death being activated in Columbia roots. ATM and ATR mutants showed greatly reduced cell death at this concentration, again usually one dead initial. Higher doses at 80 Gray showed a more significant change in cell death within the meristem. Large levels of cell death were witnessed within the control seedlings whereas the level of cell death appeared not to change in *atm-1* between 40 and 80 Gray. The *atr-2* allele appeared to show scattered cell death throughout the meristem, cell death was not observed to be specific to the root initials.

Reduction of cell death was seen clearly in ATM and ATR mutants, I then attempted to quantify this showing this reduction was statistically significant. Images were scored by counting roots showing at least one dead root initial in

response to zeocin or x-ray treatment (Table 3.1.). Using the Fisher exact test to determine significance in small sample sizes, *atm* and *atr* roots were shown to exhibit significantly reduced cell death (see materials and methods for description of statistical analysis).

Results from ATM and ATR mutants therefore confirmed a role of DNA damage signalling proteins in the activation of cell death. Both zeocin and x-ray treatments showed reduction in initial-specific cell death in *atm-1*, *atm-2* and *atr-2* mutant alleles. This cell death was shown to be significantly lower than levels shown in wild type roots.

Figure 3.3. ATM and ATR mutants showed inhibition of the cell death in response to zeocin treatment

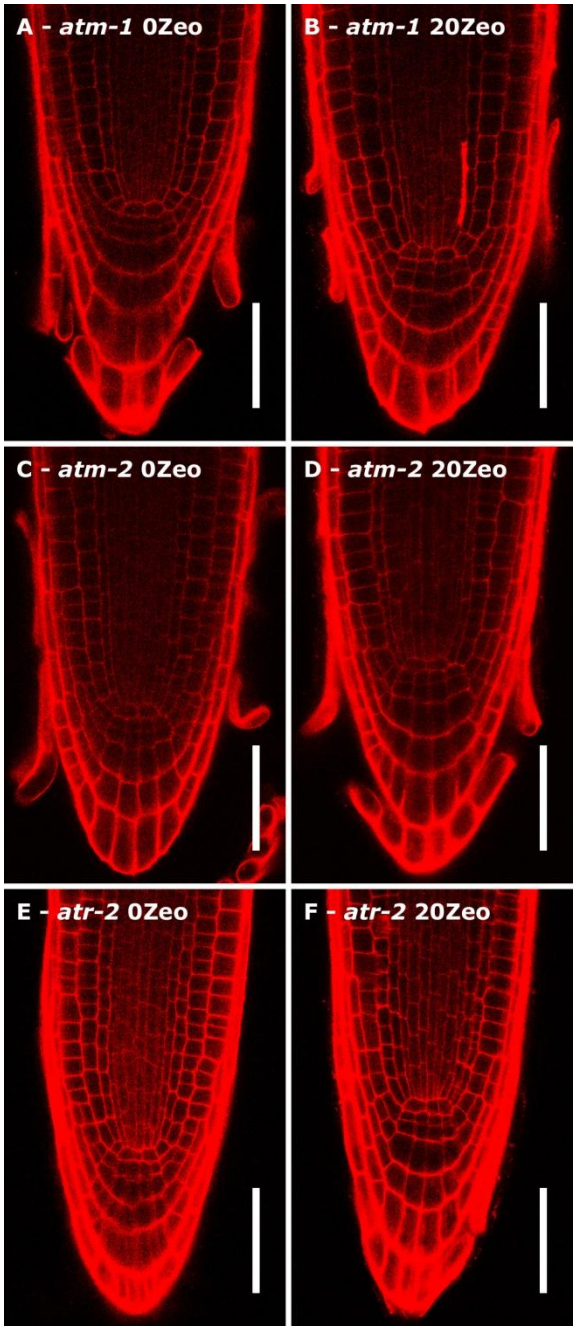

Two *ATM* mutant alleles (*atm-1* and *atm-2*) and one *ATR* allele (*atr-2*) were unable to initiate cell death in the root initials after zeocin treatment. Some single cell death was seen in some roots, this was thought to be due to possible residual ATM or ATR activity (see fig 3.1. for wild type controls). (Scale Bars: 50 μm).

Figure 3.4. X-ray irradiation of *atm-1* and *atr-2* confirmed results obtained with zeocin

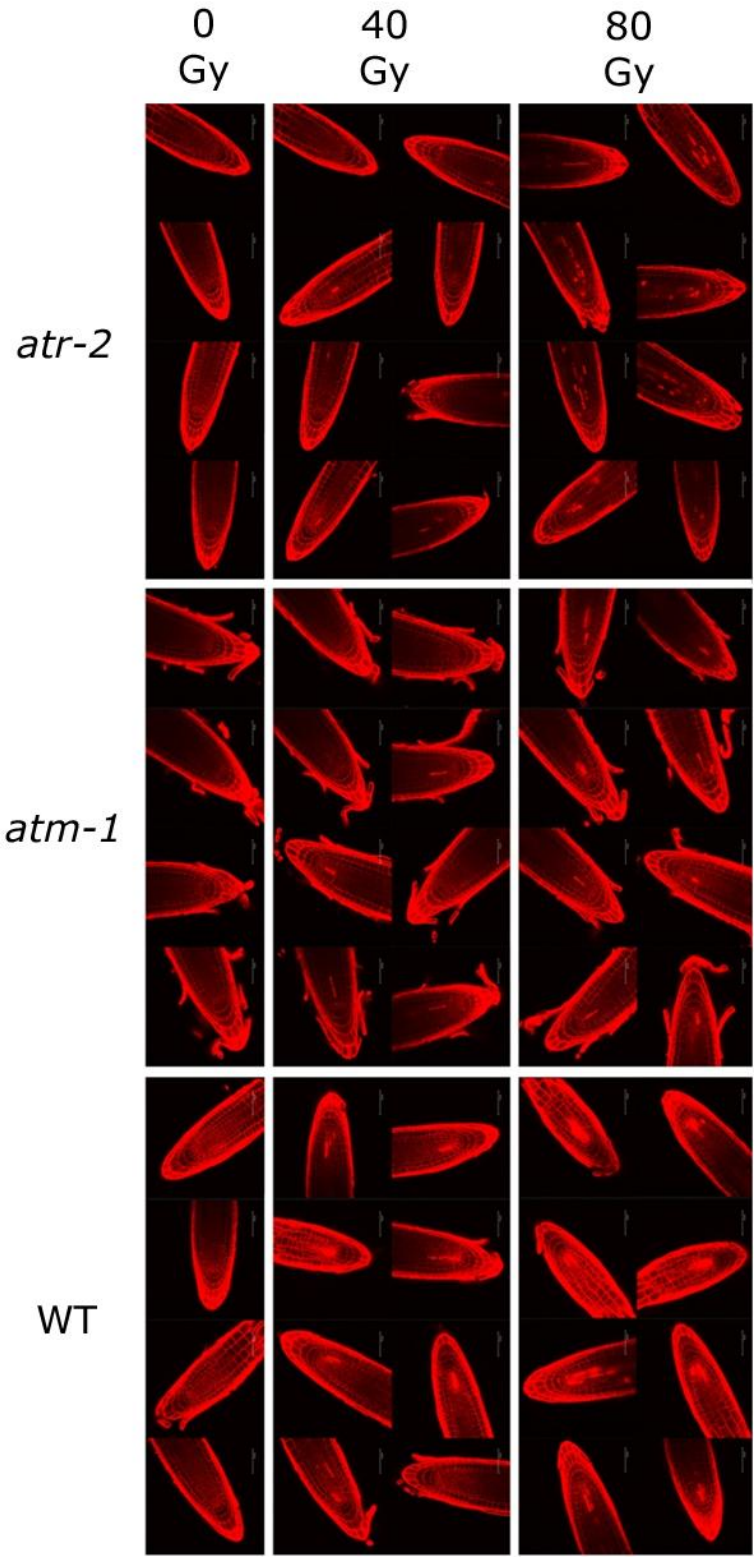

Columbia, *atm-1* and *atr-2* seedlings were irradiated at doses of 40 and 80 Gray. Cell death was greatly reduced in root initials of *atm-1* and *atr-2* seedlings. Additional cell death was seen in the *atr-2* seedlings in stele cells above the root initials.

Table 3.1. Frequency of roots containing at least one dead initial cell 24 h after exposure to zeocin or x-rays

	Control	Zeocin, 20 µg/mL	X-rays, 0 Gy	X-rays, 40 Gy	X-rays, 80 Gy
WT	0 (n = 21)	20 (n = 20)	0 (n = 8)	7 (n = 9)	10 (n = 10)
atm-1	0 (n = 17)	2 (n = 14), $p < 10^{-6}$	0 (n = 8)	0 (n = 9), $p < 10^{-2}$	5 (n = 10)
atr-2	0 (n = 16)	2 (n = 13), $p < 10^{-6}$	0 (n = 6)	0 (n = 9), $p < 10^{-2}$	5 (n = 10)

p values are shown for treatments with significant difference from the WT (Fisher's exact test).

3.2.4. Plants defective in non-homologous end joining (NHEJ) showed spontaneous cell death of untreated root initials

In addition to analysing mutants for DNA damage perception, mutants implicated in DNA repair by homologous recombination (HR) and non-homologous end joining (NHEJ) were also treated with zeocin. NHEJ is the predominant pathway for DNA repair in animals and is active mostly in G0 and G1 (Shrivastav*, et al.* 2008). This form of repair is however prone to introducing mutations as broken DNA ends are processed and simply religated (Pardo*, et al.* 2009). This end processing (thought to be performed by MRE11 at the perception stage) creates compatible ends for rejoining but disregards sequence homology. This process contrasts to HR which utilises sister chromatids during S phase to act as a template for accurate repair (Bernstein and Rothstein 2009). For a detailed review of these processes see chapter 1.

To begin analysing these pathways, mutants implicated in NHEJ were first treated with zeocin. Activity of KU proteins is crucial in the first step of NHEJ, KU70 and KU80 join to form a heterodimer which is loaded onto exposed DNA ends (Jackson 2002). Recruitment of DNA-PK mediates downstream activation of the ligase complex XRCC4/LIGIV enabling successful end joining (Cann and Hicks 2007). Homologous genes for KU proteins have been identified in *Arabidopsis* and have shown a number of interesting phenotypes including sensitivity to DNA damage and lengthening of telomeres (Bundock*, et al.* 2002, West*, et al.* 2002, Zellinger*, et al.* 2007). Plants were also shown to contain a homolog of DNA ligase IV which showed similar sensitivity to DNA damage (van Attikum*, et al.* 2003). Treatment of the *ku80* (West*, et al.* 2002, WS background) and *lig4-4* (unpublished, obtained from Chris West) mutants showed extensive cell death within the root meristem, much more than shown in wild type roots (Fig 3.5.). More importantly, spontaneous cell death of root initials was often witnessed within untreated roots.

In addition to NHEJ mutants, a known mutant proposed to affect homologous recombination was also analysed. RAD51 is well known from animal studies to be involved in the strand invasion of broken DNA ends, this forms a key step in holiday junction formation as part of HR (Bernstein and Rothstein 2009). Several mutants have been implicated as homologs in *Arabidopsis* (Bleuyard*, et al.* 2005); the *rad51-1* allele characterised by Li *et al.* (2004) has previously shown sensitivity to mitomycin C (Markmann-Mulisch*, et al.* 2007). Mutants homozygous for *rad51-1* were shown to display complete infertility; for these experiments, 10 seedlings from a heterozygous line were treated with zeocin for 24 hrs and imaged. After imaging, seedlings were removed from microscope slides and placed back onto germination media. Seedlings were labelled in order to match with microscope images and grown to maturity. Homozygous lines were easily identified through fertility defects which prevented seed formation. Unfortunately, only one treated homozygous plant survived imaging which showed wild type levels of cell death. This root tip however exhibited death within the QC, this is also shown in wild type roots at higher zeocin doses (shown in chapter 2, figure 2.4) which suggests the *rad51-1* mutants may be sensitive to zeocin treatments.

Results with NHEJ proteins therefore showed that defective repair of endogenous DNA breaks was enough to activate death within root initials. I then aimed to identify the frequency of roots exhibiting cell death by scoring microscope images. Images of 20 untreated *ku80* and *lig4-4* mutants were scored for roots showing 1 and more than 1 dead root initial (Table 3.2.). Statistical analysis was performed using the Fisher's exact test to see if levels of spontaneous cell death were significantly higher in the mutants (See materials and methods for formula). The *p* values indicated that *ku80* ($p < 0.001$) and *lig4-4* ($p < 0.01$) contained significantly higher levels of spontaneous cell death. I also included *rad51-1* mutants to see if spontaneous breaks occurred within this line. Because *rad51-1* plants are infertile, I screened 80 heterozygous

seedlings, 20 of which would segregate as homozygous. 5 roots out of 80 showed death of at least 1 root initial, these numbers were divided by 4 to represent this 25% segregation (1.25 out of 20). The *rad51-1* mutant was shown not to exhibit significantly higher levels of spontaneous death of root initials ($p > 0.2$). Plants deficient in NHEJ repair pathways were therefore shown to initiate cell death in the absence of zeocin, the HR mutant *rad51* however showed no rise in spontaneous cell death.

Figure 3.5. Mutants involved in DNA repair through NHEJ but not HR pathways showed spontaneous death of root initials

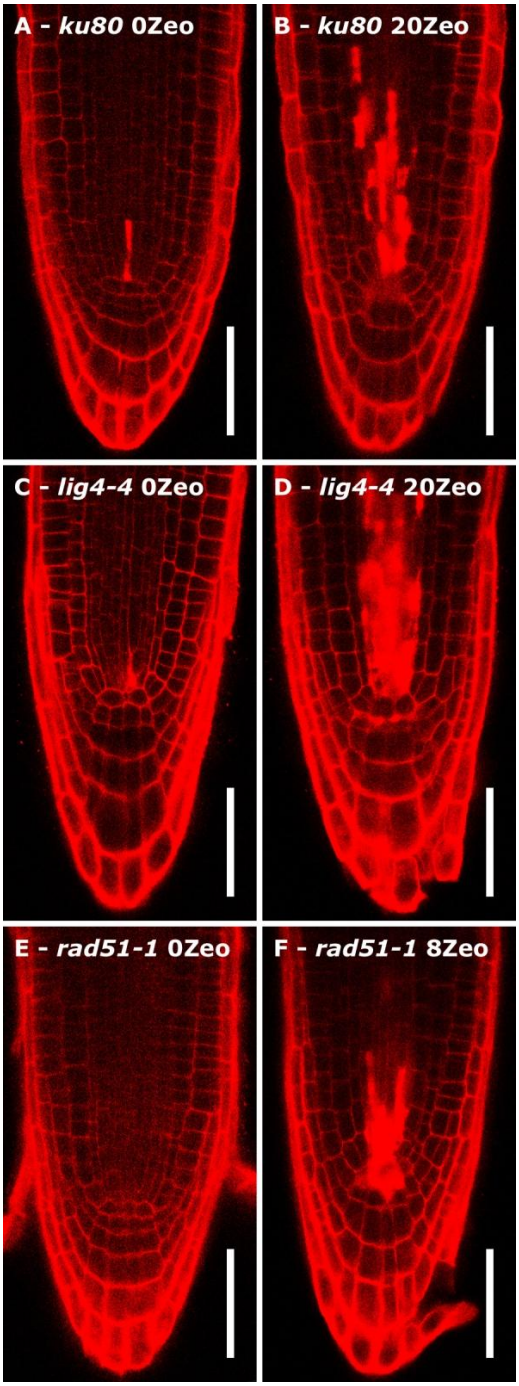

Mutants implicated in *Arabidopsis* NHEJ (*ku80* and *lig4-4*) and HR (*rad51-1*) pathways were treated with zeocin at shown concentrations for 24 hrs. Different zeocin stocks required different concentrations to achieve the same effect. Mutants defective in NHEJ showed spontaneous cell death in the absence of zeocin treatment. Zeocin treatment caused extensive death in the root meristem much higher than in wild type roots (see fig 3.1. for wild type controls). The *rad51-1* mutant showed no evidence of spontaneous cell death or rise in cell death levels in comparison. (Scale Bars: 50 μm).

Table 3.2. Frequency of roots showing spontaneous cell death of root initials

	0 dead initials	1 dead initial	>1 dead initial	Total roots
WT	19	1	0	20
ku80 -/-	9	9	2	20
lig4-4 -/-	12	7	1	20
rad51-1 -/+	75	2	3	80

Table showing numbers of roots with spontaneous cell death in NHEJ and HR mutants. Homozygous *ku80* and *lig4-4* mutants showed cell death in ~50% of roots, 80 roots were examined for heterozygous *rad51-1*, 20 were expected to be homozygous dependent on normal segregation of the mutant.

3.2.5. Mutants affecting cell cycle control in *Arabidopsis* showed no change in cell death levels

Cell cycle control in response to DNA damage is well established in animals. Cell cycle arrest allows more time to activate and complete DNA repair, after which the cell cycle resumes. DNA damage is known to arrest cell cycle through ATM and ATR signalling kinases, which use different mechanisms at G1 and G2 checkpoints (Bucher and Britten 2008). In animals, activation of ATM and ATR leads to phosphorylation of checkpoint kinases (CHK1 and 2) which modulate cell cycle by regulating CDC25 activity. The CDC25 family of phosphatases comprising of CDC25A, CDC25B and CDC25C act to remove inhibitory phosphates from CDKs allowing cell cycle progression (Karlsson-Rosenthal and Millar 2006). ATM and ATR mediated activation of CHK1 and 2 leads to inhibition of CDC25 phosphatases leading to cell cycle arrest. Presence of another phosphatase, WEE1, acts to add inhibitory phosphates on CDKs and acts downstream of ATM and ATR (De Schutter*, et al.* 2007). Activity of CDC25 and WEE1 in animals therefore functions as a switch allowing positive and negative regulation of cell cycle in response to DNA damage.

This mechanism appears to be largely absent within *Arabidopsis*. Homologous proteins for CHK1, CHK2 and CDC25 phosphatase are yet to be identified (Cools and De Veylder 2009). A homolog for WEE1 has however been identified and has been shown to phosphorylate CDKA;1 *in vitro* (De Schutter*, et al.* 2007). This homolog was also sensitive to DNA damage leading to its proposal as a cell cycle regulator in plants by De Schutter *et al.* (2007). Mutants for *WEE1* were therefore suggested in this paper to lack cell cycle arrest after DNA damage leading to their sensitivity. The effects of defective cell cycle arrest were examined by treating *wee1-1* and *wee1-2* mutants with 20 µg/ml zeocin for 24 hrs (Fig 3.6.). These mutants failed to show any response in initial specific cell death, cell death levels were comparable to wild type.

DNA damage is also known to influence mammalian cell cycle control in G1/S phase through Retinoblastoma and E2F genes. E2F transcription factors are required for activation of target genes involved in the G1/S phase transition (Attwooll *et al.* 2004). E2F activity is complemented by binding with DP proteins which mediate association with DNA to activate transcription (Polager and Ginsberg 2008). E2Fs are inhibited through binding of the Retinoblastoma protein (pRB), this inhibition is lifted through phosphorylation by CDK/Cyclin complexes (Sun *et al.* 2007). The DNA damage signalling transducer ATM is known to interact with pRB and E2F genes in response to genotoxic stress (Polager and Ginsberg 2008). Because of this interaction, plant E2F genes were investigated for possible effects on cell death. *Arabidopsis* contains several homologous genes for E2F pathway members including E2F, DP and pRB (Francis 2007). To investigate the role of these genes on zeocin induced cell death, the *e2fa* mutant was first treated with zeocin which showed no effect on cell death induction (Fig 3.7.). In addition to treating *e2fa* mutants, overexpression lines for E2Fa and DPa were also investigated. These overexpression lines showed no change in cell death levels. In conclusion, *E2F* genes were not found to show any effect on initiating cell death within these experiments.

Figure 3.6. Mutants lacking cell cycle arrest after DNA damage showed no reduction in cell death of root initials

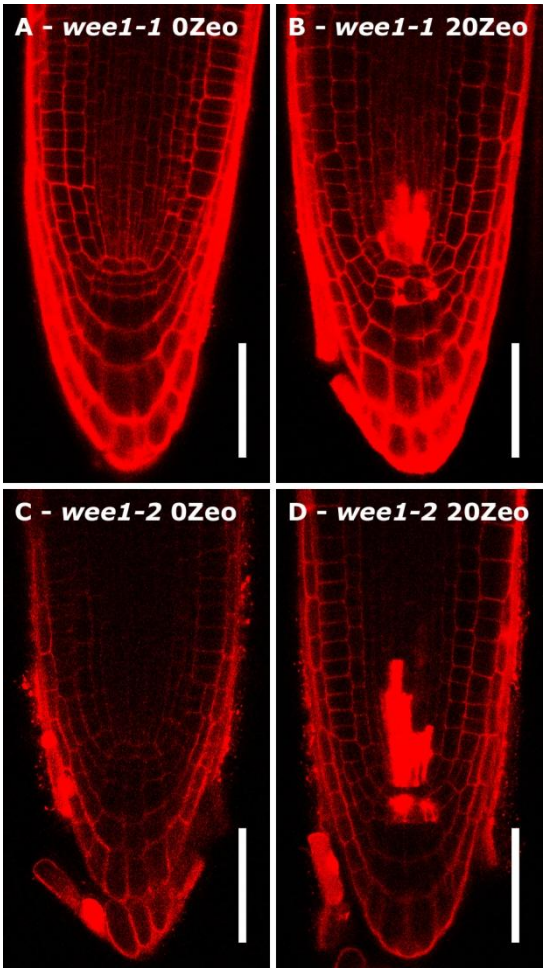

Mutants shown to lack cell cycle arrest after DNA damaging treatments were exposed to 20 µg/ml zeocin for 24 hrs. Cell death in both *wee1-1* and *wee1-2* mutant alleles was shown to be similar to that of wild type plants (see fig 3.1. for wild type controls). (Scale Bars: 50 µm).

Figure 3.7. Mutants affecting *Arabidopsis* E2F genes showed no change in cell death levels

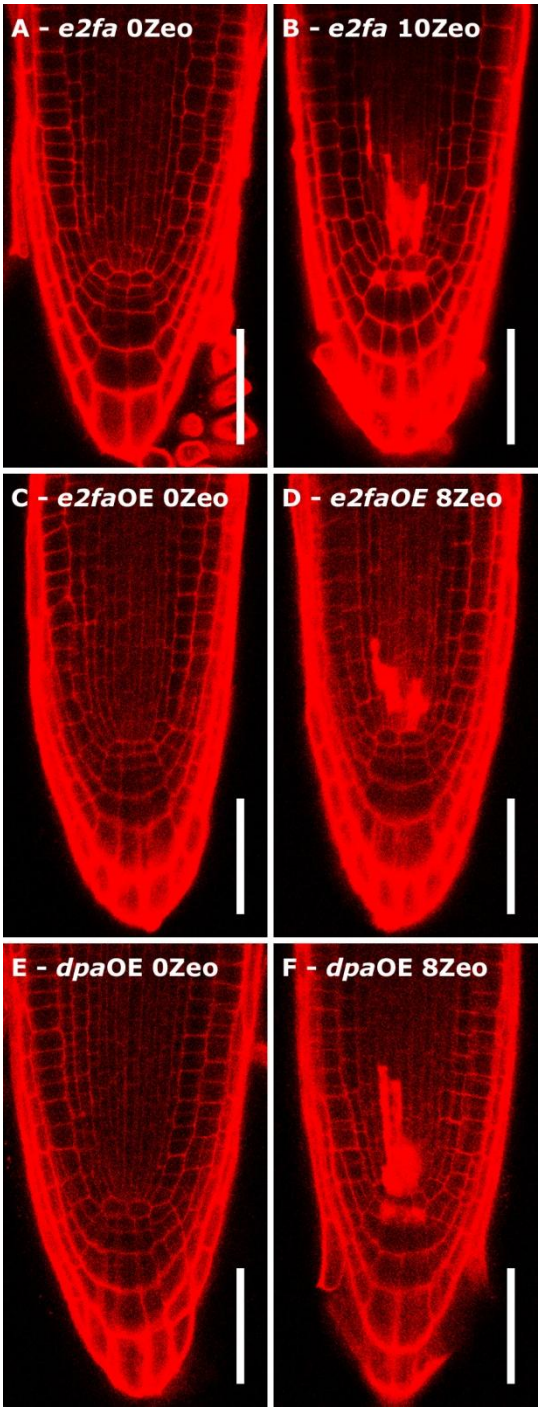

***E2F* mutant and *E2F/Dpa* overexpressors were treated with zeocin for 24 hrs.** No effect of cell death was seen in either mutants or overexpressors. Different zeocin stocks required different concentrations to achieve the same effect (see fig 3.1. for wild type controls). (Scale bars: 50 μm).

3.2.6. Telomerase (TERT) mutants showed slight sensitivity to DNA damage

Results obtained earlier in this chapter from mutants defective in NHEJ showed spontaneous death of root initials in the absence of zeocin. Genomic instability was proposed to result from unrepaired DSBs which can be induced though endogenous cellular processes such as ROS production (West *et al.* 2004). These background DNA breaks were therefore thought to be enough to activate cell death mechanisms within NHEJ mutants. To further analyse the effect of genomic instability, I tested cell death induction in mutants for telomerase which are known to show defects in telomere elongation (Fitzgerald *et al.* 1999).

Telomeres function to protect chromosome ends from DNA damage repair mechanisms. This enables the cell to differentiate between broken DNA ends and chromosome ends suppressing the activation of repair at telomeres. Telomeres shorten during each cell division due to the end replication problem (Osterhage and Friedman 2009). Stem cell populations utilise telomerase, a reverse transcriptase with a RNA subunit, to maintain telomere length (Denchi 2009). Loss of telomerase activity results in critically shortened telomeres which can fuse together using NHEJ pathways (Riha *et al.* 2006). This forms dicentric chromosomes that can break during anaphase and cause mass chromosomal arrangements and therefore genomic instability. An *Arabidopsis* telomerase (*TERT*) mutant has shown sensitivity to DNA damaging agents and shortened telomeres (Fitzgerald*, et al.* 1999, Watson *et al.* 2005). The aim was to test the telomerase mutant in order to identify possible spontaneous death and increased sensitivity to zeocin.

Telomerase mutants survive for 10 generations although they lose 250-500 bp from telomeres in each generation (Watson*, et al.* 2005). The 3rd generation *tert* mutant was treated with 0, 15 and 30 µg/ml zeocin for 24 hrs; with this stock, 30 µg/ml was the optimum treatment to induce cell death. In

control roots (0 µg/ml), no spontaneous cell death was seen in either wild type Columbia or *tert* mutants (Fig 3.8.). Roots treated with half the usual zeocin dose (15 µg/ml) displayed some cell death in WT (3 out of 10 roots) but *tert* mutants seemed to be slightly more sensitive (6 out of 10 roots showed cell death). Treatments of 30 µg/ml induced cell death in the majority of WT roots although some lacked consistent death of root initials. This compared to tert mutants which all displayed high levels of cell death. Death of the QC cells occurred in 3 out of 10 roots which were not shown in the WT; QC death was shown in chapter 2 to occur after exposure to high zeocin concentrations. These results suggests 3rd generation *tert* mutants display a slight sensitivity to DNA damage, less than that of the NHEJ mutants with showed spontaneous cell death in the absence of zeocin.

Figure 3.8. Genomically unstable roots lacking telomerase activity showed slight sensitivity to zeocin treatments

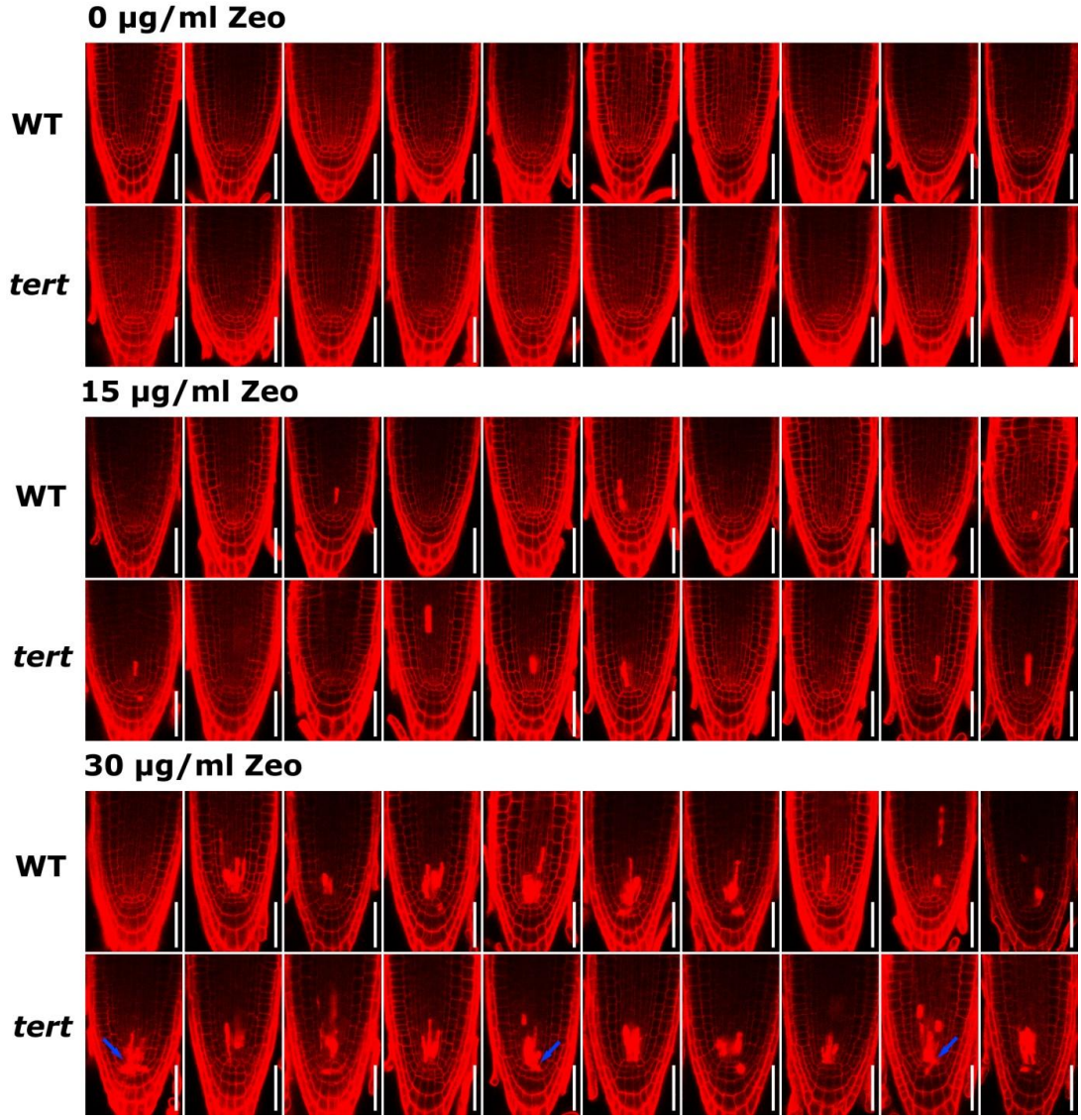

3rd generation *tert* mutants were treated with 0, 15 and 30 µg/ml zeocin for 24 hrs. No spontaneous cell death was seen in untreated controls. Slight sensitivity was shown at 15 µg/ml with 6 out of 10 roots displaying cell death (compared to 3 out of 10 in WT Columbia controls). A higher concentration of 30 µg/ml produced QC death (marked by blue arrows) not seen in wild type controls (3 out of 10 roots). (Scale Bars: 50 µm).

3.3. Discussion

Molecular pathways involved in activation of DNA damage responses appear to be reasonably conserved between animals and plants. This chapter aimed to investigate the role of homologous DNA repair genes in activating stem cell specific cell death in *Arabidopsis*. As described throughout this chapter, *Arabidopsis* contains many homologous genes for DNA damage perception and downstream responses such as DNA repair, cell cycle arrest and cell death. Unfortunately, not much is known about interactions between these proteins during damage signalling in plants. What is known about these signalling pathways is implicated from animal studies which are considerably more detailed. We therefore identified relevant *Arabidopsis* mutants suggested to have similar roles in plants and treated with zeocin to see if cell death levels were affected.

The majority of mutants tested were obtained from SALK and GABI-KAT collections, these T-DNA insertions are present within the Columbia background. Some mutants were however obtained in the WS background, Landsberg plants are also used in chapter 4 for shoot meristem imaging (mutants with ecotypes different to Columbia are indicated within the text). The first experiments aimed to investigate zeocin treatments of wild type Columbia, WS and Landsberg *erecta* seedlings to see if different accessions displayed similar hypersensitivity to zeocin. Results showed that WS and Columbia seedlings displayed a similar level of cell death within the root meristem. Landsberg seedlings however appeared to show slightly higher sensitivity to the same zeocin treatment with a larger area of cell death. These seedlings did not show death of QC cells which is a characteristic of roots treated with high levels of zeocin (shown in chapter 2). Cell death levels therefore appeared to vary amongst accessions of *Arabidopsis*.

Differences in cell death levels between accessions is not surprising, evidence has shown separate ecotypes to respond differently to certain stresses.

Nam *et al.* (1997) showed *Arabidopsis* ecotypes displayed variable susceptibility to crown gall disease as a result of *Agrobacterium* inoculation. Comparison of 11 ecotypes revealed a reduced crown gall phenotype in UE-1, this contrasted to Aa-0 which showed consistent development of tumours after inoculation. The difference between these ecotypes was eventually shown to be due to the effectiveness of T-DNA integration. More importantly, seeds and seedlings were treated with varying doses of γ-radiation to investigate the sensitivity of both ecotypes to DNA damage. Sensitivity of a certain ecotype was thought to reflect the ability for integration of T-DNA into the plants genome. UE-1, which displayed a reduced crown gall phenotype, was found to be considerably more sensitive to DNA damage. Previous evidence has therefore shown variable DNA damage responses within different *Arabidopsis* ecotypes.

The initial step of DNA damage signalling is known to be dependent on the MRN complex. This complex consisting of MRE11 (end resection), RAD50 (end anchoring) and NBS1 (downstream signalling) is well established in animals (Czornak*, et al.* 2008); see Chapter 1 for review on this process. Studies investigating mutations in components of the mammalian MRN complex have revealed their key roles in the DNA damage response. Three phosphosite mutants of *NBS1* in human fibroblasts which contain amino acid substitutions in sites phosphorylated by ATM were shown to affect cell survival. Cell survival was decreased due to defects in damage perception causing lack of a signalling response. Cell survival was also decreased in skin fibroblasts derived from patients with reduced MRE11 activity (Stewart *et al.* 1999). Disruption of mouse RAD50 resulted in early embryonic cell death (Luo *et al.* 1999). Null mutations of mammalian MRN components all cause embryonic lethality (Stracker *et al.* 2004); this contrasts to homologous genes in *Arabidopsis* where homozygous mutants survive, but are not without defects. Experiments treating mutants for MRN proteins with zeocin aimed to investigate their role in cell death activation.

Mutants of *Arabidopsis* MRE11 and NBS1 were obtained and treated with zeocin for 24 hrs; Different responses were however seen in each mutant. Mutants of *MRE11* showed spontaneous cell death within root initials in the absence of zeocin. Addition of zeocin however did not cause a significant increase in cell death. MRE11 is proposed to function as a nuclease in the repair of DSBs, resection by MRE11 at exposed ends is thought to create compatible ends for religation (Pardo*, et al.* 2009). In the absence of MRE11, broken ends may not be resected meaning incompatible ends are not joined. This would leave unrepaired endogenous DSBs which maybe enough to activate cell death within the root initials. Zeocin treatment however, which would induce more DSBs, did not cause a rise in cell death within the root meristem. Experiments with *nbs1* mutants showed wild type levels of cell death with no spontaneous cell death observed in untreated roots. NBS1 mutants in *Arabidopsis* do not display the defects observed with *rad50* and *mre11* plants. The AtNBS1 protein was shown to interact with MRE11 in a yeast 2 hybrid experiment and to have a synergistic role with ATM, but did not show hypersensitivity to x-rays or UV treatment (Waterworth*, et al.* 2007). This protein was selected due to sequence homology with other plant orthologs and human NBS1; it is however possible that plant NBS1 is not functional in DNA damage perception. The role of MRN components in DSB perception in plants is not entirely certain; this role is implied from mammalian studies. Results from *mre11* mutants indicate a possible role due to presence of spontaneous cell death; this is not clear as zeocin treatment did not induce higher levels of cell death as seen with DNA repair mutants. The role of MRN components would therefore need to be studied further. Future experiments could also use mutants for RAD50, the third component of the mammalian MRN complex, to further study effects of suggested MRN homologs.

Ataxia-telangiectasia mutated (ATM) is a well established target of the MRN complex and known key regulator of the DNA damage response (Lee and Paull 2005). Human deficiency of ATM results in many age related phenotypes

including cerebellar degradation, immunodeficiency, radiation sensitivity, chromosomal instability and cancer predisposition (Uziel *et al.* 2003). Disruption of *Atm* function in mice also showed presence of these phenotypes including male and female sterility (Barlow *et al.* 1996). While ATM deficiency causes abnormalities in normal development and sensitivity to DNA damage, mice homozygous mutants for *Atr* (Ataxia-telangiectasia related) are embryonic lethal (Ruzankina *et al.* 2007). ATM and ATR are similar based on sequence homology; despite this relation, both appear to contribute specific roles in DNA damage signalling. Roles for ATM and ATR in DNA damage signalling are thought to be specific to perception of DSB and replication stress respectively (See chapter 1 for review on ATM and ATR signalling in response to DNA damage).

Homologous *ATM* and *ATR* genes have been identified in *Arabidopsis*. An *ATM* homolog was first described by Garcia *et al.* (2000), its expression was found to be upregulated after γ-irradiation. A later paper (Garcia*, et al.* 2003) showed partial sterility in the *atm-1* mutant, defects in meiosis and sensitivity to irradiation. Characterisation of the ATR allele in *Arabidopsis* showed sensitivity to replication blocking treatments with hydroxyurea and UV (Culligan*, et al.* 2004). Irradiation treatments however showed only slight sensitivity mimicking roles proposed in animal studies where ATM is essential after DSB formation and ATR after replication stress. Microarray analysis of ATM dependent genes induced after γ-irradiation has also shown upregulation of many genes involved in DNA repair (Culligan*, et al.* 2006). These results point to a very strong role for ATM and ATR homologs in the DNA damage response in *Arabidopsis*.

Initial experiments using two mutant alleles of *ATM* (*atm-1* & *atm-2*) and one of *ATR* (*atr-2*) showed exciting results. All *ATM* and *ATR* alleles showed lack of cell death after zeocin and x-ray treatment indicating an important role in cell death activation. This lack of cell death was shown to be statistically significant through use of the Fisher exact test, used to determine significance with small sample sizes. Previous studies in mouse have shown ATM to be essential in

activating cell death in stem cell populations (Heyer*, et al.* 2000). This study showed mouse ESCs (embryonic stem cells) were hypersensitive to low doses of irradiation, mice deficient for *Atm* and *p53* showed stem cell survival after DNA damaging treatment. It therefore appears here that the role of ATM in DNA repair and cell death activation is conserved in plants and animals. Plants however lack a known homolog for *p53*, a gene essential for activating a wide range of DNA damage responses downstream of ATM in animals (See chapter 1 for review).

Roles for ATR in normal development appear to be essential, mice carrying homozygous mutations for *Atr* are embryonic lethal. Ruzankina *et al.* (2007) created a recombinase based system to remove ATR activity in mature mice. Cre recombinase was fused to the estrogen receptor ERT2 which is activated in the presence of tamoxifen. This enabled removal of functional ATR from transgenic mice harbouring a construct containing wild type *Atr* flanked by lox recombination sites. Removal of *Atr* in adult mice results in generation of a number of age related phenotypes and stem cell depletion. This contrasts greatly to plants where homozygous mutants of *ATR* are developmentally normal under standard growth conditions (Culligan*, et al.* 2004). Culligan *et al.* (2004) showed *ATR* mutants were susceptible to replication stress but not especially sensitive to DNA damage. ATR is however seen to be essential in activating stem cell specific cell death in response to zeocin and x-rays. It is therefore possible that the role of ATR is not entirely specific to replication stress. A study by Garcia-Muse & Boulton (2005) showed *C. elegans atl-1* (ATR homolog) is involved in processing of DSBs. Experiments showed *atl-1* is recruited to DSBs independently of ATM and is involved in initiating apoptosis in response to DSBs. A model proposed in this paper suggests exonuclease activity by MRN in the processing of broken DSB ends leads to binding of RPA to ssDNA. Presence of RPA is essential in activating ATR in conjunction with ATRIP, this RPA binding may explain ATR activity in activating cell death in root initials. This however

does not explain why remaining ATM activity in the *ATR* mutant does not activate cell death. These results suggest that ATM and ATR interaction may be essential to activate stem cell specific cell death in *Arabidopsis*.

In experiments using zeocin and x-rays, some residual cell death was seen in *ATM* and *ATR* mutants. These mutants represent strong loss of function alleles, it is however possible that some residual ATM and ATR activity may remain. Another explanation for this cell death is that continuation through the cell cycle without activation of repair mechanisms could result in cell death independently of ATM or ATR signalling. High x-ray treatments (80 gray) of the *atr-2* mutant showed cell death within stele cells above the population of root initials. *Arabidopsis* ATR has been shown to regulate cell cycle checkpoints in response to genotoxic stress (Culligan*, et al.* 2004). Loss of ATR activity could therefore result in cell death of cells undergoing cell division but not drastically affect the stem cells, which divide relatively slowly in the root meristem.

In animals, ATM and ATR activation leads to activation of downstream processes including initiation of DNA repair mechanisms which can re-ligate broken DNA ends. Two primary pathways are known to act in the repair of DSBs in animals, homologous recombination (HR) and non-homologous end joining (NHEJ). HR requires a homologous template such as a sister chromatid to mediate repair. This pathway is relatively error free but is active only at late S-G2 phase (Bernstein and Rothstein 2009). This contrasts to NHEJ where broken ends are processed by the MRN complex and relegated directly; this is the predominant pathway and is predominant in G1. See chapter 1 for an extensive review of the HR and NHEJ pathways.

For experiments investigating DSB repair pathways, mutants were identified for involvement in both mechanisms. As NHEJ is the predominant repair pathway in animals, conserved components between plants and animals were investigated. *Arabidopsis* lacks known homologs for *DNA-PK* but related KU70, KU80, XRCC4 and LIGIV proteins have been identified (Riha *et al.* 2002,

van Attikum*, et al.* 2003, West*, et al.* 2000, West*, et al.* 2002). The *atKU80* mutants show high sensitivity to DNA damaging agents including bleomycin and menadione (West*, et al.* 2002). Mutants for *AtKU70* also show sensitivity to MMS and γ-radiation, telomeres are also affected in this mutant (Riha*, et al.* 2002). The *AtLIGIV* homolog also displayed sensitivity to MMS and x-rays; T-DNA integration was not affected in this mutant suggesting a specific role for DNA repair (van Attikum*, et al.* 2003). *Arabidopsis* LIGIV was also shown to be upregulated after γ-irradiation and to interact with and *XRCC4* homolog (West*, et al.* 2000). Presence of these mutants in *Arabidopsis* suggests a similar role for a NHEJ type mechanism in the repair of DSBs in plants.

Results obtained from zeocin treatments of *ku80* and *lig4* mutants showed increased sensitivity within stem cell populations. In the absence of zeocin, spontaneous cell death was observed within the root initials which occurred very frequently (~50% of untreated roots showed at least one dead cell). This was shown to be statistically significant using Fisher's exact test. Cell death was shown to be extensive after treatment of both mutants with zeocin indicating high sensitivity to DNA damage compared with wild type. This high sensitivity is to be expected within mutants unable to repair DSBs. Endogenous DNA breaks occur under normal cellular conditions from metabolic processes; this appears to be enough to initiate cell death of stem cells. Increase in DSBs from zeocin treatment therefore results in higher levels of cell death than experienced in wild type roots. These results are also consistent with studies involving mice LIGIV mutants. Null mutants of the mouse *Lig4* gene result in early embryonic lethality which is a common feature among DNA repair proteins, expression of a hypomorphic allele enabled Nijnik *et al.* (2007) to study effects of mutated *Lig4*. The $Lig4^{Y288C}$ hypomorphic mutant displayed ageing phenotypes similar to those described by Ruzankina *et al.* (2007) in the knock out of ATR. Maintenance of stem cells was found to be impaired in the $Lig4^{Y288C}$ mice resulting in loss of stem cells. This loss at attributed to overactive apoptosis in

stem populations, this was proposed to be due to defective LIGIV being unable to repair endogenous DSBs. In addition, *Ku80* deficient mice also experienced hypersensitivity to DNA damage (Nussenzweig *et al.* 1997). These results are therefore consistent with animal studies into deficiency of NHEJ components.

In addition to treating mutants for NHEJ pathways, the *RAD51* mutant proposed to be defective in HR was also treated with zeocin. RAD51 proteins function downstream of ATM and ATR and act to direct strand invasion of broken DNA ends into the homologous template (Bernstein and Rothstein 2009). Seven RAD51 paralogs exist in vertebrates and *Arabidopsis* which include *RAD51*, *RAD51B*, *RAD51C*, *RAD51D*, *XRCC2*, *DMC1* and *XRCC3* (Bleuyard*, et al.* 2005). *Arabidopsis* RAD51 has been shown to be essential for meiosis and homozygous *rad51-1* mutants are sterile (Li*, et al.* 2004). Bleuyard *et al.* (2005) found three paralogs *AtRAD51B*, *AtRAD51C* and *AtXRCC2* were sensitive to crosslinking agent mitomycin C but not ionizing radiation. To investigate the effects of zeocin on cell death of RAD51 proteins, the *rad51-1* mutant as used by Li *et al.* (2004) was treated with zeocin. Homozygous mutants for *rad51* showed no effect on cell death, QC death was however observed in the single surviving homozygous mutant. This could reflect a higher sensitivity to DNA damage as higher zeocin concentrations activate QC death in wild type seedlings. QC death was observed occasionally in wild type roots meaning this result cannot confirm a lower DNA damage tolerance; future experiments could use larger numbers of seedlings to compare QC death between *rad51-1* and wild type. Experiments investigating occurrence of spontaneous death in *rad51-1* seedlings however failed to show a significant increase in death in the absence of zeocin treatment. Spontaneous death was therefore thought not to occur in the *rad51* mutant. Roles for specific RAD51 paralogs maybe different in *Arabidopsis*, this allele could be more specific to meiotic recombination and not to DNA repair (Li*, et al.* 2004). It would be interesting to test additional RAD51 paralogs in plants to study sensitivity to DNA damage and potential occurrence of spontaneous cell death.

DNA repair mechanisms activated after DNA damage require time to act on DSBs before entering the next stage of the cell cycle. Cell cycle arrest is also a well characterised response to DNA damage in animals allowing stalling at G1 and G2 checkpoints. ATM and ATR signalling in response to a DSB can act to inhibit progression into S or M phase (Bucher and Britten 2008). ATM and ATR phosphorylate checkpoint kinases 1 and 2 which then act to inhibit activity of CDC25 phosphatases. CDC25 phosphatases act to remove inhibitory phosphates from CDK/cyclin complexes and aid cell cycle progression. Blocking CDC25 activity leads to cell cycle arrest. WEE1 kinase also functions downstream of ATM/ATR and acts to attach inhibitory phosphates to CDKs which inhibits cell cycle progression. CDC25 and WEE1 can therefore act as a switch, acting downstream of DNA damage to release or repress cell cycle progression. Additional functions of p53 and p21 act downstream of ATM and ATR to stall the cell cycle at G1, p53 activated downstream of ATM and ATR activates CDK inhibitor p21. Activity of p21 stops the cyclinE/CDK2 complex from affecting the pRB-E2F interaction and prevents transcription of E2F target genes. For a detailed review of cell cycle arrest after DNA damage see chapter 1.

To assess the connections between cell cycle arrest and death of root initials, mutants for *Arabidopsis* cell cycle arrest were treated with zeocin. Plants lack homologous genes for *CHK1*, *CHK2* and *CDC25* phosphatases. A candidate gene for *CDC25* was identified by Landrieu *et al.* (2004); further studies however suggest other functions for this gene in arsenate metabolism and not cell cycle control (Dissmeyer*, et al.* 2009). Despite lack of essential mammalian cell cycle arrest homologs, a WEE1 kinase was identified within the *Arabidopsis* genome (De Schutter*, et al.* 2007). This paper showed *in vitro* phosphorylation of CDKA;1 dependent on WEE1, sensitivity to DNA damage and requirement of ATM for activation. Seeds for *wee1-1* and *wee1-2* mutant alleles were obtained from the authors and treated with zeocin. These lines were proposed to abolish

DNA damage induced cell cycle arrest, no effect on cell death of root initials was observed.

More recently, Dissmeyer *et al.* (2009) suggested WEE1 activity was not essential for DNA damage dependent cell cycle arrest in *Arabidopsis*. To test the importance of P-loop phosphorylation, CDKA;1 constructs were produced by substituting this region with phosphomimicking and nonphosphorylatable animo acids. These constructs were transformed into homozygous *cdka;1* mutant backgrounds and examined for defects in cell cycle progression and sensitivity to HU. Phosphomimicking mutants displayed severely reduced cell proliferation and growth; however, the nonphosphorylatable variants unexpectedly resembled wild type plants. As *wee1* plants were proposed to lack the ability to arrest the cell cycle after DNA damage, it was expected nonphosphylatable CDKA;1 mutants would mimic the *wee1* phenotype after exposure to HU. Seedlings treated with HU responded in a similar way to wild type plants leading to the conclusion that the phosphorylation of CDKA;1 by WEE1 is not essential to arrest the cell cycle after DNA damage. Cell cycle control appears more complex in *Arabidopsis* due to presence of many additional cyclins and B-type CDKs (Francis 2007), its possible extra CDKs/cyclins could drive progression in a plant specific mechanism. Work by Dissmeyer *et al.* (2009) does not rule out the possibility that WEE1 functions to regulate the cell cycle downstream of DNA damage through phosphorylation of additional CDKs, including the plant specific B-type CDKs.

In addition to WEE1 mutants, defects in the retinoblastoma pathway were also investigated for a role in cell death. Wildwater *et al.* (2005) first characterised the *pRB* gene in *Arabidopsis*, these results were interesting because analysis of the root meristem in the RNAi knockdown line showed extensive cell death in the root initials. Retinoblastoma regulates progression of the cell cycle through binding E2F proteins; this interaction is prevented by cyclin/CDK complexes (Sun*, et al.* 2007). Released E2F transcription factors are

then able to act of cell proliferation genes. Studies in animals have also shown *E2F* genes to mediate cell death through activation of apoptosis and autophagy genes (Polager and Ginsberg 2008). Through this, E2F activity is thought to act as a switch, controlling either cell cycle progression or activating cell death. Cell death experienced in the pRB RNAi knockdown line (Wildwater*, et al.* 2005) could be due to uncontrolled release of E2F proteins activating cell death. To test this, mutants and over expression lines for E2Fa and also DPa, the E2F binding partner, were treated with zeocin. Overexpression of *E2Fa* was hypothesised to result in overactive cell death in the root initials as with the pRB RNAi line, cell death in all lines was however shown to be comparable to wild type. Experiments using cell cycle regulators therefore suggest cell death activation pathways act independently of cell cycle arrest pathways.

In addition to studying the effects on DNA repair mutants, a mutant known to exhibit genomic instability was also tested looking for occurrence of spontaneous cell death. Telomerase is a ribonucleoprotein complex composed of a RNA component (TERC) and a protein counterpart (TERT) (Deng and Chang 2007). The reverse transcriptase activity of Telomerase acts to elongate shortened telomeres using its RNA template to bind single stranded telomere ends. Progressive telomere shortening occurs through cell division due to the end replication problem (Osterhage and Friedman 2009). In mammalian somatic cells, telomerase is inactive allowing telomeres to become shorter throughout cell division. Telomerase is however active within stem cells and helps to maintain telomere length (Fitzgerald*, et al.* 1999). Loss of telomerase leads to shortening of telomeres in stem cell populations and eventually, when shortened beyond a critical length, fusion of chromosome ends through NHEJ pathways (Riha and Shippen 2003). This fusion creates genomic instability and could potentially lead to cell death activation.

A role for telomerase has been identified in plants, Fitzgerald *et al.* (1999) first characterised its activity in *Arabidopsis* and found telomere

shortening and onset of developmental defects in generation 6 (G6) of the mutant. Chromosomal fusions and sensitivity to DNA damage were also observed in G8 callus tissue (Watson*, et al.* 2005). The G3 mutant was obtained from the authors of these papers and treated with zeocin looking for enhanced susceptibility to DNA damage. In this experiment, *tert* mutants were shown to display slightly higher levels of cell death. Seedlings treated with 30 µg/ml zeocin showed normal cell death levels but contained QC death (which is a response seen in chapter 2 from high zeocin doses). Spontaneous cell death was however not witnessed in untreated seedlings. It would be interesting in future experiments to establish homozygous lines from generations up to G8 and perform the same experiment. Telomere length gets progressively shorter in subsequent generations of the mutant (Fitzgerald*, et al.* 1999). Developmental defects do not occur until G6, further telomere loss beyond G3 maybe essential to activate spontaneous cell death.

To conclude, key signalling transducers ATM and ATR were found to be essential in activating cell death of root initials in response to DNA damage. Results from the proposed MRN complex proteins involved in ATM/ATR activation in animals however did not show clear involvement in this process. Mutants deficient in NHEJ but not HR were shown to exhibit spontaneous cell death in the absence of zeocin, suggesting endogenous DSBs were enough to activate stem cell specific cell death. Overall, these results show that cell death is a genetically programmed response to DNA damage in *Arabidopsis* root initials.

Chapter 4 – Exploring mechanisms of meristem cell death after DNA damage

4.1. Introduction

All multicellular organisms are able to initiate cell suicide pathways in response to developmental cues or cellular stress (Reape*, et al.* 2008, Williams and Dickman 2008). In animals, three main categories of programmed cell death are well characterised; apoptosis, autophagy and necrosis. These categories are defined by morphological features exhibited by the dying cell (van Doorn and Woltering 2005). Key characteristics of apoptosis include nuclear fragmentation, formation of apoptotic bodies and final degradation in the lysosome of a neighbouring cell (Elmore 2007). This contrasts to autophagy ("self-eating") where cellular components are degraded within the cell's own lysosome (Geng and Klionsky 2008). Necrosis is described as a response to extreme physiological conditions (Williams and Dickman 2008); necrotic traits include swelling of the cell and collapse of the plasma membrane causing rapid lysis (Proskuryakov*, et al.* 2003). A detailed review of these cell death pathways is discussed more extensively in chapter 1.

Little is understood about cell death pathways in plants. As mentioned in chapter 2, plants are known to lack several key executioners for apoptosis including caspases, p53, CHK1 and CHK2 (Bonneau*, et al.* 2008, Cools and De Veylder 2009). Stem cell populations in mouse (Heyer*, et al.* 2000) and *C. elegans* (Garcia-Muse and Boulton 2005) have shown to induce apoptosis in response to low levels of DNA damage. Various similarities with mammalian cell death have however been described in *Arabidopsis* such as apoptotic-like cell shrinkage (McCabe *et al.* 1997) and presence of metacaspases (Vercammen*, et al.* 2004). However, true apoptotic death has been presumed not to occur in

plants (van Doorn and Woltering 2005), so the specific death of root initials in response to DNA damage described in previous chapters is likely to use a mechanism different from apoptosis.

This chapter therefore aimed to identify cell death mechanisms in plants which operate in response to DNA damage. Initial experiments involved treating mutants implied in plant cell death pathways with zeocin looking for a reduction in cell death. Mutants included those for metacaspase genes (implicated as functional homologs of mammalian caspase genes), genes involved in initiating the hypersensitive response and Poly(ADP-ribose) polymerase (PARP) implicated in necrosis. In addition to this, electron microscopy was carried out on dying cells in an attempt to spot any morphological characteristics as described for mammalian cell death programs.

4.2. Results

4.2.1. Analysis of candidate apoptosis genes showed no effect on cell death

Apoptosis is well defined in mammalian programmed cell death as an efficient mechanism to exclude damaged cells from stem cell populations (Heyer*, et al.* 2000). A number of studies have shown p53 dependent apoptotic cell death of stem cells in response to DNA damaging treatments (Aladjem *et al.* 1998, Heyer*, et al.* 2000). True apoptosis as defined in animal studies, however, was proposed not to occur in plants (van Doorn and Woltering 2005). Nevertheless, plants display similarities in other apoptotic traits such as DNA cleavage (laddering), DNA fragmentation and the activation of caspase-like proteases (Williams and Dickman 2008). It is therefore possible that a unique cell death mechanism evolutionarily related to apoptosis could be activated in response to DNA damage.

In animals, caspases are involved in the initiation of apoptotic cell death (reviewed in chapter 1). Actions of caspases are induced by stress signals produced in response to endogenous and exogenous factors. This activates a cascade of proteolytic activity, which is necessary to effectively break down the cell. *Arabidopsis* has shown to lack orthologous caspase genes based on sequence homology (Bonneau*, et al.* 2008). A family of arginine proteases called metacaspases were identified in *Arabidopsis* and cloned by Vercammen *et al.* (2004), which share structural similarities with mammalian caspases. The metacaspase family comprises of 9 genes in *Arabidopsis*, these are divided into two subcategories based on sequence homology (Watanabe and Lam 2004). Experiments on metacaspase mutants have revealed links to DNA damage responses. Expression of *AtMC8* (*ARABIDOPSIS METACASPASE 8*) is upregulated after treatment with DNA damaging agents, mutants also showed enhanced

growth on methyl viologen compared with wild type plants (He*, et al.* 2008). Analysis of genes upregulated after γ-rays also showed ATM dependent induction of *AtMC1* (Ricaud *et al.* 2007). It was therefore possible that metacaspase genes could be involved in stem cell specific cell death in *Arabidopsis*.

To test the requirement for metacaspase genes in initial specific cell death, *AtMC8* and *AtMC1* mutants were exposed to zeocin for 24 hrs (Fig 4.1.). Roots were stained with propidium iodide and examined for any reduced cell death phenotype. Unfortunately, single metacaspase mutants failed to show a reduction in cell death of initials compared with wild type plants.

Figure 4.1. Analysis of metacaspase mutants showed no reduction in cell death after zeocin treatment

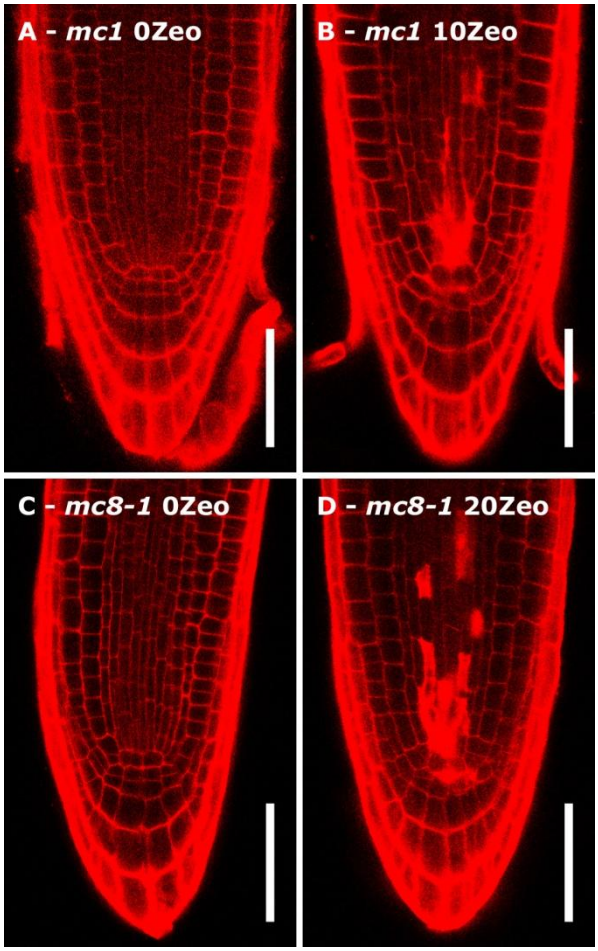

***AtMC1* and *AtMC8* mutants were treated with zeocin for 24 hrs; no difference in cell death was seen compared to controls.** Seedlings were treated with zeocin at shown concentrations. Different zeocin stocks required different concentrations to induce the same response as described in chapter 3. See fig 3.1. for examples of cell death in wild type roots. (Scale Bars: 50 μm).

4.2.2. Disruption of signals involved in the hypersensitive response (HR) showed no effect on cell death in the root meristem

One well known example of programmed cell death in plants is the hypersensitive response (HR) caused by exposure to fungi, bacteria and viruses (van Doorn and Woltering 2005). Pathogens affect plants and animals through the release of effector proteins which modify the state of the infected host cells (DeYoung and Innes 2006). The recognition of pathogen-derived avirulence (Avr) effectors by plant resistance (R) proteins triggers a defence response in *Arabidopsis* that often results in rapid cell death known as the hypersensitive response (Marathe and Dinesh-Kumar 2003). The hypersensitive response involves a burst of reactive oxygen species initiating cell death through oxidative stress (Alvarez 2000). Cell death surrounding the site of infection prevents spread of the pathogen through plant tissues.

Plant hormones are known to play important roles in activation of the hypersensitive response downstream of resistance protein interactions (Bari and Jones 2009). Salicylic acid (SA) accumulation is linked to defence responses to biotrophic pathogens where jasmonates (JA) and ethylene (ET) respond specifically to necrotrophic pathogens and herbivorous insects (Bari and Jones 2009). Accumulation of these hormones leads to an oxidative burst in the host cell. As this response is well established in plants, experiments using plants defective in these hormone signalling pathways were used to study the role of hormones in activating initial specific cell death.

A central role of SA in the plant disease response was proposed using plants expressing the bacterial *salicylate hydroxylase* (*NahG*) gene (Delaney *et al.* 1994). NahG causes depletion of SA levels, *Arabidopsis* plants expressing *NahG* showed susceptibility to fungal pathogens indicated by an increase in trypan blue staining (Delaney*, et al.* 1994). In addition, mutants of the *SALICYLIC ACID INDUCTION DEFICIENT 2* (*SID2*) gene which is involved in a

key biochemical step of the production of SA contain very little SA (Heck *et al.* 2003). Both mutants were treated with zeocin for 24 hrs and imaged looking for differences in cell death compared with WT. Unfortunately, neither *NahG* expressing plants nor *sid2-5* mutants showed any difference in cell death patterns in the root meristem compared with controls (Fig 4.2.).

In addition to salicylic acid, the gaseous hormone ethylene is also well established in responses to stress including HR (Overmyer *et al.* 2000). Ethylene has also been shown to trigger programmed cell death in a number of developmental processes (Overmyer*, et al.* 2000). Analysis of ethylene signalling genes has shown *ETHYLENE INSENSITIVE 2* (*EIN2*) to be essential for transduction of ethylene signalling (Alonso *et al.* 1999). In addition, the *RADICAL INDUCED CELL DEATH 1* (*RCD1*) gene is known to antagonise ethylene production (Wang *et al.* 2002). Using *ein2-5* and *rcd1-1* mutants, *ein2-5* resulting in loss of ethylene perception and *rcd1-1* resulting in over production of ethylene, zeocin treatments were also performed to study effects on death of initials. No change in cell death was seen in either mutant (Fig 4.3.).

Figure 4.2. *NahG* and *Sid2-1* seedlings defective in salicylic acid (SA) accumulation showed initial specific cell death comparable to wild type

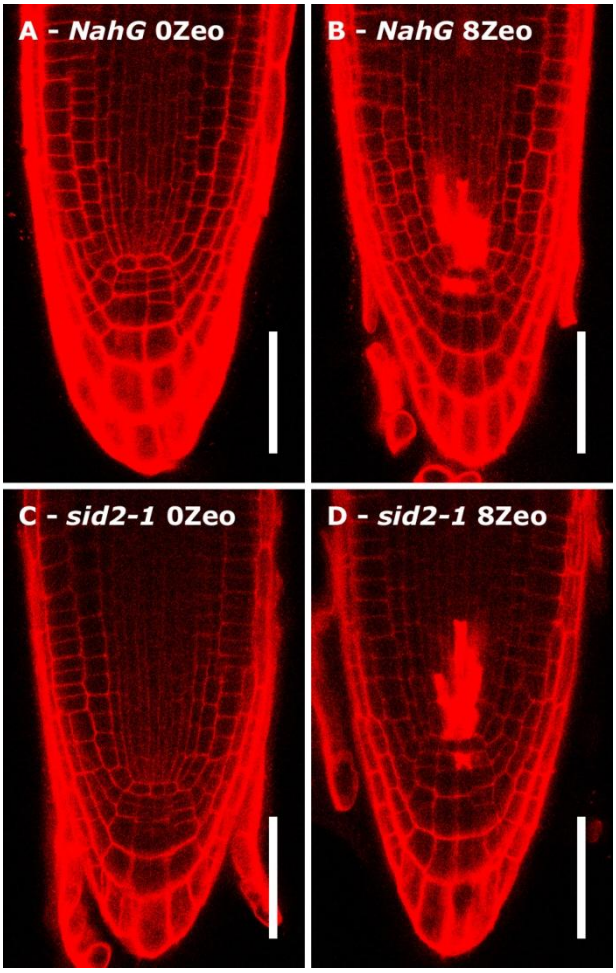

***NahG* and *sid2-1* are known to affect SA accumulation through depletion and preventing production respectively.** Seedlings were treated for 24 hrs with zeocin. Cell death was comparable to wild type levels (see fig 3.1. for wild type controls). (Scale Bars: 50 μm).

Figure 4.3. Mutants affecting ethylene signalling showed no reduction in cell death

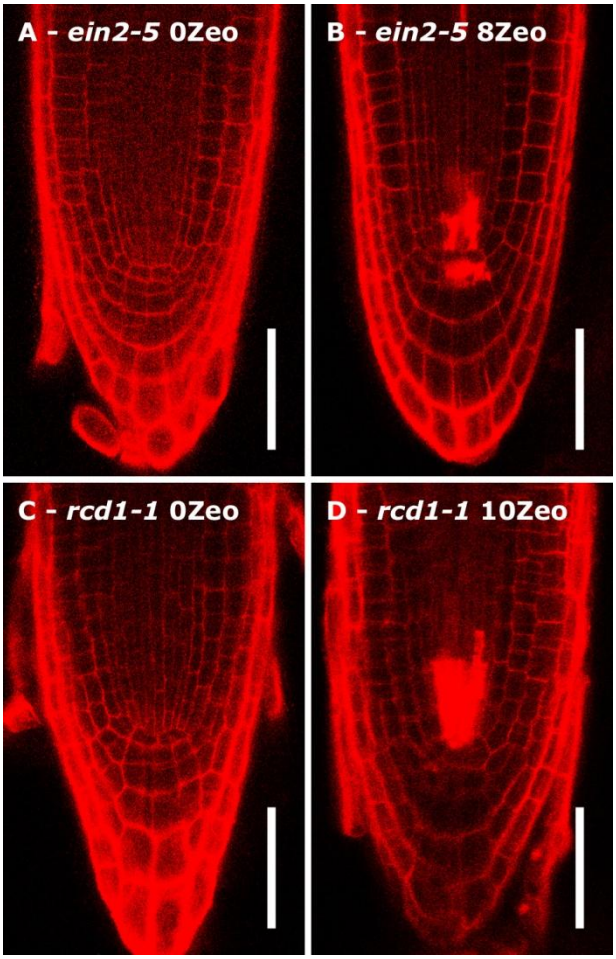

Mutants defective in ethylene signalling showed wild type levels of cell death within root initials. Seedlings were treated with 8 or 10 µg/ml (zeocin concentration differed due to the use of different stocks) for 24 hrs, stained with PI and imaged. See fig 3.1. for wild type controls. (Scale Bars: 50 µm).

4.2.3. *Poly(ADP-ribose) Polymerase* (*PARP*) genes did not influence cell death within the root meristem

To further assess known cell death activators, the actions of Poly(ADP-ribose) polymerase (PARP) were studied in relevance to death of root initials. *PARP-1* is activated in response to double and single stranded DNA breaks and is involved in the repair process of moderate levels of DNA damage (Ha and Snyder 1999). A second *PARP* gene *PARP-2* has also been identified with similarities to *PARP-1*, the latter however accounts for 85% of PARP activity in animals (Woodhouse and Dianov 2008). PARP proteins are responsible for the production of poly(ADP-ribose) polymers (PAR) in response to genotoxic stress (Heeres and Hergenrother 2007). Using NAD+ as a substrate, PARP-1 builds these polymers of ADP ribose units which are attached to a number of proteins including histones, polymerases and PARP-1 itself (Andrabi *et al.* 2006). Cellular accumulation of PAR can result in either activation of DNA repair or cell death as described by Heeres & Hergenrother (2007). In response to moderate DNA damage, PARP activation causes poly(ADP-ribosyl)ation of DNA damage proteins leading to DNA repair and cell survival. Large amounts of DNA damage leads to over accumulation of PAR produced by PARP-1. Overproduction of PAR can lead to metabolic stress on the cell severely reducing ATP levels. This metabolic stress eventually leads to activation of necrotic cell death (Ha and Snyder 1999).

Homologous genes have been identified for *PARP-1* and *PARP-2* in *Arabidopsis*; both genes were found to be highly expressed after exposure to ionizing radiation (Doucet-Chabeaud*, et al.* 2001). While in animals PARP-1 is responsible for the majority of PARP activity, Doucet-Cheabeaud *et al.* (2001) has shown both *Arabidopsis* PARP genes to be equally induced after DSB formation. To first study the effects of PARP activity on the death of root initials, seedlings of the *parp-2* mutant were treated with zeocin looking for reduction in cell death (Fig 4.4a & b). Cell death comparable to wild type was observed in

these seedlings. In addition to treating a *parp-2* mutant, I also obtained RNAi lines used previously to inhibit PARP activity. De Block *et al.* (2005) generated RNAi PARP plants to specifically target *PARP-1* and *PARP-2* activity through a shared sequence surrounding the PARP signature motif present in both genes. These plants were found to be tolerant to drought, high light intensity and methyl viologen which are known to induce DNA damage. Zeocin treatments of these lines in my experiments however showed cell death comparable with wild type seedlings (Fig 4.4d & f).

Results with the *parp-2* mutant and RNAi lines failed to show any effect on cell death. In parallel to using knockout and knock down lines, PARP inhibitor 3-methoxybenzamide (3-MB) was also used to block PARP function. This inhibitor has previously shown to strongly help survival of *Brassica napus* callus after exposure to oxidative stress (De Block*, et al.* 2005). LTI6B-GFP seedlings were treated on media containing zeocin alone and zeocin with 1 mM 3-MB (Fig 4.5.). After 24 hrs treatment, seedlings were stained with Sytox orange and imaged. Results detected a decrease in cell death compared with control treatment without zeocin. Out of 8 seedlings treated with 20 µg/ml zeocin, 19 dead initials or daughter cells were scored. This compared to 8 seedlings treated with 20 µg/ml zeocin and 1 mM 3-MB in which 8 dead initials or daughter cells were scored. No cell death was seen in the untreated control or control treated with 1 mM 3-MB.

Figure 4.4. *PARP* inactivation through T-DNA and RNAi lines showed no effect on cell death levels

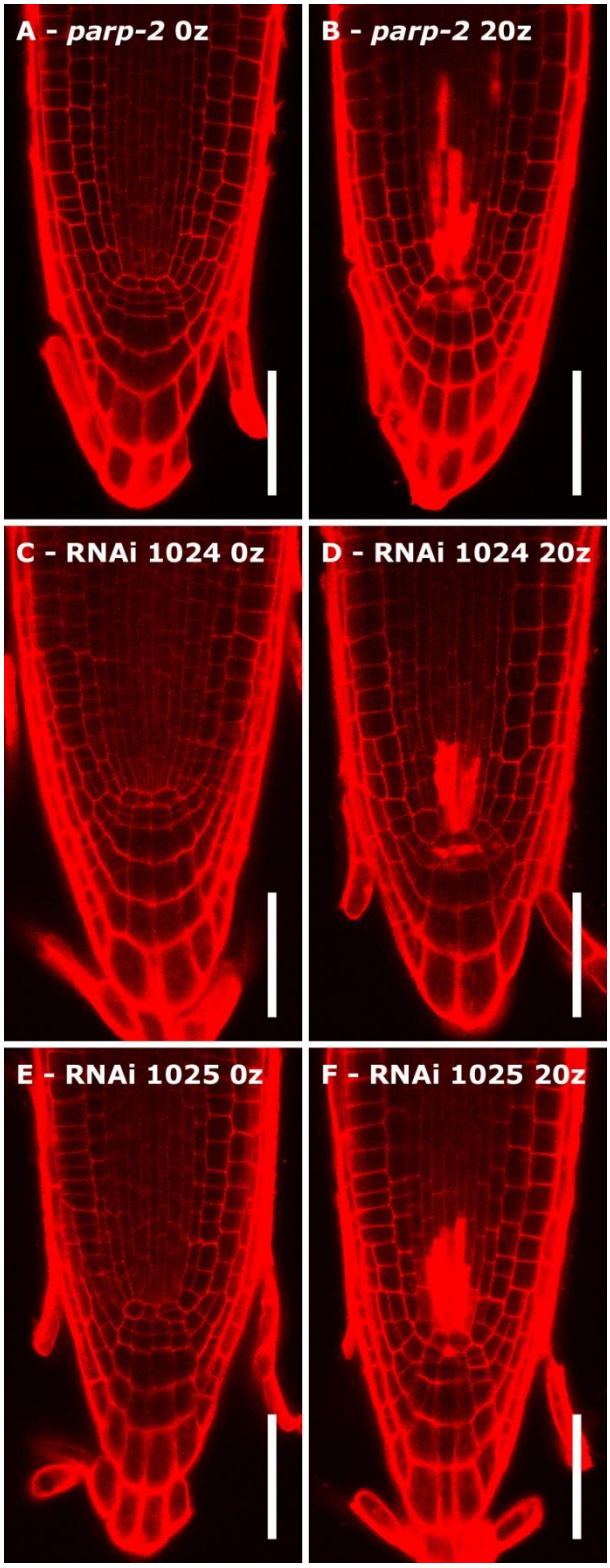

***parp-2* T-DNA mutant and two separate RNAi lines known to affect PARP activity showed no reduction in cell death.** Seedlings were treated for 24 hrs with 20 µg/ml zeocin, stained with PI and imaged. See fig 3.1. for wild type controls. (Scale Bars: 50 µg/ml).

Figure 4.5. Treatment with PARP inhibitor 3-methoxybenzamide (3-MB) showed slight decrease in cell death

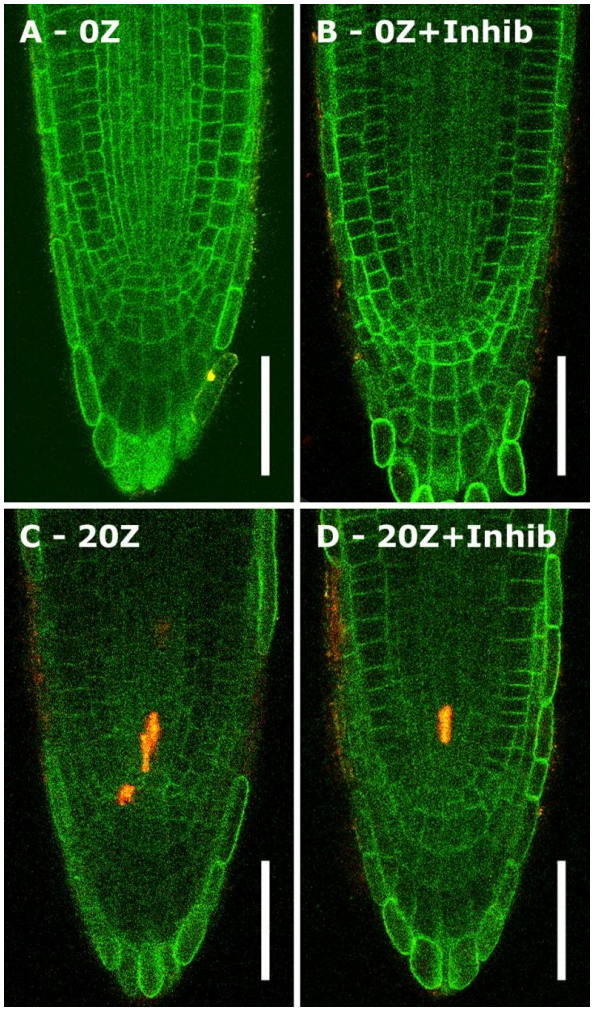

35S:GFP-LTI6B seedlings were exposed to zeocin and PARP inhibitor 3-MB on supplemented GM plates to examine the effect on cell death. (**A**) No treatment (**B**) 0 µg/ml zeocin & 1 mM 3-MB (**C**) 20 µg/ml zeocin (**D**) 20 µg/ml zeocin and 1 mM 3-MB. A slight reduction in cell death was witnessed in seedlings exposed to the PARP inhibitor. (Scale Bars: 50 µM).

4.2.4. Transmission Electron Microscopy revealed presence of autophagic-like vesicles within dying root initials

In animals, analysis of morphology within dying cells allows categorisation into one of the three mechanisms of programmed cell death. Features of apoptosis include cell shrinkage, membrane blebbing and nuclear fragmentation, which contrast to necrotic cells that display cellular swelling and rupture of the plasma membrane (Elmore 2007). Autophagy on the other hand is clearly shown by presence of large autophagosomes contained within the cytoplasm before death is initiated (Klionsky 2007). Morphological traits of programmed cell death in plants are not so well defined; some common features are however described in plant cells. Programmed cell death in carrot cells has shown retraction of the plasma membrane away from the cell wall in response to high temperature (McCabe*, et al.* 1997). This mimics the cytoplasmic condensation shown in mammalian apoptosis (Elmore 2007). McCabe *et al.* (1997) showed membrane retraction was not exhibited by cells undergoing necrotic death at higher temperatures. Features of autophagic death have also been shown in plant cells after concanamycin-A treatment using electron microscopy (Yoshimoto *et al.* 2004). Using transmission electron microscopy (TEM) imaging, I aimed to identify known cell death traits within dying root initials.

To study the morphology of dying root initials, seedlings were treated with 20 µg/ml zeocin for 16 hrs, as results from chapter 2 (Fig 2.6.) showed cell death was initiated after approximately 16 hrs treatment. Roots were then fixed, sectioned and prepared for TEM imaging (Fig 4.6.). Images showed clear presence of vesicles contained within dying cells similar to those shown in electron micrographs by Yoshimoto *et al.* (2004). Presence of these vesicles was seen in root initials and daughter cells. At more advanced stages of cell death, the cytoplasm and nucleus were stained heavily and organelles became

indisctinct (Fig 4.7.). Dead or dying cells were shown to collapse with neighbouring cells expanding to occupy space.

Figure 4.6. Electron micrographs of dying root initials show features of autophagy

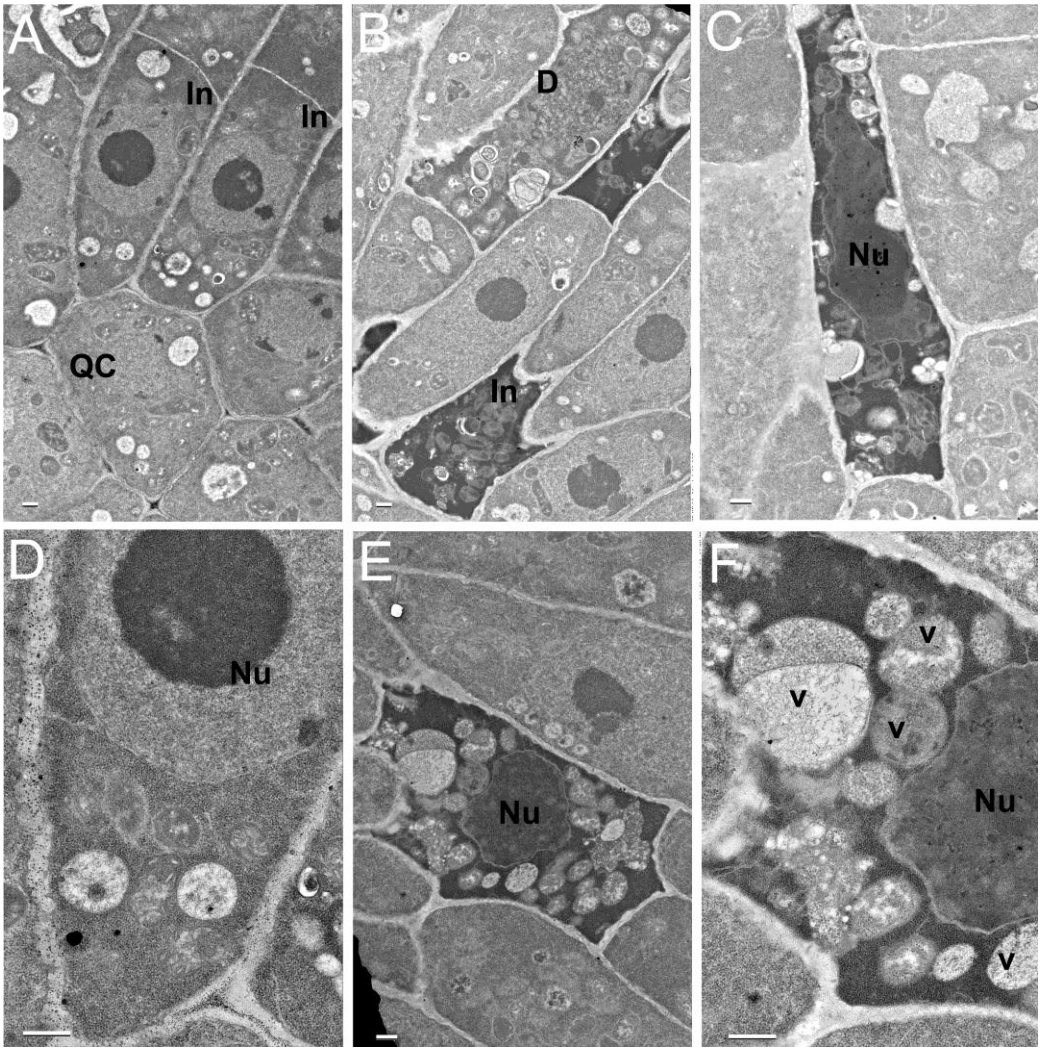

Wild type Columbia seedlings were treated for 16 hrs on 20 µg/ml zeocin, fixed and sectioned for TEM analysis. (**A** & **D**) Sections showing QC and initials (In) of an untreated root tip. Section *D* represents higher magnification of *A* showing the nucleus (Nu) and organelles of a root initial. (**B**, **C**, **E** & **F**) Sections of zeocin treated roots including initials (In) and daughter cells (D). Accumulation of vesicles (V) is shown in dying initial and daughter cells in section *B* and *C.* Clearly defined vesicles are seen in *E*, Section *F* represents *E* at higher magnification. Dense cytoplasm and vesicles resemble features of autophagic cell death (Klionsky 2007). (Scale Bars: 500 nm).

Figure 4.7. Dying cells in terminal stage of PCD shown to collapse

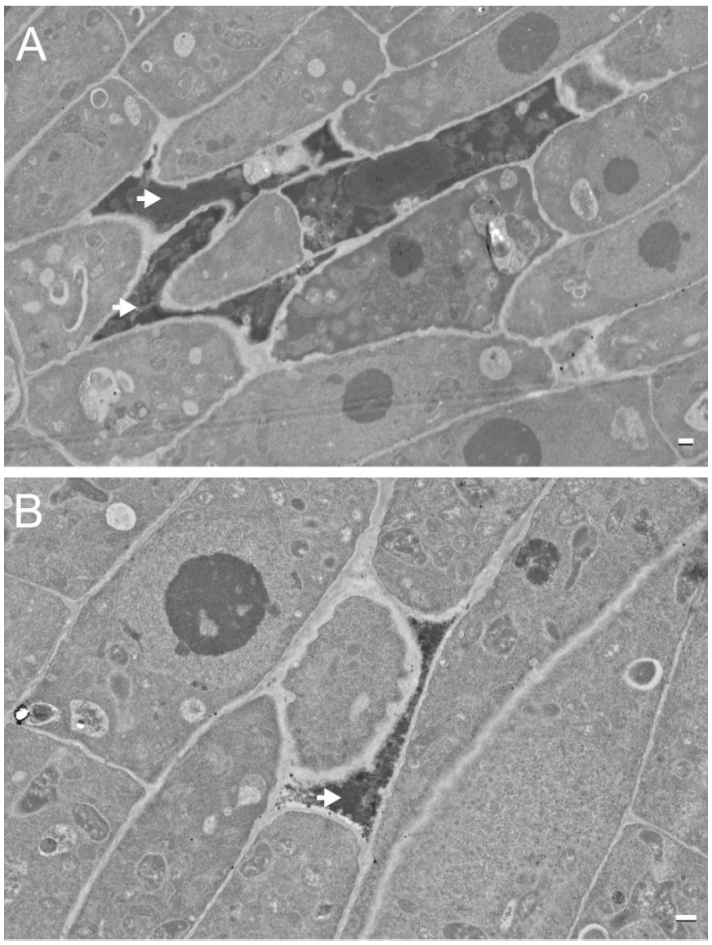

Terminal stages of cell death induced by DNA damage in the root meristem. (**A** and **B**) Electron micrographs of root meristem cells at 24 h after zeocin treatment. Arrows indicate collapsed cells, with neighbouring cells expanding to occupy their space. (Scale bars: 0.5 μm.)

4.2.5. *AUTOPHAGY-RELATED* (*ATG*) mutants affecting vesicle formation showed no change in cell death levels

Results obtained from TEM imaging showed presence of putative autophagic vesicles within dying root initials. In order to further study autophagy within these cells, mutants known to be defective in autophagy pathways in plants were examined. In mammals, autophagy-related (*ATG*) genes have been shown to regulate autophagic processes (Longatti and Tooze 2009). These genes are involved in production of double-membrane vesicles which engulf portions of cytoplasm in macroautophagy forming the autophagosome (Geng and Klionsky 2008). The autophagosome is then degraded within the lysosome of the dying cell (for detailed review of the autophagy process see chapter 1).

Arabidopsis also shows plant autophagic processes that are mediated by *ATG* genes. Experiments by Inoue *et al.* (2006) showed autophagic features in root cells exposed to the membrane-permeable cysteine protease inhibitor E-64d. Mutants for ATG proteins showed significant reduction of autophagic death after E-64d treatment, the role for *ATG* in plant autophagy appears similar to that of mammals. Autophagy genes *ATG5*, *ATG6*, *ATG7*, *ATG10*, *ATG18* have shown to be essential for vesicle formation in *Arabidopsis* (Phillips *et al.* 2008, Qin *et al.* 2007, Xiong *et al.* 2005). In order to investigate the role of ATG genes in death of root initials, I treated mutants of *ATG5*, *ATG6*, *ATG7* and *ATG18* with zeocin for 24 hrs looking for any reduction in cell death due to defective autophagy pathways (Fig 4.8.). Treatment of these mutants failed to shown any significant reduction in cell death of root initials compared to wild type.

In parallel to experiments using mutants for autophagy genes, I also aimed to label vesicles for imaging by confocal microscopy. Use of lysotracker has been used previously to stain cytoplasmic vesicles in palisade parenchyma cells undergoing autophagic death (Hofius*, et al.* 2009). To allow labelling of autophagic cells with lysotracker, I treated wild type seedlings for 16 hrs with 20

µg/ml zeocin (initiation of cell death was witnessed after 16 hr in chapter 2). Roots were then stained with lysotracker and imaged; membrane stains were omitted due to their ability to enter dead or dying cells (Fig 4.9.). Dead initials at first appeared to be marked by the stain which saturated the whole cell. This does not compare to staining by Hofius *et al.* (2009) where specific vesicles were marked within cells, not the entire cell. The area of staining in these roots appears to be due to collection of stain within dead cells rather than specific staining of vesicles (marked by arrows in fig 4.9b). Lysotracker can enter all cells, but specifically labels organelles with acidic pH levels such as autophagosomes (Lysotracker manual, Invitrogen and Liu *et al.* 2005). Lines expressing the *ATG8:GFP* construct have been used previously to show initiation of autophagy in plants (Yoshimoto*, et al.* 2004). When using this line in a similar approach to that of the lysotracker imaging, the possibility of stain collecting within dead cells would be eliminated. Unfortunately, use of membrane stains could also saturate dead or dying initials so PI staining was omitted. Image stacks were taken when imaging roots of *ATG8:GFP* expressing seedlings, no clear presence of clusters of vesicles were present in root initials (Fig 4.9d). Presence of vesicles was however detected in root cap cells; this GFP signal was not detected in Columbia root tips. In conclusion, use of markers for autophagic vesicles failed to provide positive markers for autophagy within dying root initials.

Figure 4.8. Zeocin treatment of mutants defective in autophagy showed wild type levels of cell death in the root

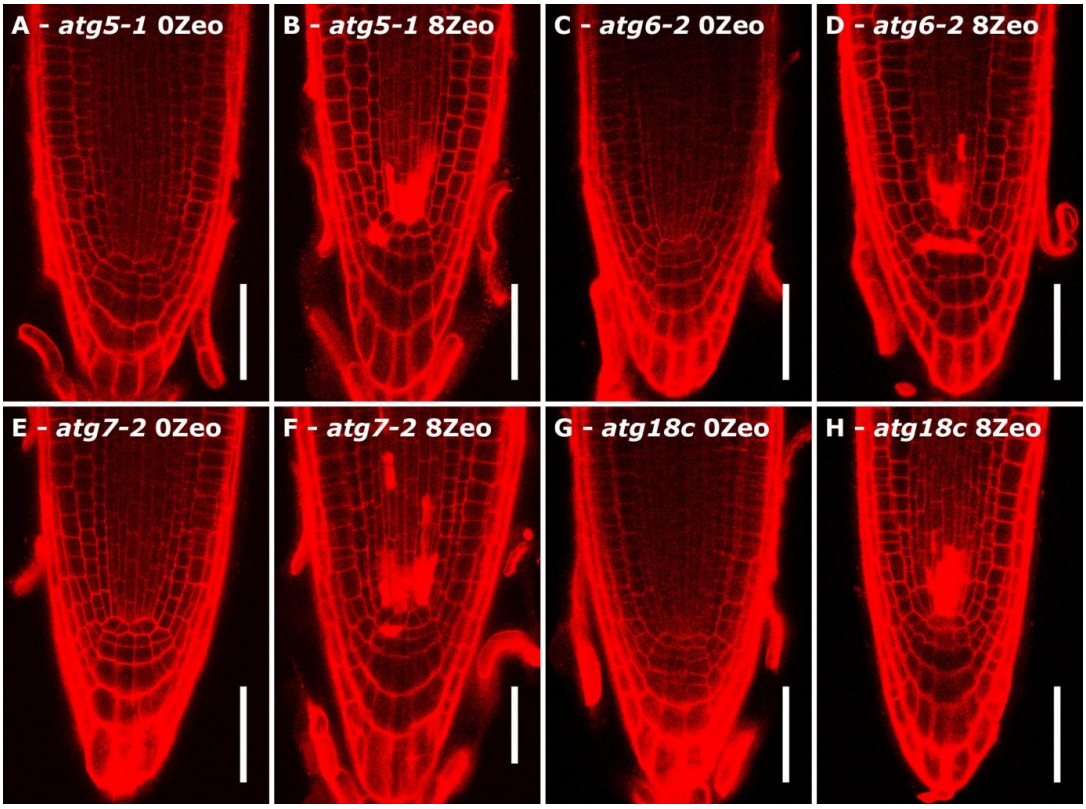

Mutants for ATG proteins known to be defective in plant autophagy were treated with 8 µg/ml zeocin for 24 hrs. (Note: Different stocks of zeocin needed different optimum concentrations). Cell death levels in these mutants were shown to be comparable to wild type (see fig 3.1. for examples of wild type cell death). (Scale Bars: 50 µm).

Figure 4.9. Lysotracker staining and *ATG8:GFP* expression failed to label vesicles within dying root initials

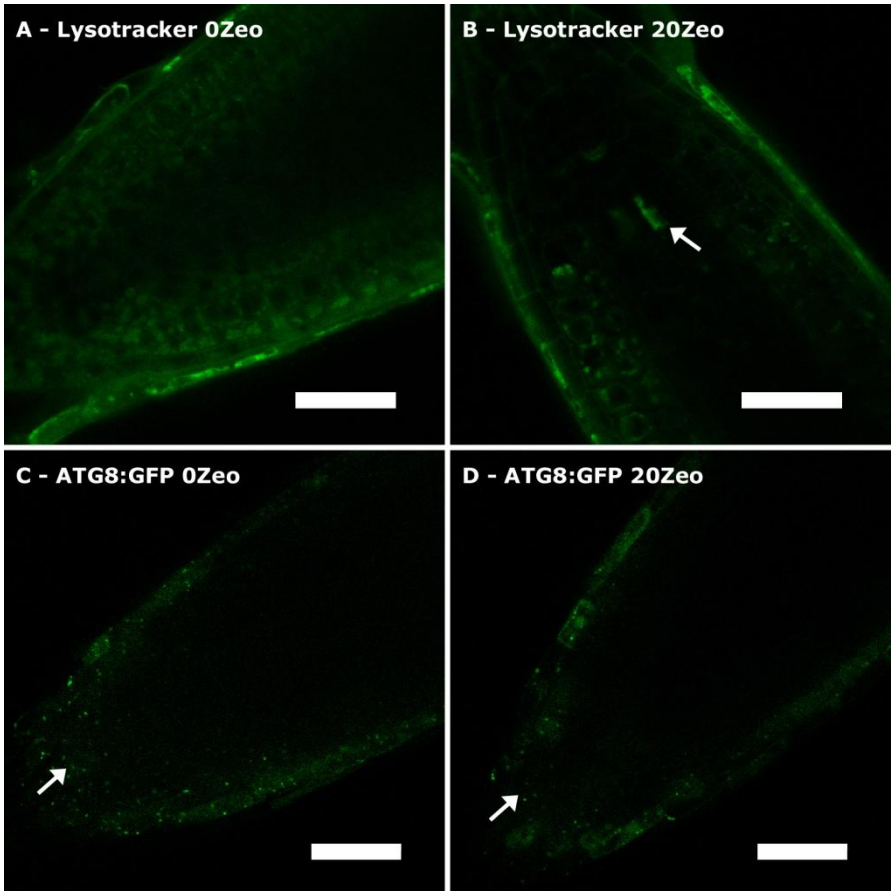

Columbia and ATG8:GFP seedlings were treated for 16 hrs with 20 µg/ml zeocin. Confocal imaging was then performed with 40 x objective. Columbia seedlings were stained with Lysotracker (**A** & **B**); stain was shown to enter dead cells but not stain vesicles within root initials (marked by arrow). (**C** & **D**) ATG8:GFP, a marker for induction of vesicle formation, showed no expression within dying root initials. Vesicles were however seen in root cap cells of treated and untreated roots (marked by arrows). (Scale Bars: 31.75 µm).

4.3. Discussion

Programmed cell death pathways in plants are relatively unknown compared to the well established mammalian mechanisms of PCD. The aim of this chapter was to identify pathways involved in activating DNA damage induced cell death in *Arabidopsis*. The apoptotic response to DNA damage is well characterised from animal studies, it is known that stem cells initiate apoptosis in response to DNA damage (Garcia-Muse and Boulton 2005, Heyer*, et al.* 2000). This response is known to be dependent on DNA damage signalling proteins ATM/ATR and also p53, a key transducer of cell cycle arrest and cell death activation (Garner and Raj 2008). This chapter aimed to identify initial specific cell death mechanisms through studying mutants implicated in plant cell death pathways and cell morphology of dying root initials.

As apoptosis is the best studied cell death response to DNA damage in animals, I began to investigate mutants of metacaspase genes suggested to share related function to mammalian caspases. Experiments studying the cleavage of caspase substrates in plants have shown caspase-like activity in cell death (Woltering *et al.* 2002). Caspase specific peptide inhibitors Ac-YVAD-CMK and Ac-DEVD-CHO were found to suppress cell death in tobacco leaves after infiltration with the bacterial pathogen *Pseudomonas syringae pv. Phaseolicola* (del Pozo and Lam 1998). Metacaspases have however shown to play no part in the cleavage of these substrates (Bonneau*, et al.* 2008). Results from metacaspase mutants do however propose a function downstream of DNA damage signalling. Mutants for *AtMC8* have shown increased resistance to DNA damage induced by methyl viologen (He*, et al.* 2008). Microarray studies based on genes upregulated after DNA damage have also shown ATM dependent induction of *AtMC1* (Ricaud*, et al.* 2007). These studies therefore present conflicting evidence for the role of metacaspases in plant cell death.

Because of the established relationship with metacaspases and DNA damage in plants, mutants were treated with zeocin to see if cell death was reduced or abolished in the root tip. Cell death levels were however comparable to wild type in these experiments implying no immediate role for metacaspases in activating cell death of root initials. Other experiments could also be performed to conclude this; creating double mutants could potentially show an effect on cell death as removing activity of a single metacaspase was insufficient to abolish cell death. Also, seedlings could be treated with caspase inhibitors as used by Del Pozo & Lam (1998) to see if cell death of root initials is dependent on caspase-like protease activity. These results indicate that individually, none of the metacaspases tested play an essential role in initial specific cell death. The role of caspase-like proteolytic activity in plant stem cell death remains unknown.

The hypersensitive response is the best studied programmed cell death response known in *Arabidopsis*. This response is primarily mediated by rising hormone levels including jasmonic acid (JA), salicylic acid (SA) and ethylene (ET) (Dong 1998). Once hormone levels have accumulated an oxidative burst initiates cell death in cells surrounding the infection site (Bari and Jones 2009, Lamb and Dixon 1997). To investigate the role of these hormones in activating cell death of root initials, mutants and transgenic lines affecting hormone accumulation were treated with zeocin looking for any reduction in cell death.

To begin analysing defence pathways and their role in activating cell death of root initials we first investigated components of the salicylic acid pathway. Disruption of the salicylic acid accumulation was targeted using transgenic plants expressing the bacterial *salicylate hydoxylase* (*NahG*) gene which is known to prevent SA accumulation in plants (Heck 2003). Also, *SALICYLIC ACID INDUCTION–DEFICIENT* (*SID*) Mutants of *Arabidopsis* showed increased susceptibility to fungal pathogens (Nawrath and Metraux 1999). Because these mutants were unable to activate the hypersensitive response

after pathogen attack, it was thought SA could also affect DNA damage induced cell death. This was however shown not to be the case as *NahG* expressing lines and the *sid2-5* mutant failed to show a reduction in DNA damage induce cell death (Fig 4.2.). Salicylic acid signalling was shown in these experiments not to be essential in the activation of DNA damage induced cell death.

In addition to analysing SA levels in activating programmed cell death of root initials, ET levels were also disrupted using mutants for ethylene signalling. The *ETHYLENE INSENSITIVE 2* (EIN2) mutant has shown to be an essential transducer of stress responses (Alonso*, et al.* 1999). RCD1 is known to antagonise ethylene production; Ethylene production in *rcd1* is higher than that of the wild type (Wang*, et al.* 2002). The mutant *rcd1-1* has shown increased susceptibility to O_3 but not genotoxic conditions including methyl viologen and UV (Fujibe *et al.* 2004, Overmyer *et al.* 2005, Overmyer*, et al.* 2000). Disruption of the ethylene pathway was also shown to have no effect on the activation of initial specific cell death (Fig 4.3.). These results provide no evidence for the role of hormones related to the hypersensitive response in stem cell specific cell death. Activation of cell death through ATM and ATR signalling kinases is likely to be independent of these hormones.

The oxidative burst, which results in rapid generation of ROS, acts downstream of hormone accumulation to mediate cell death in the hypersensitive response (Alvarez 2000). Experiments which manipulate the rise in hormone levels failed to show any response in activating cell death; it is however possible that the oxidative burst still plays a role in activating death of root initials. Methods to label ROS accumulation such as 3,3'-diaminobenzidine (DAB) staining have been used previously to show elevated H_2O_2 levels (Nakagami *et al.* 2006). Preliminary experiments using DAB staining has however shown no evidence for ROS accumulation in root initials (data not shown). Future experiments could also investigate downstream responses to ROS accumulation by examining *OXIDATIVE SIGNAL-INDUCIBLE1* (*OXI1*)

mutants. *OXI1* expression was found to be strongly increased after exposure to H_2O_2; also, *oxi1* mutants were found to be more susceptible to *Phytophthora parasitica* suggesting a role in the hypersensitive response (Rentel *et al.* 2004). It is therefore important to determine whether ROS plays a role in DNA damage induced cell death due to its central role in the hypersensitive response.

Experiments investigating the role of PARP in cell death showed no cell death changes in the *Arabidopsis parp-2* mutant and PARP RNAi lines. As mentioned in the results, *PARP-2* only accounts for around 15% of overall PARP activity in animals; the rest is dependent on *PARP-1*. It appears however that PARP genes are equally involved in DNA damage responses in plants (Doucet-Chabeaud*, et al.* 2001). De Block *et al.* (2005) showed PARP-2 inactivation was more effective at obtaining stress tolerance than with PARP-1 knockdown lines. Unfortunately, I was unable to test the *PARP-1* mutant due to time constraints; it will be interesting to test this mutant in future experiments. The effects of reduced PARP activity in the RNAi lines however also showed no effect on cell death. PARP inhibitor 3-MB slightly decreased cell death shown by Sytox staining. Sytox was used in these experiments as it has shown reduced sensitivity compared with PI staining (See chapter 2). It was thought that Sytox staining would make scoring of dead cells easier to compare with treatments lacking 3-MB. The results using PARP inhibitors justify further investigation into the role of PARP in cell death. Future experiments involving PARP inhibitors could test nicotinamide (NA) which was also shown to protect *Brassica napus* callus tissue from oxidative stress (De Block*, et al.* 2005). This paper however mentions that these inhibitors are not entirely specific to PARP activity and could potentially inhibit other enzymes.

In parallel to performing zeocin treatments on mutants implicated in programmed cell death in plants, electron microscopy was also used to study cell morphology of dying cells. Because cell death in animals is defined by morphological changes within dying cells, the aim was to study the appearance

of similar features in plants. As mentioned previously, apoptotic-like cell death was not expected due to lack of key executioners in this form of cell death such as caspases and p53. However, features of apoptosis, autophagy and necrosis have been observed in plants. One morphological trait of apoptotic death in animals is loss of membrane integrity and cell shrinkage (Reape and McCabe 2008). Experiments by McCabe *et al.* (1997) showed cell shrinkage of carrot cells in response to temperatures of 55°C. The cell membrane was shown to retract from the cell wall leaving a visible gap, higher temperatures of 75°C caused necrotic cell death without membrane retraction (Reape and McCabe 2008). Electron micrographs have shown presence of autophagic vesicles in *Arabidopsis* after treatment with concanamycin-A, which is known to induce autophagic vesicles through its ability to raise pH levels (Yoshimoto*, et al.* 2004). The aim of these experiments was therefore to look for features of cell death, typically cell shrinkage and vesicle formation as described previously in plants, after zeocin treatment.

Transmission electron microscopy (TEM) imaging revealed presence of numerous vesicles in dying root initials and daughter cells in response to zeocin. These vesicles appeared to fuse and contained varied cellular contents, similar to autophagic vesicles. Thus my results suggest that root initials primarily activate an autophagic-like cell death in response to DNA damage. Autophagic cell death was proposed to be the dominant form of cell death in plants due to lack of apoptotic death components (van Doorn and Woltering 2005); in this case it appears to also be true. Autophagy however is defined by production of double membrane bound vesicles known as the autophagosome (Longatti and Tooze 2009). Presence of the double membrane is visible by electron microscopy (Klionsky 2007), but such a double membrane was not identified in my experiments. This maybe due to preparation techniques used for imaging, images presented by Klionsky *et al.* (2007) used freeze fracture electron microscopy to visualise autophagosomes. This process maybe essential to obtain

high resolution images meaning additional membranes can be identified. Because I was unable to confidently describe these structures as containing a double membrane, death was described as showing autophagic-like symptoms and not confirmed as true autophagy.

Autophagic cell death has been previously described in plants in response to programmed cell death signals. The hypersensitive response is initiated in response to pathogen attack and causes programmed cell death around sites of pathogen infection. Occurrence of autophagic vesicles was seen in cells undergoing death in the hypersensitive response (Hofius*, et al.* 2009). Vesicle formation was shown by staining with lysotracker green and expression of ATG8:GFP after infection with *Pseudomonas syringae.* Evidence for autophagy has also been shown during developmental processes including formation of xylem cells, aerenchyma formation, phloem cell development, formation of root cap cells, and senescence (van Doorn and Woltering 2005). Examples of autophagic death have therefore also been described in response to developmental cues and the stress induced hypersensitive response.

It has been known for some time that plant autophagy is important for nutrient remobilization during sugar and nitrogen starvation and leaf senescence (Bassham 2007). More recently is has been shown that autophagy plays an important role in programmed cell death in plants (Hofius*, et al.* 2009). In order to further test the role of autophagy in the programmed death of stem cells, defective mutants were identified and treated with zeocin determine the effect on cell death. Involvement of the autophagy-related (*ATG*) family in vesicle formation is well characterised in animals (Klionsky 2007). A group of approximately 30 proteins are known to be involved, ATG proteins join in a similar way to the way the ubiquitination pathway attached Ub to proteins targeted for degradation (Geng and Klionsky 2008). Conjugation with other ATG proteins and membrane lipids mediate the formation of autophagic vesicles (this process is described in more detail in chapter 1). In *Arabidopsis*, at least 36

genes have been characterised to have a role in autophagy (Qin*, et al.* 2007). To investigate the role of these genes in cell death, 4 *ATG* mutants (*atg5-1*, *atg6-2*, *atg7-2*, and *atg18c*) all shown to be defective in plant autophagy were treated with zeocin. Thompson *et al.* (2005) investigated autophagy in *atg5* and *atg7* mutants and found enhanced sensitivity to N-deficiency and lack of ATG8:GFP labelled vesicles after concanamycin-A treatment. Monodansylcadaverine (MDC) staining of ATG18 RNAi lines showed disruption of autophagosome formation, ATG8:GFP expression was also diffused in sucrose-starved protoplasts (Xiong*, et al.* 2005). ATG6 was also shown to be essential for normal plant development and autophagy was affected in *atg6* mutants (Qin*, et al.* 2007). Treatment of ATG mutants with zeocin however showed no reduction in cell death levels.

In addition to testing mutants deficient in autophagy, I used known markers for autophagic vesicles to show autophagic traits in dying cells. The first experiments involved using Lysotracker green, a fluorescent stain that labels autophagosome structures as used by Hofius *et al.* (2009) to label autophagy in cells during the hypersensitive response. The Lysotracker stain enables visualisation of acidic vesicles such as the autophagosome by fluorescing at low pH levels (Liu*, et al.* 2005). Staining of 16 hr treated roots did not reveal staining to autophagosome structures within dying root initials. Instead, the stain appeared to saturate cells which had already died. Presence of autophagic vesicles did however appear in root cap cells which indicate staining was successful in cells showing a small amount of endogenous autophagy. As autophagy is known to be implemented to conserve nutrients, some small amount of background vesicle formation could occur (Bassham 2007). In addition to Lysotracker staining, the ATG8:GFP marker line has been used in many studies as a GFP marker for autophagy induction. Papers characterising loss of autophagic activity in ATG mutants often show reduced ATG8:GFP expression (Phillips*, et al.* 2008, Thompson*, et al.* 2005, Xiong*, et al.* 2005). Unfortunately, membrane stains could not be used in conjunction with ATG8:GFP

experiments as absorption of stains into dead cells could prevent visualisation of GFP. These experiments were therefore conducted without PI or FM464 staining. No clear GFP expression was found in root initials but was again shown in root cap cells as with the Lysotracker experiments. Detection of root initials was difficult due to lack of membrane staining.

As mentioned previously, ATG mutants completely abolish autophagosome formation marked by the lack of *ATG8:GFP* expression (Thompson*, et al.* 2005). Results however showed that cell death was not decreased after zeocin treatments of *ATG* mutants. Results from electron microscopy however show clear formation of vesicles in dying cells reminiscent of autophagy. These results therefore show conflicting evidence for the role of autophagy in DNA damage induced cell death; it is possible that autophagy is not the sole mechanism by which plants remove damaged stem cells. As mentioned at the start of this discussion, plants were shown to exhibit proteolytic activity of known caspase substrates (Woltering*, et al.* 2002). It could be that plants use a unique form of apoptosis which utilises this proteolytic activity to mediate cell death. In the absence of autophagy genes, plants could choose to activate either cell death mechanism. It is also possible that autophagy could accompany other plant specific cell death mechanisms to execute PCD. Unfortunately, not enough is known about caspase-like protease activity in plants to couple it to autophagic responses. Perhaps future experiments could examine ATG mutants after treatment with zeocin and caspase inhibitors mentioned earlier in this discussion to see if cell death is reduced or completely absent.

I also believe future experiments could investigate the use of autophagy markers further. Higher magnification and screening of a greater number of treated root tips could generate better results. The magnifications used (40x and 60x) were not enough to clearly visualise small amounts of GFP in the root initials. Root stem cells are much smaller than epidermal cells of the leaf by

which Hofius *et al.* (2009) observed lysotracker staining. Also, as I was unable to use membrane staining for ATG8:GFP imaging, it would be beneficial to cross this marker to the 35S:GFP:LTI6B membrane marker to enable easier identification of root initials, possibly at higher magnifications than used in these experiments. Electron microscopy indicated clear presence of large cytoplasmic vesicles showing strong evidence for autophagic like death. Unfortunately, I did not have time to fully investigate vesicle marking with these markers.

Chapter 5 – Effects of DNA damage on the shoot meristem

5.1. Introduction

Results from previous chapters have shown that root initials are hypersensitive to relatively low levels of DNA damage. These results raised the question of the functional significance of cell death activation in *Arabidopsis* stem cell populations. Root growth is known to be affected by DNA damaging conditions with *atm* and *atr* mutants showing sensitivity to γ-irradiation (Culligan*, et al.* 2006). This highlights the requirement for a protection mechanism in the root which would allow sustained root growth and effective competition for nutrients. Cell death was hypothesised to help maintain root growth after exposure to genotoxic conditions (See chapter 6). The effects of DNA damage in the shoot meristem has however not been studied so far. Protecting from genotoxic stress in stem cells of the shoot is deemed important to protect the genomic integrity of future generations. The stem cell niche in the shoot meristem will eventually produce floral organs; any potentially negatively impacting mutations could therefore be passed onto future generations. It therefore appeared likely that a similar mechanism of DNA damage induced cell death would be also present in the shoot.

The experiments outlined in this chapter aimed to investigate programmed cell death within the shoot in response to DNA damage. Zeocin and x-ray treatments were carried out on shoot meristems which were then analysed by confocal microscopy looking for cell death within stem cell populations. In addition, I aimed to analyse *atm* and *atr* mutants to identify any reduction in cell death. Mutants for *lig4* and *ku80*, which showed spontaneous cell death within the root meristem, were also imaged in order to reveal any spontaneous death within the shoot meristem.

5.2. Results

5.2.1. Stem cells within the shoot meristem showed specific cell death after zeocin treatment

Treating the root with radiomimetic drugs is fairly straightforward as germination media can be supplemented with zeocin or bleomycin. Roots can then be imaged without any dissection by placing directly onto a microscope slide. Access to the shoot apex is however more difficult due to being surrounded by flowers and developing floral buds. Imaging the shoot meristem is also difficult as delicate dissection is necessary to mount the apex onto a microscope slide. A slightly different approach was therefore needed to examine shoots treated with DNA damaging drugs.

To treat shoot tips, 0.2 ml PCR tubes were filled with either 0 or 20 µg/ml solution of zeocin. Siliques, flowers and larger floral buds were then removed from the shoot with forceps. Shoot tips were dipped into zeocin containing tubes and held onto the stem with surgical tape. After 24 hrs, tubes were removed from the shoot; remaining buds were removed until the apex was exposed. The apex was dissected away from the stem and mounted onto a microscope slide. The apex was stained with 10 µg/ml Propidium iodide and imaged by confocal microscopy.

Imaging of Columbia shoots showed large patches of cell death within the zeocin treated shoot apex (Fig 5.1.). This region of cell death appeared to correspond to the *CLV3* expressing domain shown in experiments by Reddy & Meyerowitz (2005). Cells at the centre of emerging buds, where *CLV3* expression has also been reported, also showed preferential cell death (Fig 5.1d.). To confirm that cell death occurred within the *CLV3* expressing domain which marks stem cells in the shoot, a CLV3:GFP line used previously by Reddy & Meyerowitz (2005) & Yadav (2009) was obtained from the authors. Treated

shoots of this line showed cell death associated with the GFP expressing region (Fig 5.2b). Zeocin treatment did however not appear to kill all GFP expressing cells within the shoot meristem and not all dead cells were located within the *CLV3* expression domain. This was reminiscent of the results seen in the root meristem although cell death was seen preferentially in root initials, not all initials died and death was also seen in early descendants of the initials.

In chapter 2, the CYCB1;1:GFP line was used to monitor cell cycle arrest in the root meristem after zeocin treatments. Similarly, treatment of CYCB1;1:GFP shoots showed surrounding meristem cells also expressed GFP (Fig 5.2d) indicating that the cell cycle arrest in response to DNA damage occurred throughout the shoot meristem, in contrast to the more localised cell death response.

In summary, cell death was also seen in the stem cell niche of the shoot meristem. Expression of *CLV3:GFP* co-localised with cell death regions within the shoot apex. Also, cell cycle arrest but not cell death was activated in surrounding cells, suggesting death was cell type specific.

Figure 5.1. Preferential cell death was seen in the central region of the inflorescence and floral meristems

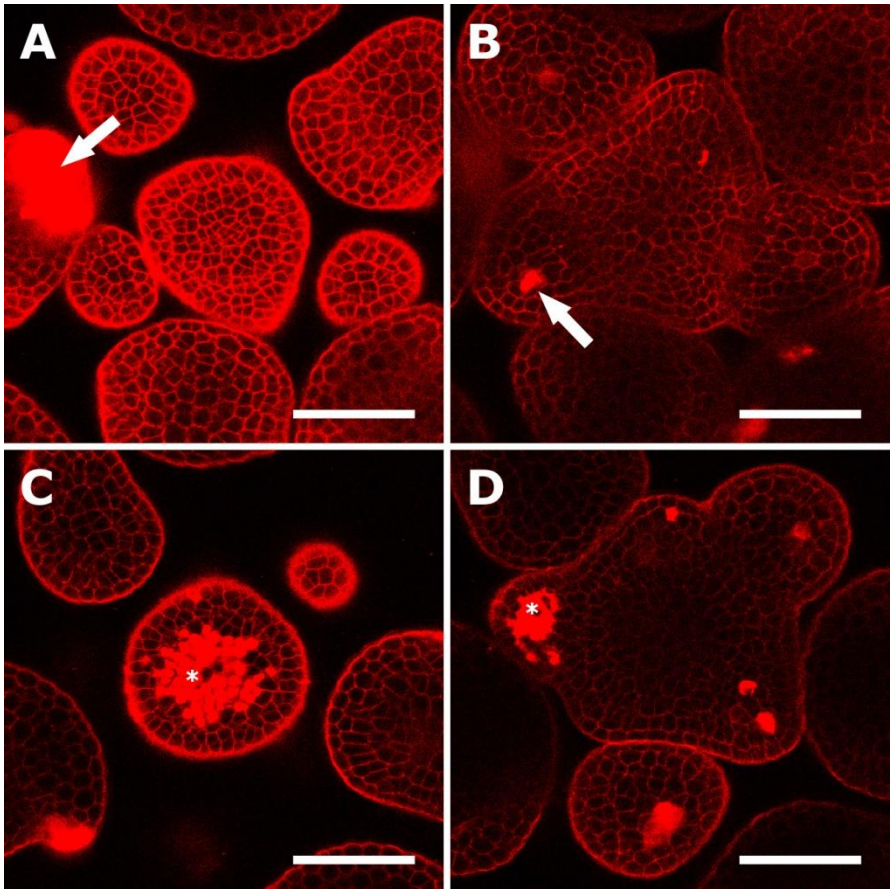

Columbia shoot tips were treated with 20 µg/ml zeocin for 24 hrs, dissected, stained with propidium iodide and imaged. Small amounts of cell death were seen in untreated controls and may result from dissection and manipulation of the shoot apex (Shown with arrows). This was easily distinguished from zeocin induced cell death (Shown with asterisks). (**A**) Control shoot apex showing no cell death (**B**) Same control shoot imaged further into meristem showing emerging buds (**C**) Zeocin treated apex showing cell death (**D**) Zeocin induced cell death seen in emerging floral buds. (Scale bars: 50 µm).

Figure 5.2. Analysis of CLV3:GFP plants confirmed death was associated with the stem cell niche, CYCB1;1:GFP showed cell cycle arrest in surrounding meristem cells

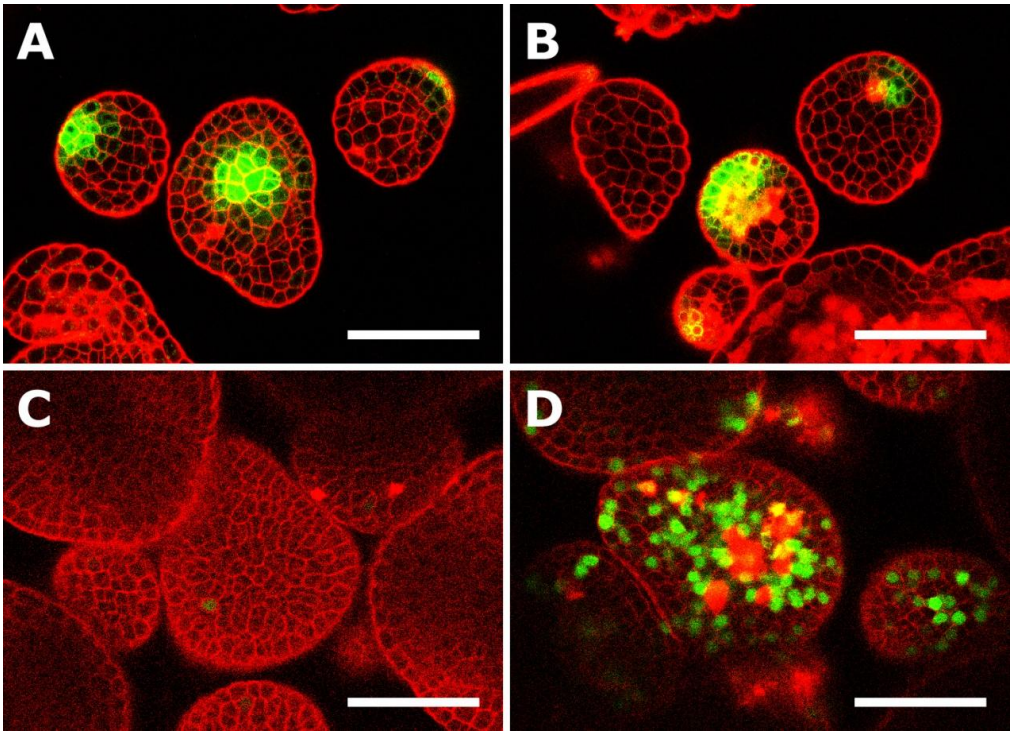

Cell death was detected in the shoot meristem of CLV3:GFP and CYCB1;1:GFP marker lines. Position of CLV3:GFP showed cell death in the shoot apex. Resulting GFP expression was thought to be due to surviving stem cells. Surrounding meristem cells also showed a similar cell cycle response as seen in the root meristem. Shoots were treated with 20 µg/ml zeocin for 24 hrs. (**A**) CLV3:GFP Control (**B**) CLV3:GFP Treated (**C**) CYCB1;1:GFP Control (**D**) CYCB1;1:GFP Treated. (Scale bars: 50 µm).

5.2.2. Uniform treatment with x-rays also preferentially killed cells in the central zone of the shoot meristem

It was suggested in chapter 2 that radiomimetic drugs could be transported or metabolised differently in stem cells. This, rather than a differential response to DNA damage, could have potentially resulted in death of root initials. This possibility prompted experiments using x-rays to induce DNA damage in seedlings. Exposure to x-rays is expected to be uniform across all tissues; these irradiation experiments showed that cell death was cell type specific and not a result of zeocin collection in the root tip.

A similar x-ray treatment was used in the shoot meristem. For this treatment, mature Landberg *erecta* (L*er*) plants were sealed in polythene bags and irradiated in a similar manner to seedlings in chapter 2. L*er* plants proved easier than Columbia to prepare for imaging because of their thicker stems and dense floral bud arrangement. Plants were irradiated at 40 and 80 Gray doses as performed previously with ATM and ATR mutant seedlings in chapter 3. Plants were left for 24 hrs after irradiation, stained with propidium iodide and imaged looking for cell death within the shoot apex.

Images of irradiated shoot tips showed cell death preferentially within the central region of the shoot meristem, in patches that compare to the cell death region after zeocin treatments (Fig 5.3.). X-ray treatment however appeared to cause a more scattered cell death pattern than with zeocin. No cell death was detected in untreated shoots. Cell death was observed at 40 and 80 Gray indicating that the sensitivity to x-rays was similar in the shoot and root meristems. From these results we concluded that x-rays also activated cell death preferentially in the central zone of the shoot meristem, where the stem cell niche is located.

Figure 5.3. X-rays induced stem cell specific cell death in the shoot meristem

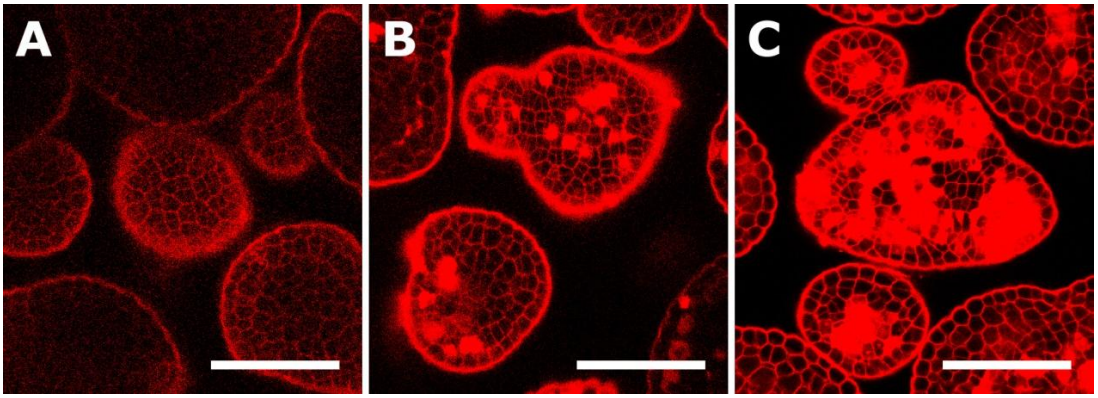

X-ray irradiation at 40 and 80 Gray activated cell death in the shoot apex and developing floral buds. Plants were irradiated and placed back into long day growth conditions for 24 hrs before imaging. (**A**) 0 Gray (**B**) 40 Gray (**C**) 80 Gray. (Scale bars: 50 μm).

5.2.3. ATM was important for cell death activation in the shoot meristem

In the root meristem, *atm* and *atr* mutant alleles were shown to inhibit cell death when treated with 20 µg/ml zeocin for 24 hrs (chapter 2). These key DNA damage signalling regulators were therefore shown to be essential in activating stem cell specific cell death. To see if the same responses are found in to shoot meristem, *atm-2* and *atr-2* were treated with zeocin for 24 hrs, dissected and imaged. Interestingly, *atr-2* showed death of stem cells whereas no *atm-2* shoots displayed dead cells (Fig 5.4.). This suggests different roles for ATM and ATR in shoot and root stem cells.

Occurrence of spontaneous cell death of root initials was also seen in *ku80, mre11-4* and *lig4-4* mutants (chapter 2). This was thought to be due to lack of DNA repair by non-homologous end joining (NHEJ); generation of endogenous DNA breaks seems to be sufficient to activate cell death in root initials. These experiments were also applied to the shoot meristem. Untreated *ku80* mutants (West*, et al.* 2002) were imaged looking for spontaneous death in the shoot apex. Untreated Columbia shoots were also imaged as a control to assess damage done to shoots through the imaging process. Unfortunately, due to the technique used in preparation of the shoot apex for imaging, a small amount of background cell death is often seen in wild type shoots (Fig 5.5a & b). Out of 7 Columbia shoots, 2 showed death of ~ 2 cells in the meristem region. The same amount of death was seen in *ku80* plants with 2 out of 8 showing death of 2 to 3 cells. Images from *ku80* untreated (Fig 5.5c & d) show death which seems to be more centred on the shoot apex, it is however uncertain whether this death is due to defects caused by loss of KU80 or damage by preparation.

Figure 5.4. ATM and ATR mutants were shown to play different roles in activating cell death in the shoot meristem

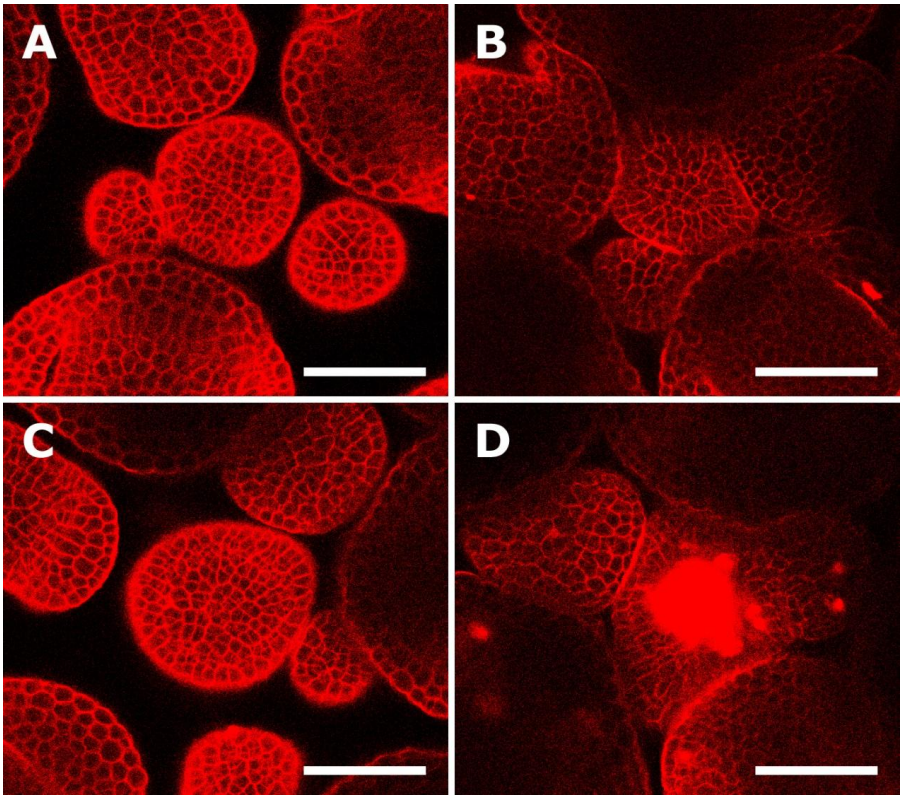

Preferential cell death was seen in *atr-2* but absent in *atm-2* in the shoot meristem. Shoots were treated for 24 hrs with 0 or 20 µg/ml zeocin, stained with propidium iodide and prepared for imaging. (**A**) *atm-2* control (**B**) *atm-2* 20 µg/ml zeocin (**C**) *atr-2* control (**D**) *atr-2* 20 µg/ml zeocin. (Scale bars: 50 µm).

Figure 5.5. Spontaneous cell death in *ku80* mutants was hard to identify due to imaging preparation techniques

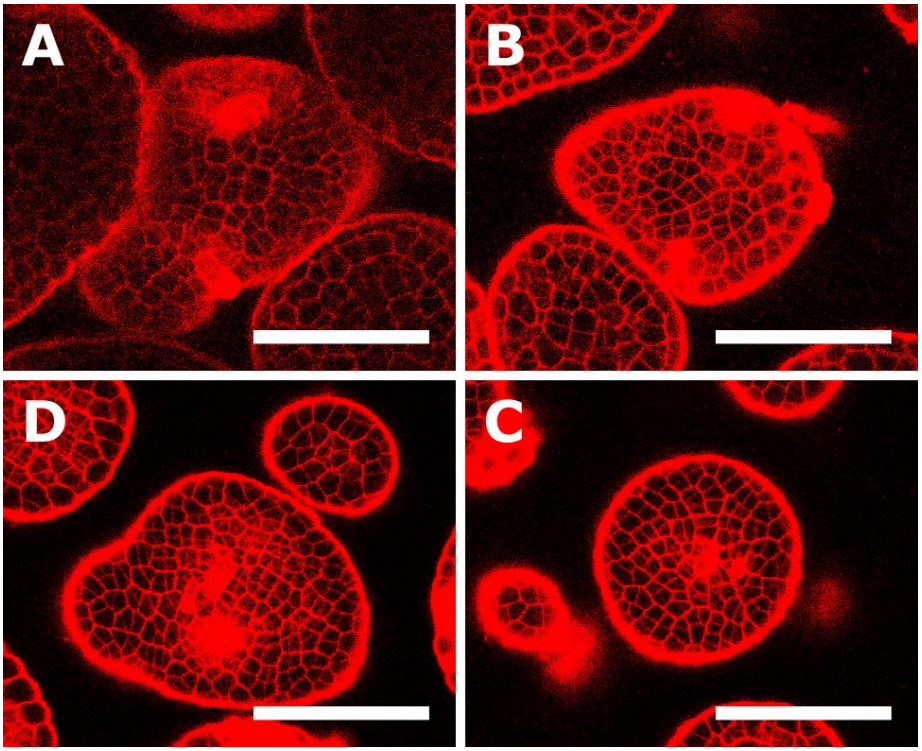

Preparation of the shoot meristem for imaging produces a small amount of cell death in the shoot apex. (**A** & **B**) Two representative images of untreated Columbia shoot meristems showing death of a few single cells. (**D** & **C**) Two representative images of *ku80* also showing a small amount of cell death. Although the cell death in the *ku80* mutant is more central to the apex in the stem cell region compared with Columbia, it is difficult to prove this death is stem cell specific. (Scale bars: 50 μm).

5.3. Discussion

Plants produce reproductive organs throughout their lifetime; these organs are derived from stem cell populations present within the shoot meristem. DNA damage could potentially inflict mutations onto the stem cell population; any negative effects could be passed onto future generations in the absence of a protection mechanism. As shown previously in earlier chapters, stem cell specific death is seen within the root meristem in response to DNA damage. It is shown here that programmed cell death also appears to have evolved to protect the stem cell niche in the shoot meristem.

Treatments of Columbia wild type plants showed sectors of cell death that seemed to correspond with the stem cell niche in the shoot apex. Also, stem cell niches established in emerging floral meristems were shown to be highly sensitive to DNA damage. The question however remained whether these cells constituted those of the stem cell niche. To answer this question we obtained a *CLV3:GFP* expressing line as used by Reddy & Meyerowitz (2005) & Yadav *et al.* (2009) in 3d shoot meristem imaging. Treated CLV3:GFP lines exhibited cell death within the GFP expressing region of these plants. Some GFP expression did remain within the shoot apex, experiments in the root meristem showed that not all root initials seemed to die in response to zeocin. In fact, surviving initials were shown to expand to fill space left by dead cells (See chapter 6). It is therefore likely that remaining GFP expression is due to survival of a fraction of the stem cell population.

In chapter 2, it was suggested that cell death seen in root initials could be due to non-uniform distribution of zeocin and not cell identity. Collection of zeocin in segments of the root tip could result in higher concentrations within certain areas; this could activate cell death regardless of stem cell identity. The root already displays a precedent for non-uniform transport of molecules. Auxin is transported by PIN proteins to the root tip where it acts to specify positional

information to establish the quiescent centre (QC) (Tucker and Laux 2007). Experiments were designed to show DNA damage responses throughout the root meristem using CYCB1;1:GFP to show that surrounding meristem cells activated a DNA damage mediated cell cycle arrest. In addition to this, root tips were irradiated with x-rays to provide a uniform exposure to DNA damage. PCD of root initials was still observed after a uniform x-ray treatments indicating death was stem cell specific.

To further investigate uniform DNA damage responses in the shoot, *CYCB1;1:GFP* expressing plants were exposed to zeocin. Preferential cell death was shown in the shoot apex of these plants; surrounding cells were also shown to activate proposed cell cycle checkpoints, indicated by high levels of GFP expression. X-ray irradiation experiments also highlighted preferential death of stem cells with patches of cell death observed within the stem cell region of the shoot apex. Cell death was therefore also concluded to be cell type specific within the shoot meristem.

Results from chapter 3 revealed ATM and ATR, key DNA damage signalling kinases, are essential in activating root initial specific cell death within the root. The role of these kinases was also investigated in the shoot which highlighted different roles in activating cell death between shoot and root meristems. PCD was triggered in the *atr-2* mutant allele whereas *atm-2* failed to induce cell death. This result differed to that of the root meristem where *atm-1*, *atm-2* and *atr-2* failed to initiate cell death of root initials. It therefore appears that ATM and ATR differ in their ability to activate cell death within shoot and root meristems of *Arabidopsis*.

The differences observed between ATM and ATR are however not surprising as their roles have been shown to be varied in different tissues and organisms. Human fibroblasts have shown to require ATM but not ATR in response to IR induced DNA damage (Wilson *et al.* 2010). Activation of DNA damage response was monitored by tracking formation of γ-H2AX foci (a key

step in DNA damage signalling, see chapter 1 for review). ATR mutants showed presence of γ-H2AX foci comparable to wild type after ionizing radiation (IR). ATM mutants were however shown to be defective in foci γ-H2AX formation. These experiments are consistent with the view that ATM is specifically activated after DSBs and ATR after blocks in replication (Cann and Hicks 2007). Other experiments in *C. elegans* have however indicated a direct role for ATR in the DSB damage response. MRN dependent recruitment of ATR homolog *atl-1* was seen in *C. elegans* after IR treatment (Garcia-Muse and Boulton 2005). A model was proposed (as discussed in chapter 3) where processing by MRN creates ssDNA and enables RPA binding. ATR is activated through association with ATRIP (ATR interacting protein) and RPA which triggers the DNA damage response. The DSB response in *C. elegans* was found to act independently of ATM, RNAi knockdowns of ATM showed continued recruitment of ATR after IR (Garcia-Muse and Boulton 2005). Cuadrado *et al.* (2006) also shows ATR recruitment to DSBs in human Raji lymphoblastoid cells, this is however dependent on ATM. Human AT patients with ATM deficiency show an absence of ATR recruitment after IR. It has long been assumed that ATM and ATR activation depends solely on DSB formation and replication stress respectively, evidence therefore shows a wider role for ATR in DNA damage signalling (Cann and Hicks 2007).

As PCD was also activated within the shoot stem cell niche in response to DNA damage, this could provide a mechanism to protect future generations from genomic instability. Hypersensitivity to DNA damage in stem cell populations which contribute to the germline is well established in animal studies. Exposure to low levels of DNA damage in mouse embryonic stem cells initiates selective programmed cell death, dependent on ATM and p53 (Heyer*, et al.* 2000). A similar result confirming p53 initiated apoptosis in germ line cells has been shown in *C. elegans* (Garcia-Muse and Boulton 2005). Low levels of γ-rays also initiated apoptosis in stem cell intestinal crypts in mice which was also shown to be p53 dependent (Merritt *et al.* 1994). Programmed cell death is therefore a

widely accepted response to low levels of DNA damage in stem cells and germline cells in particular. Cell death is therefore also proposed to act in *Arabidopsis* to protect genomic integrity of germline stem cells.

Components of the non-homologous end joining (NHEJ) pathways were shown to induce spontaneous cell death in the root in the absence of zeocin. Mutants for *ku80* and *lig4* also showed increased cell death in the root meristem in response to DNA damage (chapter 3). Endogenous damage to DNA occurs in consequence to hydrolysis, lipid peroxidation events and formation of other reactive small molecules intracellularly (Lindahl 2000). Results from the root suggest that endogenous DNA breaks that are not repaired in mutants for NHEJ are enough to induce spontaneous death of stem cells. These experiments were therefore also applied to shoot stem cells where mutants for KU80 were examined for spontaneous cell death. I was unable to determine whether spontaneous cell death occurred within the shoot meristem due to background damage caused by the dissection of the shoot apex. To image the shoot apex, floral buds are removed till the apex is exposed; the apex is then removed under the dissection microscope. This technique causes mechanical stress on the apex results in occasional death of a few cells within the shoot apex. Because of this, true spontaneous cell death can not be distinguished from those caused by preparation.

Using different approaches, it may be possible to determine spontaneous death with shoots of *ku80* and *lig4* mutants. The number of apices showing cell death should perhaps be higher in the mutants as these plants could potentially incur both spontaneous and mechanical cell death. The numbers of shoots showing cell death was however similar between control and *ku80* shoots. In order to establish whether these mutants show spontaneous death in future experiments, it may be necessary to image more shoot tips. Around 7-8 were successfully dissected for these experiments, imaging a larger number may allow for statistical analysis. Also, scoring shoots for numbers of dead cells and

their position in the apex could help eliminate those with dead cells outside the stem cell domain. This could be done in conjunction with the CLV3:GFP marker for clear labelling of the stem cell niche. Unfortunately, there was not enough time to complete these experiments.

In summary, cell death was shown to function in both shoot and root meristems to eliminate genomically damaged cells. In the shoot, these cells are essential for generation of floral organs, removing them from the niche could help to protect future generations from genomic instability. Different roles for ATM and ATR in initiating cell death were found between shoot and root meristems. It is possible that different mechanisms could operate specifically in the shoot to initiate cell death. Also, I was unfortunately unable to determine whether NHEJ mutants formed spontaneous stem cell death without zeocin treatment.

Chapter 6 – Tracking cell lineage from the QC and recovery of the root meristem

6.1. Introduction

This chapter aims to address two main questions; (1) Short and long term changes after cell death with emphasis on the behaviour of the QC (2) Testing the functional significance of root responses to DNA damage. Results from chapter 2 show root initials were selectively killed in response to radiomimetic drugs. Survival of the quiescent centre (QC) was seen with relatively mild DNA damaging treatments, it was questioned whether the QC could establish a new population of initials through activation of cell division. The long mitotic cycles of the QC were proposed to act in protecting the genome through homologous recombination (HR) which utilises sister chromatids to mediate DNA repair (See chapter 1 for review of HR). Results from chapter 2 however failed to show any evidence of QC activation after DNA damage. Additionally, it is not known what happens to dead cells within the root meristem during recovery. If programmed cell death has evolved to exclude genetically unstable cells, how does the meristem deal with this? In this chapter, I aimed to test the QC potential for repopulating the root initials by developing a unique cell lineage labelling system allowing spatial and temporal marking of QC descendents. Also, I aimed to investigate the fate of dead initials by imaging propidium iodide stained roots up to 48 hrs during recovery.

Images from 35S:GFP-LTI6B roots left to recover from a 48 hr bleomycin treatment showed significant restoration of meristem structure in chapter 2. These results however do not show recovery of root growth after exposure to DNA damage. Root growth has shown to be stunted after genotoxic treatments, whether growth resumes after the death of initials needs to be investigated

(Culligan*, et al.* 2004, Culligan*, et al.* 2006). Also, ATM and ATR mutants were shown to be resistant to initial specific cell death highlighting them as key signalling kinases in the cell death response (See chapter 3). It is uncertain whether cell death in the initials is essential to recover root growth. To test this, in this chapter root growth was be monitored after zeocin treatments in wild type, *atm* and *atr* seedlings.

Cell labelling systems have previously been used in shoot and root meristems in an attempt to fully understand cell lineage. Heat shock-responsive GUS constructs were used to create clonal sectors in *Arabidopsis* leaves (Kilby *et al.* 2000). Kurup *et al.* (2005) employed a heat shock inducible Ac transposase system to create YFP labelled sectors within the root. Descendents of heat shock labelled cells are clearly marked by YFP expressing nuclei, fluorescence was however rarely observed in the central cells of the QC. Campilho *et al.* (2006) utilised the 35S:GFP-LTI6B membrane marker to track cell divisions in whole roots, an approach also used by Reddy *et al.* (2004) using 35S::YFP29-1 in the shoot meristem. I aimed to develop an improved 4-component recombinase based system to label cell lineage from the QC in my experiments. This would allow us to further investigate work by Clowes (1959, 1961) on activation of QC division after DNA damage.

6.2. Results

6.2.1. Recovery after cell death within the root meristem

DNA damaging treatments have shown root initials undergo selective programmed cell death, the fate of dead cells during recovery of the meristem is however unknown. Previous experiments using 35S:GFP-LTI6B (Chapter 2, Fig 2.1.) showed recovery of meristem structure after bleomycin treatment. Propidium iodide (PI) staining is needed to show presence of dead initials, but repeated staining is toxic (Truernit and Haseloff 2008) so tracking recovery of a single root would be difficult.

For this experiment, 30 WOX5:GFP seedlings were treated with 20 µg/ml zeocin for 24 hrs. 10 seedlings were prepared for imaging (0 hr recovery) and the remaining 20 were added to media without zeocin to allow recovery. 10 seedlings were then imaged after 24 and 48 hr recovery periods. Three representative images out of 10 were selected for each time point (Fig 6.1.). After 0 hr recovery, cell death of initials was clearly seen with *WOX5:GFP* expression being maintained within the QC. Dead cells had sharp, clearly defined cell outlines. After 24 hrs recovery, *WOX5* expression was still present within the QC although with a slightly expanded domain of expression. Cell death was still seen but was reduced, dead cells no longer showed clear outlines and cell death appeared as irregular patches of high PI staining. After 48 hrs of recovery, even less cell death was visible. PI staining still appeared patchy and it seemed surrounding cells were squashing dead initials. Cell death appeared to be displaced from the QC; this could be due to activation of QC division or to activity of new initials derived from the stem cells that survived the treatment. The majority of cell death was removed from the meristem gradually over a period of 48 hrs.

Figure 6.1. Cell death marked by propidium iodide is less visible after 24 and 48 hrs recovery

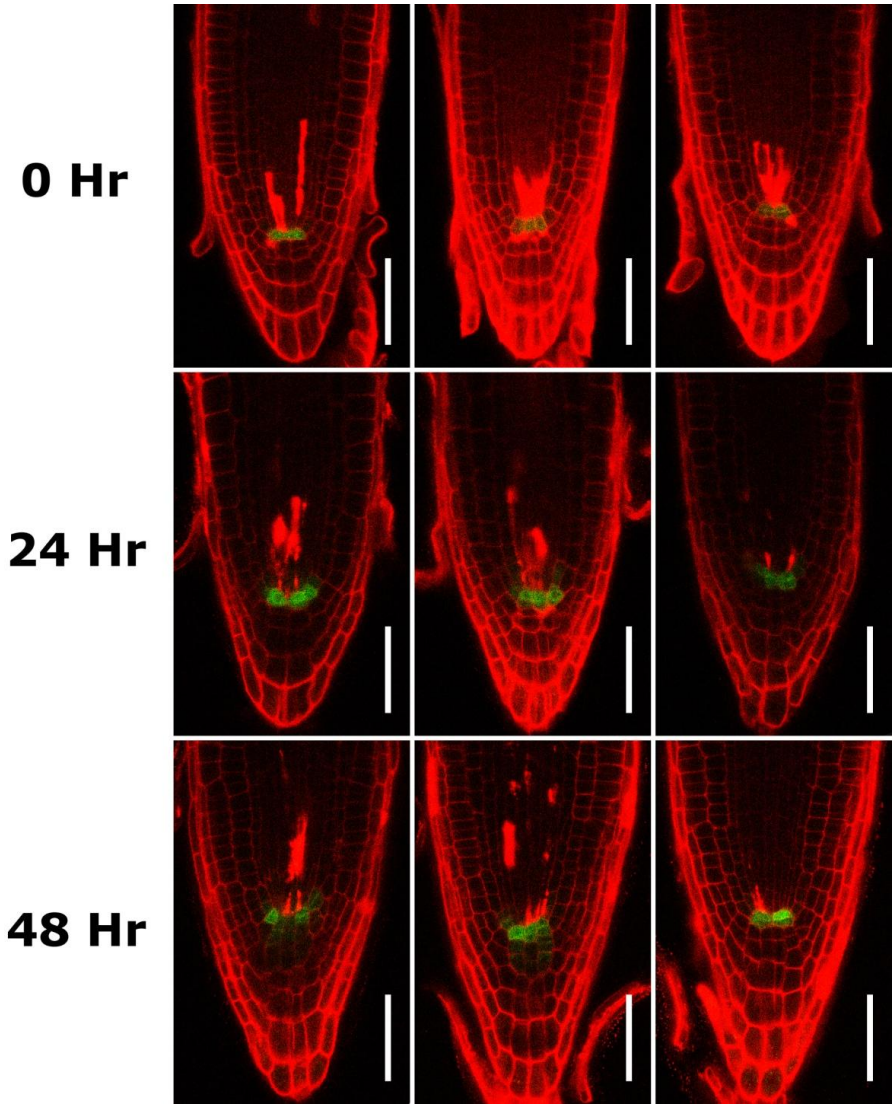

Seedlings were treated for 24 hrs with 20 µg/ml zeocin and moved back to media without zeocin for recovery. Roots were imaged at 0, 24 and 48 hrs after treatment. Three representative images are shown for each time point. Dead cells appear to be squashed by surrounding initials and displaced away from the QC. (Scale bars: 50 µm).

6.2.2. Live imaging of *WOX5:GFP/35S:GFP-LTI6B* expressing roots showed no evidence of QC activation

Experiments from chapter 2 demonstrated that following QC identity was difficult based solely on cell morphology. For subsequent experiments to track the QC after DNA damage, the WOX5:GFP QC specific marker was crossed to the 35S:GFP-LTI6B membrane marker. This line enabled easy visualisation of cell membranes and QC identity within a single root tip. A live imaging approach was used to view the same root at 0, 8, 16 and 24 hr intervals. Presence of LTI6B meant use of toxic membrane stains such as FM464 and propidium iodide was not required. To avoid repetitively moving roots to and from media and microscope slides, a slide was produced containing a thin layer of growth medium overlaid with cellophane to sustain root growth. Seedlings were positioned on the cellophane and a cover slip was placed over the roots. Slides were kept vertically for up to 24 hrs in a wet chamber between imaging. This enabled imaging for up to 24 hrs, after this point repeated imaging would damage the root tip. Live imaging experiments did not show any evidence of QC activation after 24 hrs recovery on media without zeocin (Fig 6.2.). Instead, surrounding initials which survived the treatment were shown to expand and fill space left by dead cells (Fig 6.2. marked by arrows). These cells also expressed GFP suggesting they were also acquiring QC identity, perhaps as a result of disrupted auxin signalling (see below). As QC division was not seen in a 24 hr period, longer recovery was needed to see if the QC would be activated at a later time.

To further analyse *WOX5:GFP* expression after zeocin treatment, *WOX5:GFP* seedlings were treated with 20 µg/ml zeocin and moved back to normal media for 24 and 48 hrs to recover. 3 treated roots were imaged at each recovery period; roots were stained with FM464 to label cell membranes but not cell death. Significant expansion of the *WOX5* expressing domain was seen after

24 hrs (Fig 6.3.) and seemed to be reduced after 48 hrs (2 out of 3 seedlings). Significant disorganisation of meristem structure and a large *WOX5* expression domain was seen in one seedling after 48 hrs recovery. This pattern of extreme disruption was not seen in any previous recovery experiments including treatment of GFP-LTI6B in chapter 2 and fig 6.1 of this chapter. Occurrence of this extremely disrupted root tip therefore was deemed an anomaly. Only 3 seedlings were analysed at each time point in this experiment. The remaining 2 seedlings showed apparent restoration of meristem structure and reduction of the WOX5 domain. These seedlings were therefore assumed as a typical result of this experiment.

Expansion of the WOX5 domain suggested cell division in the QC after DNA damage. However, this was ruled out after a similar expression pattern was seen after experiments involving ablation of the QC (Xu *et al.* 2006). Removal of the QC by laser ablation showed GFP expression in surrounding cells after 16 hrs, which continued for up to 3 days. Position of the QC seemed to be restored after 3 days, when surrounding cells took up QC identity. This suggested tracking QC divisions solely by *WOX5:GFP* expression would not be sufficient. *WOX5* is expressed downstream of SCR in the root meristem which is dependent of the auxin maxima (see chapter 1 for review of auxin controlled gene expression in the root), so an enlargement of the *WOX5* expression domain can reflect changes in auxin distribution rather than division of the cells initially expressing *WOX5*.

These experiments only addressed the short term responses to DNA damage; it remained entirely possible QC activation could be activated after a longer recovery time point. To look at QC activation in a longer time frame, cell lineage labelling would allow visualisation of QC descendents without the need for live imaging.

Figure 6.2. Live imaging of WOX5:GFP/35S:GFP-LTI6B expressing roots showed no evidence of QC activation

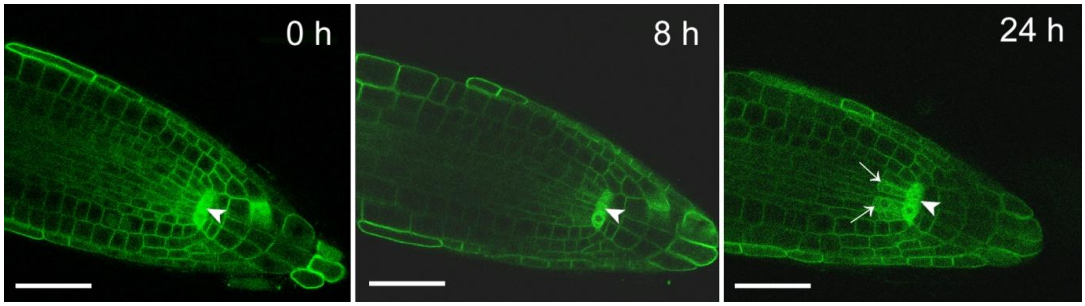

Confocal imaging of the same root (LTI6B, WOX5) imaged up to 24 hr after zeocin treatment showed no evidence of QC activation. Roots were treated with zeocin (24 hr, 20 µg/ml), moved to media without zeocin and imaged at 0, 8, 16 and 24 hr intervals. No difference was seen between 8 and 16 hr images. After 24 hrs, surviving initials (marked by arrows) expanded to fill space left by dead cells (QC marked by arrowhead). (Scale bars: 50 µm).

Figure 6.3. WOX5:GFP expression expanded in recovering roots

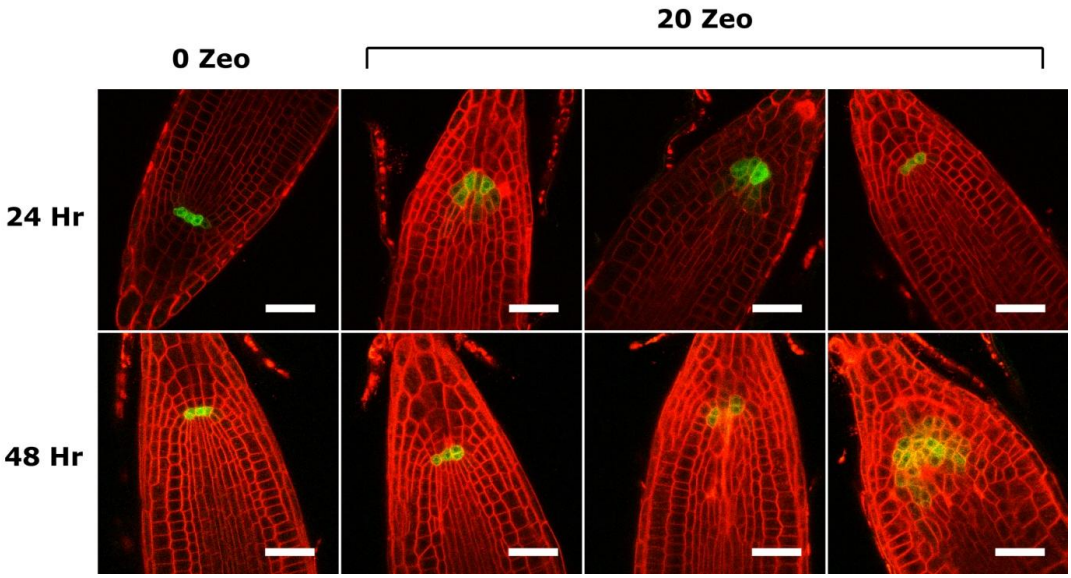

WOX5:GFP expressing roots were treated with zeocin (20 µg/ml, 24 hrs) and imaged after 24 and 48 hr recovery. Cell outlines are marked with FM4-64 staining, which is not known to label cell death. Untreated controls show typical *WOX5* expression in QC cells. Treated images represent 3 separate roots at each stage of recovery. Expansion of the *WOX5* expressing domain was increased after 24 hr recovery (2 out of 3 roots), whereas expression area was reduced after 48 hrs (2 out of 3 roots). (Scale bars: 27.5 µm).

6.2.3. Using a 4-component system to label descendents of the QC

In order to investigate the long term contribution of the QC to surrounding cells after DNA damage, a cell lineage marking system was constructed based on the Cre-*lox*P recombination system. The Cre recombinase is able to cleave DNA at specified lox recombination sites in *Arabidopsis* (Marjanac *et al.* 2008). Heat-shock inducible Cre has been shown previously to act upon a double reporter construct to generate random GFP sectors (Gallois*, et al.* 2002). The double reporter 35S:lox-GUS-lox-GFP expresses GUS constitutively until it is excised by Cre activity at lox sites activating GFP expression. Gallois *et al.* (2002) showed heat shock activated GFP sectors in cotyledons and hypocotyls, the double reporter was eventually changed to express WUS instead of GFP allowing random induction of WUS in seedlings. This approach, however, would be problematic for my experiments as sectors are induced randomly. In my case, Cre function would need to be specifically targeted to the QC at an experimentally controlled time.

To tag dividing QC cells under spatial and temporal control, I aimed to create a variant of the GFP tagging system established by Gallois *et al.* (2002). My system would utilise the same double reporter construct used by Gallois *et al.* (2002) to mark cells with GFP (Fig 6.3.), but instead of inducing Cre randomly, recombination would be induced in specific cells and at a specific time. To control Cre activity, I created a fusion between Cre and the GFP-tagged LTI6B membrane protein. This would anchor the Cre recombinase to the cell membrane, preventing it from acting upon its target construct in the nucleus. Between the Cre and GFP-LTI6B sequences, I placed a cleavage site for the tobacco etch virus (TEV) sequence-specific protease. The TEV protease is able to cleave proteins containing a unique amino acid sequence consisting of ENLYFQG (Kapust and Waugh 2000) and has been used previously to cleave engineered target proteins in *Arabidopsis* (Mathieu *et al.* 2007). To express the Cre-TEVr-

GFP-LTI6B protein in specific cells, such as the QC, an operator construct *Op:Cre-TEVr-GFP-LTI6B* was produced. QC-specific expression would be provided by placing this construct under the control of a WOX5:LhG4 driver (Fig 6.3.). To achieve temporal control over Cre induction, the TEV protease was placed under the control of the hsp18.2 heat shock promoter, which can be activated after dipping seedlings into a water bath at 38°C. Thus, ubiquitous activation of TEV protease was expected to cleave the Cre-TEVr-GFP-LTI6B protein specifically in the QC. After cleavage, Cre would be released from the plasma membrane and be able to localise to the nucleus (Le *et al.* 1999). In the nucleus Cre would be able to excise the GUS fragment from the double reporter construct, resulting in GFP expression in the QC and in any of its descendants.

In addition to using the WOX5:LhG4 driver to target membrane Cre to QC cells only, this system could also be applied to the shoot meristem to track cell lineage from stem cells within the shoot apex. The stem cell region within the shoot is marked by expression of *CLV3* (See chapter 1 for review of stem cell maintenance in the shoot, also see chapter 5 for an example of *CLV3:GFP* expression). It might be possible to direct expression of the membrane Cre construct to stem cells in the shoot using a CLV3:LhG4 driver. Therefore, I also placed *Op:Cre-TEVr-GFP-LTI6B* under the control of CLV3:LhG4 to test whether my tagging system could be put to general use.

Figure 6.4. 4-component cell lineage labelling system

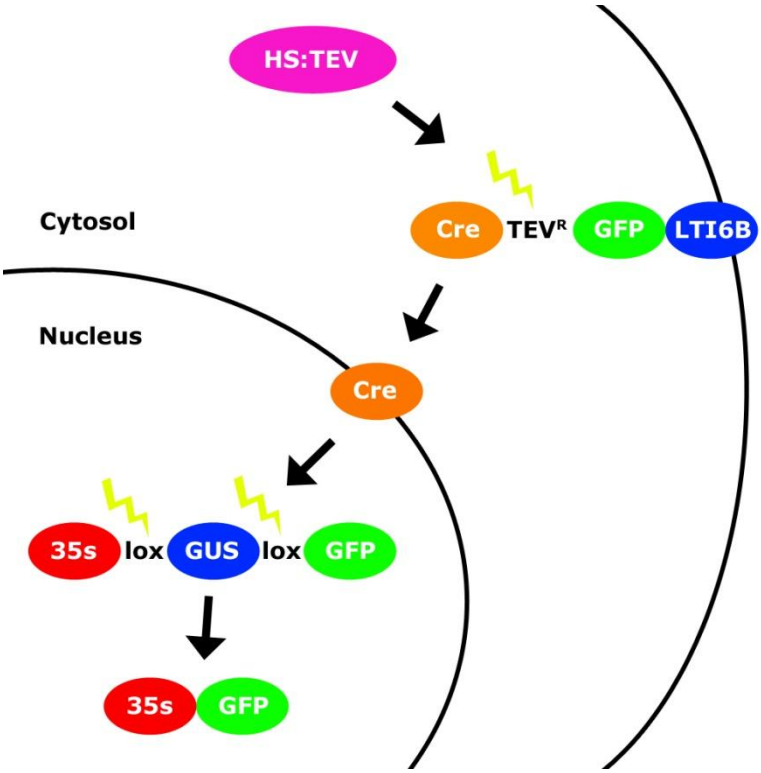

Schematic diagram showing 4-component system which allows specific labelling of cells descended from the QC. The LhG4:pOp mosaic expression system will drive *Op:Cre-TEVr-GFP-LTI6B* within the QC under control of WOX5:LhG4. *HS:TEV* will cleave at the TEV recognition site (TEVr) releasing Cre from its connection to the cell membrane. Cre can then locate to the nucleus where it excises GUS from the *35S-lox-GUS-lox-GFP* construct.

6.2.4. Applying the 4-component system to the shoot and root meristem

To begin arranging the 4-component system proposed in the previous section, the required constructs would first need to be cloned. Out of the 4 constructs needed for this system, only one was available in the lab from previous experiments. The *35S:lox-GUS-lox-GFP* construct was used previously in experiments to induce random GFP sectors as described (Gallois*, et al.* 2002). This left the three remaining constructs, *Op:Cre-TEVr-GFP-LTI6B* (membrane anchored Cre), *HS:TEV* (heat shock inducible TEV protease) and *WOX5:LhG4* (WOX5 driver). As a *WOX5:LhG4* driver was not available, I planned to construct *Op:Cre-TEVr-GFP-LTI6B* first and test it with an established CLV3:LhG4 driver used previously by the lab. Presence of membrane GFP in the shoot meristem of transformed plants would confirm correct expression of the new construct.

The strategy for creating the 4 component system involved introducing *Op:Cre-TEVr-GFP-LTI6B* into CLV3:LhG4 plants and *HS:TEV* into plants already containing the double reporter. Lines homozygous for each construct would then be crossed to generate plants with each of the 4 constructs. *Op:Cre-TEVr-GFP-LTI6B* was first tested with a CLV3:LhG4 driver to establish a working line before crossing to the *WOX5:LhG4* line which was still being constructed. Successfully transformed plants were expected to express membrane GFP in the shoot meristem. *Op:Cre-TEVr-GFP-LTI6B* was transformed into CLV3:LhG4 plants by the floral dip method (Clough and Bent 1998). Out of 15 primary transformants, 1 plant showed good expression of membrane GFP in the shoot meristem (Fig 6.5.). The GFP expression domain detected in the shoot was however much larger than expected. Experiments from chapter 5 using a published CLV3:GFP line showed clear GFP expression in the shoot apex (Yadav*, et al.* 2009). The expression domain using the CLV3:LhG4 driver was much larger in comparison. The use of this CLV3:LhG4 driver therefore may not be

entirely limited to the shoot apex; this requires further experiments to examine the specificity of its expression.

Additional problems were highlighted which suggest the membrane Cre operator construct may be prone to silencing in the next generation. The presence of membrane GFP was detected in the inflorescence meristem but not in floral buds. In addition, some possible areas of cell death are visible in the meristem indicated by bright green patches of fluorescence (Fig. 6.5b and 6.5d, cell death marked with asterisks). It is possible the shoot meristem may be highly sensitive to Cre because of its DNA cleaving properties. This would select for cells in which the construct has been inactivated. Plants in the next generation failed to show any expression of membrane GFP, it is possible the Cre expressing construct may have been targeted by gene silencing mechanisms. A study on Cre toxicity in plants also suggested gene silencing may inactivate Cre expression (Coppoolse *et al.* 2003).

HS:TEV was transformed into the double reporter construct (35S:lox-GUS-lox-GFP) which yielded 15 primary transformants. RT-PCR was performed on these primary transformants to determine expression of TEV protease in heat shocked and non-heat shocked plants. Around 6 inflorescence meristems were collected from each plant and divided into 2 tubes; one tube was exposed 38^{o}C in a waterbath for 30 minutes whereas the other tube was left at room temperature. Immediately after heat shock, RNA was extracted from control and heat shocked samples and RT-PCR was performed. Unfortunately, in both heat shocked and non-heat shocked plants, bands were present indicating presence of TEV in both. Tsukaya *et al.* (1993) suggested that the heat shock promoter is endogenously activated in floral organs by normal developmental processes. This procedure was instead repeated on seedlings of primary transformants which showed significant increase in expression of TEV after heat shock (Fig 6.6.).

A WOX5:LhG4 driver was required in order to drive expression of *Op:Cre-TEVr-GFP-LTI6B* within the central cells. Expression of the operator construct may not be silenced in the QC due to these stem cells not contributing to the germline. To test its function, *WOX5:LhG4* was transformed into the L*er* background and crossed to the Op:ER-GFP reporter. Seeds from the cross were sown onto plates with antibiotic resistance for both constructs; resulting seedlings were screened for presence of GFP within the QC. No GFP was detected in seedlings from 18 crosses.

Multiple difficulties experienced with cloning and gene silencing led to the abandonment of these experiments. Interestingly, the problems experienced with localising Cre recombinase to the meristem suggest stem cells are sensitive to recombinase activity. Other mechanisms to label sensitive cells will therefore need to be developed in order to directly label stem cell descendents. Cell lineage experiments remain important in monitoring the long-term contribution of QC division to maintenance of the root meristem after DNA damage.

Figure 6.5. Expression of *Cre-TEVr-GFP-LTI6B* in the shoot was detected after transformation into CLV3:LhG4 background

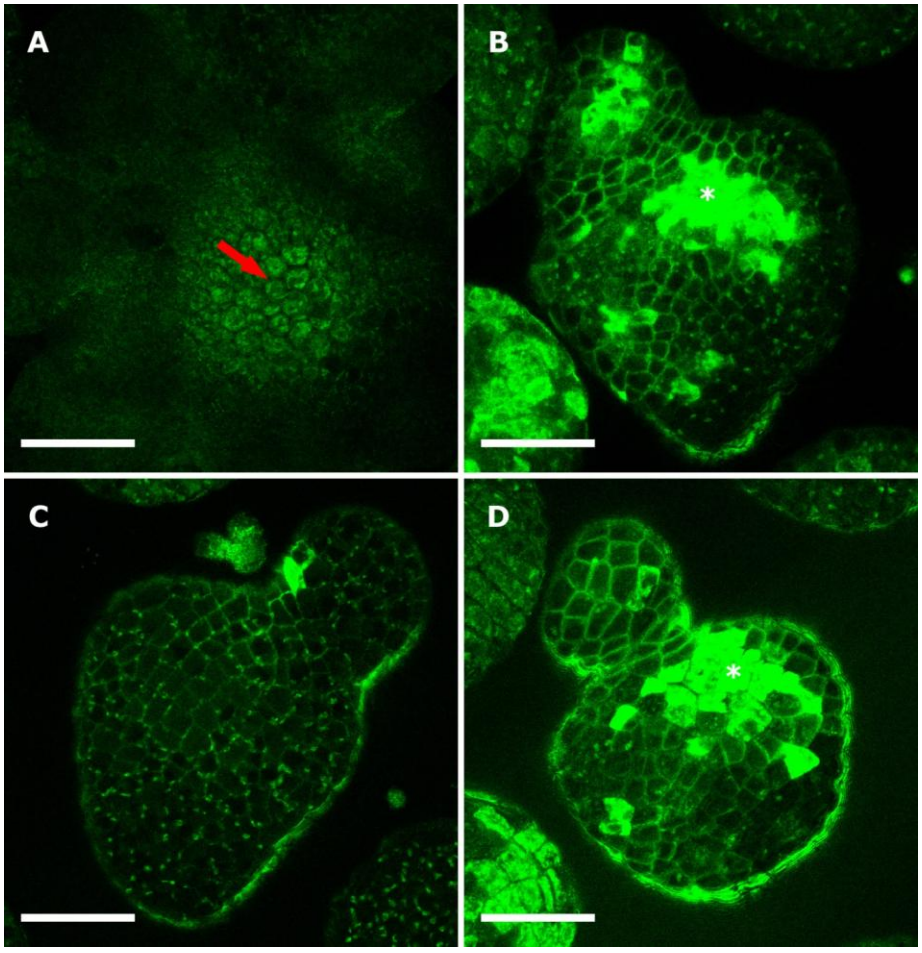

Plants expressing *CLV3:LhG4* which were transformed with the *Op:Cre-TEVr-GFP-LTI6B* construct showed membrane GFP in the shoot meristem. Images represent 3 shoot tips derived from the same primary transformant (**B**, **C** & **D**) and a wild type control not expressing GFP (**A**). The CLV3 expressing domain was however observed to be larger than expected. (Scale Bars: 50 μm).

Figure 6.6. Heat shock induced expression of TEV protease was confirmed by RT-PCR

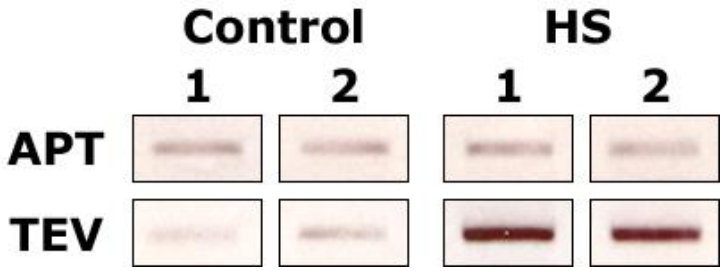

Experiments using RT-PCR to test the *HS:TEV* construct showed enhanced expression after heat shock. Seedlings were exposed to 38^{o}C for 30 minutes and prepared for RT-PCR, 2 primary transformants showed elevated TEV levels whereas expression of APT control remained constant.

6.2.5. Monitoring long term root growth and survival after exposure to DNA damaging conditions

Recovery of meristem structure after DNA damage suggests this mechanism may also allow continued root growth. This raised the question of how selective death of initials affected overall root growth. Death of root initials might be expected to initially cause a growth disadvantage, but this might be compensated in the long run if there is a penalty for allowing cells with damaged DNA to populate the stem cell niche.

Other studies have examined root growth after DNA damage induced by bleomcyin, hydroxyurea, aphidicolin and UV-B which cause stunted roots (Culligan*, et al.* 2004, Culligan*, et al.* 2006, De Schutter*, et al.* 2007, Dissmeyer*, et al.* 2009). Most of these experiments however are the result of continuous treatment by these chemical agents allowing no time for recovery. Culligan (2006) investigated root length recovery after γ-irradiation, WT roots recovered growth 7-8 days after irradiation at 100 gray whereas *atm-3*, *atr-2* and *ku80-1* showed complete growth termination. Treatment at 100 gray is however far more severe than the 40 gray irradiation which initiated cell death in root tips (see chapter 2, Fig 2.8.).

To investigate recovery of root growth at lower doses of DNA damage, seedlings were treated for 24 hrs with 20 µg/ml zeocin to induce cell death. Seedlings were then moved to normal media for 7 days to track continued growth of the root. To genetically test the effect of cell death on overall root growth, the only available mutants that suppress cell death are *atm* and *atr* (see chapter 3). One limitation of these mutants, however, is that they also lack cell cycle arrest and DNA repair, which are also expected to affect cell fitness and growth. Defects in DNA repair and in cell cycle checkpoints might eventually cause these plants to undergo mitotic catastrophe and arrest root growth. Accordingly, analysis of root growth showed recovery of root growth in Columbia

wild type plants, but total arrest by *atm* and *atr* mutant alleles (Fig 6.7.). Length of treated wild type roots was considerably longer than those of atm and atr mutants, which seem to have terminated growth. Thus if atm and atr mutants had an initial growth advantage due to survival of root initials, this was subsequently negated by the consequences of DNA damage on cell fitness.

Figure 6.7. Analysis of root growth after DNA damage in ATM and ATR mutants

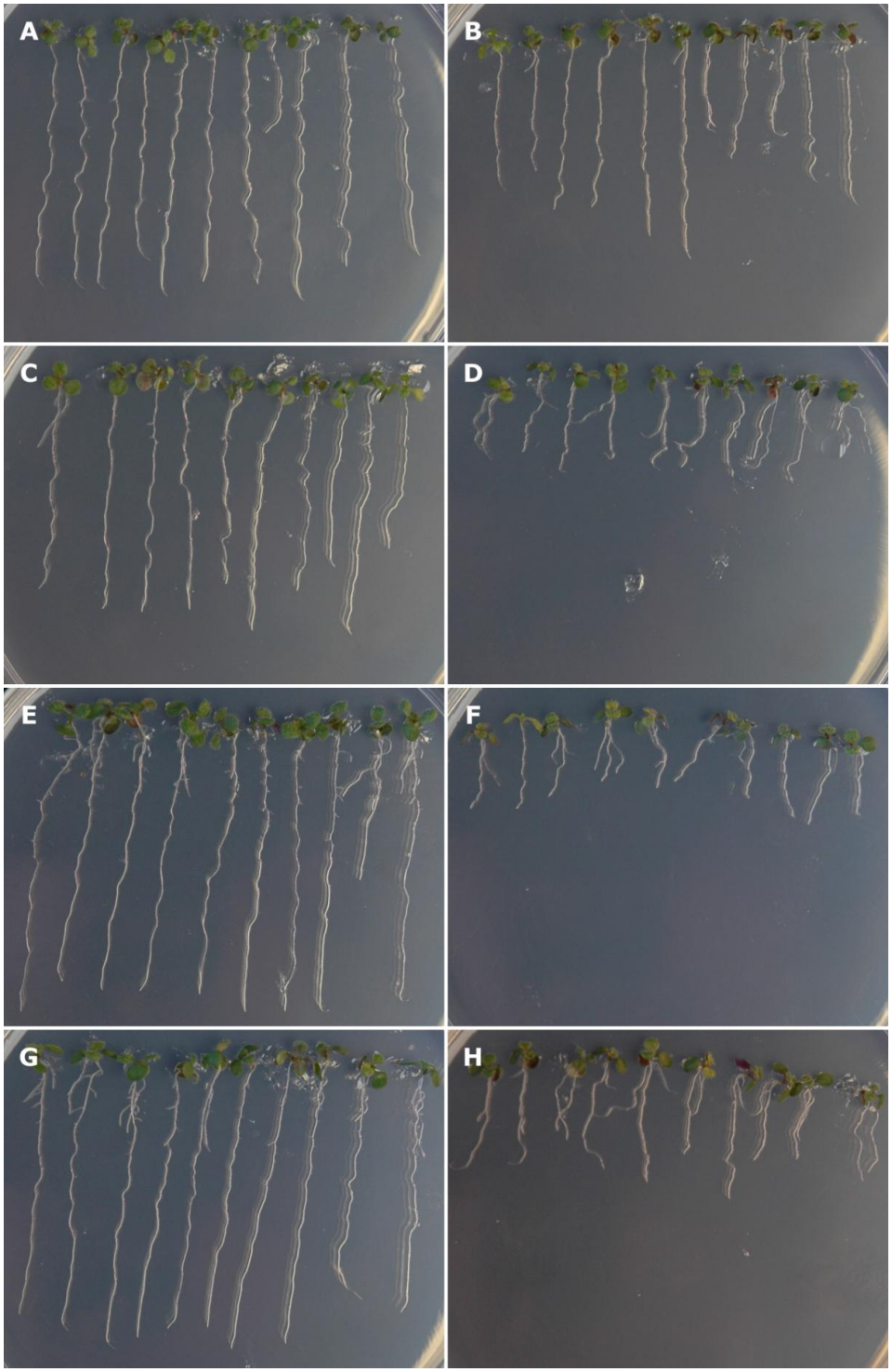

Seedlings were treated with 0 & 20 µg/ml zeocin for 24 hrs then moved to untreated media for 7 days. Columbia untreated (**A**) treated (**B**), *atm-1* untreated (**C**) and treated (**D**), *atm-2* untreated (**E**) and treated (**F**) and *atr-2* untreated (**G**) and treated (**H**). Root growth appears to recover in treated Columbia roots whereas *atm* and *atr* show termination of growth.

6.3. Discussion

One of the main objectives of this chapter was to assess short and long term changes to the root meristem after cell death. As programmed cell death was hypothesised to exclude genetically damaged initials from the meristem, it was important to discover what happens to these cells during recovery of root structure. To investigate this, treated roots expressing *WOX5:GFP* were left to recover for 24 and 48 hrs after treatment with zeocin. Staining with propidium iodide revealed after 0 hrs recovery, clearly defined death of initials with clear cell outlines was seen in the root meristem (Fig 6.1.). After 24 and 48 hrs, dead initials appeared to be squashed by surrounding cells and levels of cell death were reduced. Dead cells seemed to be pushed away from the QC, the possibility still remained that QC activation was excluding dead cells from the stem cell niche.

To assess QC activation, live imaging was used to visualise the meristem over a 24 hr recovery period after zeocin treatment. WOX5:GFP was crossed to the LTI6B membrane marker to label both membranes and QC identity. Imaging at 8, 16 and 24 hr time points showed surviving root initials to expand and fill space left by dead cells. QC activation was however not seen within this 24 hr period, division could however occur at a later time point. Live imaging by this approach could not be used for longer periods, because prolonged exposure to high laser intensities and photobleaching during confocal imaging can damage roots (Oparka *et al.* 1994). Also, quick growth of the root can limit the imaging lifespan on a microscope slide (Campilho*, et al.* 2006). These factors limited the effectiveness of this live imaging approach meaning the root could only be imaged for relatively short periods of growth on a slide.

In addition to live imaging, recovery experiments using WOX5:GFP seedlings stained with FM464 showed expansion of the WOX5 domain after 24 hrs recovery. This enlargement of *WOX5* expression was thought to be possibly

due to activation of QC division. The enlarged domain was observed to be reduced after 48 hrs recovery showing recovery of normal meristem structure. Enlarged expression of GUS QC markers has previously shown to label QC activation in mutants overexpressing ethylene (Ortega-Martinez*, et al.* 2007). Experiments investigating the expression of various root meristem markers however suggested otherwise (Xu*, et al.* 2006). In the study by Xu *et al*. (2006) the expression of *DR5*, *PLT*, *WOX5*, *SHR* and *SCR* were monitored after laser ablation of the QC. Expansion of the *WOX5* expressing domain was seen after QC ablation in a similar pattern as witnessed in my experiments. It was thought disrupted auxin flow could change expression of the WOX5 reporter as *WOX5* is expressed downstream of genes modulated by auxin flow (Tucker and Laux 2007). This paper also showed *DR5* expression patterns after QC ablation, which also showed an expanded domain. Experiments in chapter 2 with DR5 showed no change in expression as a result of cell death. Recovery of DR5:GFP roots was however not followed in these experiments. It would be useful to perform these experiments also with the DR5:GFP auxin marker to confirm whether expanded expression also occurs in this line after death of initials. As the expansion of the WOX5 domain did not reveal clear evidence of QC activation, other methods would be needed to examine QC contributions over time in the same root.

To further study QC activation over a longer time period, a cell lineage labelling system was designed to specifically label QC cells and track their potential contribution to the stem cell niche. This 4 component system would enable spatial and temporal activation of QC marking, once labelled the potential lineage to initials would be marked by GFP. Cloning of a *HS:TEV* construct showed good results in RT-PCR experiments investigating TEV expression after heat shock. Problems arose, however, when the *Op:Cre-TEVr-GFP-LTI6B* construct was found to be silenced in floral buds and plants of the next generation. Primary transformants displayed membrane GFP showing successful

expression of the membrane bound construct. The high frequency of silencing may result from selection against cells expressing the construct, possibly due to toxicity of the Cre recombinase. Cre is involved in DNA recombination specifically between lox sites present in DNA. Cre activity could be excluded from genetically important cells like stem cells because of these properties. Coppoolse *et al.* (2003) investigated toxicity of Cre in petunia, *N. tabacum* and *A. thaliana*. Plants expressing Cre under constitutive promoters were found to show leaf chlorosis, deformation and sterility. These Cre constructs were suggested to be targeted by gene silencing mechanisms (Coppoolse*, et al.* 2003). Consistent with the idea that Cre expression could be toxic, cell death also seemed to occur in the shoot meristem in lines containing the *Op:Cre-TEVr-GFP-LTI6B* construct in conjunction with the CLV3 driver. Cells expressing Cre could undergo cell death in response to DNA breaks, as seen in the root and shoot after zeocin treatments. It has also been reported previously that the recombination of heat shock inducible constructs is not effective within meristem cells (Kurup*, et al.* 2005). Using the Ac transposase, Kurup *et al.* (2005) aimed to label cell lineages within the root meristem using a recombinase system. This system randomly labelled cells by heat shock inducing YFP labelled sectors in the root. Kurup *et al.* (2005) reported that central cells never showed YFP expression indicating these cells may also be protected from actions of recombination proteins. Alternatively, the lack of sectors arising from recombination in central cells might result simply from the fact that random sectors would be rare in a cell population that constitutes only a very small portion of the root. This idea could be tested by targeting the recombinase to these cells; unfortunately, in our case this could not be tested due to lack of a working WOX5:LhG4 driver.

WOX5:LhG4 primary transformants were crossed to Op:ER-GFP to identify those that successfully expressed the driver, but out of 18 crosses no GFP expression was detected. It was uncertain whether *Op:Cre-TEVr-GFP-LTI6B* would be silenced in the root, the plan was to cross this line into the WOX5

driver to see if membrane GFP was detected in the QC. Further experiments with this system could include generating a working WOX5 driver to test this theory. Also, crossing the operator line into a RDR6 mutant background could eliminate silencing in the shoot. A mutant for RDR6 would stop any RNA dependent silencing (Peragine *et al.* 2004); unfortunately I did not have enough time to complete these experiments.

Programmed death was hypothesised to effectively remove damaged cells from the population to establish continuation of growth. The question remained: is cell death essential in recovering root growth? My results show that root growth is re-established after transient zeocin treatment in the wild-type, Columbia primary roots showed stunted growth after treatment. Loss of ATM or ATR function, either of which is required to detect cells with damaged DNA, showed a complete termination of root growth. These results are consistent with the idea that removing genetically instable stem cells is beneficial to root growth. However, it cannot be definitely concluded from these experiments that death of damaged cells helps roots recover and continue growing, because the *atm* and *atr* mutants have additional defects, including inability to delay the cell cycle to allow for repair, and inability to activate DNA repair genes. To answer this question, it will be necessary to identify mutants that specifically prevent cell death, without affecting the other responses downstream of *ATM* and *ATR*.

It also remains uncertain whether QC cells divide to repopulate root initials after DNA damage. My experiments monitored QC division up to 24 hrs of recovery; it remains entirely possible that QC activation could occur after cell death is removed from the meristem. To answer this question, continuation of the cell lineage labelling would be useful to show any long term effects of QC divisions. Problems would need to be overcome to eliminate the potential gene silencing within meristem cells, possibly using an *rdr6* mutant. In conclusion, although QC division was not an early response to DNA damage in *Arabidopsis*, the results from this chapter and chapter 2 do not reject the original hypothesis

proposed by Clowes *et al.* (1961) that QC activation could eventually help to repopulate damaged root meristems.

Chapter 7 – General discussion

7.1. General summary

The aim of my PhD project was to investigate responses to DNA damage in plants, specifically within shoot and root meristems. Stem cell populations are important throughout the lifetime of *Arabidopsis* to mediate growth and establish the germline; little is understood about how they tolerate harmful genotoxic conditions. It might be expected that meristems may contain enhanced mechanisms to deal with genomic instability due to their importance as the ultimate source of all new cells and their inability to escape harmful conditions. This was confronted in the second chapter when investigating the function of the QC.

The quiescent centre was hypothesised to act in safeguarding the root meristem against DNA damage through early work by Clowes (1959). Slow mitotic activity within these cells was proposed to enable enhanced DNA repair, providing the stem cell population with a genetically stable template (Ivanov 2007). In the event of DNA damage, the QC would activate division in order to form a new population of stem cells in the root tip. Initial experiments therefore focused on examining QC divisions by confocal microscopy after treatment with radiomimetic drugs that induce DNA damage. Eventual staining with propidium iodide, a stain which labels cell outlines but can also penetrate dead cells, revealed more exciting results. Cell death was found to occur specifically in the stem cell population of the root meristem in response to radiomimetic drugs and x-ray irradiation. This was surprising as cell death has not previously been described in plants as a downstream response to DNA damage. In addition, the QC was shown to survive DNA damage treatments marked by expression of the *WOX5:GFP* marker. This result upheld the hypothesis that the QC could act in

repopulating meristem cells. We however focused on the unexpected cell death phenotype to see if it was a genetically programmed response to DNA damage.

Experiments from chapter 3 focused on identifying the role of DNA damage perception proteins in activating initial specific cell death. Interactions between DNA damage signalling intermediates are well studied in animals and proteins involved in damage perception, repair and cell cycle arrest are well characterised. A number of related genes have been identified within the genome of *Arabidopsis* through sequence homology with their mammalian counterparts. Mutants for a number of these genes were found to display sensitivity to DNA damaging agents compared to wild type plants providing evidence for their role in DNA repair. Analysis of mutants for key signalling transducers *ATM* and *ATR* showed clear lack of DNA damage induced cell death, implicating these genes as being essential to DNA damage perception in plants. In addition, mutants involved in NHEJ pathways were shown to exhibit higher levels of cell death including spontaneous death of root initials in the absence of zeocin. It therefore appears that conserved mechanisms for cell death activation exist between animals and plants, despite the lack of some homologous genes such as p53 and checkpoint kinases.

After showing cell death was a genetically controlled response in chapter 3, it was next essential to determine the mechanism by which root initials committed suicide. As mentioned, three types of cell death are described in animals; apoptosis, autophagy and necrosis. These pathways were not as well characterised in plants, this is due to features of plant cells which limit apoptosis, the primary mechanism of programmed cell death in animals. Stem cells in animals have previously shown to be hypersensitive to DNA damage, activating apoptosis in response to gamma irradiation (Heyer*, et al.* 2000). Eventual electron microscopy of dying initials showed presence of vesicles resembling autophagosomes, a characteristic of autophagy. However, the idea that autophagy is the mechanism of cell death downstream of ATM/ATR, was not

confirmed through zeocin treatment of ATG mutants known to be defective in autophagy. It was concluded that other mechanisms could act alongside autophagy to affect the cell death response.

The root meristem is important for root growth; the shoot meristem however contains additional functions in establishing the germline. Because of this, the shoot was predicted to also experience cell death in response to DNA damaging treatments. Chapter 5 therefore investigated death in the shoot meristem using zeocin and x-ray irradiation. Both treatments were found to induce cell death within the shoot apex highlighting cell death as a mechanism to remove damaged stem cells in both the root and shoot. Mutants for *ATM* but not *ATR* prevented this death implicating different roles for these signalling proteins in root and shoot meristems.

Finally, I aimed to investigate the potential for the QC to activate division after DNA damage using cell lineage marking techniques. Unfortunately, I was unable to produce a working cell lineage labelling system based on the membrane bound Cre recombinase method. This was due mainly to problems experienced with silencing of transgenic plants and cell death experienced within plants containing Cre constructs. Subsequent experiments within this chapter addressed recovery of root growth after DNA damaging treatments. I showed that root growth recovers after the standard 24 hr zeocin treatment and that cell death slowly reduces in roots followed up to 3 days after exposure. This provides evidence for the role of cell death in maintenance of root growth after exposure to genotoxic conditions.

Results obtained within this thesis show evidence for cell death in protecting stem cell populations from genomic instability, removing cells with compromised genomes. Cell death would function as a mechanism to protect future generations from negatively impacting mutations in the case of the shoot meristem. In the root, cell death could help to remove damaged stem cells to help maintain growth in a competitive environment. Stem cell death may also be

required to help maintain meristem structure, which maybe essential for competitive root growth. It is also possible that cell death could operate in conjunction with already established DNA damage toleration mechanisms such as DNA translesion polymerases as mentioned in chapter 2 (Curtis & Hays 2007).

The assay developed by these experiments provides a useful tool for identifying genes that control these mechanisms. As mentioned, mutants were found to lack cell death in response to DNA damage, it will be essential to find additional mutants to further develop plant specific DNA damage response pathways. It is possible that these mutants could tolerate genotoxic stress caused by environmental conditions, allowing plants to be grown in areas previously unable to yield crops.

7.2. Future directions

In addition to future experiments described throughout the thesis, a genetic screening method could be used to reveal key signalling proteins involved in the initiation of cell death. Using this approach, seedlings from a mutagenised *Arabidopsis* population could be treated with zeocin and screened for roots lacking cell death. Preliminary experiments have attempted to establish a quick screening method in order to efficiently identify these seedlings. Using Sytox staining (used in chapter 2 to label cell death); I have managed to observe cell death at low magnifications within wild type plants. This would remove the need for oil immersion as used in confocal imaging of root tips, speeding up imaging of large numbers of seedlings. The next step will to set up a mock screen using ATM and ATR mutants which showed no cell death in chapter 2. These will be mixed with wild type seedlings and screened to see if mutants can be isolated from the mock population.

A number of known DNA repair mutants were also not tested in this study due to time constraints. *Arabidopsis BRCA1* and *BARD1* are described in the introductory chapter; mammalian homologs are involved in DNA damage perception and downstream signalling (Reidt*, et al.* 2006). The *ATRIP* homolog was also described by Sweeney *et al.* (2009) and mutants share phenotypes related to *atr-1* seedlings. It will be interesting to analyse the mutants through zeocin treatments to discover whether they play a role in cell death activation. Also, The XRCC4 protein which associates with LIGIV has been identified in plants and is shown to interact with AtLIGIV (West*, et al.* 2000). This mutant could also display spontaneous cell death within the root meristem as experienced with *ku80* and *ligiv* seedlings.

In addition to the study of DNA signalling, mutants displaying defects in cell death mediated developmental process could also prevent DNA damage induced death of initials. Cell death processes act during xylem differentiation to remove organelles from sieve elements, it's possible that similar proteins contribute to both pathways. The *ACAULIS5* (*ACL5*) gene has previously been described to act in xylem specification within *Arabidopsis* (Muniz *et al.* 2008). This paper utilised the XCP2:GUS marker to show proposed xylem specific proteolytic activity associated with cell death, the *acl5* mutant exhibited premature expression of this construct suggesting a role of *ACL5* in repression of cell death in xylem elements. If this gene has a similar role in DNA damage induced cell death, the mutant could display spontaneous death and higher cell death levels within the root meristem.

Finally, in addition to toxic metal experiments, other conditions which are known to elicit DNA damage in plants could be tested using the cell death assay. This could include exposing plants to drought and high or low temperature levels, looking for an effect within meristems. This would act to link cell death to naturally occurring environmental conditions and could help to explain tolerance to many factors.

Chapter 8 - Materials and Methods

8.1. Plant material

8.1.1. Plant lines

All mutant and transgenic plant lines used throughout the thesis are described below.

Mutants	Accession	Insertion ID	Reference
mre11-4	Columbia	SALK_028450	Unpublished
nbs1	Columbia	GK-570B09	Waterworth *et al.* (2007)
atm-1	WS	N/A (see ref)	Garcia *et al.* (2003)
atm-2	Columbia	SALK_006953	Garcia *et al.* (2003)
atr-2	Columbia	SALK_032841C	Culligan *et al.* (2004)
ku80	WS-2	N/A (see ref)	West *et al.* (2002)
lig4-4	Columbia	SALK_095962	Unpublished
rad51-1	Columbia	GABI_134A01	Li *et al.* (2004)
wee1-1	Columbia	GABI_270E05	De Schutter *et al.* (2007)
wee1-2	Columbia	SALK_147968	De Schutter *et al.* (2007)
e2fa	Columbia	N/A (see ref)	Roa *et al.* (2009)
tert (3rd Gen)	Columbia	N/A (see ref)	Fitzgerald *et al.* (1999)
mc1	Columbia	GK-096A10	Unpublished
mc8-1	WS	FLAG322_G10	He *et al.* (2008)
sid2-1	Columbia	N/A (see ref)	Nawrath & Métraux (1999)
ein2-5	Columbia	N/A (see ref)	Guzman & Ecker (1990)
rcd1-1	Columbia	N/A (see ref)	Overmyer *et al.* (2000)
parp2	Columbia	GK-380E06	Unpublished
atg5-1	Columbia	N/A (see ref)	Thompson *et al.* (2005)
atg6-2	Columbia	SALK_109281	Fujiki *et al.* (2007)
atg7-2	Columbia	GK-655B06	Hofius *et al.* (2009)
atg18c	Columbia	SALK_009459	Xiong *et al.* (2005)

Transgenic lines	Assession	Reference
35S:GFP-LTI6B	N/A	Cutler *et al.* (2000)
QC25	N/A	Sabatini *et al.* (2003)
DR5:GFP	N/A	Frimil *et al.* (2003)
PIN1:GFP	Columbia	Benkova *et al.* (2003)
CYCB1;1:GFP	Columbia	Colon-Carmona *et al.* (1999)
WOX5:GFP	Columbia	Bilou *et al.* (2005)
ATG8:GFP	Columbia	Yoshimoto *et al.* (2004)
CLV3:GFP	N/A	Yadav *et al.* (2009)
NahG	Columbia	Delaney *et al.* (1994)
e2faOE	Columbia	De Veylder *et al.* (2002)
dpaOE	Columbia	De Veylder *et al.* (2002)
parp RNAi 1024	Columbia	De Block *et al.* (2005)
parp RNAi 1025	Columbia	De Block *et al.* (2005)

I would like to acknowledge the following people for providing seeds; Chris West (*mre11-4*, *ku80*, *lig4-4* & *rad51-1*), Lieven Deveylder (*wee1-1*, *wee1-2*, *e2faOE* & *DPaO*E), Marie-Edith Chabouté (*e2fa*), Karel Riha (*tert* 3rd gen), Patrick Gallois (*mc8-1*), Morten Petersen (*atg5-1* & *atg7-2*), Keiko Sugimoto (*atm-1*), Renze Heidstra (*WOX5*:*GFP*), Liam Dolan (*QC25*), Peter Doerner (*CYCB1;1:GFP*), Kohki Yoshimoto (*ATG8:GFP*), Marc De Block (parp RNAi) & Pradeep Das (*CLV3:GFP*).

8.1.2. Seed sterilisation

Seeds were placed into a labelled 1.5 ml Eppendorf tube, 15 µl of 100% Ethanol was then pipetted into the tube under a laminar flow hood. Open tubes were placed in racks and left for approximately 3 to 4 hours. Once Ethanol had evaporated, tubes were then gently tapped to ensure seeds did not stick together.

8.1.3. Growth conditions

Seeds were sown directly onto germination media (GM): Murashige and Skoog salts (Sigma), 1% glucose, 0.5 g/mL 4-morpholineethanesulfonic acid (Sigma), 0.8% agar, pH 5.7. Media was autoclaved and left to cool before pouring into 90 mm petri dishes (Sterilin). For selection of certain transgenic lines, antibiotics were added to media after cooling to around 50°C at the following working concentrations: Kanamycin 50 µg/ml (Sigma), Gentamycin 100 µg/ml (Sigma) & Phosphinothricin (PPT) 10 µg/ml (Melford Laboratories). Once media was dry, seeds were sown directly from Eppendorf tubes onto plates, which were sealed with surgical tape (3M). After stratification for 48 hrs at 4°C in the dark, plates were transferred to long day growth chambers at 21°C (16 hrs light at 100 µmol photons $m^{-2}s^{-1}$, 8 hrs dark) or continuous light at 20°C (24 hrs at 100 µmol photons $m^{-2}s^{-1}$). Seeds used for root imaging were always transferred to continuous light where plates were placed vertically; plants grown to maturity were transferred to long day growth chambers. Antibiotic resistance was usually detectable after 1 to 2 weeks of growth in long day growth conditions.

For plants grown to maturity, seedlings were pricked out to soil after formation of the first two leaves. Plants were grown in JIC *Arabidopsis* soil mix consisting of Levingtons F2 compost (with Intercept) and grit at a ratio of 6:1. Seedlings were then placed into CER 51-10 under long day growth conditions (16 hrs light, day 18°C and night 20°C, humidity 80%)

8.1.4. Crosses

Crosses were performed using fine-pointed forceps on flowers from primary or secondary inflorescences under a dissection microscope. To isolate female pollen acceptors, mature flowers were removed from inflorescence meristems along with the shoot apex leaving only unopened floral buds. These buds were then

emasculated leaving the immature carpel; this was performed on approximately 5 to 10 buds. Emasculated plants were then labelled and left for 2 days to allow carpel to mature. The carpel was then pollinated from mature flowers by dabbing anthers onto the stigma of the emasculated floral bud. These were left to mature into siliques; just before desiccation, siliques were bagged into 88mm x 120mm cellophane bags (Cannings) to collect seeds.

8.1.5. Genotyping of T-DNA mutants

8.1.5.1. DNA extractions for PCR genotyping

To extract DNA from mutant lines, 3 cauline leaves were collected from each plant and placed into a labelled Eppendorf tube. Tubes were dipped into liquid nitrogen and tissue was ground within the Eppendorf using a micro-pestle. 500 µl of DNA extraction buffer (0.2 M Tris-HCl pH9, 0.4 M LiCl, 25 mM EDTA & 1% SDS) was added to the tube, frozen tissue was completely submerged into extraction buffer. Tubes were centrifuged for 5 mins at full speed (16000 x g), 350 µl of supernatant was then transferred to a fresh Eppendorf with 350 µl isopropanol. Tubes were then mixed by inversion and centrifuged again for 20 minutes. Liquid was poured away and the tube left to dry for ~20 mins leaving a pellet. The pellet was washed by adding 500 µl of 70% Ethanol, vortexing and centrifuging for 10 mins. Tubes were again left to dry for ~30 mins, the pellet was then resuspended in 200 µl of dH_2O.

8.1.5.2. PCR genotyping

After completing DNA extractions, PCR reactions were prepared in order to identify homozygous or heterozygous mutant plants. Hot start PCR was used in all genotyping reactions to increase the specificity of oligos used to amplify from

genomic DNA preps. This involved preparation of separate PCR and hot start mixes, the hot start mix containing Taq polymerase was added after heating samples to 94°C. Reactions were prepared as follows: PCR mix – 2 µl Genomic DNA, 1 µl Forward oligo [10 µM], 1 µl Reverse oligo [10 µM], 0.625 µl dNTPs [10 mM] (Roche), 2 µl 10x Taq Buffer (Roche) and 13.375 µl dH_2O; Hot start Mix - 0.25 µl Taq (Roche), 0.5 µl 10x Taq Buffer (Roche) and 4.25 dH_2O.

Relevant oligonucleotide combinations for each mutant were used to amplify either wild type or mutant alleles (see section 8.1.5.3. for list). Wild type and mutant reactions were prepared for each DNA sample totalling 20 µl. The following PCR programme was used for genotyping: 94°C for 2 mins then 30 cycles of 94°C for 30 secs, 55°C for 30 secs, 72°C for 1 min. Reactions were heated for 1.5 minutes, PCR programme was then paused. 5 µl of hot start mix was then added to each tube (enough was produced to cover all reactions), the lid was closed and the PCR programme resumed. On completion of PCR, samples were run on 2 % agarose gel looking for bands indicating wild type or mutant alleles.

8.1.5.3. Genotyping oligos

The following oligonucleotide combinations were used to amplify wild type or mutant alleles. For *atm-1* mutants, homozygous lines were identified by the partial sterility phenotype of mature plants.

Mutant	**Oligos**
nbs1	NF033 ATATTGACCATCATACTCATTGC NF034 GGTATTTACAAGGTTGGTCGAAAA (NF033 + NF034 = Mutant)
atm-1	N/A
atm-2	NF045 GCGTGGACCGCTTGCTGCAACT NF046 TCTCTCCTTGTTTCAAGCTCTGC (NF045 + NF046 = Mutant)
atr-2	NF039 GCAGCAAAAATTTCTTGGTTG NF040 ACTTCAAGGGTTCCGATGTTC

	NF041 ATTTTGCCGATTTCGGAAC (NF039 + NF040 = WT; NF039 + NF041 = Mutant)
ku80	NF024 CTCCAAGACGCAGCCTTTACGAAG NF025 CAAGGGCTTTCGCTATGGACCTCAG NF026 GATTCTTTTTATGCATAGATGCAC (NF024 + NF025 = WT; NF024 + NF026 = Mutant)
lig4-4	NF041 ATTTTGCCGATTTCGGAAC NF053 AAAGCCCTAAGGTCTTCATGG NF054 TTTGTTGTTTGAGGATCCGAC (NF053 + NF054 = WT; NF041 + NF054 = Mutant)
rad51-1	NF018F TTTGTGTTTTCTTCTGTGATAGCTT NF019R ATTATACGCCCTCGCATAGG NF033 ATATTGACCATCATACTCATTGC (NF018 + NF019 = WT; NF018 + NF033 = Mutant)
wee1-1	NF029 TGGTGCTGGACATTTCAGTCGG NF033 ATATTGACCATCATACTCATTGC NF042 TCAATAAGGCTTGGTTTCTTCAGT NF047 GCTATCTGTAAGAGACATAGTAC (NF029 + NF047 = WT; NF042 + NF033 = Mutant)
wee1-2	NF041 ATTTTGCCGATTTCGGAAC NF043 TCTGATGTCCAAAAGGGTCAG NF044 GAAGATTCGGAAGATGGAAGG (NF043 + NF044 = WT; NF041 + NF044 = Mutant)
e2fa	E2fa FW1 TTCCAGGTCTGTCTTTCCTATTTC E2fa RV1 CTTCCTATTTCTATGTTCATTATA E2fa LB CCCATTTGGACGTGAATGTAGACAC (FW1 + RV1 = WT)
tert	TERT-6 CTAGGACATATCCATCAAGGGCT TERT-7 GAAAGGAAGCTGTATTGCACGAA LB-CD6 GAACATCGGTCTCAATGCAA (TERT-6 + TERT-7 = WT; TERT-6 + LB-CD6 = Mutant)
mc1	NF033 ATATTGACCATCATACTCATTGC NF074 TCCTCCGCAACCTTCCTCCGC NF075 CGATATGGATCAGTTTCTTCC (NF074 + NF075 = WT; NF033 + NF075 = Mutant)
mc8-1	N/A
parp2	NF033 ATATTGACCATCATACTCATTGC NF048 AGGGAGAGAAGAGGAGAAGAAGAC (NF033 + NF048 = Mutant)
atg5-1	NF059 CAATTCACAGATGGATTGTAACTGCAGAG NF060 GCCTTTTCAGAAATGGATAAATAGCCTTGCTT (NF059 + NF060 = Mutant)
atg6-2	NF068 GCTGAAGTAAACCATCAACTG NF069 GTTACACATCGTATGGAGGAG (NF068 + NF069 = WT; No Band = Mutant)
atg7-2	NF033 ATATTGACCATCATACTCATTGC NF058 CAAGCCTCAATTACACTTTCATCA (NF033 + NF058 = Mutant)
atg18c	NF064 AAGAAAACGCAGACACGTGAA NF065 CTCTCCTCGATTGAGACCAGG NF066 GCGTGGACCGCTTGCTGCAAC (NF064 + NF065 = WT; NF064 + NF066 = Mutant)

8.2. Creating transgenic lines

8.2.1. CTAB genomic DNA extraction

The following protocol was used to extract genomic DNA for cloning of the *WOX5* promoter. 500 ml of CTAB buffer was produced: 20.54 g Sorbitol, 110 ml Tris pH8, 22 ml EDTA 0.5 M pH8, 23.38 g NaCl, 5 g Sarcosyl (N-lauroyl-sarcosine), 4 g CTAB (cetyltrimethylammonium bromide) and dH_2O up to 500ml (do not autoclave). Three cauline leaves were collected from wild type L*er* plants and placed into labelled Eppendorf tubes (3 extractions were performed). Tubes were dipped into liquid nitrogen and tissue was ground using a micro-pestle (do not allow to thaw). 1 ml of CTAB buffer was added and mixed with ground tissue, tubes were then incubated for 15 mins at 65^{o}C mixing occasionally. Under a fume hood, 0.4 ml chloroform was added and tubes were mixed by inversion. After centrifuging for 10 mins, the aqueous phase was then transferred to a fresh tube (usually 850 µl). 0.7 ml of cold isopropanol was added, the tube was incubated at -20^{o}C for 30 mins then centrifuged for 10 mins to pellet DNA. The Pellet was then resuspended in 500 µl dH_2O, an equal volume of phenol:chloroform (1:1) was added and mixed by tube inversion. After centrifuging for 10 mins, the aqueous phase was transferred to a fresh tube (450 µl). 45 µl of 3 M sodium acetate (pH 5.5) and 900 µl 100% ethanol was then added; tubes were placed at -20^{o}C for 1 hr (preferable to leave overnight). After centrifuging for 10 mins to pellet the DNA, ethanol was removed and 1 ml of fresh 100% ethanol was added to wash the pellet. The pellet was resuspended after vortexing and tubes were finally centrifuged for 5 mins. Ethanol was removed, the pellet was left to air-dry for 30 mins then resuspended in 50 µl dH_2O and vortexed.

8.2.2. Cloning strategies

8.2.2.1. Supplier information

All enzymes and buffers used in cloning reactions are supplied by Roche unless stated otherwise. The pGEM-T Easy vector system (kit including vector, T4 ligase and buffers) was supplied by Promega and oligonucleotides were supplied by Sigma.

8.2.2.2. *HS:TEV*

TEV protease was amplified from pRK793 (Addgene) using NF009 (GAAAGACGCGCAGACTAATTCGGATCCGAA) and NF011 (TAGAGGATCCTTATTAGC GACGGCGACGACGAT), underlined bases represent inserted BamH1 cloning sites. The following PCR reaction was prepared: 1 µl pRK793, 2.5 µl 10x buffer, 0.625 µl dNTPs [10 mM], 1 µl NF009 [10 µM], 1 µl NF011 [10 µM], 0.25 µl Pwo polymerase and 18.625 µl dH_2O. This reaction was run using the following PCR programme: 94°C for 1 min then 25 cycles of 94°C for 1 min, 55°C for 30 secs and 72°C for 1 min. Following PCR, the reaction was cleaned up using the QIAQUICK PCR purification kit (Qiagen). The PCR product was treated with Taq polymerase and dATP: 6 µl PCR product, 1 µl 10x buffer, 1 µl dATP [10 mM], 0.3 µl Taq polymerase and 1.7 µl dH_2O; This reaction was incubated for 5 mins at 72°C. The resulting product was then ligated into T-A cloning vector pGEM-T Easy: 5 µl dATP treated PCR product, 1 µl pGEM-T Easy, 1 µl T4 ligase, 7.5 µl 2x buffer and 0.5 µl dH_2O; this reaction was incubated overnight at 4°C.

The *TEV*-pGEM ligation was cleaned by phenol extraction (see section 8.2.3.), transformed into *E. coli* (JM110) by electroporation (See section 8.2.4.) and left overnight at 37°C. LB plates were supplemented with 100 µg/ml Carbenicillin Disodium (CD, Ampicillin analogue) to allow for selection of the

pGEM plasmid. Blue-white selection was used to identify colonies that contain the *TEV* insert. Before spreading electroporated JM110 onto plates, 80 µl X-gal (20 mg/ml) and 40 µl IPTG (200 mg/ml) was spread onto the surface of LB plates, any blue colonies would signify that *TEV* protease was not present. White colonies were picked from plates and added to 10 ml LB liquid cultures containing 100 µg/ml CD, these cultures were incubated overnight at 37^{o}C with shaker. Mini-preps were performed on cultures using the QIAPREP spin mini-prep kit (Qiagen). Mini-preps were digested with *Bam*H1 checking for correct release of *TEV* from pGEM: 3 µl Mini-prep plasmid, 1 µl *Bam*H1, 1 µl Buffer A and 5 µl dH_2O; incubate at 37^{o}C for 1 hr. Restriction digests were separated by gel electrophoresis to identify the 860bp *TEV* insert.

The *TEV* fragment was then cloned into pZP222, which contains the heat shock 18.2 promoter (pRS3024, lab stock #526, Spectinomycin 80 µg/ml in bacteria). First, BamH1 was used to open pRS3024 and release TEV from pGEM: 10 µl plasmid, 1 µl BamH1, 1.5 µl Buffer A, 2.5 µl dH_2O. Both reactions were incubated for 1 hr at 37^{o}C, pRS3024 digest was further incubated with shrimp alkaline phosphatase (SAP) to prevent religation of cut plasmid: 1 µl added to digest, incubate for 1 hr at 37^{o}C. Each reaction was run on a 1% agarose gel, correct fragments were then excised from the gel and purified using the QIAQUICK gel extraction kit (Qiagen). The following ligation reaction was then set up: 6 µl purified *TEV* insert, 2 µl purified pRS3024, 1 µl T4 ligase, 1 µl T4 buffer; the reaction was then incubated overnight at 17^{o}C. The ligation reaction was cleaned up by phenol extraction and transformed into JM110 as described previously. After identifying *TEV* containing colonies, mini-preps were produced which were again digested with *Bam*HI to identify those that contain *TEV* protease. Those that released fragments were sequenced (See section 8.2.4.) using pZP sequencing oligos from the lab stock.

Out of the plasmids containing *TEV* in the correct orientation, one was selected to create a glycerol stock. To create glycerol stock, selected plasmid

was electroporated into DH5α, selected with 80 µg/ml Spectinomycin, incubated at 37°C overnight, colonies were picked for liquid culture, incubated at 37°C overnight with shaker, 800 µl of liquid culture was then added to 500 µl autoclaved glycerol, tubes were stored at -70°C. To create HS:TEV transgenic plants, the finished plasmid was transformed into the double reporter line (35S-lox-GUS-lox-GFO-nos; lab stock – 1.03.7.84) and selected for with Gentamycin 100 µg/ml (see section 8.2.6. for plant transformation protocol).

8.2.2.3. *Op:Cre-TEVr-GFP-LTI6B*

Cre recombinase was amplified from pRS030 (lab stock #169) using NF005 (AGTTCTAGATCTATGTCCAATTTACT) and NF006 (GCTCTCTCGAGATCGCCATCTTC CAGCAG), *Xba*I (NF005) and *Xho*I (NF006) cloning sites are underlined. *GFP-LTI6B* was amplified from pBIB (lab stock #458-1) using NF007 (GGAATCTCGAGATGGTGAGCAAGGGCGAGGAG) and NF008 (ATGACTAGTCAAAAG GTGATGATATAAAGAGC), *Xho*I (NF007) and *Spe*I (NF008) cloning sites are underlined. To PCR mentioned fragments, the following reaction was prepared: 1 µl Plasmid DNA (pRS030 or pBIB), 2.5 µl 10x buffer, 0.625 µl dNTPs [10 mM], 1 µl NF005 or NF007 [10 µM], 1 µl NF006 or NF008 [10 µM], 0.25 µl Pwo polymerase and 18.625 µl dH_2O. This reaction was run using the following PCR programme: 94°C for 1 min then 25 cycles of 94°C for 1 min, 55°C for 30 secs and 72°C for 1 min. 3 µl of the PCR products were checked on 1 % agarose gel in order to confirm the correct fragment size. Following PCR, the reactions were cleaned up using the QIAQUICK PCR purification kit (Qiagen). The PCR products were treated with Taq polymerase and dATP: 25 µl Purified PCR product, 3 µl 10x Buffer, 0.625 µl dATP [10 mM], 0.3 µl Taq polymerase and 1.075 µl dH_2O; reactions were incubated for 5 mins at 72°C.

Each of the resulting PCR products were ligated into T-A cloning vector pGEM-T Easy: 3 µl dATP treated PCR product, 1 µl pGEM-T Easy, 1 µl T4 Ligase,

5 µl 2x Buffer and 1 µl dH_2O; this reaction was incubated overnight at 4°C. *Cre*-pGEM and *GFP-LTI6B*-pGEM ligations were then transformed into *E. coli* (JM110) by electroporation (See section 8.2.2. for protocol) and left overnight at 37°C. Using blue-white selection (see section 8.2.2.1. for details), white colonies from each transformation were picked to 10 ml liquid LB cultures containing 100 µl CD and moved to 37°C overnight with shaking. Mini-preps were produced from each culture using the QIAPREP spin mini-prep kit (Qiagen). Plasmid preps were digested to check correct bands were released; *Cre*-pGEM: 3 µl Plasmid prep, 1.5 µl Buffer H, 1 µl *Xba*I, 1 µl *Xho*I, 8.5 µl dH_2O; *GFP-LTI6B*-pGEM: 3 µl Plasmid prep, 1.5 µl Buffer H, 1 µl *Xho*I, 1 µl *Spe*I, 8.5 µl dH_2O. Both reactions were incubated at 37°C for 1 hr and separated by gel electrophoresis (1 % agarose gel) to check cloning sites released correct fragments.

To create the TEV protease recognition site (TEVr), oligos NF003 (TCGAAAATCTTTATTTTCAAGGAC) and NF004 (TCGAGTCCTTGAAAATAAAGATTT) were hybridised and phosphorylated to enable cloning into *Cre*-pGEM. Oligos were resuspended to 100 µM in dH_2O, 20 µl of each oligo was added to an Eppendorf with a few drops of mineral oil. The tube was then heated to 100°C in a heat block for 1 min then removed and allowed to cool to room temperature. The following was then added: 5 µl dH_2O, 5 µl kinase buffer, 10 µl T4 polynucleotide kinase (PNK), 10 µl dATP [10 mM], reaction was incubated for 1 hr at 37°C then 10 mins at 70°C.

To clone TEVr into *Cre*-pGEM, plasmid DNA was digested with Xho1: 6 µl Plasmid, 1.5 µl Buffer H, 1 µl *Xho*I and 6.5 µl dH_2O; 37°C for 1 hr. TEV oligos were designed to contain *Xho*I sites at each end; the left flanking site was adapted so that the *Xho*I was inactive after being inserted into *Cre*-pGEM. Digested plasmid DNA was then treated with SAP (1 µl, incubate for 1 hr at 37°C) and purified using the QIAQUICK PCR purification kit (Qiagen). A ligation reaction was then prepared: 15 µl Digested plasmid, 1 µl TEVr, 1 µl T4 DNA ligase, 2.5 µl T4 buffer and 5.5 µl dH_2O. Ligation reactions were incubated

overnight at 16°C. Reaction was transformed into JM110 as described previously; mini-preps were then prepared from white colonies and sequenced (see 8.2.4. for sequencing protocol).

Plasmids containing correct *Cre-TEVr* sequences were used to clone *GFP-LTI6B*. *GFP-LTI6B*-pGEM and *Cre-TEVr*-pGEM were digested with *Xho*I and *Spe*I to release *GFP-LTI6B* and to open *Cre-TEVr*-pGEM: 6 µl plasmid DNA, 1.5 µl Buffer H, 1 µl *Xho*I, 1 µl *Spe*I and 5.5 µl dH_2O. Reactions were run on a 1 % agarose gel; correct bands for vector and insert were excised and purified using the QIAQUICK gel extraction kit (Qiagen). The purified bands were then checked on another gel before preparing ligation: 10 µl Vector (*Cre-TEVr*-pGEM), 4 µl insert (*GFP-LTI6B*), 1 µl T4 DNA ligase, 2.5 µl T4 buffer and 7.5 µl dH_2O. Reaction was incubated at 16°C overnight. Reactions were transformed into JM110 and minipreps were produced from white colonies as previously described. Mini-preps were then digested with *Xba*I and *Spe*I to check for correct insertion of *GFP-LTI6B* (should release 2kb fragment): 3 µl plasmid DNA, 1.5 µl Buffer H, 1 µl *Xba*I, 1 µl *Spe*I and 8.5 µl dH_2O. After incubation for 1 hr at 37°C, reactions were separated on a 1 % agarose gel to identify which clones had received the correct fragment, which were then sequenced.

Finally, *the Cre-TEVr-GFP-LTI6B* sequence was inserted into the pZP222 vector containing the operator (pRS338, lab stock #177). *Cre-TEVr-GFP-LTI6B* was removed from pGEM by digesting with *Xba*I and *Spe*I: 10 µl plasmid DNA, 1.5 µl Buffer H, 1 µl *Xba*I, 1 µl *Spe*I and 1.5 µl dH_2O. After incubation for 1 hr at 37°C, 1 µl Klenow and 2 µl dNTPs [2 mM] was added and left at room temperature for 10 mins. Reaction was run on 1 % agarose gel; 2 kb fragment was purified and used for blunt ended ligation: 0.5 µl pRS338, 15.5 µl insert, 1 µl T4 DNA ligase, 1 µl *Sma*I, 2 µl T4 buffer. Reaction was left at room temperature overnight. Ligation was transformed into JM110; minipreps were produced from colonies and sequenced as described previously. Finished plasmids were sequenced and eventually transformed into homozygous

CLV3:LhG4 plants (lab stock number 1.06.1.50) and selected for with Gentamycin 100 µg/ml (plant transformation protocol -section 8.2.6.)

8.2.2.4. *WOX5:LhG4*

Genomic DNA preps were first produced from L*er* plants using the CTAB extraction protocol (see section 8.2.1.). The *WOX5* promoter was then amplified from genomic DNA using NF016F (TTGGGAGCTCGGTAGCGAACTAGGAATTG) and NF017R (AAGAGGTACCCAGATGTAAAGTCCTCAACTG); underlined sequences represent *Sac*I (NF016F) and *Kpn*I (NF017R) cloning sites. The Expand High Fidelity PCR System was used to amplify the 4.5kb *WOX5* promoter using the hot start technique: PCR mix – 2 µl genomic DNA, 4.5 µl 10x buffer, 5.4 µl $MgCl_2$ [25 mM], 0.2 µl NF016F [100 µM], 0.2 µl NF017R [100 µM] and 31.7 µl dH_2O; Hot start mix – 0.75 µl Expand, 0.5 µl 10x buffer, 0.6 µl $MgCl_2$ [25 mM] and 3.15 µl dH_2O. The following PCR programme was used: 94°C for 2 mins, 10 cycles of 94°C for 15 secs - 55°C for 30 secs - 68°C for 3:30 mins then 20 cycles of 94°C for 15 secs - 55°C for 30 secs - 68°C for 3:30 minutes (+5 secs per cycle) and finally 72°C for 7 mins to finish (see Expand manual by Roche for details). PCR mix was prepared and run on first PCR step (94°C) for 1.5 mins, programme was paused and 5 µl of hot start mix was added, lid was closed and PCR programme resumed.

Following PCR, 3 µl of reaction was run on 0.8 % agarose gel to check for a 4.5kb fragment. The fragment was then cloned directly into pGEM-T Easy using the following reaction: 1 µl pGEM, 3 µl PCR, 1 µl T4 ligase and 5 µl 2x buffer (ligase and buffer supplied with kit) and incubated overnight at 4°C. The Ligation was cleaned by phenol extraction (see section 8.2.3.) and transformed into JM110 *E. coli* strain by electroporation (See section 8.2.4.). Colonies were picked and cultured in 10 ml liquid LB containing CD 100 µg/ml overnight at 37°C with shaker before extracting plasmids using the QIAPREP spin mini-prep

kit (Qiagen). Plasmids were digested with *Kpn*I and *Sac*I to see if 4.5kb fragment was released: 3 µl DNA, 1 µl *Kpn*I, 1 µl *Sac*I , 1.5 µl buffer L 0.15 µl BSA (New England Biolabs) and 8.35 µl dH_2O; reaction was incubated for 1 hr at 37°C.

The *WOX5* promoter fragment was then cloned into pZP222 containing the nos terminator (pCW004, lab stock #32). 10 µl of pZP222+nos and *WOX5*-pGEM was digested with *Kpn*I and *Sac*I as mentioned previously. These reactions were then run on a 0.8 % agarose gel; correct fragments were excised and purified using the QIAQUICK gel extraction kit (Qiagen). After checking fragments had been successfully purified on an agarose gel, the following ligation reaction was prepared: 2 µl purified vector, 6 µl purified *WOX5* insert, 1 µl T4 ligase and 1 µl T4 buffer; incubated overnight at 16°C. The ligation was then cleaned by phenol extraction and transformed into JM110 as described previously. After picking colonies (selection for pZP222 is Spectinomycin 100 µg/ml) and making mini-preps of plasmids, 3 µl of plasmid DNA was again digested with *Sac*I and *Kpn*I as described earlier to check for insert.

To clone LhG4 into *WOX5*-pZP222, pRS162 (lab stock #564) which contains the LhG4 sequence in bluescript KS- and *WOX5*-pZP222 were digested with *Bam*HI: 10 µl DNA, 1 µl *Bam*HI, 1.5 µl buffer B 2.5 µl dH_2O; incubated for 1 hr at 37°C. Digested samples were run on 0.8 % agarose gel; Vector (*WOX5*-pZP222) and insert (LHG4, 1.7kb) were purified from the gel using the QIAQUICK gel extraction kit (Qiagen). The following ligation reaction was prepared: 2 µl vector, 6 µl insert, 1 µl T4 ligase and 1 µl T4 buffer; incubated overnight at 16°C. Reactions were cleaned and transformed into JM110, colonies were picked and mini-preps were produced. First, plasmids were digested with *Bam*HI checking for insert. Those plasmids that contained the LhG4 insert were then digested with *Hind*III to check for orientation: 3 µl DNA, 1 µl *Hind*III, 1.5 µl Buffer B and 9.5 µl dH_2O; incubate at 37°C for 1 hr. Those with correct orientation should yield bands of 11, 3, 1.7 and 1kb. Plasmids that produced the

correct size bands were then sequenced and transformed (plant transformation protocol -section 8.2.6.) into L*er* (lab stock 1.5.12.16).

8.2.3. Phenol extraction protocol

The following protocol was used to clean up ligations before electroporation. Reaction was brought up to 100 µl with dH_2O and 100 µl phenol:chloroform was added under fume hood. Tube was shaken until solution turned white, centrifuged at full speed (16000 x g) for 10 mins and upper phase (90 µl) was extracted to a new Eppendorf. 9 µl of sodium acetate (pH5.6, 3 M), 250 µl of 100 % ethanol and 1 µl glycogen was added to the tube, which was mixed and incubated at -20^{o}C for 15 mins. Tube was centrifuged for 20 mins and liquid removed leaving pellet. Pellet was washed with 200 µl of 70 % ethanol, and centrifuged for 10 mins. Ethanol was removed and tube and tube left to air-dry for around 30 mins before re-suspending in dH_2O.

8.2.4. Preparation of electrocompetent bacteria

To prepare electrocompetent *E.coli* cells, a single colony of JM110 strain was grown in 10 ml of LB-broth overnight, shaking at 37^{o}C. 0.5 ml of culture was then added to 500 ml SOB (super optimal broth) (20 g Bacto tryptone; 5 g Bacto yeast extract; 0.584 g NaCl; 0.186 g KCl into 1 litre of dH_2O; autoclaved) then grown with shaker at 37^{o}C until the optical density at 550 nm reached 0.5. Cells were then pelleted at 7268 x g in sterile 500 ml tubes at 4^{o}C for 10 mins. After removing liquid from tubes, cells were resuspended in 500 ml chilled washing buffer (10% glycerol). Tubes were then centrifuged at 7268 x g, 4^{o}C for 10 mins to pellet cells. Washing process was then repeated by removing liquid, adding washing buffer and centrifuging. 2 ml of 10% glycerol was then added to pellet,

cells were gently resuspended and aliquotted into Eppendorfs (110 µl). Tubes were stored at -70°C.

To prepare electrocompetent *Agrobacterium tumefaciens*, a single colony of the GV3101 strain was grown in 10 ml LB broth shaking at 29°C. Media was supplemented with gentamycin (40 µg/ml) and rifampicin (100 µg/ml) for *Agrobacterium* selection. 0.5 ml of overnight culture was then added to 500 ml SOB-broth as described for *E.coli* but containing relevant antibiotics. The 500 ml was grown shaking at 29°C until the optical density at 600 nm reached 0.5. Cells were then prepared as described above for *E.coli*.

8.2.5. Electroporation of *E. coli* and *Agrobacterium*

To transform plasmid DNA into *E. coli* or *Agrobacterium*, electrocompetent cells were first thawed on ice allowing 50 µl for each reaction. Electroporation cuvettes were also chilled on ice prior to transformation. 0.2 µl of plasmid prep was pipetted into the bottom of a cuvette, 50 µl of thawed cells were then pipetted into cuvette, mixing with plasmid DNA. The lid was added and the cuvette was placed into a Biorad Genepulser, making sure the gap was bridged. The following settings were then applied to Genepulser machine: Capacitance extender – 250 µFD, Pulse controller – 200 Ω, Capacitance – 25 µFD and Voltage – 2.5 KV. The cuvette holder was closed and pulse buttons were held to electroporate cells. 1 ml of cold LB was then pipetted into the cuvette and mixed; mixture was then pipetted into an Eppendorf and incubated for 2 hrs at 30°C for *Agrobacterium* or 37°c for *E. coli*. Tubes were then spun at low speed to pellet cells; the pellet was resuspended in 200 µl LB and spread onto LB plates containing relevant antibiotics. Plates were incubated overnight at 37°C (for *E. coli*) or 2 days at 30°C (for *Agrobacterium*).

8.2.6. DNA sequencing

Sequencing reactions were performed using the Big Dye Terminator v3.1 Cycle Sequencing Kit (Applied Biosystems). Reactions were prepared as follows: 4 µl Big Dye 3.1, 0.5 µl sequencing oligo [10 µM], 2 µl Plasmid DNA, 3.5 µl dH_2O. Sequencing reactions were performed in a PCR machine using the following programme: 25 cycles of 96°C for 30 secs, 1°C per sec to 50°C, 50°C for 15 secs, 1°C per sec to 60°C, 60°C for 4 mins and 1°C per sec to 96°C. The following sequencing oligos were used: pGEM T Easy – M13 forward (GTAAAACGACGGCCAGT) and M13 reverse (GGAAACAGCTATGACCA T), pZP222 – pZPLB2 (TCACACAGGAAACAGCTATGACCAT). DNA obtained from sequencing reactions was sent to the genome laboratory (John Innes Centre), sequence data was analysed using Vector NTI software (Invitrogen).

8.2.7. Plant transformation

To transform plants, the floral dip method was used as described by Clough and Bent (1998). Two 500 ml cultures were first prepared of GV3101 transformed with plasmid DNA, colonies from transformed plates were picked to 10 ml liquid LB containing Rifampicin 50 µg/ml and Gentamycin 25 µg/ml to select for GV3101 and relevant selection for transformed plasmid. After 2 days incubation at 30°C with shaker, cultures were then transferred to 500 ml liquid LB cultures with relevant antibiotics. Two 500 ml cultures were produced for each transformation, after a further 2 days at 30°C with shaking, cultures were ready to be used for transformation. Each culture was poured into large centrifuge bottles (2 bottles, 1 for each culture). Cultures were then centrifuged at 7268 x g for 20 mins, liquid was poured away leaving pellet. A small amount of cold infiltration medium was added to each bottle: Infiltration media (1 Ltr) – 4.3 g MS salts pack, 1 ml B_5 vitamins, 50 g sucrose, 300 µl silwet L-77, added water

to 1 ltr and mixed, adjusted pH to 5.8 with KOH and placed on ice. The pellet was resuspended in infiltration media; both resuspended cultures were then added together to give a 1 ltr culture. Siliques were removed from plants; plants were dipped into infiltration media for 30 secs and placed onto their side in a clear plastic bag, after 24 hrs plants were taken to a containment glasshouse. Just before siliques began to dehisce, plants were bagged and seeds collected.

8.2.8. Selection of transformed seeds

To select primary transformants, seeds were aliquotted into 30 Eppendorfs. Tubes were left open, placed into a tube rack and then into a large glass desiccator jar. Under a fume hood, a beaker containing 100 ml commercial bleach (Freshline) was placed into the jar. 3 ml concentrated HCl was pipetted into the beaker and the jar was sealed. The seeds were left for 4 hrs to sterilise in chlorine gas, the jar was then opened under the fume hood and tubes were closed. Tubes were then moved to a laminar flow hood and 15 µl 100% Ethanol was added to each tube to cover seeds. Tubes were left open under the laminar flow hood until all ethanol had evaporated which took around 3-4 hrs. Seeds were then sown onto large GM plates (140 mm; Sterilin) supplemented with the relevant antibiotic. Plates were sealed and stratified in the dark for 48 hrs at 4^{o}C, then moved to long day growth chambers; resistant primary transformants were pricked out to soil for growth in long day conditions.

8.2.9. Testing constructs

8.2.9.1. Testing *Op:Cre-TEVr-GFP-LTI6B* by confocal microscopy

For *Op:Cre-TEVr-GFP-LTI6B*, inflorescence meristems of primary transformants were prepared for confocal microscopy (See section 8.3.2. for protocol).

Presence of membrane GFP within the shoot apex indicates correct expression of the transformed construct under control of the *CLV3:LhG4* driver (shown in chapter 6, fig 6.4.).

8.2.9.2. Testing *WOX5:LhG4* by confocal microscopy

To test the *WOX5:LhG4* construct, primary transformants were crossed to homozygous *Op:ER:GFP* plants (15.07.3.1). Seeds from crosses were selected for both constructs on GM media supplemented with Gentamycin 100 µg/ml and PPT 10 µg/ml. Resistant seedlings were examined for presence of GFP within the QC.

8.2.9.3. Testing *HS:TEV* by RT-PCR

To test *HS:TEV*, RT-PCR was used to identify upregulated expression of TEV in heat shocked plants. Seeds from primary transformants were grown on Gentamycin 100 µg/ml and Kanamycin 50 µg/ml to select for both *HS:TEV* and *35S-lox-GUS-lox-GFP-nos*. Seeds were grown vertically in a long day growth chamber for 12 days. 40 seedlings were used for RT-PCR, 20 seedlings were heat shocked and 20 left at root temperature as control. For heat shock, 20 seedlings were collected in an Eppendorf tube, a wet cotton bud was placed into the tube to maintain humidity. Tubes were incubated for 30 minutes in a 38^{o}C waterbath; control seedlings were also placed into tubes but left at room temperature. Immediately after heat shock, RNA was extracted from seedlings.

For RNA extraction, tissue was ground using a micro-pestle after dipping tubes in liquid nitrogen. 1 ml Trizol (Sigma) was added to tubes, after 5 mins tubes were centrifuged at 13100 x g for 10 mins at 4^{o}C. Supernatant was transferred to a fresh tube and incubated at room temperature for 5 mins. 0.2 ml chloroform was added under a fume hood; tubes were shaken for 15 secs

and incubated at room temperature for 3 mins. The tubes were then centrifuged at 13100 x g for 15 mins at 4°C. The supernatant was transferred to a fresh tube and 0.5 ml of cold isopropanol was added. Tubes were incubated at room temp for 10 mins then centrifuged at 13100 x g for 10 mins at 4°C. Tubes were washed twice with 75% ethanol by extracting supernatant, adding 1 ml 75% ethanol, vortexing and centrifuging at 5100 x g for 5 mins at 4°C. Pellet was dried for approx 15 mins and 17 µl of dH_2O was added. To finish, sample was heated for 10 mins at 60°C and left on ice for 5 mins. To remove DNA from sample, 1 µl DNAse and 2 µl DNAse buffer was added and incubated at 37°C for 20 mins. To inactivate DNAse, EDTA pH8 was added to a concentration of 8 mM and sample was heated at 75°C for 10 mins. Samples were then stored at -70°C.

For RT-PCR, samples were thawed and RNA concentrations were measured using an Eppendorf Biophotometer. RNA extractions were diluted to 1000 ng/ml and the RT reaction was prepared: 1 µl oligo DT, 2 µl dNTPs [10 mM], 1 µl RNA [1000 ng/ml], 8 µl dH_2O. Reaction was denatured at 65°C for 10 mins then placed back onto ice. The following was then added: 4 µl RT buffer (Invitrogen), 2 µl DTT [0.1 M] (Invitrogen), 0.5 µl RNAse inhibitor (Invitrogen), 0.7 µl M-MLV reverse transcriptase (Invitrogen) and 0.8 µl dH_2O. Samples were incubated at 42°C for 2 mins, 25°C for 15 mins and 42°C for 50 mins. Both heat shock and control samples were then subject to PCR using APT control (APT_F: TCCCAGAATCGCTAAGATTGCC & APT_R: CCTTTCCCTTAAGCTCTG) and TEV specific (NF027F: CACGACTTTGCAACAACACC & NF028R: CCAACCACTAACCCACT GCT) oligos. The following PCR reaction was prepared: 3 µl RT reaction, 2.5 µl 10x buffer , 0.625 µl dNTPs [10 mM] , 1 µl APT_F or NF027F [10 µM], 1 µl APT_R or NF028R [10 µM], 0.25 µl Taq polymerase and 16.625 µl dH_2O. The reaction was run on the following PCR programme: 94°C for 2 mins then 30 cycles of 94°C for 30 secs, 55°C for 30 secs and 72°C for 1 min. PCR was then run on 1.2 % agarose gel; bands indicating heat shocked samples amplified with TEV oligos should provide significantly brighter bands than with control samples.

8.3. DNA damaging treatments

8.3.1. Root meristem

For bleomycin, zeocin, hydroxyurea (HU) and aphidicolin (Aph) treatments, seedlings were transferred to supplemented plates after 3 days growth in continuous light unless stated otherwise. To prepare plates, Germination medium (GM) was autoclaved and left to cool to around 50^{o}C. Media was then supplemented with either bleomycin (1 µg/ml, Sigma), zeocin (8-20 µg/ml, Invitrogen), hydroxyurea (1 mM, Sigma) or aphidicolin (12 µg/ml, Sigma) and poured into petri dishes (Sterilin). Seedlings were then transferred to plates under a laminar flow hood and sealed with surgical tape (3M). Plates were wrapped in foil to prevent degradation of light sensitive chemicals bleomycin and zeocin then placed back into continuous light (to keep temperature constant) for 24 hrs before imaging.

X-ray irradiation was performed at the Norfolk and Norwich hospital with the help of Frank Luhana. Seedlings were grown vertically in continuous light for 3 days then transferred to fresh GM plates for control and x-ray irradiated conditions. Plates were placed between tissue-mimicking wooden blocks and irradiated at 0.92 Gray/Min with a Varian Clinac 600CD linear accelerator to a final dose of 40 or 80 Gray (see appendix a for image of experimental setup). For UV treatments, seedlings were grown in continuous light for 5 days and transferred to GM plates for control and UV irradiation conditions. Plates for UV-C (254 nm) treatment were placed into a Stratagene UV Stratalinker 2400 and irradiated to a dose of 2 J cm^{-2} (20 kJ m^{-2}) using 2 treatments of 9999 µJ m^{-2} x 100. Both UV and X-ray irradiated seedlings were placed back into continuous light for 24 hrs then prepared for imaging.

Heavy metal treatments were performed differently because heavy metal solutions are incompatible with GM. Strips of 3MM paper were first cut to size

and placed vertically within magenta pots. 50ml of either Aluminium Chloride ($AlCl_3$, 300 µM) or Cadmium Sulfate ($CdSO_4$, 200 µM) solution was added (H_2O for control), 3MM paper was able to absorb solution and stick to the side of the magenta pot. Seedlings grown in continuous light for 3 days were then placed vertically onto the paper. Pots were placed back into continuous light for 24 hrs, seedlings were then prepared for imaging.

8.3.2. Shoot meristem

To treat the shoot meristem with zeocin, mature flowers and siliques were removed from inflorescence meristems, which were briefly dipped into 0.015% Silwet L-77 (Lehle Seeds). 0.2 ml PCR tubes were filled with 200 µl of either 0 or 20 µg/ml zeocin solutions, shoot tips were submerged into the solution and secured to tubes using surgical tape (3M). Plants were then watered and placed vertically within empty trays using a rack to keep tubes vertical. After 24 hrs, tubes were removed and shoots were prepared for imaging.

For X-ray treatments, 5 week old L*er* plants were separated from P40 trays into single pots. Plants were sealed into 88 x 210 mm seed bags (2 bags were placed over plant and pot which were sealed in the middle). Plants were then placed between tissue-mimicking blocks (using petri dishes as spacers) and irradiated using the same conditions as mentioned for treatment of seedlings (Section 8.3.1.). Plants were moved back to long day growth conditions for 24 hrs, shoot tips were then prepared for imaging.

8.4. Imaging

8.4.1. Slide preparation and staining

For preparation of roots for confocal microscopy, strips of 25 mm masking tape (Antalis) were added to a microscope slide to act as spacers. Propidium Iodide (PI) (10 µg/ml; Sigma) or Sytox orange solution (250 nM; Molecular Probes, Invitrogen) was pipetted directly onto the slide and seedlings added. For seedlings co-stained with Sytox and fluorescein diacetate (FD), seedlings were first transferred to tubes containing 5 µg/ml FD for 25 mins, and then transferred to slides for Sytox staining. A 22 x 50 mm cover slip was then added to cover roots leaving cotyledons exposed. Additional PI or Sytox was pipetted under cover slip if needed. For FM464 (Invitrogen) staining, dH_2O was pipetted onto the slide and seedlings were added. 1 µl of 50 µg/ml FM464 was pipetted onto the root tip and cover slip was added. For Lysotracker staining, seedlings were moved to tubes containing 1 µM Lysotracker Green (Molecular Probes, Invitrogen) for 45 minutes.

To prepare the shoot meristem for confocal imaging, flowers and floral buds were removed from inflorescence meristems until the apex was exposed. Shoot apices were removed by cutting the stem around 1 inch from the tip; tips were then placed into Eppendorf tubes containing 1 ml of H_2O. Spacers were added to microscope slides and water was pipetted onto the surface. Shoot tips were added to the microscope slide and the shoot apex was excised from the stem under a dissection microscope with a razor blade. The shoot apex was then positioned upright using fine pointed forceps. Water was blotted away from the slide and 10 µg/ml PI solution was then added, a cover slip was then placed onto the slide.

8.4.2. GUS staining

Bleomycin-treated QC25 seedlings were first fixed in 90% acetone for 10 mins on ice. The following GUS staining buffer was prepared: 200 µl EDTA (Ethylenediaminetetraacetic Acid) 0.5 M, 10 µl Triton X100, 5 ml phosphate buffer 0.1 M pH7.5, 150 µl $K_3[Fe(CN)_6]$ (Potassium ferricyanide), 150 µl $K_4[Fe(CN)_6]$ (Potassium ferrocyanide), 100 µl X-Gluc (5-bromo-4-chloro-3-indolyl-β-D-glucuronide) 100 mg/ml (Sigma), dH_2O was added up to 10ml. GUS wash buffer was prepared which was same as staining buffer but without X-Gluc. Seedlings were washed 3 times after fixing, then incubated in GUS staining buffer at 37^oC for 6-7 hrs. Seedlings were then washed in 70 % ethanol and mounted onto slides for imaging.

8.4.3. Microscopy

Confocal imaging was performed using a Leica SP1 equipped with an argon krypton laser, except for the images shown in Figures 6.1. and 6.2. which used a Leica SP2. GFP, PI and FD were excited using the 488-nm argon ion laser and emission was collected between 500 - 550 nm (GFP), 600 - 656 nm (PI) and 505 – 525 nm. (FD). Lysotracker green used the same settings as for GFP fluorescence. Sytox Orange was excited using the 543-nm laser line and emitted light was collected between 580 and 610 nm. Z stacks were obtained by imaging 4 µm sections of the shoot meristem, which were averaged two times. Images were processed using Leica Confocal Software and Adobe Photoshop 6.0 (Adobe Systems).

For transmission electron microscopy (TEM) analysis, seedlings were treated for 16 h on GM with 20 µg/ml zeocin and untreated controls were fixed in 2.5% glutaraldehyde/0.05 M Na cacodylate pH 7.2, vacuum-infiltrated, and left overnight. Seedlings were postfixed in 1% osmium tetroxide/0.05 M Na

cacodylate for 1 h; washed with water; and dehydrated for up to 1 h each step in ethanol 30%, 50%, 70%, 90%, and 100%. Samples were then infiltrated in London Resin White resin (London Resin Co., Ltd.) and sectioned for TEM imaging with an FEI Technai G2 20 Twin TEM.

8.4.4. Photography

For analysis of root length (figure 6.7.), a Nikon D70 digital camera was used to photograph roots directly on germination media. The camera was positioned on a tripod and a lamp was angled at 45^{o} to allow for illumination of roots in the photo. Images showing the experimental set up of x-ray irradiation (appendix A) were taken by a Samsung F480.

8.4.5. Live imaging

Three-day-old LTI6B/WOX5:GFP seedlings were treated with 20 µg/ml zeocin for 24 h and transferred to a microscope slide covered with a thin layer of GM overlaid with wet cellophane. A coverslip was placed over the roots; the slides were placed vertically in a wet chamber in the dark; and images of the same root were taken at 0, 8, and 16 hr intervals.

8.5. Statistical analysis

Fisher's exact test was used for all statistical analyses (Quenouille 1950). This test is specifically used to determine significance in small sample sizes. To perform the test, the following table was constructed in Microsoft Excel.

	Death	No death	Total
WT	a	b	a + b
Mutant	c	d	c + d
total	a + c	b + d	n

In chapter 3, microscope images were scored for spontaneous cell death in *lig4-4*, *ku80* and *rad51-1* mutants (Table 3.2). For example, data collected from *lig4-4* images showed 12 out of 20 roots contained at least one dead initial compared to 1 out of 20 out of wild type roots. This information was placed into the table as shown.

	Death	No death	Total
WT	1	19	20
Mutant	12	8	20
Total	13	27	40

The following equation was then applied to the table in order to calculate the *p* value. For the *lig4-4* mutant, the *p* value was calculated at 0.000209 < than 0.05 (95% confidence). This indicates *lig4-4* experiences a significant number of spontaneous cell death compared with wild type seedlings.

$$p = \frac{(a+b)!\,(c+d)!\,(a+c)!\,(b+d)!}{a!\,b!\,c!\,d!\,n!}$$

APPENDICES

Appendix A

Images showing the set up for x-ray irradiation of seedlings. Petri dishes containing seedlings on germination media were placed between tissue mimicking wooden blocks (shown by the blue arrow). Seedlings were then irradiated from above using conditions described in the materials and methods. Irradiation of mature plants was performed in a similar way by inserting the aerial portions of the plant into the gap marked by the blue arrow.

REFERENCES

Abe, M., Takahashi, T. and Komeda, Y. (1999) Cloning and characterization of an L1 layer-specific gene in Arabidopsis thaliana. *Plant Cell Physiol*, **40**, 571-580.

Aida, M., Beis, D., Heidstra, R., Willemsen, V., Blilou, I., Galinha, C., Nussaume, L., Noh, Y.S., Amasino, R. and Scheres, B. (2004) The PLETHORA genes mediate patterning of the Arabidopsis root stem cell niche. *Cell*, **119**, 109-120.

Aladjem, M.I., Spike, B.T., Rodewald, L.W., Hope, T.J., Klemm, M., Jaenisch, R. and Wahl, G.M. (1998) ES cells do not activate p53-dependent stress responses and undergo p53-independent apoptosis in response to DNA damage. *Current Biology*, **8**, 145-155.

Alonso, J.M., Hirayama, T., Roman, G., Nourizadeh, S. and Ecker, J.R. (1999) EIN2, a bifunctional transducer of ethylene and stress responses in Arabidopsis. *Science*, **284**, 2148-2152.

Alvarez, M.E. (2000) Salicylic acid in the machinery of hypersensitive cell death and disease resistance. *Plant Mol Biol*, **44**, 429-442.

Andrabi, S.A., Kim, N.S., Yu, S.W., Wang, H., Koh, D.W., Sasaki, M., Klaus, J.A., Otsuka, T., Zhang, Z., Koehler, R.C., Hurn, P.D., Poirier, G.G., Dawson, V.L. and Dawson, T.M. (2006) Poly(ADP-ribose) (PAR) polymer is a death signal. *Proc Natl Acad Sci U S A*, **103**, 18308-18313.

Apel, K. and Hirt, H. (2004) Reactive oxygen species: metabolism, oxidative stress, and signal transduction. *Annu Rev Plant Biol*, **55**, 373-399.

Armakolas, A. and Klar, A.J. (2006) Cell type regulates selective segregation of mouse chromosome 7 DNA strands in mitosis. *Science*, **311**, 1146-1149.

Attwooll, C., Lazzerini Denchi, E. and Helin, K. (2004) The E2F family: specific functions and overlapping interests. *EMBO J*, **23**, 4709-4716.

Bakkenist, C.J. and Kastan, M.B. (2003) DNA damage activates ATM through intermolecular autophosphorylation and dimer dissociation. *Nature*, **421**, 499-506.

Banerjee, A.K., Mandal, A., Chanda, D. and Chakraborti, S. (2003) Oxidant, antioxidant and physical exercise. *Mol Cell Biochem*, **253**, 307-312.

Bao, Q. and Shi, Y. (2007) Apoptosome: a platform for the activation of initiator caspases. *Cell Death Differ*, **14**, 56-65.

Bari, R. and Jones, J.D. (2009) Role of plant hormones in plant defence responses. *Plant Mol Biol*, **69**, 473-488.

Barlow, C., Hirotsune, S., Paylor, R., Liyanage, M., Eckhaus, M., Collins, F., Shiloh, Y., Crawley, J.N., Ried, T., Tagle, D. and Wynshaw-Boris, A. (1996) Atm-deficient mice: a paradigm of ataxia telangiectasia. *Cell*, **86**, 159-171.

Bassham, D.C. (2007) Plant autophagy--more than a starvation response. *Curr Opin Plant Biol*, **10**, 587-593.

Batista, L.F., Kaina, B., Meneghini, R. and Menck, C.F. (2009) How DNA lesions are turned into powerful killing structures: insights from UV-induced apoptosis. *Mutat Res*, **681**, 197-208.

Baurle, I. and Laux, T. (2003) Apical meristems: the plant's fountain of youth. *Bioessays*, **25**, 961-970.

Benfey, P.N., Linstead, P.J., Roberts, K., Schiefelbein, J.W., Hauser, M.T. and Aeschbacher, R.A. (1993) Root development in Arabidopsis: four mutants with dramatically altered root morphogenesis. *Development*, **119**, 57-70.

Benjamins, R. and Scheres, B. (2008) Auxin: the looping star in plant development. *Annu Rev Plant Biol*, **59**, 443-465.

Benkova, E., Michniewicz, M., Sauer, M., Teichmann, T., Seifertova, D., Jurgens, G. and Friml, J. (2003) Local, efflux-dependent auxin gradients as a common module for plant organ formation. *Cell*, **115**, 591-602.

Berleth, T. and Jurgens, G. (1993) The role of the monopteros gene in organising the basal body region of the Arabidopsis embryo. *Development*, **118**, 575-587.

Bernstein, K.A. and Rothstein, R. (2009) At loose ends: resecting a double-strand break. *Cell*, **137**, 807-810.

Bleuyard, J.Y., Gallego, M.E., Savigny, F. and White, C.I. (2005) Differing requirements for the Arabidopsis Rad51 paralogs in meiosis and DNA repair. *Plant J*, **41**, 533-545.

Blilou, I., Xu, J., Wildwater, M., Willemsen, V., Paponov, I., Friml, J., Heidstra, R., Aida, M., Palme, K. and Scheres, B. (2005) The PIN auxin efflux facilitator network controls growth and patterning in Arabidopsis roots. *Nature*, **433**, 39-44.

Bonneau, L., Ge, Y., Drury, G.E. and Gallois, P. (2008) What happened to plant caspases? *J. Exp. Bot.*, **59**, 491-499.

Bracken, A.P., Ciro, M., Cocito, A. and Helin, K. (2004) E2F target genes: unraveling the biology. *Trends Biochem Sci*, **29**, 409-417.

Brand, U., Grunewald, M., Hobe, M. and Simon, R. (2002) Regulation of CLV3 expression by two homeobox genes in Arabidopsis. *Plant Physiol*, **129**, 565-575.

Bray, C.M. and West, C.E. (2005) DNA repair mechanisms in plants: crucial sensors and effectors for the maintenance of genome integrity. *New Phytol*, **168**, 511-528.

Bucher, N. and Britten, C.D. (2008) G2 checkpoint abrogation and checkpoint kinase-1 targeting in the treatment of cancer. *Br J Cancer*, **98**, 523-528.

Bundock, P. and Hooykaas, P. (2002) Severe developmental defects, hypersensitivity to DNA-damaging agents, and lengthened telomeres in Arabidopsis MRE11 mutants. *Plant Cell*, **14**, 2451-2462.

Bundock, P., van Attikum, H. and Hooykaas, P. (2002) Increased telomere length and hypersensitivity to DNA damaging agents in an Arabidopsis KU70 mutant. *Nucleic Acids Res*, **30**, 3395-3400.

Burger, R.M. (1998) Cleavage of Nucleic Acids by Bleomycin. *Chem Rev*, **98**, 1153-1170.

Burma, S., Chen, B.P., Murphy, M., Kurimasa, A. and Chen, D.J. (2001) ATM phosphorylates histone H2AX in response to DNA double-strand breaks. *J Biol Chem*, **276**, 42462-42467.

Byrne, M.E., Barley, R., Curtis, M., Arroyo, J.M., Dunham, M., Hudson, A. and Martienssen, R.A. (2000) Asymmetric leaves1 mediates leaf patterning and stem cell function in Arabidopsis. *Nature*, **408**, 967-971.

Byrne, M.E., Simorowski, J. and Martienssen, R.A. (2002) ASYMMETRIC LEAVES1 reveals knox gene redundancy in Arabidopsis. *Development*, **129**, 1957-1965.

Cairns, J. (1975) Mutation selection and the natural history of cancer. *Nature*, **255**, 197-200.

Campilho, A., Garcia, B., Toorn, H.V., Wijk, H.V. and Scheres, B. (2006) Time-lapse analysis of stem-cell divisions in the Arabidopsis thaliana root meristem. *Plant J*, **48**, 619-627.

Cann, K.L. and Hicks, G.G. (2007) Regulation of the cellular DNA double-strand break response. *Biochem Cell Biol*, **85**, 663-674.

Chen, L., Trujillo, K., Sung, P. and Tomkinson, A.E. (2000) Interactions of the DNA ligase IV-XRCC4 complex with DNA ends and the DNA-dependent protein kinase. *J Biol Chem*, **275**, 26196-26205.

Child, E.S. and Mann, D.J. (2006) The intricacies of p21 phosphorylation: protein/protein interactions, subcellular localization and stability. *Cell Cycle*, **5**, 1313-1319.

Chinnaiyan, A.M., O'Rourke, K., Tewari, M. and Dixit, V.M. (1995) FADD, a novel death domain-containing protein, interacts with the death domain of Fas and initiates apoptosis. *Cell*, **81**, 505-512.

Cho, U.-H. and Seo, N.-H. (2005) Oxidative stress in Arabidopsis thaliana exposed to cadmium is due to hydrogen peroxide accumulation. *Plant Science*, **168**, 113-120.

Claussen, C.A. and Long, E.C. (1999) Nucleic Acid recognition by metal complexes of bleomycin. *Chem Rev*, **99**, 2797-2816.

Clough, S.J. and Bent, A.F. (1998) Floral dip: a simplified method for Agrobacterium-mediated transformation of Arabidopsis thaliana. *Plant J*, **16**, 735-743.

Clowes, F.A.L. (1959) Reorganization of Root Apices after Irradiation. *Ann Bot*, **23**, 205-210.

Clowes, F.A.L. (1961) Duration of the Mitotic Cycle in a Meristem. *J. Exp. Bot.*, **12**, 283-293.

Clowes, F.A.L. (1965) The Duration of the G1 Phase of the Mitotic Cycle and its Relation to Radiosensitivity. *New Phytologist*, **64**, 355-359.

Colon-Carmona, A., You, R., Haimovitch-Gal, T. and Doerner, P. (1999) Technical advance: spatio-temporal analysis of mitotic activity with a labile cyclin-GUS fusion protein. *Plant J*, **20**, 503-508.

Cooke, M.S., Evans, M.D., Dizdaroglu, M. and Lunec, J. (2003) Oxidative DNA damage: mechanisms, mutation, and disease. *FASEB J*, **17**, 1195-1214.

Cools, T. and De Veylder, L. (2009) DNA stress checkpoint control and plant development. *Curr Opin Plant Biol*, **12**, 23-28.

Coppoolse, E.R., de Vroomen, M.J., Roelofs, D., Smit, J., van Gennip, F., Hersmus, B.J., Nijkamp, H.J. and van Haaren, M.J. (2003) Cre recombinase expression can result in phenotypic aberrations in plants. *Plant Mol Biol*, **51**, 263-279.

Creagh, E.M., Conroy, H. and Martin, S.J. (2003) Caspase-activation pathways in apoptosis and immunity. *Immunol Rev*, **193**, 10-21.

Cuadrado, M., Martinez-Pastor, B., Murga, M., Toledo, L.I., Gutierrez-Martinez, P., Lopez, E. and Fernandez-Capetillo, O. (2006) ATM regulates ATR chromatin loading in response to DNA double-strand breaks. *J Exp Med*, **203**, 297-303.

Culligan, K., Tissier, A. and Britt, A. (2004) ATR regulates a G2-phase cell-cycle checkpoint in Arabidopsis thaliana. *Plant Cell*, **16**, 1091-1104.

Culligan, K.M., Robertson, C.E., Foreman, J., Doerner, P. and Britt, A.B. (2006) ATR and ATM play both distinct and additive roles in response to ionizing radiation. *Plant J*, **48**, 947-961.

Curtis, M.J. and Hays, J.B. (2007) Tolerance of dividing cells to replication stress in UVB-irradiated Arabidopsis roots: requirements for DNA translesion polymerases eta and zeta. *DNA Repair (Amst)*, **6**, 1341-1358.

Cutler, S.R., Ehrhardt, D.W., Griffitts, J.S. and Somerville, C.R. (2000) Random GFP::cDNA fusions enable visualization of subcellular structures in cells of Arabidopsis at a high frequency. *Proc Natl Acad Sci U S A*, **97**, 3718-3723.

Czornak, K., Chughtai, S. and Chrzanowska, K.H. (2008) Mystery of DNA repair: the role of the MRN complex and ATM kinase in DNA damage repair. *J Appl Genet*, **49**, 383-396.

Danial, N.N. (2007) BCL-2 family proteins: critical checkpoints of apoptotic cell death. *Clin Cancer Res*, **13**, 7254-7263.

Danon, A. and Gallois, P. (1998) UV-C radiation induces apoptotic-like changes in Arabidopsis thaliana. *FEBS Lett*, **437**, 131-136.

De Block, M., Verduyn, C., De Brouwer, D. and Cornelissen, M. (2005) Poly(ADP-ribose) polymerase in plants affects energy homeostasis, cell death and stress tolerance. *Plant J*, **41**, 95-106.

de Jager, M., van Noort, J., van Gent, D.C., Dekker, C., Kanaar, R. and Wyman, C. (2001) Human Rad50/Mre11 is a flexible complex that can tether DNA ends. *Mol Cell*, **8**, 1129-1135.

De Schutter, K., Joubes, J., Cools, T., Verkest, A., Corellou, F., Babiychuk, E., Van Der Schueren, E., Beeckman, T., Kushnir, S., Inze, D. and De Veylder, L. (2007) Arabidopsis WEE1 kinase controls cell cycle arrest in response to activation of the DNA integrity checkpoint. *Plant Cell*, **19**, 211-225.

De Smet, I., Vassileva, V., De Rybel, B., Levesque, M.P., Grunewald, W., Van Damme, D., Van Noorden, G., Naudts, M., Van Isterdael, G., De Clercq, R., Wang, J.Y., Meuli, N., Vanneste, S., Friml, J., Hilson, P., Jurgens, G., Ingram, G.C., Inze, D., Benfey, P.N. and Beeckman, T. (2008) Receptor-like kinase ACR4 restricts formative cell divisions in the Arabidopsis root. *Science*, **322**, 594-597.

De Veylder, L., Beeckman, T., Beemster, G.T., de Almeida Engler, J., Ormenese, S., Maes, S., Naudts, M., Van Der Schueren, E., Jacqmard, A., Engler, G. and Inze, D. (2002) Control of proliferation,

endoreduplication and differentiation by the Arabidopsis E2Fa-DPa transcription factor. *EMBO J*, **21**, 1360-1368.

De Veylder, L., Beeckman, T., Beemster, G.T., Krols, L., Terras, F., Landrieu, I., van der Schueren, E., Maes, S., Naudts, M. and Inze, D. (2001) Functional analysis of cyclin-dependent kinase inhibitors of Arabidopsis. *Plant Cell*, **13**, 1653-1668.

De Veylder, L., Beeckman, T. and Inze, D. (2007) The ins and outs of the plant cell cycle. *Nat Rev Mol Cell Biol*, **8**, 655-665.

del Pozo, O. and Lam, E. (1998) Caspases and programmed cell death in the hypersensitive response of plants to pathogens. *Curr Biol*, **8**, R896.

Delaney, T.P., Uknes, S., Vernooij, B., Friedrich, L., Weymann, K., Negrotto, D., Gaffney, T., Gut-Rella, M., Kessmann, H., Ward, E. and Ryals, J. (1994) A central role of salicylic Acid in plant disease resistance. *Science*, **266**, 1247-1250.

DeLeo, F.R. and Quinn, M.T. (1996) Assembly of the phagocyte NADPH oxidase: molecular interaction of oxidase proteins. *J Leukoc Biol*, **60**, 677-691.

Dello Ioio, R., Linhares, F.S., Scacchi, E., Casamitjana-Martinez, E., Heidstra, R., Costantino, P. and Sabatini, S. (2007) Cytokinins determine Arabidopsis root-meristem size by controlling cell differentiation. *Curr Biol*, **17**, 678-682.

Denchi, E.L. (2009) Give me a break: how telomeres suppress the DNA damage response. *DNA Repair (Amst)*, **8**, 1118-1126.

Deng, C.X. (2006) BRCA1: cell cycle checkpoint, genetic instability, DNA damage response and cancer evolution. *Nucleic Acids Res*, **34**, 1416-1426.

Deng, C.X. and Wang, R.H. (2003) Roles of BRCA1 in DNA damage repair: a link between development and cancer. *Hum Mol Genet*, **12 Spec No 1**, R113-123.

Deng, Y. and Chang, S. (2007) Role of telomeres and telomerase in genomic instability, senescence and cancer. *Lab Invest*, **87**, 1071-1076.

DeYoung, B.J. and Innes, R.W. (2006) Plant NBS-LRR proteins in pathogen sensing and host defense. *Nat Immunol*, **7**, 1243-1249.

Dissmeyer, N., Weimer, A.K., Pusch, S., De Schutter, K., Kamei, C.L., Nowack, M.K., Novak, B., Duan, G.L., Zhu, Y.G., De Veylder, L. and Schnittger, A. (2009) Control of cell proliferation, organ growth, and DNA damage response operate independently of dephosphorylation of the Arabidopsis Cdk1 homolog CDKA;1. *Plant Cell*, **21**, 3641-3654.

Doerner, P. (2001) Plant meristems: a menage a trois to end it all. *Curr Biol*, **11**, R785-787.

Doil, C., Mailand, N., Bekker-Jensen, S., Menard, P., Larsen, D.H., Pepperkok, R., Ellenberg, J., Panier, S., Durocher, D., Bartek, J., Lukas, J. and Lukas, C. (2009) RNF168 binds and amplifies ubiquitin conjugates on damaged chromosomes to allow accumulation of repair proteins. *Cell*, **136**, 435-446.

Dolan, L., Janmaat, K., Willemsen, V., Linstead, P., Poethig, S., Roberts, K. and Scheres, B. (1993) Cellular organisation of the Arabidopsis thaliana root. *Development*, **119**, 71-84.

Dong, X. (1998) SA, JA, ethylene, and disease resistance in plants. *Curr Opin Plant Biol*, **1**, 316-323.

Donnelly, P.M., Bonetta, D., Tsukaya, H., Dengler, R.E. and Dengler, N.G. (1999) Cell cycling and cell enlargement in developing leaves of Arabidopsis. *Dev Biol*, **215**, 407-419.

Doucet-Chabeaud, G., Godon, C., Brutesco, C., de Murcia, G. and Kazmaier, M. (2001) Ionising radiation induces the expression of PARP-1 and PARP-2 genes in Arabidopsis. *Mol Genet Genomics*, **265**, 954-963.

Dutta, A. and Stillman, B. (1992) cdc2 family kinases phosphorylate a human cell DNA replication factor, RPA, and activate DNA replication. *EMBO J*, **11**, 2189-2199.

Elledge, S.J. (1996) Cell cycle checkpoints: preventing an identity crisis. *Science*, **274**, 1664-1672.

Elmore, S. (2007) Apoptosis: a review of programmed cell death. *Toxicol Pathol*, **35**, 495-516.

Esashi, F., Christ, N., Gannon, J., Liu, Y., Hunt, T., Jasin, M. and West, S.C. (2005) CDK-dependent phosphorylation of BRCA2 as a regulatory mechanism for recombinational repair. *Nature*, **434**, 598-604.

Falck, J., Coates, J. and Jackson, S.P. (2005) Conserved modes of recruitment of ATM, ATR and DNA-PKcs to sites of DNA damage. *Nature*, **434**, 605-611.

Feraru, E. and Friml, J. (2008) PIN polar targeting. *Plant Physiol*, **147**, 1553-1559.

Fitzgerald, M.S., Riha, K., Gao, F., Ren, S., McKnight, T.D. and Shippen, D.E. (1999) Disruption of the telomerase catalytic subunit gene from Arabidopsis inactivates telomerase and leads to a slow loss of telomeric DNA. *Proc Natl Acad Sci U S A*, **96**, 14813-14818.

Fletcher, J.C. (2002) Coordination of cell proliferation and cell fate decisions in the angiosperm shoot apical meristem. *Bioessays*, **24**, 27-37.

Fram, R.J. and Kufe, D.W. (1982) DNA strand breaks caused by inhibitors of DNA synthesis: 1-beta-D-arabinofuranosylcytosine and aphidicolin. *Cancer Res*, **42**, 4050-4053.

Francis, D. (2007) The plant cell cycle--15 years on. *New Phytol*, **174**, 261-278.

Friesner, J.D., Liu, B., Culligan, K. and Britt, A.B. (2005) Ionizing radiation-dependent gamma-H2AX focus formation requires ataxia telangiectasia mutated and ataxia telangiectasia mutated and Rad3-related. *Mol Biol Cell*, **16**, 2566-2576.

Friml, J., Vieten, A., Sauer, M., Weijers, D., Schwarz, H., Hamann, T., Offringa, R. and Jurgens, G. (2003) Efflux-dependent auxin gradients establish the apical-basal axis of Arabidopsis. *Nature*, **426**, 147-153.

Fujibe, T., Saji, H., Arakawa, K., Yabe, N., Takeuchi, Y. and Yamamoto, K.T. (2004) A methyl viologen-resistant mutant of Arabidopsis, which is allelic to ozone-sensitive rcd1, is tolerant to supplemental ultraviolet-B irradiation. *Plant Physiol*, **134**, 275-285.

Fujie, M., Kuroiwa, H., Suzuki, T., Kawano, S. and Kuroiwa, T. (1993) Organelle DNA Synthesis in the Quiescent centre of Arabidopsis thaliana (Col.). *J. Exp. Bot.*, **44**, 689-693.

Fujiki, Y., Yoshimoto, K. and Ohsumi, Y. (2007) An Arabidopsis homolog of yeast ATG6/VPS30 is essential for pollen germination. *Plant Physiol*, **143**, 1132-1139.

Fukuda, H. (1996) Xylogenesis: Initiation, Progression, and Cell Death. *Annu Rev Plant Physiol Plant Mol Biol*, **47**, 299-325.

Galinha, C., Hofhuis, H., Luijten, M., Willemsen, V., Blilou, I., Heidstra, R. and Scheres, B. (2007) PLETHORA proteins as dose-dependent master regulators of Arabidopsis root development. *Nature*, **449**, 1053-1057.

Gallego, M.E., Jeanneau, M., Granier, F., Bouchez, D., Bechtold, N. and White, C.I. (2001) Disruption of the Arabidopsis RAD50 gene leads to plant sterility and MMS sensitivity. *Plant J*, **25**, 31-41.

Gallois, J.L., Woodward, C., Reddy, G.V. and Sablowski, R. (2002) Combined SHOOT MERISTEMLESS and WUSCHEL trigger ectopic organogenesis in Arabidopsis. *Development*, **129**, 3207-3217.

Garcia-Muse, T. and Boulton, S.J. (2005) Distinct modes of ATR activation after replication stress and DNA double-strand breaks in Caenorhabditis elegans. *EMBO J*, **24**, 4345-4355.

Garcia, V., Bruchet, H., Camescasse, D., Granier, F., Bouchez, D. and Tissier, A. (2003) AtATM is essential for meiosis and the somatic response to DNA damage in plants. *Plant Cell*, **15**, 119-132.

Garcia, V., Salanoubat, M., Choisne, N. and Tissier, A. (2000) An ATM homologue from Arabidopsis thaliana: complete genomic organisation and expression analysis. *Nucleic Acids Res*, **28**, 1692-1699.

Garner, E. and Raj, K. (2008) Protective mechanisms of p53-p21-pRb proteins against DNA damage-induced cell death. *Cell Cycle*, **7**, 277-282.

Gechev, T.S., Van Breusegem, F., Stone, J.M., Denev, I. and Laloi, C. (2006) Reactive oxygen species as signals that modulate plant stress responses and programmed cell death. *Bioessays*, **28**, 1091-1101.

Geng, J. and Klionsky, D.J. (2008) The Atg8 and Atg12 ubiquitin-like conjugation systems in macroautophagy. 'Protein modifications: beyond the usual suspects' review series. *EMBO Rep*, **9**, 859-864.

Grieneisen, V.A., Xu, J., Maree, A.F., Hogeweg, P. and Scheres, B. (2007) Auxin transport is sufficient to generate a maximum and gradient guiding root growth. *Nature*, **449**, 1008-1013.

Gustafsson, A.B. and Gottlieb, R.A. (2007) Bcl-2 family members and apoptosis, taken to heart. *Am J Physiol Cell Physiol*, **292**, C45-51.

Guzman, P. and Ecker, J.R. (1990) Exploiting the triple response of Arabidopsis to identify ethylene-related mutants. *Plant Cell*, **2**, 513-523.

Ha, H.C. and Snyder, S.H. (1999) Poly(ADP-ribose) polymerase is a mediator of necrotic cell death by ATP depletion. *Proc Natl Acad Sci U S A*, **96**, 13978-13982.

Hakem, R. (2008) DNA-damage repair; the good, the bad, and the ugly. *EMBO J*, **27**, 589-605.

Hamann, T., Benkova, E., Baurle, I., Kientz, M. and Jurgens, G. (2002) The Arabidopsis BODENLOS gene encodes an auxin response protein inhibiting MONOPTEROS-mediated embryo patterning. *Genes Dev*, **16**, 1610-1615.

Han, P., Li, Q. and Zhu, Y.X. (2008) Mutation of Arabidopsis BARD1 causes meristem defects by failing to confine WUSCHEL expression to the organizing center. *Plant Cell*, **20**, 1482-1493.

Hardtke, C.S. (2006) Root development--branching into novel spheres. *Curr Opin Plant Biol*, **9**, 66-71.

Hardtke, C.S. and Berleth, T. (1998) The Arabidopsis gene MONOPTEROS encodes a transcription factor mediating embryo axis formation and vascular development. *EMBO J*, **17**, 1405-1411.

Hay, A., Craft, J. and Tsiantis, M. (2004) Plant hormones and homeoboxes: bridging the gap? *Bioessays*, **26**, 395-404.

He, R., Drury, G.E., Rotari, V.I., Gordon, A., Willer, M., Farzaneh, T., Woltering, E.J. and Gallois, P. (2008) Metacaspase-8 modulates programmed cell death induced by ultraviolet light and H2O2 in Arabidopsis. *J Biol Chem*, **283**, 774-783.

Heck, S., Grau, T., Buchala, A., Metraux, J.P. and Nawrath, C. (2003) Genetic evidence that expression of NahG modifies defence pathways independent of salicylic acid biosynthesis in the Arabidopsis-Pseudomonas syringae pv. tomato interaction. *Plant J*, **36**, 342-352.

Heeres, J.T. and Hergenrother, P.J. (2007) Poly(ADP-ribose) makes a date with death. *Curr Opin Chem Biol*, **11**, 644-653.

Hefner, E., Preuss, S.B. and Britt, A.B. (2003) Arabidopsis mutants sensitive to gamma radiation include the homologue of the human repair gene ERCC1. *J Exp Bot*, **54**, 669-680.

Heyer, B.S., MacAuley, A., Behrendtsen, O. and Werb, Z. (2000) Hypersensitivity to DNA damage leads to increased apoptosis during early mouse development. *Genes Dev*, **14**, 2072-2084.

Hochstrasser, M. (1996) Ubiquitin-dependent protein degradation. *Annu Rev Genet*, **30**, 405-439.

Hof, J.V.t. (1966) Experimental Control of Dna Synthesizing and Dividing Cells in Excised Root Tips of Pisum. *American Journal of Botany*, **53**, 970-976.

Hofius, D., Schultz-Larsen, T., Joensen, J., Tsitsigiannis, D.I., Petersen, N.H., Mattsson, O., Jorgensen, L.B., Jones, J.D., Mundy, J. and Petersen, M. (2009) Autophagic components contribute to hypersensitive cell death in Arabidopsis. *Cell*, **137**, 773-783.

Holler, N., Zaru, R., Micheau, O., Thome, M., Attinger, A., Valitutti, S., Bodmer, J.L., Schneider, P., Seed, B. and Tschopp, J. (2000) Fas triggers an alternative, caspase-8-independent cell death pathway using the kinase RIP as effector molecule. *Nat Immunol*, **1**, 489-495.

Ikegami, S., Taguchi, T., Ohashi, M., Oguro, M., Nagano, H. and Mano, Y. (1978) Aphidicolin prevents mitotic cell division by interfering with the activity of DNA polymerase-alpha. *Nature*, **275**, 458-460.

Inoue, Y., Suzuki, T., Hattori, M., Yoshimoto, K., Ohsumi, Y. and Moriyasu, Y. (2006) AtATG genes, homologs of yeast autophagy genes, are involved in constitutive autophagy in Arabidopsis root tip cells. *Plant Cell Physiol*, **47**, 1641-1652.

Inze, D. (2005) Green light for the cell cycle. *EMBO J*, **24**, 657-662.

Inze, D. and De Veylder, L. (2006) Cell cycle regulation in plant development. *Annu Rev Genet*, **40**, 77-105.

Ip, S.C., Rass, U., Blanco, M.G., Flynn, H.R., Skehel, J.M. and West, S.C. (2008) Identification of Holliday junction resolvases from humans and yeast. *Nature*, **456**, 357-361.

Ivanov, V.B. (2007) [Stem cells in the root and the problem of stem cells in plants]. *Ontogenez*, **38**, 406-419.

Jackson, S.P. (2002) Sensing and repairing DNA double-strand breaks. *Carcinogenesis*, **23**, 687-696.

Jasinski, S., Piazza, P., Craft, J., Hay, A., Woolley, L., Rieu, I., Phillips, A., Hedden, P. and Tsiantis, M. (2005) KNOX action in Arabidopsis is mediated by coordinate regulation of cytokinin and gibberellin activities. *Curr Biol*, **15**, 1560-1565.

Joubes, J., De Schutter, K., Verkest, A., Inze, D. and De Veylder, L. (2004) Conditional, recombinase-mediated expression of genes in plant cell cultures. *Plant J*, **37**, 889-896.

Kapust, R.B. and Waugh, D.S. (2000) Controlled intracellular processing of fusion proteins by TEV protease. *Protein Expr Purif*, **19**, 312-318.

Karlsson-Rosenthal, C. and Millar, J.B. (2006) Cdc25: mechanisms of checkpoint inhibition and recovery. *Trends Cell Biol*, **16**, 285-292.

Kilby, N.J., Fyvie, M.J., Sessions, R.A., Davies, G.J. and Murray, J.A. (2000) Controlled induction of GUS marked clonal sectors in Arabidopsis. *J Exp Bot*, **51**, 853-863.

Klionsky, D.J. (2007) Autophagy: from phenomenology to molecular understanding in less than a decade. *Nat Rev Mol Cell Biol*, **8**, 931-937.

Klutstein, M., Shaked, H., Sherman, A., Avivi-Ragolsky, N., Shema, E., Zenvirth, D., Levy, A.A. and Simchen, G. (2008) Functional conservation of the yeast and Arabidopsis RAD54-like genes. *Genetics*, **178**, 2389-2397.

Kono, A., Umeda-Hara, C., Lee, J., Ito, M., Uchimiya, H. and Umeda, M. (2003) Arabidopsis D-type cyclin CYCD4;1 is a novel cyclin partner of B2-type cyclin-dependent kinase. *Plant Physiol*, **132**, 1315-1321.

Kotchoni, S.O. and Gachomo, E.W. (2006) The reactive oxygen species network pathways:an essential prerequisite for perception of pathogen attack and the acquired disease resistance in plants. *J Biosci*, **31**, 389-404.

Kozhevnikova, A., Seregin, I., Bystrova, E. and Ivanov, V. (2007) Effects of heavy metals and strontium on division of root cap cells and meristem structural organization. *Russian Journal of Plant Physiology*, **54**, 257-266.

Kroemer, G. and Levine, B. (2008) Autophagic cell death: the story of a misnomer. *Nat Rev Mol Cell Biol*, **9**, 1004-1010.

Kuhlemeier, C. and Reinhardt, D. (2001) Auxin and phyllotaxis. *Trends Plant Sci*, **6**, 187-189.

Kumar, S. (2007) Caspase function in programmed cell death. *Cell Death Differ*, **14**, 32-43.

Kurup, S., Runions, J., Kohler, U., Laplaze, L., Hodge, S. and Haseloff, J. (2005) Marking cell lineages in living tissues. *Plant J*, **42**, 444-453.

Lafarge, S. and Montane, M.H. (2003) Characterization of Arabidopsis thaliana ortholog of the human breast cancer susceptibility gene 1: AtBRCA1, strongly induced by gamma rays. *Nucleic Acids Res*, **31**, 1148-1155.

Lamb, C. and Dixon, R.A. (1997) The Oxidative Burst in Plant Disease Resistance. *Annu Rev Plant Physiol Plant Mol Biol*, **48**, 251-275.

Landrieu, I., da Costa, M., De Veylder, L., Dewitte, F., Vandepoele, K., Hassan, S., Wieruszeski, J.M., Corellou, F., Faure, J.D., Van Montagu, M., Inze, D. and Lippens, G. (2004) A small CDC25 dual-specificity tyrosine-phosphatase isoform in Arabidopsis thaliana. *Proc Natl Acad Sci U S A*, **101**, 13380-13385.

Lane, D.P. (1992) Cancer. p53, guardian of the genome. *Nature*, **358**, 15-16.

Laux, T., Mayer, K.F., Berger, J. and Jurgens, G. (1996) The WUSCHEL gene is required for shoot and floral meristem integrity in Arabidopsis. *Development*, **122**, 87-96.

Le, Y., Gagneten, S., Tombaccini, D., Bethke, B. and Sauer, B. (1999) Nuclear targeting determinants of the phage P1 cre DNA recombinase. *Nucleic Acids Res*, **27**, 4703-4709.

Lee, J.H. and Paull, T.T. (2005) ATM activation by DNA double-strand breaks through the Mre11-Rad50-Nbs1 complex. *Science*, **308**, 551-554.

Lenhard, M., Bohnert, A., Jurgens, G. and Laux, T. (2001) Termination of stem cell maintenance in Arabidopsis floral meristems by interactions between WUSCHEL and AGAMOUS. *Cell*, **105**, 805-814.

Li, W., Chen, C., Markmann-Mulisch, U., Timofejeva, L., Schmelzer, E., Ma, H. and Reiss, B. (2004) The Arabidopsis AtRAD51 gene is dispensable for vegetative development but required for meiosis. *Proc Natl Acad Sci U S A*, **101**, 10596-10601.

Liang, Y., Du, F., Zhou, B.R., Zhou, H., Zou, G.L., Wang, C.X. and Qu, S.S. (2002) Thermodynamics and kinetics of the cleavage of DNA catalyzed by bleomycin A5. *Eur J Biochem*, **269**, 2851-2859.

Lindahl, T. (2000) Suppression of spontaneous mutagenesis in human cells by DNA base excision-repair. *Mutat Res*, **462**, 129-135.

Liu, Y., Schiff, M., Czymmek, K., Talloczy, Z., Levine, B. and Dinesh-Kumar, S.P. (2005) Autophagy regulates programmed cell death during the plant innate immune response. *Cell*, **121**, 567-577.

Long, J.A., Moan, E.I., Medford, J.I. and Barton, M.K. (1996) A member of the KNOTTED class of homeodomain proteins encoded by the STM gene of Arabidopsis. *Nature*, **379**, 66-69.

Longatti, A. and Tooze, S.A. (2009) Vesicular trafficking and autophagosome formation. *Cell Death Differ*, **16**, 956-965.

Longhese, M.P., Mantiero, D. and Clerici, M. (2006) The cellular response to chromosome breakage. *Mol Microbiol*, **60**, 1099-1108.

Lundin, C., Erixon, K., Arnaudeau, C., Schultz, N., Jenssen, D., Meuth, M. and Helleday, T. (2002) Different roles for nonhomologous end joining and homologous recombination following replication arrest in mammalian cells. *Mol Cell Biol*, **22**, 5869-5878.

Luo, G., Yao, M.S., Bender, C.F., Mills, M., Bladl, A.R., Bradley, A. and Petrini, J.H. (1999) Disruption of mRad50 causes embryonic stem cell lethality, abnormal embryonic development, and sensitivity to ionizing radiation. *Proc Natl Acad Sci U S A*, **96**, 7376-7381.

Marathe, R. and Dinesh-Kumar, S.P. (2003) Plant defense: one post, multiple guards?! *Mol Cell*, **11**, 284-286.

Marjanac, G., De Paepe, A., Peck, I., Jacobs, A., De Buck, S. and Depicker, A. (2008) Evaluation of CRE-mediated excision approaches in Arabidopsis thaliana. *Transgenic Res*, **17**, 239-250.

Markmann-Mulisch, U., Wendeler, E., Zobell, O., Schween, G., Steinbiss, H.H. and Reiss, B. (2007) Differential requirements for RAD51 in Physcomitrella patens and Arabidopsis thaliana development and DNA damage repair. *Plant Cell*, **19**, 3080-3089.

Marteijn, J.A., Bekker-Jensen, S., Mailand, N., Lans, H., Schwertman, P., Gourdin, A.M., Dantuma, N.P., Lukas, J. and Vermeulen, W. (2009) Nucleotide excision repair-induced H2A ubiquitination is dependent on MDC1 and RNF8 and reveals a universal DNA damage response. *J Cell Biol*, **186**, 835-847.

Mathieu, J., Warthmann, N., Kuttner, F. and Schmid, M. (2007) Export of FT protein from phloem companion cells is sufficient for floral induction in Arabidopsis. *Curr Biol*, **17**, 1055-1060.

Mayer, K.F., Schoof, H., Haecker, A., Lenhard, M., Jurgens, G. and Laux, T. (1998) Role of WUSCHEL in regulating stem cell fate in the Arabidopsis shoot meristem. *Cell*, **95**, 805-815.

McCabe, P., F., Levine, A., Meijer, P.-J., Tapon, N., A. and Pennell, R., I. (1997) A programmed cell death pathway activated in carrot cells cultured at low cell density. *The Plant Journal*, **12**, 267-280.

Merritt, A.J., Potten, C.S., Kemp, C.J., Hickman, J.A., Balmain, A., Lane, D.P. and Hall, P.A. (1994) The role of p53 in spontaneous and radiation-induced apoptosis in the gastrointestinal tract of normal and p53-deficient mice. *Cancer Res*, **54**, 614-617.

Miller, G., Schlauch, K., Tam, R., Cortes, D., Torres, M.A., Shulaev, V., Dangl, J.L. and Mittler, R. (2009) The plant NADPH oxidase RBOHD mediates rapid systemic signaling in response to diverse stimuli. *Sci Signal*, **2**, ra45.

Mittler, R. (2002) Oxidative stress, antioxidants and stress tolerance. *Trends Plant Sci*, **7**, 405-410.

Mittler, R., Vanderauwera, S., Gollery, M. and Van Breusegem, F. (2004) Reactive oxygen gene network of plants. *Trends Plant Sci*, **9**, 490-498.

Muniz, L., Minguet, E.G., Singh, S.K., Pesquet, E., Vera-Sirera, F., Moreau-Courtois, C.L., Carbonell, J., Blazquez, M.A. and Tuominen, H. (2008) ACAULIS5 controls Arabidopsis xylem specification through the prevention of premature cell death. *Development*, **135**, 2573-2582.

Musacchio, A. and Hardwick, K.G. (2002) The spindle checkpoint: structural insights into dynamic signalling. *Nat Rev Mol Cell Biol*, **3**, 731-741.

Muschel, R.J., Soto, D.E., McKenna, W.G. and Bernhard, E.J. (1998) Radiosensitization and apoptosis. *Oncogene*, **17**, 3359-3363.

Nakagami, H., Soukupova, H., Schikora, A., Zarsky, V. and Hirt, H. (2006) A Mitogen-activated protein kinase kinase kinase mediates reactive oxygen species homeostasis in Arabidopsis. *J Biol Chem*, **281**, 38697-38704.

Nakajima, K., Sena, G., Nawy, T. and Benfey, P.N. (2001) Intercellular movement of the putative transcription factor SHR in root patterning. *Nature*, **413**, 307-311.

Nam, J., Matthysse, A.G. and Gelvin, S.B. (1997) Differences in susceptibility of Arabidopsis ecotypes to crown gall disease may result from a deficiency in T-DNA integration. *Plant Cell*, **9**, 317-333.

Nawrath, C. and Metraux, J.P. (1999) Salicylic acid induction-deficient mutants of Arabidopsis express PR-2 and PR-5 and accumulate high levels of camalexin after pathogen inoculation. *Plant Cell*, **11**, 1393-1404.

Niida, H. and Nakanishi, M. (2006) DNA damage checkpoints in mammals. *Mutagenesis*, **21**, 3-9.

Nijnik, A., Woodbine, L., Marchetti, C., Dawson, S., Lambe, T., Liu, C., Rodrigues, N.P., Crockford, T.L., Cabuy, E., Vindigni, A., Enver, T., Bell, J.I., Slijepcevic, P., Goodnow, C.C., Jeggo, P.A. and Cornall, R.J. (2007) DNA repair is limiting for haematopoietic stem cells during ageing. *Nature*, **447**, 686-690.

Nussenzweig, A., Sokol, K., Burgman, P., Li, L. and Li, G.C. (1997) Hypersensitivity of Ku80-deficient cell lines and mice to DNA damage: the effects of ionizing radiation on growth, survival, and development. *Proc Natl Acad Sci U S A*, **94**, 13588-13593.

Oparka, K.J., Duckett, C.M., Prior, D.A.M. and Fisher, D.B. (1994) Real-time imaging of phloem unloading in the root tip of Arabidopsis. *The Plant Journal*, **6**, 759-766.

Ortega-Martinez, O., Pernas, M., Carol, R.J. and Dolan, L. (2007) Ethylene modulates stem cell division in the Arabidopsis thaliana root. *Science*, **317**, 507-510.

Osterhage, J.L. and Friedman, K.L. (2009) Chromosome end maintenance by telomerase. *J Biol Chem*, **284**, 16061-16065.

Overmyer, K., Brosche, M., Pellinen, R., Kuittinen, T., Tuominen, H., Ahlfors, R., Keinanen, M., Saarma, M., Scheel, D. and Kangasjarvi, J. (2005) Ozone-induced programmed cell death in the Arabidopsis radical-induced cell death1 mutant. *Plant Physiol*, **137**, 1092-1104.

Overmyer, K., Tuominen, H., Kettunen, R., Betz, C., Langebartels, C., Sandermann, H., Jr. and Kangasjarvi, J. (2000) Ozone-sensitive arabidopsis rcd1 mutant reveals opposite roles for ethylene and jasmonate signaling pathways in regulating superoxide-dependent cell death. *Plant Cell*, **12**, 1849-1862.

Panier, S. and Durocher, D. (2009) Regulatory ubiquitylation in response to DNA double-strand breaks. *DNA Repair (Amst)*, **8**, 436-443.

Parcy, F., Bomblies, K. and Weigel, D. (2002) Interaction of LEAFY, AGAMOUS and TERMINAL FLOWER1 in maintaining floral meristem identity in Arabidopsis. *Development*, **129**, 2519-2527.

Pardo, B., Gomez-Gonzalez, B. and Aguilera, A. (2009) DNA repair in mammalian cells: DNA double-strand break repair: how to fix a broken relationship. *Cell Mol Life Sci*, **66**, 1039-1056.

Paull, T.T. and Gellert, M. (1998) The 3' to 5' exonuclease activity of Mre 11 facilitates repair of DNA double-strand breaks. *Mol Cell*, **1**, 969-979.

Peragine, A., Yoshikawa, M., Wu, G., Albrecht, H.L. and Poethig, R.S. (2004) SGS3 and SGS2/SDE1/RDR6 are required for juvenile development and the production of trans-acting siRNAs in Arabidopsis. *Genes Dev*, **18**, 2368-2379.

Phillips, A.R., Suttangkakul, A. and Vierstra, R.D. (2008) The ATG12-conjugating enzyme ATG10 Is essential for autophagic vesicle formation in Arabidopsis thaliana. *Genetics*, **178**, 1339-1353.

Polager, S. and Ginsberg, D. (2008) E2F - at the crossroads of life and death. *Trends Cell Biol*, **18**, 528-535.

Porceddu, A., Stals, H., Reichheld, J.P., Segers, G., De Veylder, L., Barroco, R.P., Casteels, P., Van Montagu, M., Inze, D. and Mironov, V. (2001) A plant-specific cyclin-dependent kinase is involved in the control of G2/M progression in plants. *J Biol Chem*, **276**, 36354-36360.

Proskuryakov, S.Y., Konoplyannikov, A.G. and Gabai, V.L. (2003) Necrosis: a specific form of programmed cell death? *Exp Cell Res*, **283**, 1-16.

Przemeck, G.K., Mattsson, J., Hardtke, C.S., Sung, Z.R. and Berleth, T. (1996) Studies on the role of the Arabidopsis gene MONOPTEROS in vascular development and plant cell axialization. *Planta*, **200**, 229-237.

Qin, G., Ma, Z., Zhang, L., Xing, S., Hou, X., Deng, J., Liu, J., Chen, Z., Qu, L.J. and Gu, H. (2007) Arabidopsis AtBECLIN 1/AtAtg6/AtVps30 is essential for pollen germination and plant development. *Cell Res*, **17**, 249-263.

Quenouille, M.H. (1950) *Introductory Statistics*: pp. xii. 248. Butterworth-Springer: London.

Ramsden, D.A. and Gellert, M. (1998) Ku protein stimulates DNA end joining by mammalian DNA ligases: a direct role for Ku in repair of DNA double-strand breaks. *EMBO J*, **17**, 609-614.

Reape, T.J. and McCabe, P.F. (2008) Apoptotic-like programmed cell death in plants. *New Phytol*, **180**, 13-26.

Reape, T.J., Molony, E.M. and McCabe, P.F. (2008) Programmed cell death in plants: distinguishing between different modes. *J Exp Bot*, **59**, 435-444.

Reddy, G.V., Heisler, M.G., Ehrhardt, D.W. and Meyerowitz, E.M. (2004) Real-time lineage analysis reveals oriented cell divisions associated with morphogenesis at the shoot apex of Arabidopsis thaliana. *Development*, **131**, 4225-4237.

Reddy, G.V. and Meyerowitz, E.M. (2005) Stem-cell homeostasis and growth dynamics can be uncoupled in the Arabidopsis shoot apex. *Science*, **310**, 663-667.

Reidt, W., Wurz, R., Wanieck, K., Chu, H.H. and Puchta, H. (2006) A homologue of the breast cancer-associated gene BARD1 is involved in DNA repair in plants. *EMBO J*, **25**, 4326-4337.

Reinhardt, D., Pesce, E.R., Stieger, P., Mandel, T., Baltensperger, K., Bennett, M., Traas, J., Friml, J. and Kuhlemeier, C. (2003) Regulation of phyllotaxis by polar auxin transport. *Nature*, **426**, 255-260.

Rentel, M.C., Lecourieux, D., Ouaked, F., Usher, S.L., Petersen, L., Okamoto, H., Knight, H., Peck, S.C., Grierson, C.S., Hirt, H. and Knight, M.R. (2004) OXI1 kinase is necessary for oxidative burst-mediated signalling in Arabidopsis. *Nature*, **427**, 858-861.

Ricaud, L., Proux, C., Renou, J.P., Pichon, O., Fochesato, S., Ortet, P. and Montane, M.H. (2007) ATM-mediated transcriptional and developmental responses to gamma-rays in Arabidopsis. *PLoS One*, **2**, e430.

Rich, T., Allen, R.L. and Wyllie, A.H. (2000) Defying death after DNA damage. *Nature*, **407**, 777-783.

Riedl, S.J. and Salvesen, G.S. (2007) The apoptosome: signalling platform of cell death. *Nat Rev Mol Cell Biol*, **8**, 405-413.

Riha, K., Heacock, M.L. and Shippen, D.E. (2006) The role of the nonhomologous end-joining DNA double-strand break repair pathway in telomere biology. *Annu Rev Genet*, **40**, 237-277.

Riha, K. and Shippen, D.E. (2003) Telomere structure, function and maintenance in Arabidopsis. *Chromosome Res*, **11**, 263-275.

Riha, K., Watson, J.M., Parkey, J. and Shippen, D.E. (2002) Telomere length deregulation and enhanced sensitivity to genotoxic stress in Arabidopsis mutants deficient in Ku70. *EMBO J*, **21**, 2819-2826.

Roa, H., Lang, J., Culligan, K.M., Keller, M., Holec, S., Cognat, V., Montane, M.H., Houlne, G. and Chaboute, M.E. (2009) Ribonucleotide reductase regulation in response to genotoxic stress in Arabidopsis. *Plant Physiol*, **151**, 461-471.

Roldan-Arjona, T. and Ariza, R.R. (2009) Repair and tolerance of oxidative DNA damage in plants. *Mutat Res*, **681**, 169-179.

Rothkamm, K., Kruger, I., Thompson, L.H. and Lobrich, M. (2003) Pathways of DNA double-strand break repair during the mammalian cell cycle. *Mol Cell Biol*, **23**, 5706-5715.

Rounds, M.A. and Larsen, P.B. (2008) Aluminum-dependent root-growth inhibition in Arabidopsis results from AtATR-regulated cell-cycle arrest. *Curr Biol*, **18**, 1495-1500.

Ruzankina, Y., Pinzon-Guzman, C., Asare, A., Ong, T., Pontano, L., Cotsarelis, G., Zediak, V.P., Velez, M., Bhandoola, A. and Brown, E.J. (2007) Deletion of the developmentally essential gene ATR in adult mice leads to age-related phenotypes and stem cell loss. *Cell Stem Cell*, **1**, 113-126.

Sabatini, S., Heidstra, R., Wildwater, M. and Scheres, B. (2003) SCARECROW is involved in positioning the stem cell niche in the Arabidopsis root meristem. *Genes Dev*, **17**, 354-358.

Sablowski, R. (2004) Plant and animal stem cells: conceptually similar, molecularly distinct? *Trends Cell Biol*, **14**, 605-611.

Sablowski, R. (2007) The dynamic plant stem cell niches. *Curr Opin Plant Biol*, **10**, 639-644.

Sakamoto, T., Kamiya, N., Ueguchi-Tanaka, M., Iwahori, S. and Matsuoka, M. (2001) KNOX homeodomain protein directly suppresses the expression of a gibberellin biosynthetic gene in the tobacco shoot apical meristem. *Genes Dev*, **15**, 581-590.

Sarkar, A.K., Luijten, M., Miyashima, S., Lenhard, M., Hashimoto, T., Nakajima, K., Scheres, B., Heidstra, R. and Laux, T. (2007) Conserved factors regulate signalling in Arabidopsis thaliana shoot and root stem cell organizers. *Nature*, **446**, 811-814.

Savitsky, K., Sfez, S., Tagle, D.A., Ziv, Y., Sartiel, A., Collins, F.S., Shiloh, Y. and Rotman, G. (1995) The complete sequence of the coding region of the ATM gene reveals similarity to cell cycle regulators in different species. *Hum Mol Genet*, **4**, 2025-2032.

Scheres, B., Di Laurenzio, L., Willemsen, V., Hauser, M.T., Janmaat, K., Weisbeek, P. and Benfey, P.N. (1995) Mutations affecting the radial organisation of the Arabidopsis root display specific defects throughout the embryonic axis. *Development*, **121**, 53-62.

Schumacher, B., Hofmann, K., Boulton, S. and Gartner, A. (2001) The C. elegans homolog of the p53 tumor suppressor is required for DNA damage-induced apoptosis. *Curr Biol*, **11**, 1722-1727.

Scofield, S. and Murray, J.A. (2006) KNOX gene function in plant stem cell niches. *Plant Mol Biol*, **60**, 929-946.

Shinin, V., Gayraud-Morel, B., Gomes, D. and Tajbakhsh, S. (2006) Asymmetric division and cosegregation of template DNA strands in adult muscle satellite cells. *Nat Cell Biol*, **8**, 677-687.

Shrivastav, M., De Haro, L.P. and Nickoloff, J.A. (2008) Regulation of DNA double-strand break repair pathway choice. *Cell Res*, **18**, 134-147.

Skoog, F. and Miller, C.O. (1957) Chemical regulation of growth and organ formation in plant tissues cultured in vitro. *Symp Soc Exp Biol*, **54**, 118-130.

Stahl, Y., Wink, R.H., Ingram, G.C. and Simon, R. (2009) A signaling module controlling the stem cell niche in Arabidopsis root meristems. *Curr Biol*, **19**, 909-914.

Stewart, G.S., Maser, R.S., Stankovic, T., Bressan, D.A., Kaplan, M.I., Jaspers, N.G., Raams, A., Byrd, P.J., Petrini, J.H. and Taylor, A.M. (1999) The DNA double-strand break repair gene hMRE11 is mutated in individuals with an ataxia-telangiectasia-like disorder. *Cell*, **99**, 577-587.

Stracker, T.H., Theunissen, J.W., Morales, M. and Petrini, J.H. (2004) The Mre11 complex and the metabolism of chromosome breaks: the importance of communicating and holding things together. *DNA Repair (Amst)*, **3**, 845-854.

Stucki, M. and Jackson, S.P. (2006) gammaH2AX and MDC1: anchoring the DNA-damage-response machinery to broken chromosomes. *DNA Repair (Amst)*, **5**, 534-543.

Sun, A., Bagella, L., Tutton, S., Romano, G. and Giordano, A. (2007) From G0 to S phase: a view of the roles played by the retinoblastoma (Rb) family members in the Rb-E2F pathway. *J Cell Biochem*, **102**, 1400-1404.

Sweeney, P.R., Britt, A.B. and Culligan, K.M. (2009) The Arabidopsis ATRIP ortholog is required for a programmed response to replication inhibitors. *Plant J*, **60**, 518-526.

Taylor, R.C., Cullen, S.P. and Martin, S.J. (2008) Apoptosis: controlled demolition at the cellular level. *Nat Rev Mol Cell Biol*, **9**, 231-241.

Teale, W.D., Paponov, I.A., Ditengou, F. and Palme, K. (2005) Auxin and the developing root of *Arabidopsis thaliana*. *Physiologia Plantarum*, **123**, 130-138.

Thompson, A.R., Doelling, J.H., Suttangkakul, A. and Vierstra, R.D. (2005) Autophagic nutrient recycling in Arabidopsis directed by the ATG8 and ATG12 conjugation pathways. *Plant Physiol*, **138**, 2097-2110.

Truernit, E. and Haseloff, J. (2008) A simple way to identify non-viable cells within living plant tissue using confocal microscopy. *Plant Methods*, **4**, 15.

Tsukaya, H., Takahashi, T., Naito, S. and Komeda, Y. (1993) Floral organ-specific and constitutive expression of an Arabidopsis thaliana heat-shock HSP18.2::GUS fusion gene is retained even after homeotic conversion of flowers by mutation. *Mol Gen Genet*, **237**, 26-32.

Tucker, M.R. and Laux, T. (2007) Connecting the paths in plant stem cell regulation. *Trends Cell Biol*, **17**, 403-410.

Uemukai, K., Iwakawa, H., Kosugi, S., de Uemukai, S., Kato, K., Kondorosi, E., Murray, J.A., Ito, M., Shinmyo, A. and Sekine, M. (2005) Transcriptional activation of tobacco E2F is repressed by co-transfection with the retinoblastoma-related protein: cyclin D expression overcomes this repressor activity. *Plant Mol Biol*, **57**, 83-100.

Umeda, M., Shimotohno, A. and Yamaguchi, M. (2005) Control of cell division and transcription by cyclin-dependent kinase-activating kinases in plants. *Plant Cell Physiol*, **46**, 1437-1442.

Uziel, T., Lerenthal, Y., Moyal, L., Andegeko, Y., Mittelman, L. and Shiloh, Y. (2003) Requirement of the MRN complex for ATM activation by DNA damage. *EMBO J*, **22**, 5612-5621.

van Attikum, H., Bundock, P., Overmeer, R.M., Lee, L.Y., Gelvin, S.B. and Hooykaas, P.J. (2003) The Arabidopsis AtLIG4 gene is required for the repair of DNA damage, but not for the integration of Agrobacterium T-DNA. *Nucleic Acids Res*, **31**, 4247-4255.

van den Berg, C., Willemsen, V., Hendriks, G., Weisbeek, P. and Scheres, B. (1997) Short-range control of cell differentiation in the Arabidopsis root meristem. *Nature*, **390**, 287-289.

van Doorn, W.G. and Woltering, E.J. (2005) Many ways to exit? Cell death categories in plants. *Trends Plant Sci*, **10**, 117-122.

Vercammen, D., van de Cotte, B., De Jaeger, G., Eeckhout, D., Casteels, P., Vandepoele, K., Vandenberghe, I., Van Beeumen, J., Inze, D. and Van Breusegem, F. (2004) Type II metacaspases Atmc4 and

Atmc9 of Arabidopsis thaliana cleave substrates after arginine and lysine. *J Biol Chem*, **279**, 45329-45336.

Vermeulen, K., Van Bockstaele, D.R. and Berneman, Z.N. (2003) The cell cycle: a review of regulation, deregulation and therapeutic targets in cancer. *Cell Prolif*, **36**, 131-149.

Wajant, H. (2002) The Fas signaling pathway: more than a paradigm. *Science*, **296**, 1635-1636.

Wang, K.L., Li, H. and Ecker, J.R. (2002) Ethylene biosynthesis and signaling networks. *Plant Cell*, **14 Suppl**, S131-151.

Ward, I.M. and Chen, J. (2001) Histone H2AX is phosphorylated in an ATR-dependent manner in response to replicational stress. *J Biol Chem*, **276**, 47759-47762.

Ward, I.M., Minn, K. and Chen, J. (2004) UV-induced ataxia-telangiectasia-mutated and Rad3-related (ATR) activation requires replication stress. *J Biol Chem*, **279**, 9677-9680.

Watanabe, N. and Lam, E. (2004) Recent advance in the study of caspase-like proteases and Bax inhibitor-1 in plants: their possible roles as regulator of programmed cell death. *Molecular Plant Pathology*, **5**, 65-70.

Waterworth, W.M., Altun, C., Armstrong, S.J., Roberts, N., Dean, P.J., Young, K., Weil, C.F., Bray, C.M. and West, C.E. (2007) NBS1 is involved in DNA repair and plays a synergistic role with ATM in mediating meiotic homologous recombination in plants. *Plant J*, **52**, 41-52.

Watson, J.M., Bulankova, P., Riha, K., Shippen, D.E. and Vyskot, B. (2005) Telomerase-independent cell survival in Arabidopsis thaliana. *Plant J*, **43**, 662-674.

Weinert, T.A. and Hartwell, L.H. (1988) The RAD9 gene controls the cell cycle response to DNA damage in Saccharomyces cerevisiae. *Science*, **241**, 317-322.

Welch, D., Hassan, H., Blilou, I., Immink, R., Heidstra, R. and Scheres, B. (2007) Arabidopsis JACKDAW and MAGPIE zinc finger proteins delimit asymmetric cell division and stabilize tissue boundaries by restricting SHORT-ROOT action. *Genes Dev*, **21**, 2196-2204.

West, C.E., Waterworth, W.M., Jiang, Q. and Bray, C.M. (2000) Arabidopsis DNA ligase IV is induced by gamma-irradiation and interacts with an Arabidopsis homologue of the double strand break repair protein XRCC4. *Plant J*, **24**, 67-78.

West, C.E., Waterworth, W.M., Story, G.W., Sunderland, P.A., Jiang, Q. and Bray, C.M. (2002) Disruption of the Arabidopsis AtKu80 gene

demonstrates an essential role for AtKu80 protein in efficient repair of DNA double-strand breaks in vivo. *Plant J*, **31**, 517-528.

West, C.E., Waterworth, W.M., Sunderland, P.A. and Bray, C.M. (2004) Arabidopsis DNA double-strand break repair pathways. *Biochem Soc Trans*, **32**, 964-966.

Wildwater, M., Campilho, A., Perez-Perez, J.M., Heidstra, R., Blilou, I., Korthout, H., Chatterjee, J., Mariconti, L., Gruissem, W. and Scheres, B. (2005) The RETINOBLASTOMA-RELATED gene regulates stem cell maintenance in Arabidopsis roots. *Cell*, **123**, 1337-1349.

Williams, B. and Dickman, M. (2008) Plant programmed cell death: can't live with it; can't live without it. *Mol Plant Pathol*, **9**, 531-544.

Wilson, P.F., Nham, P.B., Urbin, S.S., Hinz, J.M., Jones, I.M. and Thompson, L.H. (2010) Inter-individual variation in DNA double-strand break repair in human fibroblasts before and after exposure to low doses of ionizing radiation. *Mutat Res*, **683**, 91-97.

Woltering, E.J., van der Bent, A. and Hoeberichts, F.A. (2002) Do plant caspases exist? *Plant Physiol*, **130**, 1764-1769.

Wong, H.L. and Shimamoto, K. (2009) Sending ROS on a bullet train. *Sci Signal*, **2**, pe60.

Woodhouse, B.C. and Dianov, G.L. (2008) Poly ADP-ribose polymerase-1: an international molecule of mystery. *DNA Repair (Amst)*, **7**, 1077-1086.

Xiong, Y., Contento, A.L. and Bassham, D.C. (2005) AtATG18a is required for the formation of autophagosomes during nutrient stress and senescence in Arabidopsis thaliana. *Plant J*, **42**, 535-546.

Xu, J., Hofhuis, H., Heidstra, R., Sauer, M., Friml, J. and Scheres, B. (2006) A molecular framework for plant regeneration. *Science*, **311**, 385-388.

Yadav, R.K., Girke, T., Pasala, S., Xie, M. and Reddy, G.V. (2009) Gene expression map of the Arabidopsis shoot apical meristem stem cell niche. *Proc Natl Acad Sci U S A*, **106**, 4941-4946.

Yanai, O., Shani, E., Dolezal, K., Tarkowski, P., Sablowski, R., Sandberg, G., Samach, A. and Ori, N. (2005) Arabidopsis KNOXI proteins activate cytokinin biosynthesis. *Curr Biol*, **15**, 1566-1571.

Yoshimoto, K., Hanaoka, H., Sato, S., Kato, T., Tabata, S., Noda, T. and Ohsumi, Y. (2004) Processing of ATG8s, ubiquitin-like proteins, and their deconjugation by ATG4s are essential for plant autophagy. *Plant Cell*, **16**, 2967-2983.

Zellinger, B., Akimcheva, S., Puizina, J., Schirato, M. and Riha, K. (2007) Ku suppresses formation of telomeric circles and alternative telomere lengthening in Arabidopsis. *Mol Cell*, **27**, 163-169.

Zhou, B.B. and Elledge, S.J. (2000) The DNA damage response: putting checkpoints in perspective. *Nature*, **408**, 433-439.

Zhou, J., Lim, C.U., Li, J.J., Cai, L. and Zhang, Y. (2006) The role of NBS1 in the modulation of PIKK family proteins ATM and ATR in the cellular response to DNA damage. *Cancer Lett*, **243**, 9-15.